

# Two L-histidine transporters and one sensor kinase

## Molecular mechanisms of regulation of histidine metabolism and transport in *Pseudomonas putida* KT2440

Dissertation der Fakultät für Biologie  
zur Erlangung des Doktorgrades der Naturwissenschaften  
(Dr. rer. nat.)  
der Ludwig-Maximilians-Universität München

Larissa Marie Aniela Wirtz  
aus München



München, 2022

# Two L-histidine transporters and one sensor kinase

## Molecular mechanisms of regulation of histidine metabolism and transport in *Pseudomonas putida* KT2440

Dissertation der Fakultät für Biologie  
zur Erlangung des Doktorgrades der Naturwissenschaften  
(Dr. rer. nat.)  
der Ludwig-Maximilians-Universität München

Larissa Marie Aniela Wirtz  
aus München



München, 2022

Diese Dissertation wurde angefertigt  
unter der Leitung von Prof. Heinrich Jung  
im Bereich Mikrobiologie  
an der Ludwig-Maximilians-Universität München

Erstgutachter/in: Prof. Dr. Heinrich Jung  
Zweitgutachter/in: Prof. Dr. Thorben Cordes  
Tag der Abgabe: 03. Mai 2022  
Tag der mündlichen Prüfung: 28. September 2022

## **Eidesstattliche Erklärung**

Ich versichere hiermit an Eides statt, dass meine Dissertation selbstständig und ohne unerlaubte Hilfsmittel angefertigt worden ist. Die vorliegende Dissertation wurde weder ganz noch teilweise bei einer anderen Prüfungskommission vorgelegt.

Ich habe noch zu keinem früheren Zeitpunkt versucht, eine Dissertation einzureichen oder an einer Doktorprüfung teilzunehmen.

## **Statutory declaration**

Herewith I declare that the presented dissertation was written autonomously without illegal help. Moreover, I certify that I have not previously submitted a dissertation and that I have not undergone a doctoral examination in the past without success.

The presented dissertation was not submitted completely or essential parts of it to another examination board.

München, 03. Mai 2022

Larissa Wirtz

---

Larissa Wirtz

# Contents

<b>Eidesstattliche Erklärung</b>	<b>ii</b>
<b>Statutory declaration</b>	<b>ii</b>
<b>Publications and Manuscripts originating from this Thesis</b>	<b>vi</b>
<b>Contributions to Publications and Manuscripts presented in this Thesis</b>	<b>vii</b>
<b>Nomenclature</b>	<b>viii</b>
<b>Abbreviations</b>	<b>ix</b>
<b>Summary</b>	<b>x</b>
<b>Zusammenfassung</b>	<b>xii</b>
<b>1 Introduction</b>	<b>1</b>
1.1 <i>Pseudomonas putida</i> KT2440 as a model organism . . . . .	1
1.2 Regulation of gene expression in <i>Pseudomonas putida</i> KT2440 . . . . .	3
1.2.1 Histidine sensor kinases . . . . .	3
1.2.2 Carbon catabolite repression . . . . .	4
1.2.3 Histidine utilization is tightly controlled . . . . .	6
1.3 Membrane transport mechanisms . . . . .	9
1.3.1 Diversity of transport systems . . . . .	9
1.3.2 The APC-transporter superfamily and the role of the LeuT fold . . . . .	10
1.4 Histidine uptake in $\gamma$ -Proteobacteria . . . . .	13
1.4.1 The APC transporter HutT takes up histidine in <i>Pseudomonas</i> . . . . .	14
1.5 CbrA is a histidine kinase and a SSSF-transporter . . . . .	15
1.6 Aim of this work . . . . .	18
<b>2 Transport and kinase activities of CbrA of <i>Pseudomonas putida</i> KT2440</b>	<b>19</b>
<b>3 HutT functions as the main L-Histidine transporter in <i>Pseudomonas putida</i> KT2440</b>	<b>42</b>
<b>4 Prokaryotic solute/sodium symporters: versatile functions of a transporter family</b>	<b>68</b>

---

<b>5 Discussion</b>	<b>96</b>
5.1 Histidine uptake and utilization in <i>P. putida</i> KT2440 . . . . .	96
5.1.1 CbrA and HutT as members of the APC superfamily . . . . .	97
5.1.2 Comparison of transport activity between CbrA and HutT . . . . .	98
5.1.3 Differences in histidine transport between <i>Pseudomonas</i> species . . . . .	99
5.2 CbrA's regulatory role . . . . .	101
5.2.1 CbrA regulates carbon catabolite repression . . . . .	101
5.2.2 CbrA regulates expression of <i>hut</i> genes . . . . .	102
5.2.3 Role of CbrA's domains . . . . .	103
5.2.4 Transporters as information transmitters . . . . .	104
5.3 Model of CbrA and HutT functions . . . . .	106
5.4 Outlook . . . . .	108
<b>Bibliography</b>	<b>109</b>
<b>Acknowledgements</b>	<b>122</b>

## List of Figures

1	Electron microscopy image of wild type <i>Pseudomonas putida</i> KT2440 cells in the exponential growth phase. . . . .	1
2	Typical histidine sensor kinase (HK) and response regulator (RR) scheme. . .	3
3	Schematic representation of carbon catabolite repression in <i>Pseudomonas aeruginosa</i> . . . . .	5
4	The histidine utilization ( <i>hut</i> ) operon and the histidine degradation pathway.	7
5	Examples of transport systems. . . . .	9
6	Domain structure of CbrA und CbrB. . . . .	15
7	Uptake of histidine in <i>P. putida</i> via CbrA and HutT. . . . .	106

## List of Tables

1	Comparison of parameters between L-histidine transporters CbrA and HutT of <i>P. putida</i> KT2440. . . . .	99
---	-------------------------------------------------------------------------------------------------------------	----

## Publications and Manuscripts originating from this Thesis

### Chapter 2

Wirtz L, Eder M, Schipper K, Rohrer S, Jung H. Transport and kinase activities of CbrA of *Pseudomonas putida* KT2440. Sci rep 2020;10:5400.  
<https://doi.org/10.1038/s41598-020-62337-9>

### Chapter 3

Wirtz L, Eder M, Brand A-K, Jung H. HutT functions as the main L-Histidine transporter in *Pseudomonas putida* KT2440. FEBS Lett 2021, 595(16)  
<https://doi.org/10.1002/1873-3468.14159>

### Chapter 4

Henriquez T, Wirtz L, Su D, Jung H. Prokaryotic solute/sodium symporters: versatile functions of a transporter family. Int J Mol Sci 2021, 22(4).  
<https://doi.org/10.3390/ijms22041880>

## Contributions to Publications and Manuscripts originating from this Thesis

### Chapter 2

Larissa Wirtz, Michelle Eder, Stefanie Rohrer and Kerstin Schipper generated the strains and plasmids; L.W. and M.E. performed growth curves and reporter assays; L.W. and M.E. performed transport measurements; L.W. performed the DRaCALA; L.W. purified the proteins; L.W. performed thermal shift assays; L.W. synthesized the  $^{32}\text{P}$ -ACP; K. S., S. R., L.W. and M.E. performed phosphorylation assays; L.W. and Heinrich Jung planned and supervised the experiments; L.W. and H.J. wrote the manuscript.

### Chapter 3

L.W. and H.J. planned and supervised the experiments; L.W. and M.E. generated the strains and plasmids; L.W. performed the growth analysis; Anna-Katharina Brand and M.E. performed transport measurements; L.W. purified and reconstituted protein; L.W. and M.E. performed the DRaCALA; L.W. and H.J. wrote the manuscript.

### Chapter 4

L.W. researched and wrote the chapter "5.2 Structure-function relationships in SSSF-dependent sensor kinases".

I hereby confirm the above statements:

**Larissa Wirtz**

---

Larissa Wirtz

---

Prof. Heinrich Jung

## Nomenclature

Amino acid positions in a protein are abbreviated according to the one-letter code (e.g., T27) or three-letter code (e.g. Thr27). For amino acid substitutions, the amino acid introduced by directed mutagenesis is added to the native amino acid position in one-letter code or three-letter code (e.g., T27A or Thr27Ala).

Nucleotide positions indicate the distance to the transcriptional start site (+1).

Deletions are marked with  $\Delta$ .

---

## Abbreviations

3AT	3-amino-1,2,4-triazole
AA	amino acid
ABC	ATP binding cassette
APC family	amino acid-polyamine-organocation family
ATP	adenosine triphosphate
bp	base pair
CCCP	m-chlorophenyl hydrazine
CM	cytoplasmic membrane
Da	Dalton
DNP	2,4-dinitrophenol
his	L-histidine
$K_M$	Michaelis constant
MFS	major facilitator superfamily
NEM	N-ethylmaleimide
OAA	oxaloacetate
OD <sub>x</sub>	optical density at wavelength x
PAGE	polyacrylamide gel electrophoresis
pmf	proton motive force
SDS	sodium dodecyl sulfate
SLC5	sodium solute symporter family 5
smf	sodium motive force
SSSF	sodium solute symporter family
suc	succinate
TCDB	Transporter classification database
TM	transmembrane
TRA	1,2,4-triazolyl alanine
Tris	tris(hydroxymethyl)-aminomethane
V <sub>max</sub>	maximum rate

---

## Summary

The Gram-negative soil bacterium *Pseudomonas putida* KT2440 colonizes the rhizosphere of plants and promotes their growth. It is genetically accessible, solvent-resistant and biosafe and therefore, serves as a platform for industrial biosyntheses (for example, plastic-like polymers and biosurfactants). The bacterium is metabolically extremely versatile and can utilize diverse nutrients as carbon and nitrogen sources. Two-component systems consisting of a sensor kinase and a response regulator play an important role in the adaptation of the cell metabolism to environmental and nutrient conditions. These regulatory systems control, among other things, the expression of genes encoding nutrient-specific transporters. The focus of this thesis is on the two-component system CbrA/CbrB and the transporter HutT of *P. putida* KT2440. CbrA/CbrB is a key regulatory system involved in catabolite repression and control of various catabolic pathways in other pseudomonads. Remarkably, in addition to sensor kinase-typical domains, the sensor kinase CbrA also contains a membrane-integral transporter domain that belongs to the solute:Na<sup>+</sup> symporter family (SSSF). The physiological significance and molecular function of the SSSF domain of CbrA are unknown. HutT is also a protein localized in the cytoplasmic membrane and belongs to the amino acid transporter (AAT) family within the amino acid polyamine organocation (APC) transporter superfamily. The function of HutT in *P. putida* KT2440 has not been studied experimentally before. The task of this thesis was to elucidate the functional properties of CbrA/CbrB and HutT of *P. putida* KT2440.

This investigation confirmed also for *P. putida* KT2440 that the CbrA/CbrB system is involved in catabolite repression by regulating the expression of the small RNA CrcZ. Furthermore, the two-component system controls the catabolism of basic amino acids such as histidine. For biochemical analyses, CbrA and CbrB of *P. putida* KT2440 were produced heterologously in *Escherichia coli* and purified. Experiments with cells and purified proteins revealed that CbrA can bind and transport histidine. The transport was found to be specific for histidine. The inhibition pattern obtained with ionophores suggests an electrochemical proton gradient as the driving force. The kinase domain was not required for the uptake of histidine by the SSSF domain of CbrA and did not significantly affect transport kinetics. In addition, the histidine kinase domain was experimentally shown to autophosphorylate and transfer the phosphoryl group to the response regulator CbrB. The SSSF domain was not essential for these activities but modulated autokinase activity. Phosphatase activity of CbrA was not detectable. None of the phosphotransfer activities are significantly affected by L-histidine. The results indicate that CbrA functions as an L-histidine transporter and sensor kinase in *P. putida* KT2440. For HutT, this thesis showed that deletion of the corresponding gene inhibited the growth of *P. putida* KT2440 on histidine. This suggests that the transporter plays a central role in the uptake of histidine in this bacterium. Transport experiments with cells and purified and reconstituted protein revealed that HutT is a histidine:H<sup>+</sup> symporter. Analyses of histidine

binding and transport kinetics, as well as competition experiments, showed that HutT is highly specific for histidine and binds it with high affinity. Substitutional analyses provided evidence for amino acids possibly involved in substrate binding or coupling of histidine transport to an electrochemical proton gradient.

In summary, the sensor kinase CbrA plays a central role as a metabolic regulator and transports the amino acid histidine in *P. putida* KT2440. The physiological significance of this transport remains unclear. HutT, on the other hand, plays a central role in the uptake of histidine when the amino acid is used as a carbon source.

---

## Zusammenfassung

Das Gram-negative Bodenbakterium *Pseudomonas putida* KT2440 besiedelt die Rhizosphäre von Pflanzen und fördert deren Wachstum. Es ist genetisch zugänglich, lösungsmittelbeständig, und biologisch sicher und dient deshalb als Plattform für industrielle Biosynthesen (zum Beispiel kunststoffähnliche Polymere und Biotenside). Das Bakterium ist metabolisch äusserst versatil und kann vielfältige Nährstoffe als Kohlenstoff- und Stickstoffquelle nutzen. Bei der Anpassung des Stoffwechsels an Umwelt- und Nährstoffbedingungen spielen Zwei-Komponenten-Systeme bestehend aus einer Sensorkinase und einem Antwortregulator eine wichtige Rolle. Diese Regulationssysteme kontrollieren unter anderem die Expression von Genen, die für nährstoffspezifische Transporter kodieren. Im Mittelpunkt dieser Arbeit stehen das Zweikomponenten-System CbrA/CbrB und der Transporter HutT von *P. putida* KT2440. CbrA/CbrB ist ein zentrales regulatorisches System, das in anderen Pseudomonaden unter anderem an der Katabolitrepression und an der Kontrolle verschiedener kataboler Stoffwechselwege beteiligt ist. Bemerkenswert ist, dass die Sensorkinase CbrA neben Sensorkinase-typischen Domänen auch eine membranintegrale Transporterdomäne enthält, die zur Substrat:Na<sup>+</sup>-Symporter-Familie (SSSF) gehört. Physiologische Bedeutung und molekulare Funktion der SSSF-Domäne von CbrA sind nicht bekannt. HutT ist ebenfalls ein in der Zytoplasmamembran lokalisiertes Protein, das innerhalb der Superfamilie der Aminosäure-Polyamin-Organokationen (APC) Transporter zur Aminosäuretransporter (AAT)-Familie gehört. Die Funktion von HutT in *P. putida* KT2440 wurde bisher noch nicht experimentell untersucht. Aufgabe der Arbeit war die Aufklärung der funktionellen Eigenschaften von CbrA/CbrB und HutT von *P. putida* KT2440.

In dieser Arbeit wurde auch für *P. putida* KT2440 nachgewiesen, dass das CbrA/CbrB-System an der Katabolitrepression durch Regulierung der Expression der kleinen RNA CrcZ beteiligt ist. Weiterhin kontrolliert das Zweikomponenten-System den Katabolismus von basischen Aminosäuren wie zum Beispiel L-Histidin. Für biochemische Analysen wurden CbrA und CbrB von *P. putida* KT2440 heterolog in *Escherichia coli* produziert und gereinigt. Untersuchungen mit Zellen und gereinigten Proteinen zeigten, dass CbrA L-Histidin binden und transportieren kann. Der Transport erwies sich als spezifisch für L-Histidin. Das mit Ionophoren erhaltene Inhibitions muster wies auf einen elektrochemischen Protonengradienten als Triebkraft hin. Die Kinasedomäne war für die Aufnahme von L-Histidin durch die SSSF-Domäne von CbrA nicht erforderlich und hatte keinen wesentlichen Einfluss auf die Transportkinetik. Darüber hinaus wurde experimentell nachgewiesen, dass sich die Sensorkinase autophosphoryliert und die Phosphorylgruppe auf den Antwortregulator CbrB überträgt. Die SSSF-Domäne war für diese Aktivitäten nicht essentiell, modulierte aber die Autokinase-Aktivität. Eine Phosphataseaktivität von CbrA war nicht nachweisbar. Keine der Phosphotransferaktivitäten wird durch L-Histidin signifikant beeinflusst. Die Ergebnisse zeigen, dass CbrA als L-Histidin-Transporter und Sensorkinase in *P. putida* KT2440 fungiert.

Für HutT wurde in dieser Arbeit gezeigt, dass die Deletion des entsprechenden Gens das Wachstum von *P. putida* KT2440 auf Histidin inhibiert. Dies deutet darauf hin, dass der Transporter eine zentrale Rolle bei der Aufnahme von Histidin in diesem Bakterium spielt. Transportexperimente mit Zellen und gereinigtem und rekonstituierten Protein ergaben, dass HutT ein Histidin:H<sup>+</sup>-Symporter ist. Analysen von Histidinbindung und Transportkinetik sowie Konkurrenzexperimente zeigten, dass HutT hochspezifisch für Histidin ist und dieses mit hoher Affinität bindet. Durch Substitutionsanalysen wurden Hinweise auf Aminosäuren erhalten, die möglicherweise an der Substratbindung oder der Kopplung an einen elektrochemischen Protonengradienten beteiligt sind.

Zusammenfassend ist festzustellen, dass die Sensorkinase CbrA in *P. putida* KT2440 eine zentrale Rolle als Stoffwechselregulator spielt und die Aminosäure Histidin transportiert. Die physiologische Bedeutung dieses Transports bleibt unklar. HutT hingegen spielt eine zentrale Rolle bei der Aufnahme von Histidin, wenn die Aminosäure als Kohlenstoffquelle genutzt wird.

# Introduction

## 1.1 *Pseudomonas putida* KT2440 as a model organism

*Pseudomonas putida* KT2440 has become an important model organism and a workhorse for the biotechnological industry in the last years [Loeschcke and Thies, 2015], but it has been studied for a much longer time. The genus *Pseudomonas*, was first described rather vaguely in 1894 as “cells with polar organs of motility” by Professor Migula in Karlsruhe [Migula, 1894] (Fig. 1). He also assumed that they form spores, according to what he observed under the microscope, which was later falsified [Palleroni, 2010]. The knowledge about this organism expanded rapidly over the next 127 years until today. As early as 1926, *Pseudomonas*'s remarkable ability to degrade a large variety of organic compounds was found by Louis Edmond den Doreen de Jong [den Dooren de Jong, 1926]. Among the *Pseudomonads* are several strains that were especially well characterized in the past. *P. aeruginosa*, *P. fluorescens*, and *P. putida* are fluorescent *Pseudomonads* that belong to the rRNA group I or *Pseudomonas sensu stricto* [Palleroni, 2010].

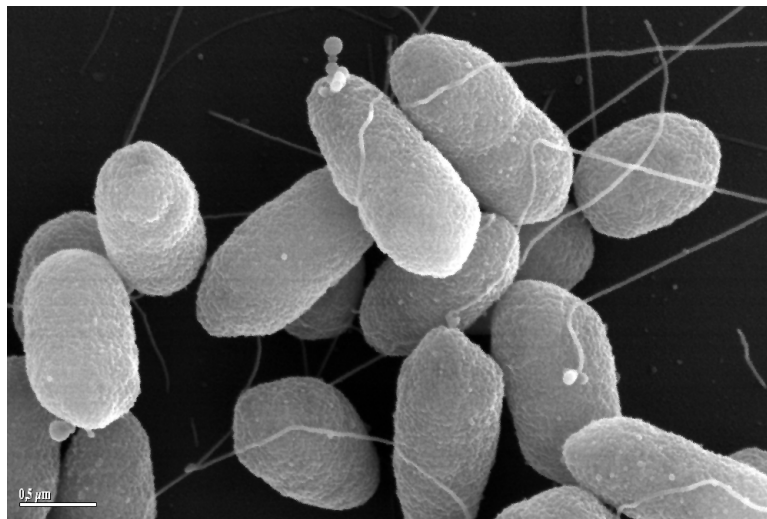


Figure 1: Electron microscopy image of wild type *Pseudomonas putida* KT2440 cells in the exponential growth phase. The polar flagella are clearly visible. Scalebar = 0.5  $\mu$ M. Image provided by Prof. Gerhard Wanner (2005).

The  $\gamma$ -Proteobacterium *P. putida* is an opportunistic bacterium since it can adapt to a great variety of environmental circumstances, including interactions with eukaryotic hosts. Its toolbox contains the ability to use more than one hundred different carbon sources for energy supply and is famous for using compounds that are toxic to most other organisms, like aromatic and aliphatic hydrocarbons [Timmis, 2002]. The original isolate *P. putida* mt-2 from

Japan contains the TOL plasmid pWW0, which encodes a metabolic pathway for toluene and xylene [Regenhardt et al., 2002]. A plasmid-free, restriction negative variant of the strain was described in 1981 and named KT2440 [Bagdasarian et al., 1981]. *P. putida* KT2440 was certified as a biosafety system for gene cloning in 1982 by the Recombinant DNA Advisory Committee [Moore et al., 2006]. First sequenced completely in 2002 [Nelson et al., 2002] and resequenced in 2016 [Belda et al., 2016], *P. putida* KT2440 shares 85% sequence identity of predicted coding regions with *P. aeruginosa* but is non-pathogenic since it is missing key virulence factors [Nelson et al., 2002], while *P. aeruginosa* is often involved in nosocomial infections [Bodey et al., 1983]. Other *Pseudomonads* like *P. syringae* cause plant disease [Silby et al., 2011] and *P. tolaasii* was even shown to cause blotch disease on cultivated mushrooms [Brodey et al., 1991]. *P. putida* KT2440 is not only non-pathogenic but is even known to be beneficial for plant growth, colonizing roots and the rhizosphere of e.g., corn, wheat and strawberry [Espinosa-Urgel et al., 2002].

Today, *P. putida* KT2440 and its rifampicin-resistant variant KT2442 are used as hosts of choice for the analysis, cloning and manipulation of genes from soil bacteria [Timmis, 2002]. The extremely high versatility of *Pseudomonads* is reflected in its ubiquitous dispersion all over the planet in different soils but also in the human body [Silby et al., 2011, Timmis, 2002]. Therefore, it is not surprising that the genome of *P. putida* KT2440 is relatively large with 6.1 Mbp and 5592 coding sequences annotated [Belda et al., 2016, Rodrigue et al., 2000], while almost 10% of the genes encode products that are involved in gene regulation [Moore et al., 2006]. *P. putida* KT2440 possesses around 350 cytoplasmic membrane transport systems to take up or excrete different chemical substances [Nelson et al., 2002]. This large number of transporters and the high level of genetic regulation might explain why the organism can survive in a large variety of environments and utilize compounds that most other organisms consider as toxic.

## 1.2 Regulation of gene expression in *Pseudomonas putida* KT2440

Strict regulation of cellular processes is required to adapt to different environmental circumstances in all prokaryotes. This regulation can happen on different levels in the cell, mainly the transcriptional or translational level. To react fast to environmental cues, such as the availability of nutrients, enables bacterial cells to save energy and efficiently use the available resources. Transcription regulation is usually the most effective way to achieve this goal [Savada et al., 2011]. Several mechanisms of gene regulation that are important for *P. putida* KT2440 will be explained in the following chapters.

### 1.2.1 Histidine sensor kinases

A typical signal transduction system in prokaryotes and also eukaryotes is the two-component system (TCS), consisting of a membrane-bound histidine sensor kinase (HK) and a response regulator (RR) (Fig. 2) [Bretl et al., 2011]. The N-terminal domain of the HK usually senses a signal e.g., binding of a ligand or a physical stimulus. This signal is relayed through conformational changes to the transmitter domain, which results in autophosphorylation of a conserved histidine residue with ATP being the phosphor donor. This orthophosphate ( $\text{H}_3\text{PO}_4^-$ ) is then transferred to a conserved aspartate in the RR that, in turn, causes a cellular response e.g., a change in gene expression [Mascher et al., 2006].

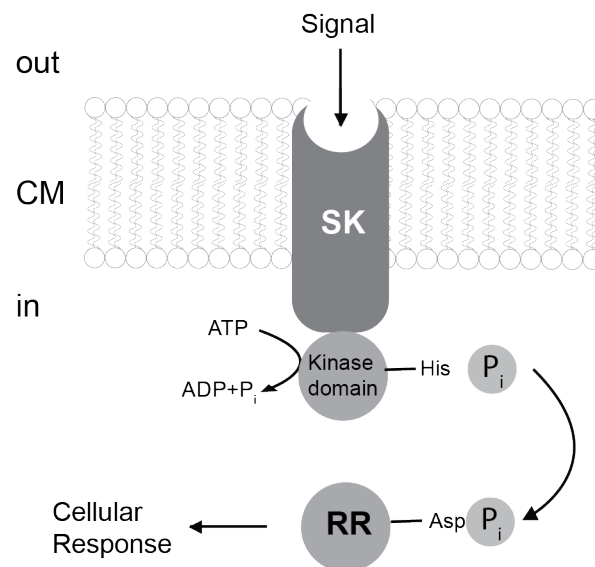


Figure 2: Typical histidine sensor kinase (HK) and response regulator (RR) scheme. The sensor receives an intra- or extracellular signal that leads to autophosphorylation of a conserved histidine residue in the kinase. The phosphor group is transferred to the RR, which leads to a cellular response. Scheme is based on Bretl, Demetriadou and Zahrt (2011). ADP, adenosine diphosphate; Asp, aspartate; ATP, adenosine triphosphate; CM, cytosolic membrane; His, histidine;  $\text{P}_i$ , orthophosphate; SK, sensor domain

In some cases, the kinase can also act as a phosphatase and dephosphorylate the RR [Parkinson, 1993]. The cytoplasmic transmitter or autokinase domains (consisting of DHp = histidine phosphotransfer domain and CA = catalytic ATP binding domain) of HKs are highly conserved while the signal receiving domains vary strongly, allowing for a wide spectrum of recognized signals [Rodrigue et al., 2000]. Many HKs carry an extracellular sensory domain in the periplasm that allows extracellular signals to be transduced to the inside of the cell e.g., CitA in *Klebsiella pneumoniae* senses citrate availability in the periplasm [Kaspar et al., 1999]. This requires transmembrane signal transduction, and consequently, these proteins have several membrane-spanning helices (TMs= transmembrane helices); two to twenty were observed so far [Mascher et al., 2006]. Then again, several kinases have their sensory domain in the intracellular space and receive intracellular signals, like TodS from *Pseudomonas putida* DOT-T1E sensing toluene in the cytosol [Busch et al., 2007].

*P. aeruginosa* is predicted to have 63 HKs and 64 RRs, most of which have homologs in *P. putida* [Nelson et al., 2002, Rodrigue et al., 2000]. This number of TCS is above average for sequenced bacterial genomes, which is about 52 [Cock and Whitworth, 2007, Krell et al., 2010]. This could help explain the ubiquity of *Pseudomonads* and their ability to respond fast to changing environmental circumstances.

### 1.2.2 Carbon catabolite repression

A well-described mechanism in bacteria for efficient use of available nutrients is carbon catabolite repression (CCR). The term describes the general phenomenon in microorganisms that carbon sources are utilized in a hierarchical order beginning with the most preferred one. This entails repression of the expression of genes that encode products needed for the utilization of less preferred carbon sources [Brückner and Titgemeyer, 2002]. The most described example is the diauxic growth of *Escherichia coli* in a medium containing both glucose and lactose as carbon sources. In the presence of glucose, the *lac* operon is repressed, and the preferred sugar glucose is metabolized first [Inada et al., 1996].

In *P. putida* and *P. aeruginosa*, the preferred carbon sources are not sugars but intermediates of the tricarboxylic acid cycle (TCA) like succinate [Rojo, 2010, Valentini et al., 2014]. In *pseudomonads*, CCR is regulated in a cascade involving proteins, small RNAs (sRNAs), and transcriptional regulation (Fig. 3) [Sonnleitner and Haas, 2011]. The master regulator Crc is an RNA-binding protein that, upon binding, blocks the formation of a productive translation initiation complex and therefore prevents translation of its target mRNAs [Hester et al., 2000, Moreno et al., 2007, Rojo, 2010]. Crc, however, can be sequestered by the small RNAs CrcZ and CrcY, allowing the expression of the Crc targets [García-Mauriño et al., 2013]. *crcZ* and *crcY* expression, in turn, is directly regulated by the transcription factor CbrB. The two-component system CbrA/B is a high-ranked element in the *P. putida* metabolic regulation [García-Mauriño et al., 2013, Nishijyo et al., 2001]. Crc regulates the hierarchical usage of amino acids (AAs) as carbon sources e.g., blocking the metabolism of arginine,

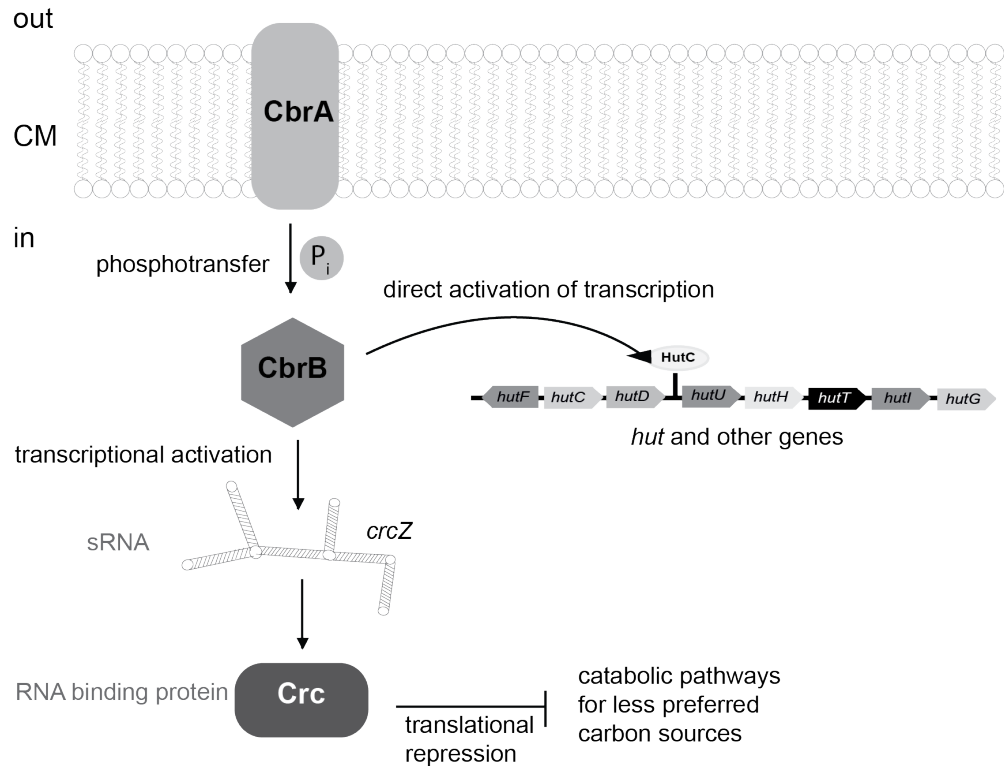


Figure 3: Schematic representation of carbon catabolite repression in *Pseudomonas aeruginosa*. CbrA receives an unknown signal and phosphorylates CbrB, which in turn activates transcription of *crcZ*. The small RNA CrcZ sequesters Crc, which can no longer block translation of genes required for less preferred catabolic pathways. CbrB can also directly activate the expression of target genes e.g., the *hut* gene cluster. When a preferred carbon source is available, CbrA does not become active. Figure based on Sonnleitner and Haas (2011), Zhang (2015) and Bender (2012). CM, cytosolic membrane;  $P_i$ , orthophosphate; sRNA, small RNA

lysine, aspartate, and asparagine, but not inhibiting pathways for proline, alanine, glutamate, glutamine and histidine [Moreno et al., 2009]. CbrA/B (encoded by *cbrA* (PP4695) and *cbrB* (PP4696) is strongly involved in carbon utilization by regulating the RNA-binding protein Crc via the small RNAs CrcZ and CrcY, but also by directly activating the expression of metabolic gene clusters, e.g. the *histidine utilization* (*hut*) genes by binding to  $\sigma_{54}$  dependent promoter regions of non-preferred catabolic pathways and activate transcription [Abdou et al., 2011, Barroso et al., 2018]. The direct binding of promoters by CbrB appears to be an alternative or addition to regulation via Crc as in the case of histidine utilization.

### 1.2.3 Histidine utilization is tightly controlled

The utilization of histidine in *Pseudomonads* requires several regulatory mechanisms to work in concert for the efficient transcription of the histidine utilization (*hut*) genes. Despite some differences, the *hut*-operons in *Pseudomonads* are organized in a very similar way.

The *hut* cluster in *P. putida* is transcribed in three or possibly four transcriptional units (Fig. 4a) [Hu and Phillips, 1988a], whereby *hutF* (PP5036), encoding the formiminoglutamate deiminase (FIGdeiminase), is the first gene of the cluster and is transcribed leftwards [Hu and Phillips, 1988b]. The genes *hutC* (PP5035) and *hutD* (PP5034), encoding regulatory proteins, are transcribed rightwards [Allison and Phillips, 1990, Hu et al., 1989]. The biggest operon is made up of *hutU* (PP5033) (encoding an urocanase), *hutH* (PP5032) (encoding a histidase), *hutT* (PP5031) (encoding a histidine permease), *hutI* (PP5030) (encoding an imidazolone propionate hydrolase = IPase) and *hutG* (PP5029) (encoding a formylglutamate hydrolase = FGase) [Allison and Phillips, 1990, Hu and Phillips, 1988b]. It appears that *hutG* can also be transcribed separately, which would make up the 4th transcriptional unit, although its promoter is unknown [Bender, 2012, Hu and Phillips, 1988a]. In *P. fluorescens* and *P. aeruginosa*, the *hut*-operons are arranged similarly, except several insertions of other genes encoding putative permeases and ABC transporters (*hutT<sub>u</sub>* and *hutXWV*), that cannot replace *hutT* regarding growth on histidine as C- or N-source [Zhang and Rainey, 2007]. Homologs of these genes can be found in *P. putida* in other regions of the chromosomal genome (pp\_3558-pp\_3560).

The metabolic utilization of histidine is well studied and understood (Fig. 4b) and consists of two conserved pathways, one of which applies for *Pseudomonas* species [Kendrick and Wheelis, 1982, Tabor and Hayaishi, 1952]. Pathway one yields two moles ammonia, one mole formate and one mole glutamate per mole histidine, resulting in one more mole of usable nitrogen than the other pathway (pathway 2) that is found in other species. Glutamate can then either be used for biosynthesis of proteins or be further degraded for ATP generation [Zhang and Rainey, 2007]. When Pathway two is used e.g., in *Bacillus* or *Klebsiella*, in the final step FIG, instead of FG, is hydrolyzed, which results in formamide and glutamate [Bender, 2012]. The first three steps of the pathway are common to all known pathways for histidine degradation, even in humans [Reitzer, 2005].

The regulation of the *hut*-operon is well characterized. Histidine is a metabolically expensive amino acid, since its biosynthesis requires more energy than all other amino acids except tryptophane and tyrosine [Akashi and Gojobori, 2002]. Therefore it makes sense that its degradation is tightly controlled. Several proteins (HutC, CbrA/B, and NtrB/C) play an essential role in different situations that the bacteria might face. Transcription of the *hut* genes depends on induction, carbon catabolite repression and nitrogen limitation in *P. putida* [Bender, 2012], with HutC acting as a repressor that binds to conserved sites in the *hut* cluster e.g., in front of the *hutUHIG* promoter when histidine utilization is not required [Zhang and

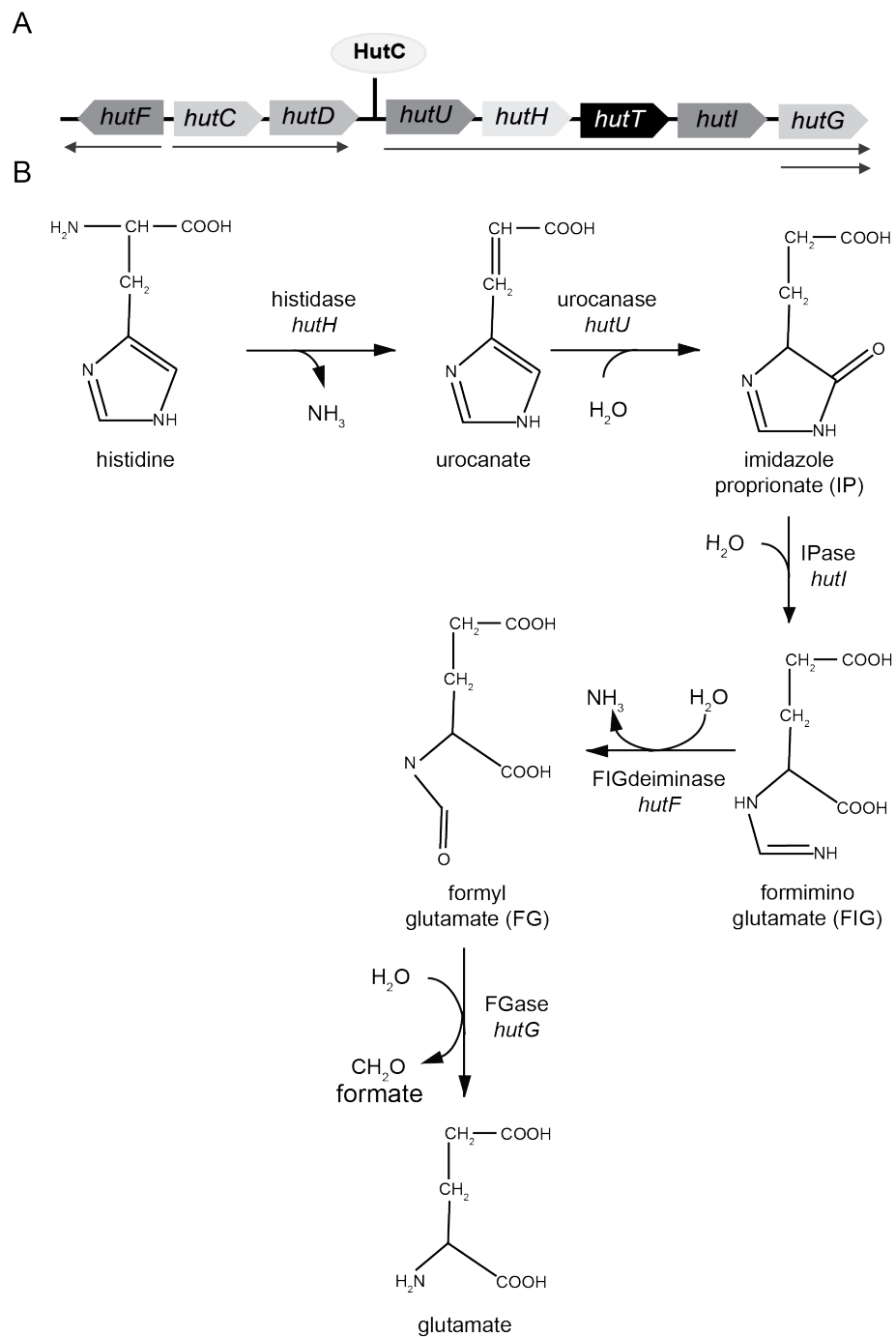


Figure 4: The histidine utilization (*hut*) operon and the histidine degradation pathway. (A) The *hut* genes are organized in three or possibly four operons. The binding site of repressor HutC lies in front of *hutUHTIG*. (B) *P. putida* uses a histidine degradation pathway that yields 3 moles of usable nitrogen per mole histidine. Figure based on Bender (2012)

Rainey, 2007]. Only in the presence of the inducer urocanate, the repression is relieved, and the genes can be transcribed [Allison and Phillips, 1990]. Recently, the binding of HutC to the

promoter region in front of *hutU* was proven via electrophoretic mobility shift assay (EMSA) in *P. fluorescens* [Naren and Zhang, 2020]. The same study could show that HutC not only regulates the *hut* genes but plays global regulatory roles beyond histidine catabolism, by binding with low affinity to other operator sites. The function of the relatively small protein HutD is not entirely understood, but it might play a role in limiting overexpression [Zhang and Rainey, 2007]. Recently, the structure of HutD from *P. fluorescens* was solved, revealing that it is a bicupin protein, possibly binding the pathway intermediate (FG) as a ligand [Gerth et al., 2017].

In *P. aeruginosa* and *P. fluorescens*, a strongly conserved binding site for CbrB can be found in the upstream region of *hutU* (TGTTACCGAA) [Abdou et al., 2011, Bender, 2012, Itoh et al., 2007]. A similar motif is described upstream of other targets of CbrB, including *crcZ* and *crcY* in *P. aeruginosa*, *P. fluorescens*, and *P. putida* [Abdou et al., 2011, Barroso et al., 2018, García-Mauriño et al., 2013]. Interestingly, this conserved binding site for CbrB is missing in the *hut-operon* of *P. putida*. It is unknown if CbrB binds to a different promoter site or if the regulation takes place differently in this case. In addition to induction by urocanate via HutC, nitrogen availability plays a role in the regulation of the *hut-operon*. When histidine is utilized as the sole nitrogen source, the *hut* genes in *P. fluorescens* can be activated by either CbrA/B or NtrB/C [Zhang and Rainey, 2008]. In *Pseudomonas*, the interplay of different regulatory mechanisms is required for optimal utilization of histidine as a carbon or nitrogen source.

The *hut* genes are broadly conserved between  $\gamma$ -Proteobacteria, also other bacteria and, to a lesser extent, archaea and eukaryotes [Bender, 2012].

The next chapter will focus on mechanisms needed to transport the substrates (e.g., histidine) into the cytoplasmic space.

## 1.3 Membrane transport mechanisms

Biological membranes make up the osmotic barriers that separate all living cells from their surroundings and control which molecules can enter into the cellular cytoplasm [Mitchell, 1991]. The lipid bilayer prevents any charged ions and hydrophilic substrates from passage. Proteins that are integral to the membrane have hydrophobic transmembrane domains and often hydrophilic domains sticking out of the lipid bilayer. The integral membrane proteins enable the controlled transport of substrates inside and out of cells. They are essential for all pro- and eukaryotic cells, which is illustrated by the fact that in sequenced prokaryotic genomes, between three and sixteen percent of open reading frames (ORFs) are predicted to be membrane transport proteins [Ren and Paulsen, 2007]. *Pseudomonas putida* KT2440 possesses approximately 350 cytoplasmic membrane transporters, encoded by approximately six percent of its genes. [Nelson et al., 2002]. Membrane transporters can be classified according to their underlying driving force [Mitchell, 1991], which will be described in the following.

### 1.3.1 Diversity of transport systems

The Transporter Classification Database (TCDB) distinguishes five major types of transporters based on their driving force [Saier et al., 2013]. Channels and pores rely on passive diffusion, whereas electrochemical potential driven transporters, primary active transporters, and group translocators rely on active transport against the concentration gradient of the substrate (Fig. 5).

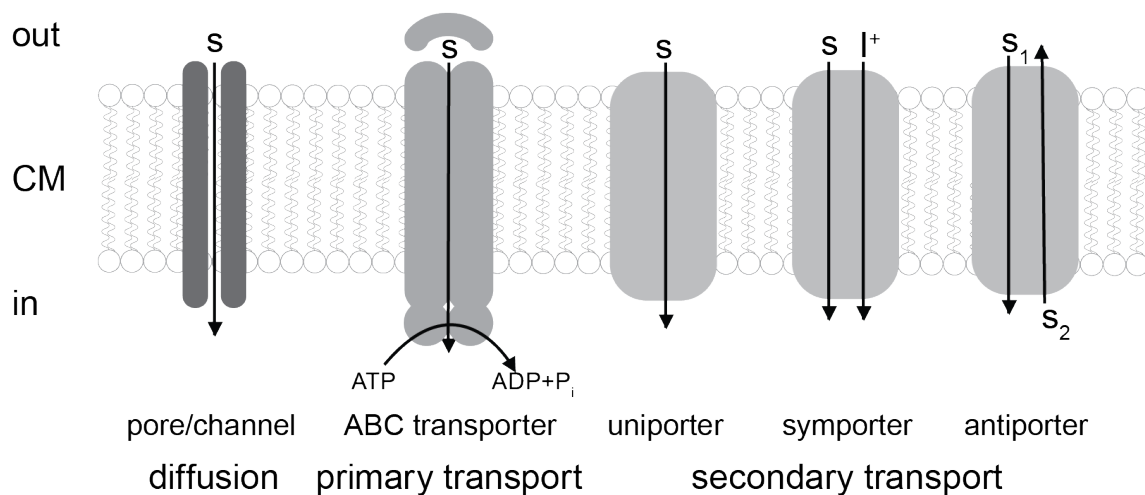


Figure 5: Classes of transport systems. Transporters are classified according to their underlying driving force. Passive substrate translocation can happen through facilitated diffusion via channels or pores. Primary active transporters such as ABC transporters consume ATP. Secondary transporters can be further distinguished by their form of substrate uptake. They all require an electrochemical proton gradient for energetic supply. ABC, ATP-binding cassette; ADP, adenosine diphosphate; ATP, adenosine triphosphate;  $I^+$ , ion;  $P_i$ , orthophosphate; S, substrate.

Nonspecific porins and specific channels are necessary to permit diffusion through the

additional layer of the outer membrane in Gram-negative bacteria. Pores or channels can be coupled to inner membrane transporters with a membrane fusion protein in the periplasmic space, e.g., PvdRT-OpmQ or MdtABC-OpmB involved in pyoverdine secretion in *P. putida* KT2440 with OpmQ and OpmB being the outer membrane porins [Henríquez et al., 2019]. Passive transport, however, can only work until the concentration gradient has been eliminated. For many biological purposes, transport against the concentration gradient is required, which makes active transport under energy consumption necessary. Active transporters can be grouped according to their energy supply. Primary transport proteins use chemical energy supplied by ATP hydrolysis. A well-known example for this type of transport is the sodium-potassium-pump in all animal cells that transports two  $K^+$  in and three  $Na^+$  out of the cell [Savada et al., 2011]. The principle of secondary active transporters is that a substrate can be transported against its concentration gradient when another solute is diffusing along its own gradient and carrying the substrate with it (symporter). Primary pumps can create the necessary ion gradients for secondary transport. The two substrates can also be translocated in opposite directions (antiporter) or a single substrate moves along its own concentration gradient (uniporter) [Mitchell, 1991]. If the secondary source of energy is present in the form of an electrochemical gradient made up of protons or sodium ions, it is termed proton motive force (pmf) or sodium motive force (smf), respectively [Saier, 2000]. There appears to be no relation between substrate and ion specificity [Lolkema et al., 1994]. Transporters have highly diverse substrates and can also be classified accordingly [Saier, 2000]. Secondary transporters are known to take up inorganic ions, sugars, vitamins, and amino acids, among other substrates [Saier, 2000].

Another example of active transport are the group translocators like the phosphotransferase system (PTS), only found in bacteria so far, that is used for sugar uptake, with the source of energy being phosphoenolpyruvate (PEP) [Saier, 2015]. It is a complex mechanism that involves chemical modification of the transported metabolites [Bramley and Kornberg, 1987]. The last group of transporters described in the transporter classification database are electron carriers in the respiratory chain, coupling redox reactions and proton transfer [Saier et al., 2006].

### 1.3.2 The APC-transporter superfamily and the role of the LeuT fold

Amino acid transporters are essential for all organisms since they provide the building blocks of proteins. However, some AAs can also be used as a nutrient source for nitrogen or carbon mainly [Shi, 2013]. Many of these transporters are secondary carriers that rely on the creation of solute gradients by primary pumps [Västermark et al., 2014]. Secondary transporters are often observed to have two duplicated segments in an antiparallel orientation or opposite topology [Vinothkumar and Henderson, 2010], which means the core TM (transmembrane) domains exhibit twofold pseudosymmetry [Shi, 2013]. A common antiparallel fold occurs in many transporters families that are not homologous on the sequence level and have diverse

functions. After LeuT of *Aquifex aeolicus* was structurally characterized [Yamashita et al., 2005], the benzyl-hydantoin:Na<sup>+</sup> transporter Mhp1 from *Microbacterium liquefaciens* [Weyand et al., 2008] and the galactose:Na<sup>+</sup> transporter vSGLT from *Vibrio parahaemolyticus* [Faham et al., 2008] were found to have the same general fold. This core LeuT fold comprises 10 TMs that are organized into two inverted structural repeats, each containing 5 TMs [Shi, 2013]. The first TMs in the two inverted repeats, TMs 1 and 6, consist of two short alpha-helices connected by an unwound segment [Abramson and Wright, 2009], a feature important for the transport mechanism of LeuT-fold transporters [Shi, 2013]. The transporter families that share this fold are grouped in the APC superfamily, which was extended to include 18 families until the present [Shi, 2013, Wong et al., 2012, Västermark et al., 2014]. These include for example the betaine/carnitine/choline transporter (BCCT) family with CaiT [Bracher et al., 2019], the amino acid-polyamine-organocation (APC) family with AdiC [Fang et al., 2009, Gao et al., 2009], GadC [Ma et al., 2012] and HutT [Jack et al., 2000] and the Na<sup>+</sup>:solute symporter (SSS) family with PutP [Jung et al., 2012]. The APC family is the second-largest family of secondary transporters, the MFS (major facilitator superfamily) being the largest. Members of those families like vSGLT (APC) or the well studied LacY (MFS) do not share sequence homology but still operate on a similar basic mechanism [Abramson and Wright, 2021].

The LeuT fold proteins may exist as a monomer, dimer or trimer [Shi, 2013]. Crystal structures obtained from transport proteins can only represent one distinct conformational state, outward-facing, occluded or inward-facing [Li et al., 2015a], confirming that in these proteins the alternating access mechanism is the mode of action [Forrest et al., 2011]. This model was proposed more than sixty years ago by Prof. Oleg Jardetzky [Jardetzky, 1966], who suggested that in order to move substrate across a membrane, a transporter must open to one side of the membrane to load cargo and to the opposite side for cargo release [Shi, 2013]. Computational and experimental analysis revealed that SSS transporters, including LeuT, vSGLT and PutP, have two substrate-binding sites [Li et al., 2015b]. Several TMs are involved in forming the substrate binding site in APC transporters, but TMs 1 and 6 are always involved [Li et al., 2015a]. One or more aromatic amino acids are often present at or adjacent to the substrate-binding sites [Shi, 2013]. Symporters can only function when the binding of substrate is accompanied by the presence of ions that provide the energy [Saier, 2000], as is the case for LeuT, where two Na<sup>+</sup> were found to bind at Na1 and Na2 close to the substrate leucine [Yamashita et al., 2005]. In vSGLT, however, only one Na<sup>+</sup> binding site was present [Watanabe et al., 2010]. Proteins belonging to this family often have additional TMs apart from the core LeuT fold, which have separate functions [Shi, 2013].

Interestingly, not all APC transporters use a sodium gradient for transport, it can also be proton-coupled transport. The structure of the amino acid transporter ApcT from *Methanocaldococcus jannaschii* revealed that protonation of a lysine in TM5 fulfills the role of Na<sup>+</sup> binding to Na2 in sodium-coupled transporters [Shaffer et al., 2009].

The transporters described above were mostly found and studied in prokaryotes, however, proteins of the APC superfamily are widespread and are also found in eukaryotes and archaea [Jung, 2002]. The SSSF transporter NIS ( $\text{Na}^+:\text{I}^-$  symporter) plays a crucial role in the human thyroid gland and other tissues. SGLT  $\text{Na}^+$ :glucose transporters are essential for health since they are responsible for intestinal glucose absorption and renal glucose reabsorption in humans [Wright et al., 2007]. These and other sugar uptake systems in the duodenum were implicated to play a role in diabetes [Dyer et al., 2002] and the inherited diseases GGM (glucose-galactose malabsorption) and FRG (familial renal glucosuria) are caused by mutations in SGLT 1 and SGLT2 respectively [Melin and Meeuwisse, 1969]. In *Arabidopsis thaliana* AAT1, another APC transporter harboring 14 TMs, was identified as essential for histidine uptake in the plant but can transport other basic amino acids and to a lesser extent, even neutral and acidic ones [Wolf et al., 1995].

## 1.4 Histidine uptake in $\gamma$ -Proteobacteria

Amino acid uptake is essential since all life on this planet is based on 20 amino acids, with two additional ones (pyrrolysine and selenocysteine) for some bacteria and archaea [Copeland, 2005]. The ingested amino acids can be used directly for protein biosynthesis or metabolized as carbon, nitrogen and energy source [Burkovski and Krämer, 2002]. As mentioned before (chapter 1.1), *P. putida* KT2440 is especially efficient in using different carbon sources, among which are amino acids [Timmis, 2002]. One of the substrates that is enough to sustain *P. putida* as a carbon and nitrogen source is histidine [Clarke, 1982, den Dooren de Jong, 1926], whose metabolism is well studied and described in detail in chapter 1.2.3.

It was found in *P. aeruginosa* and zoonotic pathogen *Brucella abortus* that urocanate, the first degradation product of histidine, and HutC, a transcriptional repressor of the *hut* genes, have important functions that promote bacterial infections in hosts [Zhang et al., 2014]. For another  $\gamma$ -Proteobacteria *Acinetobacter baumannii*, which has very similar *hut* genes to *P. putida*, histidine is a crucial nitrogen source during infections and might enable colonization of the lung [Lonergan et al., 2020]. While many  $\gamma$ -Proteobacteria can infect humans and other eukaryotes, some *Pseudomonas* species have beneficial effects on plant growth. Root colonizing bacteria require plant exudates to thrive, among them amino acids like histidine [Phillips et al., 2004, Bacilio-Jiménez et al., 2003, Zhang et al., 2006, Regaiolo et al., 2020].

Naturally, the transport of histidine is in this regard also essential for the  $\gamma$ -Proteobacteria. Histidine transport proteins were well studied in *Salmonella enterica* serovar Typhimurium, where the HisJQMP complex serves as a model for ABC-transporters [Reitzer, 2005]. HisJ is a high-affinity periplasmic binding protein and HisQMP are the membrane components of the system [Ames and Lever, 1970, Ames and Lever, 1972]. Additionally, ArgT (formerly called HisK) can also serve as periplasmic binding protein for the system, but with lower affinity. The secondary transporter AroP that usually catalyzes uptake of aromatic amino acids, like tyrosine, phenylalanine or tryptophan, can also transport histidine to a lesser extent [Ames, 1964].

In several other  $\gamma$ -Proteobacteria, like *Pseudomonas*, however, the *his* genes are not conserved. In these organisms, the main transporter is encoded within the *hut*-cluster, responsible for metabolization of histidine as well [Rietsch et al., 2004]. The deletion of *hutT* in *P. fluorescens* leads to a mutant that is no longer able to grow on histidine as a sole carbon and nitrogen source [Zhang et al., 2006]. HutT is, in contrast to HisJQMP, a secondary transporter, it was originally annotated as *proY* since in *S. typhimurium* it was shown that overexpression of a cryptic gene (*proY*) could compensate deletion of *putP*, encoding the main proline transporter and restore growth on proline [Liao et al., 1997]. ProY of *S. typhimurium* and HutT (pp\_5031) of *P. putida* share 60 % sequence identity on the amino acid level, wherefore HutT is still annotated as ProY in some databases and genome annotations.

### 1.4.1 The APC transporter HutT takes up histidine in *Pseudomonas*

The Amino Acid-Polyamine-Organocation (APC, TCDB 2.A.3) superfamily (see chapter 1.3.2) is the second-largest superfamily of secondary transporters in nature, after the major facilitator superfamily (MFS, TCDB 2.A.1) [Wong et al., 2012]. The APC superfamily has a broad substrate specificity, including many members transporting a variety of amino acids [Västermark et al., 2014]. Examples for amino acid transporters are LysP (lysine transporter from *E. coli*, TCDB 2.A.3.1.2) [Rauschmeier et al., 2014] or HutT (TCDB 2.A.3.1.9) [Rietsch et al., 2004], both belonging to the Amino acid transporter (AAT) subfamily, within the APC family that, in turn, is part of the APC superfamily, according to the transporter classification database. HutT is predicted to have twelve transmembrane domains and, typical for an APC transporter, displays the LeuT fold (TMs 1-10).

HutT's capacity to catalyze histidine uptake was first described in *P. fluorescens*, showing different uptake rates for wild type and  $\Delta hutT$  mutants depending on the carbon source used for cultivation sbw25 [Zhang et al., 2012, Zhang et al., 2015]. Also, it is possible that histidine was metabolized during the course of the experiments. Neither details on the kinetics, the energetic requirements or the specificity of the transporter are provided, nor was HutT analyzed on a biochemical level. A thorough investigation and functional characterization of HutT is therefore still lacking.

Besides HutT, *P. putida* possesses another histidine transporter, CbrA (TCDB 2.A.21.9.1), a protein with a dual function as transporter [Zhang et al., 2015] and histidine sensor kinase [Nishijyo et al., 2001], as mentioned already in chapter 1.2, which will be described in more detail in the following section.

## 1.5 CbrA is a histidine kinase and a SSSF-transporter

In 2001, *P. aeruginosa* PAO1 mutants that cannot utilize histidine or arginine and poorly use other carbon and nitrogen sources, were described by Nishiyo et al. The mutated genes responsible for this phenotype were named *cbrA* (catabolic regulation) and *cbrB*, respectively [Nishijyo et al., 2001]. The first half of the protein CbrA appeared to be a sensor membrane domain, with strong homology to members of the Na<sup>+</sup>:solute symporter family (SSSF, TCDB 2.A.21) (Fig. 6), classifying it as a member of the APC superfamily, that shares the LeuT fold. CbrA has thirteen TMs in total, with the C- and N-terminus located in the cytosol [Sepulveda and Lupas, 2017]. The second half showed homology to the sensor kinase NtrB, while CbrB appeared similar to the response regulator NtrC. CbrA has, with a PAS (Per-Arnt-Sim), DHp (histidine phosphotransfer) and CA (catalytic ATP-binding) domain, the typical features of a sensor kinase and also contains an only recently described STAC (SLC and TCST-Associated Component) domain between the transmembrane and kinase halves [Sepulveda and Lupas, 2017].

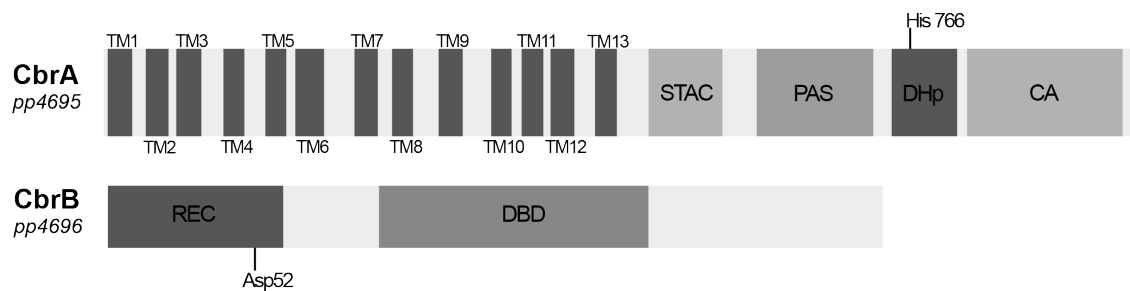


Figure 6: CbrA has 13 transmembrane helices that make up the SSSF transporter-like domain of the protein in the N-terminal half. The C-terminal half contains DHp (histidine phosphotransfer), CA (catalytic ATP-binding) and PAS (Per-Arnt-Sim) domains, typical for a histidine sensor kinase. The two halves are connected by an only recently described STAC (SLC and TCST-Associated Component) domain. CbrB has a REC (receiver) and a DBD (DNA binding domain). Domain prediction relies on SMART [Letunic et al., 2014, Letunic and Bork, 2017] and [Sepulveda and Lupas, 2017]. Scheme was designed with use of DOG 2.0 illustrator [Ren et al., 2009].

Nishiyo *et al.* conclude from their analysis that the two-component system CbrA/B is required for *Pseudomonas* growth on several single carbon sources and they suggest that CbrA/B is needed to maintain a healthy balance between C4-dicarboxylate and ammonia availability [Nishijyo et al., 2001]. Another study that found NtrB/C can partly replace CbrA/B for growth on N-containing compounds, but not TCA-cycle intermediates, corroborates the conclusion that both systems are required for a healthy C/N balance in the cell [Li and Lu, 2007]. Zhang and Rainey first found that CbrB is necessary in *P. fluorescens* for expression of the *histidine utilization (hut)* genes from a  $\sigma^{54}$  (RpoN) dependent promoter when histidine is the only C-source [Zhang and Rainey, 2007]. A short while later, they discovered that transcription from a  $\sigma^{70}$  (RpoD) dependent promoter is possible and relies on either CbrB or

NtrC when histidine is only required as an N-source [Zhang and Rainey, 2008].

In 2009, a major role of CbrA/B was described as regulators of the carbon catabolite repression master protein Crc via the small RNAs *crcZ* and *crcY* in *P. aeruginosa* [Sonnleitner et al., 2009] (see chapter 1.2.2). CbrB can upregulate the transcription of *crcZ* and *crcY* by binding to their respective promoter regions. Higher levels of *crcZ* and *crcY* lead to sequestering of the RNA-binding protein Crc, which then no longer can block the translation of mRNAs required for less preferred nutrients [Sonnleitner and Haas, 2011]. The Crc protein can only carry out its function together with Hfq, a hexameric RNA-binding protein to form stable tripartite complexes with RNA and inhibit translation [Sonnleitner and Bläsi, 2014].

The role of CbrB was further explored in *P. putida*, and its role as a high-ranked regulatory element could be proved. CbrB not only affects the assimilation of amino acids and other carbon sources but also influences chemotaxis, stress tolerance and biofilm formation [Amador et al., 2010]. Zhang et al. confirmed CbrB's role of regulating *crcZ* expression in *P. fluorescens* by recruiting the  $\sigma^{54}$  holoenzyme and showed that CbrB can initiate transcription of *pcnB*, a poly(A)polymerase gene involved in polyadenylation of RNA from a  $\sigma^{70}$  promoter [Zhang et al., 2010]. CbrA/B also controls the metabolization of leucine by regulating the *liu* genes translationally via Crc in *P. aeruginosa* since it is, like histidine, a less preferred carbon source [Díaz-Pérez et al., 2018].

The CbrA/B and Crc/Hfq systems are highly relevant in generally regulating metabolism in the *Pseudomonaceae* family, demonstrated for example by the fact that they control glucose uptake in *Azotobacter vinelandii* through GluP, even though *gluP* is not widely distributed in the *Pseudomonas* genus and the GtsABC sugar ABC transporter is more commonly found [Quiroz-Rocha et al., 2017b]. Another target of CbrA/B in *A. vinelandii* is the production of alginate, a bacterial polymer, since a *cbrA* mutant increased the synthesis by up to 500% [Quiroz-Rocha et al., 2017a].

In the reannotation of the *P. putida* genome, a small peptide encoded upstream and overlapping *cbrA*, named CbrX, was found [Belda et al., 2016] and its role directing the translation of *cbrA* by a mechanism of translational coupling [Monteagudo-Cascales et al., 2019] described. It was also found that levels of CbrA depend on the C-source via carbon catabolite repression and not via autoregulation. Interestingly, it was described in the same publication that a  $\Delta$ TM-CbrA mutant could still grow on histidine as a C-source. This cytosolic variant of CbrA, when overproduced, led to transcriptional activation of the target gene *pp\_2810* suggesting, that CbrA probably detects an intracellular, still unknown, signal, possibly via the PAS domain [Monteagudo-Cascales et al., 2019].

The physiological role of CbrA in signal transduction is fairly well studied and understood in several bacteria, mainly in *Pseudomonas*, and many target genes of the TCS CbrA/B were described.

However, only one publication has reported on the transport function of the SSSF-domain

of CbrA so far. Zhang *et al.* described in 2015 that CbrA catalyzes the uptake of  $^3\text{H}$ -L-histidine in *P. fluorescens* [Zhang et al., 2015] and concluded that CbrA is a constitutive histidine transporter that does not rely on induction, in contrast to HutT [Zhang et al., 2015]. In their experimental setup, however, it is possible that histidine is metabolized during the time of the experiment, which is the reason why the kinetic parameters given might not be accurate. Details on the specificity and the energetic requirements of CbrA catalyzed histidine uptake are not given. Additionally, the signal transduction cascade is not completely understood. Phosphorylation of CbrA and transfer of the phosphate to CbrB were never shown. It is still unclear why the SSSF domain and HK domain are combined in one large polypeptide and what signal is recognized by CbrA.

## 1.6 Aim of this work

The Na<sup>+</sup>:solute symporter (SSS) family is part of the APC superfamily and comprises integral membrane transport proteins that use an electrochemical sodium gradient to drive the uptake of various organic and inorganic solutes into cells [Jung, 2002]. CbrA was first described in 2002 as a representative of an unusual type of sensor kinases [Nishijyo et al., 2001]. These kinases are characterized by an N-terminal domain similar to members of the SSS family at the structural level, while the C-terminal domain is a histidine sensor kinase. The physiological role of CbrA as a sensor kinase is fairly well understood, as described in chapter 1.5.

However, it is unknown why these two seemingly unrelated domains are combined in one large protein. Therefore, the first aim of this thesis was to investigate the functional properties of the individual domains of CbrA. A thorough biochemical study should give insights into the molecular mechanism of function of CbrA. For this purpose, truncated variants of CbrA were planned to be analyzed and compared to wild type CbrA. I have attempted to determine the kinase and phosphatase activity of CbrA and CbrA variants in membrane vesicles and with purified protein using <sup>32</sup>P-ATP. Also, the transport function of CbrA was to be characterized thoroughly *in vivo* in the native *P. putida* strain using <sup>3</sup>H-L-histidine as the substrate. The results describing the transport and kinase activities of CbrA are given in chapter 2.

The analysis of CbrA as a histidine uptake system in *P. putida* led to the realization that it plays only a minor role in the efficient transport of histidine and mainly functions as a major regulator of metabolism together with the response regulator CbrB. The main histidine transporter is HutT, another member of the APC superfamily, belonging to the APC family and not the SSS family [Zhang et al., 2006]. The utilization of histidine as a nutrient source was characterized before (chapter 1.2.3), as well as the regulation of the *hut* genes. However, a functional characterization of HutT of *P. putida* was never performed. Therefore, HutT's role in transporting histidine was to be analyzed in the native *P. putida* and in *E. coli*. In addition, the task was to purify and reconstitute membrane protein into proteoliposomes for further analysis. Amino acid residues important for function were of interest. For this purpose, amino acids conserved within the APC family should be identified by sequence comparisons. These should be individually substituted and the resulting protein variants functionally analyzed. A characterization of HutT is presented in chapter 3.

From these experiments, we expected to gain new insights into the molecular mechanisms of regulation of histidine metabolism and transport in *P. putida* KT2440 were investigated in-depth in this thesis. Finally, a comprehensive review of SSSF-dependent sensor kinases sums up the current knowledge on the versatile functions of this unusual protein family (chapter 4). The task was to describe the diversity of SSSF transporters and their physiological role. Furthermore, the occurrence of sensor kinases that have an N-terminal SSSF domain was to be investigated. The role and functionality of CbrA and CrbS (MexS) were in focus since they are the most studied representatives of this family.

# Transport and kinase activities of CbrA of *Pseudomonas putida* KT2440

This research was originally published in *Scientific Reports* in March 2020.

**Larissa Wirtz**, Michelle Eder, Kerstin Schipper, Stefanie Rohrer and Heinrich Jung. Transport and kinase activities of CbrA of *Pseudomonas putida* KT2440 *Sci Rep* **10**, 5400.

<https://doi.org/10.1038/s41598-020-62337-9>

OPEN

# Transport and kinase activities of CbrA of *Pseudomonas putida* KT2440

Larissa Wirtz<sup>1</sup>, Michelle Eder<sup>1</sup>, Kerstin Schipper<sup>1,2</sup>, Stefanie Rohrer<sup>1,3</sup> & Heinrich Jung<sup>1\*</sup>

The CbrA/CbrB system is a two-component signal transduction system known to participate in the regulation of the cellular carbon/nitrogen balance and to play a central role in carbon catabolite repression in *Pseudomonas* species. CbrA is composed of a domain with similarity to proteins of the solute/sodium symporter family (SLC5) and domains typically found in bacterial sensor kinases. Here, the functional properties of the sensor kinase CbrA and its domains are analyzed at the molecular level using the system of the soil bacterium *P. putida* KT2440 as a model. It is demonstrated that CbrA can bind and transport L-histidine. Transport is specific for L-histidine and probably driven by an electrochemical proton gradient. The kinase domain is not required for L-histidine uptake by the SLC5 domain of CbrA, and has no significant impact on transport kinetics. Furthermore, it is shown that the histidine kinase can autophosphorylate and transfer the phosphoryl group to the response regulator CbrB. The SLC5 domain is not essential for these activities but appears to modulate the autokinase activity. A phosphatase activity of CbrA is not detected. None of the activities is significantly affected by L-histidine. The results demonstrate that CbrA functions as a L-histidine transporter and sensor kinase.

Transporters integral to cytoplasmic membranes usually catalyze the selective uptake of nutrients or the extrusion of metabolic end products and toxic solutes. However, some of these transporters play a central role also in signal transduction<sup>1,2</sup>. In bacteria, so-called trigger transporters (temporarily) interact with membrane components of signal transduction systems and modulate their activity<sup>2</sup>. For example, the lysine transporter LysP allows activation of a CadC-dependent acid stress response only when lysine can be taken up from the environment<sup>3</sup>. The C<sub>4</sub>-dicarboxylate transporter DcuB and the glucose-6-phosphate transporter UhpC interact with histidine kinases of specific two-component systems (TCSs) and stimulate phosphotransfer to the cognate response regulators when the respective substrate is present<sup>1,4</sup>.

While the interaction of transporters with separate signal transductions systems and the functional consequences are relatively well understood, little is known about the role of transporters that are covalently linked to domains typically found in bacterial signaling cascades. Prominent examples are members of the solute/sodium symporter family (SLC5)<sup>5,6</sup>. Besides sodium-motive force-dependent transporters for proline (PutP of archaea and bacteria<sup>7</sup>), monosaccharides (SGLT of bacteria and higher eukaryotes<sup>8</sup>) and others<sup>9–11</sup>, the family contains bacterial proteins in which a complete SLC5 domain is connected via a STAC (SLC5 and TCS Associated Component) domain to domains found in histidine kinases or diguanylate cyclase<sup>5,12,13</sup>. SLC5 transporters fused via STAC to histidine kinase domains are usually associated with response regulators and resemble TCSs. CbrA/CbrB represents such a histidine kinase/response regulator pair<sup>14–16</sup>. The TCS functions as a global metabolic regulator that impacts virulence, biofilm formation, and antibiotic resistance of *Pseudomonas* species<sup>16,17</sup>. More specifically, CbrA/CbrB regulates carbon utilization and together with NtrB/NtrC ensures a balanced carbon/nitrogen relationship<sup>16,18</sup>. Thereby, CbrB can directly regulate expression of different  $\sigma^N$  dependent catabolic pathways, e.g., the *histidine utilization (hut)* operon<sup>18,19</sup>. In addition, CbrA/CbrB is involved in carbon catabolite repression (CCR)<sup>15,20–22</sup>. In the presence of less-favorable substrates (e.g., L-histidine), the phosphorylation cascade of CbrA/CbrB is activated leading to the expression of the small RNAs *crcZ* and *crcY* that in turn bind the CCR protein Crc resulting in an increased translation of Crc target mRNAs<sup>23,24</sup>.

<sup>1</sup>Division of Microbiology, Department of Biology 1, Ludwig Maximilians University Munich, D-82152, Martinsried, Germany. <sup>2</sup>Present address: Institute of Microbiology, Department of Biology, Heinrich-Heine-University, D-40225, Düsseldorf, Germany. <sup>3</sup>Present address: Technical University of Munich, D-80333, Munich, Germany. \*email: [hjung@lmu.de](mailto:hjung@lmu.de)

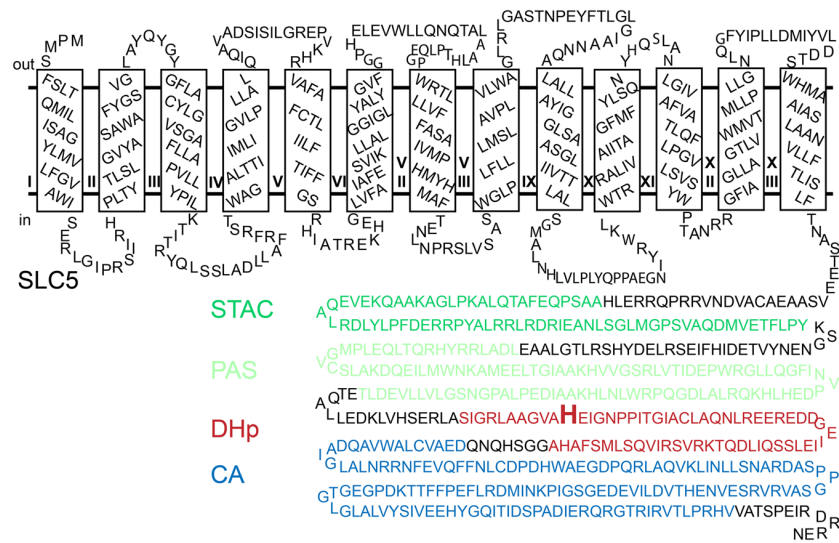


**Figure 1.** Topology model of CbrA of *P. putida* KT2440 showing the domains predicted by Sepulveda and Lupas (2017)<sup>13</sup>. The SLC5 domain (black) entails 13 TMDs connected by hydrophilic loops, a STAC domain (green) connects the SLC5 domain to the cytosolic domain and is followed by the domains PAS (light green), DHp (red) and CA (blue). The predicted phosphorylation site (His766) in the DHp domain is highlighted.

Similar to other bacterial members of the SLC5 family (e.g., the proline/sodium symporter Put<sup>S</sup>), the SLC5 domain of CbrA (about 500 amino acids) consists of 13 transmembrane domains (TMDs) that are connected by short hydrophilic loops (Fig. 1). The cytoplasmic C terminus of the SLC5 domain is covalently linked to the above mentioned STAC domain (72 amino acids). The STAC domain is suggested to mediate interactions with other proteins or control the transport cycle of the SLC5 domain<sup>12</sup>. It follows a PAS domain (about 115 amino acids) that may bind a yet to be identified signal molecule, a dimerization and histidine phosphotransfer domain (DHp, about 65 amino acids), and a catalytic ATP-binding domain CA (about 115 amino acids)<sup>13</sup>. The individual domains are connected by linker sequences (Fig. 1). Upstream of *cbrA* and partially overlapping with the gene, an ORF encoding a small hydrophobic peptide termed CbrX (58 amino acids) is located<sup>25</sup>. Translation of *cbrX* and *cbrA* are coupled, thereby the amino acid sequence of CbrX seems to be unimportant for the stability and function of CbrA<sup>14</sup>.

A mutant of *Pseudomonas fluorescens* SBW25 devoid of known histidine uptake systems was previously shown to grow on L-histidine, and CbrA was identified as being responsible for L-histidine uptake in that strain<sup>26</sup>. These results suggest that CbrA responds to extracellular L-histidine, and that transport and signal transduction are coupled<sup>26</sup>. Later investigations revealed, however, that the histidine kinase can function independently from the SLC5 domain and more likely relies on a not yet identified intracellular signal<sup>13,14</sup>.

Here, we set out to further explore the functional properties and interactions of the individual domains of CbrA in the soil bacterium *Pseudomonas putida* KT2440. For this purpose, we deleted individual domains of CbrA and analyzed the impact of the deletion on the expression of known target genes in *P. putida* KT2440. In addition, we genetically engineered, expressed, and purified individual domains and truncated versions of CbrA and compared the functional properties with wild type CbrA. We demonstrated that the SLC5 domain of CbrA transports L-histidine, and analyzed transport kinetics, substrate specificity, and driving force of the transport process. Furthermore, using <sup>32</sup>P-ATP, we show that CbrA and CbrAΔSLC5 can autophosphorylate at His766 and transfer the phosphoryl group to CbrB. The SLC5 domain is not essential for these activities but appears to modulate the autokinase activity. A phosphatase activity of CbrA or CbrAΔSLC5 leading to dephosphorylation of CbrB-<sup>32</sup>P was not detected. Although CbrA can transport L-histidine, autokinase, phosphotransfer and phosphatase activities are not influenced by the amino acid.

## Results

**The SLC5 domain of CbrA of *P. putida* KT2440 transports L-histidine.** Based on the previous observation that CbrA of *P. fluorescens* SBW25 transports histidine<sup>26</sup>, we set out to test if this is also the case for CbrA of *P. putida* KT2440 and, if so, to further characterize the transport process. For this purpose we generated a strain devoid of *cbrA* and other genes for putative histidine transporters [*hutT* (PP\_5031, encodes the main inducible histidine transporter) and *hutXW* (PP\_3558/PP\_3559, encode a putative periplasmic binding protein and an integral membrane component of a putative ABC transporter)<sup>19</sup>. In addition, *hutH* (PP\_5032) encoding the enzyme for the first step of histidine degradation<sup>19</sup> was deleted. Gene deletions were generated by homologous recombination using the pNPTS138-R6KT suicide vector<sup>27</sup>. The resulting mutant *P. putida* LW1 was transformed with pUCP-Tc-*cbrA* or pUCP-Tc (negative control), *cbrA* expression from the *lac* promoter was induced by IPTG, and uptake of <sup>3</sup>H-L-histidine was analyzed (Fig. 2a). While the strain without *cbrA* transported <sup>3</sup>H-L-histidine with an initial rate of 0.15 ± 0.06 nmol min<sup>-1</sup>mg<sup>-1</sup>, expression of *cbrA* increased the uptake rate about 2fold (0.27 ± 0.09

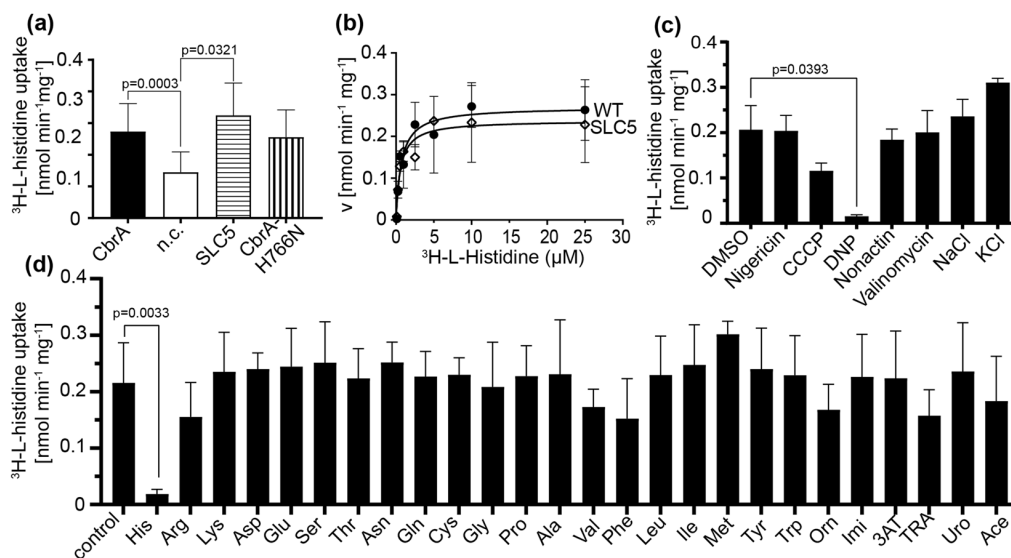


**Figure 2.** Properties of the CbrA-dependent transport of L-histidine. **(a)** Initial rates of  $^3\text{H}$ -L-histidine uptake into cells of *P. putida* LW1 ( $\Delta cbrA \Delta hutTH \Delta hutWX$ ) harboring pUCP-Tc (n.c.), pUCP-Tc-*cbrA*, or pUCP-Tc with given *cbrA* variants. Cells were suspended in 100 mM Tris/MES buffer, pH6.0 ( $\text{OD}_{600} = 5$ ), and transport was initiated by addition of  $^3\text{H}$ -L-histidine at a final concentration of 1  $\mu\text{M}$ . **(b)** Michaelis-Menten kinetics of  $^3\text{H}$ -L-histidine uptake by CbrA and the SLC5 domain of CbrA. Transport was measured as described in **(a)** with substrate concentrations ranging from 0.1 to 25  $\mu\text{M}$ . The initial rate of transport determined at each substrate concentration was corrected for background activity (rate without CbrA or SLC5 domain). Data were fitted and kinetic parameters were determined using GraphPad Prism. **(c)** Effect of ionophores, NaCl, and KCl on the initial rate of  $^3\text{H}$ -L-histidine uptake in cells transformed with pUCP-Tc-*cbrA*. The activity of cells in the presence of the solvent DMSO served as reference for all measurements with ionophores. Activities in the presence of NaCl and KCl were compared with the activities of CbrA shown in **(a)**. **(d)** Analysis of the substrate specificity of CbrA.  $^3\text{H}$ -L-histidine uptake by CbrA was measured as described in **(a)** without additions (control) and in the presence of 100  $\mu\text{M}$  (100fold molar excess) of proteinogenic amino acids, ornithine (Orn), imidazole (Imi), 3-amino-1,2,4-triazole (3AT), 1,2,4-triazolyl-3-alanine (TRA), urocanate (Uro), or acetate (Ace). For all experiments, standard deviations were calculated from minimum three independent experiments. Welch's t-test was applied for statistical analyses.

$\text{nmol min}^{-1} \text{mg}^{-1}$ ). Next, we tested whether the sensor kinase domain is required for the stimulation of  $^3\text{H}$ -L-histidine transport by CbrA. We found that the SLC5 domain alone (amino acids 3 to 544 of CbrA) is sufficient to stimulate transport to about the same extent as the full-length protein. In addition, alteration of the predicted phosphorylation site (His766) in the DHP domain (CbrA-H766N) did not significantly impact the stimulatory effect of CbrA on  $^3\text{H}$ -L-histidine uptake (Fig. 2a).

To obtain more detailed information on the kinetics of  $^3\text{H}$ -L-histidine uptake catalyzed by CbrA and the SLC5 domain, initial rates of transport were determined at substrate concentrations ranging from 0.1 to 25  $\mu\text{M}$ . Transport rates were corrected for background activity (rate without CbrA or SLC5 domain at a given substrate concentration). The resulting transport rates both for CbrA and for the SLC5 domain saturated with increasing substrate concentration, as expected for a transporter-dependent process (Fig. 2b). Data analysis according to Michaelis and Menten yielded apparent  $K_m$  and  $V_{max}$  values of  $0.7 \pm 0.2 \mu\text{M}$  and  $0.27 \pm 0.02 \text{ nmol mg}^{-1} \text{min}^{-1}$  (CbrA), and  $0.58 \pm 0.18 \mu\text{M}$  and  $0.24 \pm 0.02 \text{ nmol mg}^{-1} \text{min}^{-1}$  (SLC5 domain).

Energetic requirements of the CbrA-dependent transport were analyzed by measuring  $^3\text{H}$ -L-histidine uptake into *P. putida* LW1 in the presence of different ionophores and ions (Fig. 2c). Only the proton ionophores carbonyl cyanide *m*-chlorophenyl hydrazine (CCCP) and 2,4-dinitrophenol (DNP) led to an inhibition of the CbrA-dependent transport process. Other ionophores with specificity for potassium and/or sodium (valinomycin, nigericin, nonactin) had no significant impact on transport. Since the SLC5 domain is characteristic for members of the solute/sodium symporter family, we expected sodium to stimulate transport. However, comparison of the transport rates in sodium-free Tris/MES buffer with and without NaCl or KCl did not reveal any significant difference (Fig. 2a,c). Taken together, the results suggest that transport catalyzed by CbrA is an energy-dependent process. While it seems to depend on an (electro)chemical proton gradient, there is no evidence that an (electro)chemical sodium gradient can drive transport.

The substrate specificity of CbrA was tested by recording  $^3\text{H}$ -L-histidine uptake into *P. putida* LW1 transformed with plasmid pUCP-Tc-*cbrA* in the presence of a 100fold molar excess of potential substrates (Fig. 2d). All proteinogenic amino acids were tested, and only L-histidine led to a significant inhibition of the uptake of the  $^3\text{H}$ -labeled substrate. In addition, L-ornithine, imidazole, 3-amino-1,2,4-triazole, 1,2,4-triazolyl-3-alanine, and urocanate did not have significant effects on  $^3\text{H}$ -L-histidine uptake. Also acetate, that is recognized by CrbS<sup>13</sup>, another SLC5-containing sensor kinase of *Pseudomonas* species, had no influence on the transport process. The

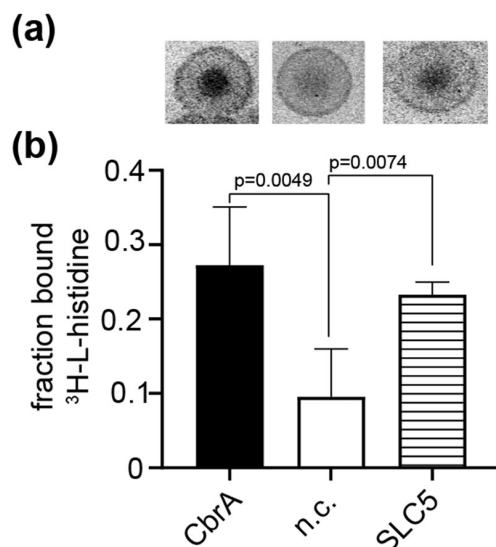


**Figure 3.** Binding of L-histidine to CbrA and the SLC5 domain of CbrA. Membrane vesicles were prepared from *E. coli* C43 containing either full length CbrA, the SLC5 domain, or none of the two proteins (negative control, n.c.). (a) The membrane vesicles were mixed with  $1.35 \mu\text{M}$   $^3\text{H}$ -L-histidine ( $37 \text{ Ci mmol}^{-1}$ ) and spotted on nitrocellulose membranes. Diffusion of radioactivity in the resulting spots was visualized using a tritium screen and a Typhoon scanner. (b) The spots were quantified using ImageJ and the bound fraction of  $^3\text{H}$ -L-histidine was calculated according to Roelofs *et al.*<sup>28</sup>. The error bars represent standard deviation of four experiments. Welch's t-test was applied for statistical analysis.

results suggest that CbrA-catalyzed transport is specific for L-histidine, with the imidazole ring and the carboxyl and amino groups being decisive for binding.

**The domains SLC5 and PAS of CbrA bind L-histidine.** Based on the ability of CbrA to take up  $^3\text{H}$ -L-histidine, we set out to test binding of the amino acid to full-length CbrA, the SLC5 domain and the PAS domain (amino acids 614 to 745 of CbrA). Binding of  $^3\text{H}$ -L-histidine to CbrA and SLC5 domain in membrane vesicles was assessed using the DRaCALA assay<sup>28</sup>. For this purpose, genes encoding the respective proteins were cloned into pET21a, heterologously expressed in *E. coli* C43, and vesicles were prepared. Membranes isolated from *E. coli* C43 transformed with the empty plasmid pET21a served as negative control. The membrane vesicles were mixed with  $1.35 \mu\text{M}$   $^3\text{H}$ -L-histidine ( $37 \text{ Ci mmol}^{-1}$ ) and spotted on nitrocellulose membranes. Diffusion of radioactivity in the resulting spots was visualized using a tritium screen and a Typhoon scanner (Fig. 3a). The observed retention of radioactivity in the center of the spot relative to the negative control was taken as evidence for binding of  $^3\text{H}$ -L-histidine to CbrA and the SLC5 domain (Fig. 3b). When cold L-histidine was added in excess, binding was reduced to the values observed for the negative control (not shown).

To analyze ligand binding to the soluble PAS domain, the respective nucleotide sequence (plus six codons at the 3' end encoding a 12His tag) was cloned into pET21a and expressed in *E. coli* BL21. The protein was purified by Ni-NTA affinity chromatography (Fig. S1a). Ligand binding was analyzed using thermal shift assays. Thereby, the impact of potential ligands on the melting temperature ( $T_m$ ) of the PAS domain was determined with Nano differential scanning fluorimetry (NanoDSF) in a Prometheus (NanoTemper). The method revealed an increase of the  $T_m$  value by  $0.73 \pm 0.13$  °C, when 1 mM L-histidine was added to the protein solution (Fig. S2). The addition of 1 mM of other amino acids, imidazole, urocanate, 3AT or TRA did not affect the  $T_m$  value (Fig. 4a). Next, the effect of L-histidine on the  $T_m$  value was titrated by adding the amino acid at concentrations between 5 and 1667  $\mu\text{M}$ . Plotting of  $\Delta T_m$  against the L-histidine concentration led to a saturation curve and yielded a  $k_d$  value for L-histidine of  $43 \pm 13$   $\mu\text{M}$  (Fig. 4b). These results were verified using a different method to detect the  $T_m$ , by adding SYPRO Orange that binds to hydrophobic regions of the protein (Fig. S3a). The  $k_d$  value for L-histidine determined with this method was  $46 \pm 17$   $\mu\text{M}$  (Fig. S3b).

Taken together, the results suggest that the membrane-integral SLC5 domain as well as the cytosolic PAS domain of CbrA can specifically bind L-histidine.

**Autophosphorylation of CbrA and phosphotransfer to CbrB.** To measure the putative autokinase activity of CbrA, the respective gene was heterologously expressed in *E. coli* TKR2000 (inactive  $F_0F_1$  ATPase)<sup>29</sup>, and membrane vesicles were prepared. Vesicles with CbrA-H766N (putative site of phosphorylation was altered) served as negative control. The vesicles were incubated with  $\gamma$ - $^{32}\text{P}$ -ATP as a phosphate donor, then subjected to SDS-PAGE, and radioactivity was detected using a phosphor screen. Autophosphorylation was observed in 50 mM Tris-HCl, pH7.5 supplemented with 10% glycerol, 10 mM  $\text{MgCl}_2$ , 2 mM dithiothreitol, and 360 mM KCl for wild type CbrA but not for CbrA-H766N (Fig. 5a). Maximum autophosphorylation was achieved within 30 s of incubation. A high concentration of potassium ions (e.g., 360 mM KCl) was required for the autokinase activity

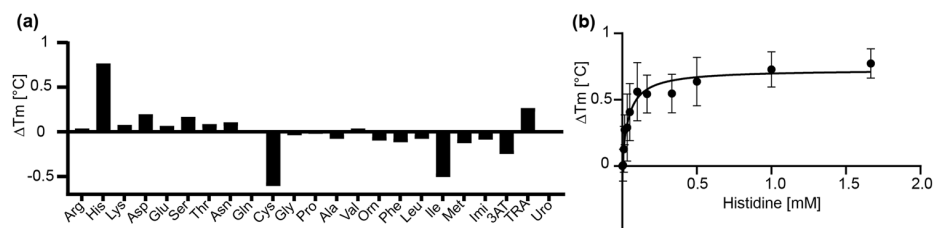


**Figure 4.** Binding of L-histidine to the PAS domain of CbrA. (a) The PAS domain was purified from *E. coli* C43 by Ni-NTA affinity chromatography, and the melting temperature  $T_m$  of the protein ( $170 \mu\text{g ml}^{-1}$  in 100 mM Tris-HCl pH7.5, 100 mM KCl and 10% glycerol) was determined in the presence of 1 mM of given amino acids and related compounds using NanoDSF. (b) The melting temperature  $T_m$  of the PAS domain was determined at given concentrations of L-histidine as described in (a). The error bars represent standard deviations of three experiments. All  $\Delta T_m$  values are minimum 3fold larger than the respective standard deviations. Plotting of  $\Delta T_m$  against the L-histidine concentration yielded a  $k_d$  value for L-histidine of  $43 \pm 13 \mu\text{M}$ .

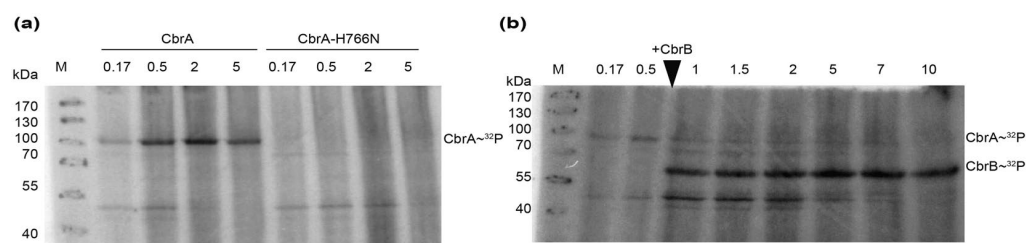


**Figure 5.** Phosphorylation of CbrA and phosphotransfer onto CbrB. (a) *E. coli* TKR2000 membrane vesicles containing either CbrA or CbrA-H766N (in 50 mM Tris-HCl, pH7.5, 10% glycerol, 10 mM  $\text{MgCl}_2$ , 2 mM dithiothreitol, 360 mM KCl) were incubated with  $\gamma\text{-}^{32}\text{P}$ -ATP. The reaction was stopped at given time points (min), and proteins were separated by SDS-PAGE. Radioactive protein bands were visualized using a phosphor screen. (b) Transfer of the phosphoryl group onto purified CbrB that was added after 45 sec of incubation of CbrA in membrane vesicles with  $\gamma\text{-}^{32}\text{P}$ -ATP. CbrA has a predicted size of 109 kDa and CbrB of 54 kDa. Representative gels of three replicates are shown. Complete gels are presented in Fig. S4a,b.

probably to simulate ionic conditions as present in the bacterial cytosol. On the contrary, NaCl did not stimulate autophosphorylation of CbrA.

Next, we tested the capability of CbrA to transfer the phosphoryl group to the response regulator CbrB. For this purpose, *cbrB* (plus six codons at the 3' end encoding a 6His tag) was cloned into pET21a, and expressed in *E. coli* BL21. The protein was purified by Ni-NTA affinity chromatography (Fig. S1b). Purified CbrB was added to the autokinase assay described in the previous paragraph 45 s after its initiation. The experiment revealed that the phosphoryl group was rapidly transferred (within < 15 s) from CbrA to CbrB (Fig. 5b).

Since CbrA was shown to bind L-histidine, we analyzed the impact of the amino acid on the CbrA phosphorylation activities. L-histidine did neither affect the autokinase nor the phosphotransfer activities of CbrA (Fig. S4c,d). The lack of an effect of L-histidine leaves open the possibility that a yet to be identified intracellular metabolite is perceived by CbrA as a signal.

Is the membrane integral transporter domain SLC5 required for the phosphorylation activities of CbrA? To answer the question, the nucleotide sequence encoding only the cytoplasmic domains of CbrA (CbrA $\Delta$ SLC5, amino acids 614 to 992 of CbrA plus twelve codons at the 3' end encoding a 12His tag) was cloned into pET21a and expressed in *E. coli* C41. The soluble protein was purified by Ni-NTA affinity chromatography (Fig. S1c). Purified CbrA $\Delta$ SLC5 (in 50 mM Tris-HCl, pH7.5 supplemented with 10% glycerol, 10 mM  $\text{MgCl}_2$ , 2 mM dithiothreitol, and 360 mM KCl) catalyzed both autophosphorylation and transfer of the phosphoryl group to CbrB indicating that the SLC5 domain is not essential for these activities (Fig. 6a,b). However, while maximum autophosphorylation of wild type CbrA in membrane vesicles occurred within 30 s, soluble CbrA $\Delta$ SLC5 needed about 10 min to reach the maximum value (Fig. 6a). Maximum phosphorylation of CbrB by CbrA $\Delta$ SLC5 was reached within about the same period of time (about 10 min) and was probably limited by the low autokinase activity (Fig. 6b). Although a precise quantitative comparison of the activities of wild type CbrA in *E. coli* TKR2000 membrane vesicles and purified soluble CbrA $\Delta$ SLC5 is not possible because the exact amount of wild type CbrA in the membranes is not known, the results seem to suggest that the SLC5 domain can modulate the autokinase activity of CbrA. Unfortunately, all trials to substitute the membrane vesicles by defined amounts of purified wild type CbrA in detergent or reconstituted into proteoliposomes failed due to the inactivity of the isolated protein under all test conditions. The results suggest that the SLC5 domain is important but not essential for the phosphorylation activities of CbrA.

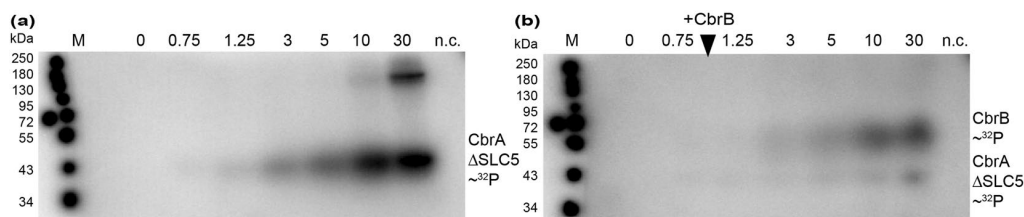


**Figure 6.** Phosphorylation of CbrA $\Delta$ SLC5 and phosphotransfer onto CbrB. (a) Purified CbrA $\Delta$ SLC5 (in 50 mM Tris-HCl, pH7.5, 10% glycerol, 10 mM MgCl<sub>2</sub>, 2 mM dithiothreitol, 360 mM KCl) was incubated with  $\gamma$ -<sup>32</sup>P-ATP. The reaction was stopped at given time points (min), and the protein was separated by SDS-PAGE. Radioactive protein bands were visualized using a phosphor screen. (b) Transfer of the phosphoryl group from CbrA $\Delta$ SLC5 to purified CbrB that was added after 45 sec of incubation with  $\gamma$ -<sup>32</sup>P-ATP. Purified CbrA $\Delta$ SLC5-H766N incubated with CbrB under the same conditions for 10 min served as negative control (n.c.). CbrA $\Delta$ SLC5 has a predicted size of 44 kDa and CbrB of 54 kDa. Representative gels of three replicates are shown. Complete gels are presented in Fig. S5.

**Phosphatase activity of CbrA.** Besides phosphotransfer from sensor kinases, phosphorylation levels of response regulators can be modulated by autophosphorylation by small-molecule phosphodonors such as acetyl phosphate (ACP) and dephosphorylation by sensor kinases<sup>30–32</sup>. To test autophosphorylation of CbrB by ACP and a possible phosphatase activity of CbrA, we synthesized <sup>32</sup>P-ACP from acetic anhydride and <sup>32</sup>P-orthophosphate. <sup>32</sup>P-ACP was then incubated with purified wild type CbrB and CbrB-D52N (Asp52 is the predicted site of phosphorylation) and the time course of phosphorylation was recorded for up to 90 min (Fig. S6). While <sup>32</sup>P labeling of wild type CbrB was visible within 10 min of incubation, phosphorylation of CbrB-D52N was not observed within 90 min indicating that Asp52 is indeed the site of phosphorylation. Before testing a possible phosphatase activity of CbrA, excess of <sup>32</sup>P-ACP was removed from the CbrB-<sup>32</sup>P solution via a HiTrap desalting column. The resulting CbrB-<sup>32</sup>P was incubated without and with CbrA in membrane vesicles prepared from *E. coli* TKR2000 or purified CbrA $\Delta$ SLC5. Typical time courses of the dephosphorylation experiment are shown in Fig. S7. The percentage of radioactivity remaining at CbrB after 10 min of incubation relative to the zero-time point was used as a quantitative measure of dephosphorylation (Fig. S7). CbrB-<sup>32</sup>P without additions was stable for minimum 10 min. Addition of CbrA containing membrane vesicles or of purified CbrA $\Delta$ SLC5 did not significantly stimulate dephosphorylation of CbrB-<sup>32</sup>P, and also the addition of L-histidine had no significant effect (Fig. S7b,e). In conclusion, CbrA did not show a significant phosphatase activity under the conditions of the experiments.

**Significance of the individual domains of CbrA for signal transduction.** To test signal transduction via CbrA/CbrB *in vivo*, a transcriptional reporter gene fusion was generated by fusing the promoter of one of the target genes (*crcZ*<sup>14,15,23</sup>) to the *luxCDABE* operon in plasmid pBBR1-MCS5-*lux*<sup>33</sup>. Genes *cbrA* (and its variants with given deletions) and *cbrB* were cloned into plasmid pUCP-Tc. Furthermore, genes *cbrA* and *cbrB* were individually deleted from the genome of *P. putida* KT2440 by homologous recombination using the suicide vector pMRS101<sup>34</sup>. The resulting mutants were co-transformed with plasmids pBBR1-P<sub>*crcZ*</sub>::*luxCDABE* and pUCP-Tc containing given *cbrA* or *cbrB* variants (Fig. 7a). To test the functionality of the reporter system, cells were grown on different carbon sources, and cell luminescence was determined. Expression of *crcZ* was (partially) repressed when cells were grown in LB medium or M9 minimal containing succinate, a preferred carbon source of *P. putida* (Fig. 7b). Less favorable carbon sources (L-histidine, L-arginine, oxaloacetate) led to maximum expression of *crcZ* as expected for a small RNA sequestering the Crc protein<sup>15</sup> (Fig. 7b). Mutants with a deletion of either *cbrA* or *cbrB* did express *crcZ* only when transformed with pUCP-Tc-*cbrA* or pUCP-Tc-*cbrB* respectively, but not when pUCP-Tc was used (Fig. 7c). These results confirmed the functionality of the reporter system.

Next, we tested the impact of the deletion of individual domains of CbrA on *crcZ* expression with L-histidine as a carbon source (Fig. 7d). Contrary to wild type CbrA, CbrA-H766N did not activate expression of *crcZ* indicating that the conserved histidine in the DHP domain (site of phosphorylation) is essential for signal transduction. Consequently, also the membrane integral domain SLC5 alone did not induce *crcZ* expression. On the contrary, when the SLC5 domain of CbrA was deleted (CbrA $\Delta$ SLC5) or replaced by the SLC5 domain of the homologous sensor kinase CbrS of *P. putida* KT2440 (CbrSA), *crcZ* expression was activated as observed with wild type CbrA. Deletion of the STAC domain (CbrA $\Delta$ STAC) allowed *crcZ* expression but at significantly reduced levels compared to wild type CbrA, while deletion of the PAS domain (CbrA $\Delta$ PAS) had relatively little impact on *crcZ* expression (Fig. 7d).

## Discussion

The TCS CbrA/CbrB is known to participate in the regulation of the cellular carbon/nitrogen balance and to play a central role in carbon catabolite repression of *Pseudomonas* species<sup>22–24,35</sup>. Here, we analyze functional properties of the sensor kinase CbrA and its domains at the molecular level using the system of the soil bacterium *P. putida* KT2440 as a model. In agreement with a previous publication on CbrA of *P. fluorescens*<sup>26</sup>, we demonstrate that CbrA of *P. putida* KT2440 can catalyze the uptake of L-histidine. The apparent  $K_m$  of CbrA for L-histidine is with 0.7  $\mu$ M similar to the  $K_m$  of PutP, another SLC5 family member, for L-proline<sup>36</sup>. The CbrA-dependent maximum rate of L-histidine uptake into cells (0.27 nmol mg<sup>-1</sup> min<sup>-1</sup>) is relatively low but in the same range as the ones detected for other L-histidine transport systems of *Pseudomonas* species<sup>26,37</sup>. In fact, it was previously

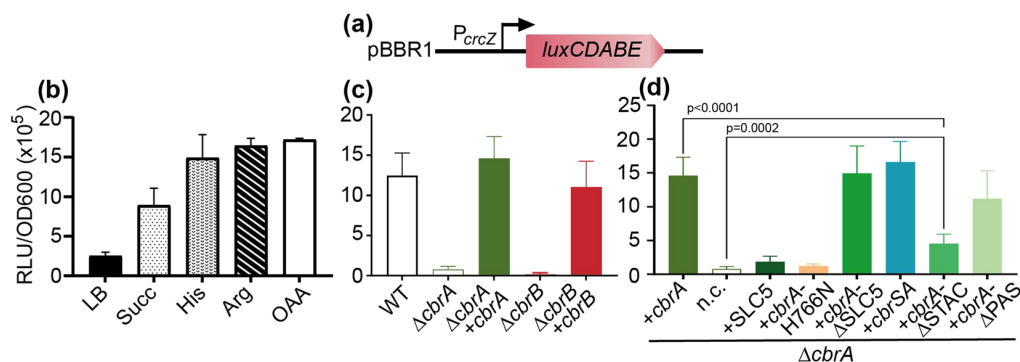


**Figure 7.** Analysis of CbrA/CbrB-dependent signal transduction using a  $P_{crcZ}::luxCDABE$  reporter gene fusion. **(a)** Scheme of the reporter gene fusion  $P_{crcZ}::luxCDABE$  plasmid pBBR1. **(b)** *P. putida* KT2440  $\Delta cbrA$  was co-transformed with plasmids pBBR1- $P_{crcZ}::luxCDABE$  and pUCP-Tc-*cbrA*. Cells were grown in LB medium (LB) or M9 medium supplemented with succinate (Suc), L-histidine (His), L-arginine (Arg), or oxaloacetate (OAA) as carbon sources under aerobic conditions at 30 °C. Luminescence (RLU) and optical density ( $OD_{600}$ ) were recorded over time in a microtiter plate reader. The RLU/ $OD_{600}$  ratios were taken as a measure of *crcZ* expression, and were calculated from values at the beginning of the exponential growth phase. **(c)** Expression of *crcZ* in *P. putida* KT2440 (wild type) and in *cbrA* and *cbrB* mutants. Cells were co-transformed with either pUCP-Tc, pUCP-Tc-*cbrA*, or pUCP-Tc-*cbrB*, and pBBR1- $P_{crcZ}::luxCDABE$ , grown in M9 medium with L-histidine as C-source, and RLU/ $OD_{600}$  ratios were determined as described in **(a)**. **(d)** Expression of *crcZ* in *P. putida* KT2440 ( $\Delta cbrA$ ) transformed with pBBR1- $P_{crcZ}::luxCDABE$  and pUCP-Tc harboring the genetic information for wild type CbrA, the SLC5 domain of CbrA, CbrA-H766N, CbrA $\Delta$ SLC5, the sensor kinase hybrid CbrSA, CbrA $\Delta$ STAC, or CbrA $\Delta$ PAS. Mean values and standard errors were calculated from five independent experiments. All values were significantly different from the n.c. except for SLC5 and CbrA-H766N ( $p \leq 0.0005$ ).

shown that CbrA supports growth of *P. fluorescens* on L-histidine when all other L-histidine transport systems are deleted<sup>26</sup>. Differing from PutP and other members of the SLC5 family, substrate uptake is not stimulated by sodium ions. This finding agrees with the observation that amino acids known to be involved in sodium binding (e.g., Ser340, Thr341 in the middle of transmembrane domain IX of PutP<sup>36</sup>) are not conserved in CbrA. Instead, studies with ionophores suggest that uptake is driven by an electrochemical proton gradient (Fig. 2b). In this case, CbrA would be the first functionally characterized member of the SLC5 family, whose transport activity is not stimulated by an electrochemical sodium gradient. Transport via the SLC5 domain is not affected by alterations in the sensor kinase domains of CbrA (e.g., CbrA-H766N) or by the complete removal of these domains. Similarly, other transporters associated with signal transductions systems (e.g., LysP, DctA, UhpC) were shown to catalyze transport independent of the interaction partner<sup>2,38,39</sup>.

Furthermore, our results suggest that besides the SLC5 domain also the PAS domain of CbrA can bind L-histidine. Both domains seem to be highly specific for L-histidine, and neither other amino acids nor structurally related molecules or degradation products of L-histidine are recognized (Figs. 2d and 4a). This result fits in principle with the concept of a dual-sensing receptor, which is able to detect and respond to both the availability of a substrate in the environment and the intracellular demand for this substrate<sup>40</sup>. However, since the CbrA/CbrB systems regulates the catabolism not only of L-histidine but of many different carbon and nitrogen sources (e.g., L-proline, L-arginine, xylose, mannose)<sup>18</sup>, the strict specificity for L-histidine is hard to understand. Instead, one would rather expect that a central metabolite acts as intracellular signaling molecule. If so, this metabolite has yet to be identified.

We show in *in vitro* experiments that CbrA autophosphorylates at the position of His766, and that the phosphoryl group is transferred to the response regulator CbrB. A CbrA-dependent dephosphorylation of CbrB~P is not observed. Despite the described binding of L-histidine to CbrA, the amino acid does not influence any of the three activities under our *in vitro* conditions. This finding further supports the idea that not L-histidine but a yet untested metabolite regulates the activities of CbrA. However, we cannot exclude that our *in vitro* test conditions do not allow detection of a L-histidine effect that might be relevant for the conditions in *P. putida* KT2440 cells.

The SLC5 domain of CbrA of *P. putida* KT2440 is not required for signal transduction. Neither substitution by the SLC5 domain of the homologous sensor kinase CrbS (regulates acetate utilization<sup>13,40</sup>) (CbrSA) nor complete removal of the SLC5 domain (CbrA $\Delta$ SLC5) have a significant effect on the expression of the CbrA/CbrB target gene *crcZ* (Fig. 7d). Similar results were previously obtained with a CbrSA hybrid of *P. fluorescens*<sup>13</sup>. All the results agree with our finding that CbrA $\Delta$ SLC5 has an autokinase activity and is capable of transferring the phosphoryl group to CbrB (Fig. 6). Nevertheless, a comparison of the time courses of autophosphorylation catalyzed by wild type CbrA and CbrA $\Delta$ SLC5 seems to suggest that the autokinase activity is lower for the latter CbrA variant compared to wild type (Figs. 5 and 6). A reduced (deregulated) autokinase activity may explain the previously observed inhibition of growth on L-histidine of a *P. fluorescens* mutant expressing a *cbrA* $\Delta$ SLC5 variant<sup>26</sup>. Another publication reports that deletion of the “transmembrane domains” of CbrA reduces the expression of the CbrA/CbrB target gene PP\_2810, and that the phenotype is reversed by overexpression of the soluble

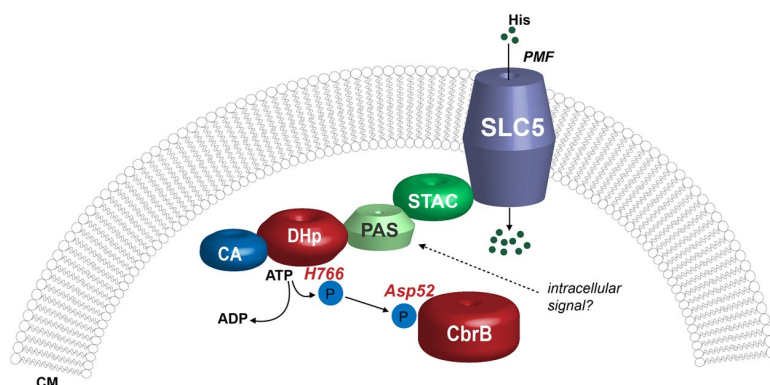


**Figure 8.** Proposed model of CbrA function. The SLC5 domain takes up L-histidine into the cell using an electrochemical proton gradient as driving force. The DHP domain autophosphorylates under ATP consumption at His766, and transfers the phosphoryl group to Asp52 of CbrB. The SLC5 domain may influence the autokinase and phosphotransfer activities. An impact of L-histidine on these activities is not observed. Instead, a yet to be identified intracellular metabolite may be perceived as a signal by the PAS domain. CM, cytoplasmic membrane; PMF, proton motive force (electrochemical proton gradient).

histidine kinase domain<sup>14</sup>. Taken together, all these observations suggest that although physical interactions between the SLC5 domain and the histidine kinase domain are not essential for signal transduction by CbrA, the SLC5 domain modulates the autokinase kinetics of the CbrA/CbrB system.

Furthermore, deletion of the STAC domain has a significant impact on signal transduction, albeit the domain is not essential for the activation of gene expression by the CbrA/CbrB system (Fig. 7d). Since it is assumed that the STAC domain mediates interactions between the SLC5 domain and the sensor kinase domain, the result further supports the idea that the SLC5 domain can modulate the phosphorylation kinetics of CbrA. Surprisingly, deletion of the PAS does not have a significant effect in signal transduction (Fig. 7d). A previous analysis revealed an impact of the PAS domain on CbrA-dependent gene expression<sup>14</sup>. The discrepancy may be explained by the different sizes of the deleted fragments and resulting effects on the remaining protein structure and functionality.

Taken together, we demonstrate here that CbrA of *P. putida* KT2440 can specifically bind and transport L-histidine using an electrochemical proton gradient as a driving force (Fig. 8). The significance of L-histidine for signal transduction remains enigmatic. First experimental evidence is presented suggesting that the transporter domain SLC5 via the STAC domain modulates the kinetics of autophosphorylation catalyzed by CbrA.

## Materials and Methods

**Strains and cultivation conditions.** All strains of *P. putida* and *E. coli* used in this investigation are listed in Table S1. Cells were cultivated aerobically at 30 °C and 37 °C, respectively. When cells were transformed with plasmids, the respective antibiotics were added at the following concentrations: ampicillin/carbenicillin (100 µg ml<sup>-1</sup>), tetracycline (50 µg ml<sup>-1</sup>), gentamycin (30 µg ml<sup>-1</sup>), and kanamycin 50 (µg ml<sup>-1</sup>). For standard cultivation and precultures, LB medium was used (1% tryptone/peptone, 1% NaCl, 0.5% yeast extract). For plates, 1.5% agar was added to the medium and poured into petri dishes. For minimal medium, a M9 salt solution supplemented with 18.7 mM NH<sub>4</sub>Cl, 0.2 mM CaCl<sub>2</sub>, 2 mM MgSO<sub>4</sub>, 2 mM thiamine and 20 mM of the appropriate C-source were used. Additionally, the following trace elements were added: 134 µM Na<sub>2</sub>-EDTA, 31 µM FeCl<sub>3</sub>, 6.2 µM ZnCl<sub>2</sub>, 0.76 µM CuCl<sub>2</sub>, 0.42 µM CoCl<sub>2</sub>, 1.62 µM H<sub>3</sub>Bo<sub>3</sub>, 0.081 µM MnCl<sub>2</sub>.

**Generation of strains and plasmids.** To individually delete *cbrA* (PP\_4695) and *cbrB* (PP\_4696) from the genome of *P. putida* KT2440, the nucleotide sequences flanking these genes (500 base pairs) were cloned up- and downstream of a FRT-kanamycin resistance cassette in the suicide vector pMRS101<sup>34</sup> followed by homologous recombination. Subsequently, the kanamycin resistance cassette was removed from the genome of the resulting mutants with FLP recombinase. *P. putida* KT2440 mutant LW1 ( $\Delta cbrA \Delta hutTH \Delta hutWX$ ) was created by cloning the flanking regions of the respective genes into the suicide vector pNPTS138-R6KT followed by double homologous recombination for insertion into the bacterial chromosomal genome<sup>27</sup>.

For complementation analyses, *cbrA* and its variants encoding CbrA without SLC5, STAC, PAS, or sensor kinase domain were amplified by PCR with primers listed in Table S3, digested with restriction enzymes *NdeI* and *XhoI* and cloned into pUCP-Tc. For overexpression, *cbrB*, *cbrA* or nucleotide sequences encoding individual domains of CbrA and a C-terminal His tag were cloned into pET21a with *NdeI* and *XhoI*. Primers used for amplification by PCR are listed in Table S3. For DNA extraction from agarose gels and purification of PCR products the HiYield<sup>®</sup> PCR Clean-up/Gel Extraction Kit (SLG<sup>®</sup>) was used. Plasmid extraction from 3 ml overnight cultures in LB was performed with the HiYield<sup>®</sup> Plasmid Mini Kit (SLG<sup>®</sup>). All plasmids used are listed in Table S2.

**Luminescence reporter assays.** A *crcZ::luxCDABE* transcriptional reporter gene fusion was generated by PCR amplification of the promoter region of gene *crcZ* with primers P<sub>crcZ</sub>\_BamHI\_s and P<sub>crcZ</sub>\_EcoRI\_as (Table S3) and cloning of the resulting fragment into the *BamHI* and *EcoRI* sites of plasmid pBBR1-*MSC5-lux*<sup>33</sup>. *P. putida* cells with a deletion of either *cbrA* or *cbrB* were co-transformed with plasmids pBBR1-*crcZ::lux* and

pUCP-Tc containing given *cbrA* or *cbrB* variants. One hundred fifty  $\mu\text{l}$  LB or M9 minimal medium containing  $30\ \mu\text{g ml}^{-1}$  gentamycin,  $50\ \mu\text{g ml}^{-1}$  tetracycline and given carbon sources were pipetted per well of black 96well-plates (Corning) and inoculated with the respective *P. putida* strain from an overnight culture (start  $\text{OD}_{600} = 0.1$ ,  $d = 1\ \text{cm}$ ). The plates were incubated shaking at  $30\ ^\circ\text{C}$  for 24–30 h in a CLARIOstar (BMG Labtech).  $\text{OD}_{600}$  and luminescence (RLU, relative light units) were measured every 30 min, and the RLU/ $\text{OD}_{600}$  ratios were determined.

**Whole cell transport measurement.** *P. putida* LW1 containing pUCP-Tc plasmids with variants of *cbrA* were cultivated in LB medium as described and gene expression was induced by adding  $0.5\ \text{mM}$  IPTG at  $\text{OD}_{600} = 0.7$  and continued incubation for 3 h. The cells were harvested and washed in Tris/MES buffer (pH6) and kept on ice. Two hundred  $\mu\text{l}$  aliquots of cell suspension with  $\text{OD}_{600} = 5.0$  were energized with  $10\ \text{mM}$  D-lactate at  $25\ ^\circ\text{C}$  for 10 min. To initiate transport,  $^3\text{H-L-histidine}$  ( $500\ \text{Ci mol}^{-1}$ ) was added to the cell suspension to a final concentration of  $1\ \mu\text{M}$ . After given periods of incubation at  $25\ ^\circ\text{C}$ , uptake was stopped by adding ice-cold stop buffer ( $0.1\ \text{M}$  LiCl,  $0.1\ \text{M}$   $\text{KH}_2\text{PO}_4$ , pH6.0) and rapid filtration through nitrocellulose filters (pore size  $0.4\ \mu\text{m}$ ) with the aid of a vacuum pump. For competition analyses, given compounds (amino acids, L-histidine degradation products) were added simultaneously with  $^3\text{H-L-histidine}$  in 100fold molar excess (final concentration  $100\ \mu\text{M}$ ) to the cell suspension and  $^3\text{H-L-histidine}$  uptake was recorded as described. Ionophores were individually added to the cell suspension at the following final concentrations:  $6\ \mu\text{M}$  nigericin,  $20\ \mu\text{M}$  carbonyl cyanide *m*-chlorophenyl hydrazone (CCCP),  $2\ \text{mM}$  2,4-dinitrophenol (DNP),  $10\ \mu\text{M}$  nonactin,  $2\ \mu\text{M}$  valinomycin. Radioactivity attached to the nitrocellulose filters was detected by liquid scintillation counting using a Tri-Carb 2910TR counter. As a standard,  $1\ \mu\text{l}$  of a  $200\ \mu\text{M}$   $^3\text{H-L-histidine}$  solution ( $500\ \text{Ci mol}^{-1}$ ) was applied. The total protein amount in the cell suspensions was determined by the Peterson Protein assay for whole cells<sup>41</sup>. Transport data were corrected for activity of cells without CbrA (negative control) and plotted according to Michaelis-Menten using GraphPad Prism.

**DRaCALA.** CbrA or CbrA-SLC5 containing membrane vesicles were prepared from *E. coli* C43 heterologously expressing the respective genes from plasmid pET21a upon induction by  $0.5\ \text{mM}$  IPTG. Cells transformed with plasmid pET21a without *cbrA* served for the preparation of the negative control. Cells were disrupted with high pressure ( $1.35\ \text{kbar}$ ) in a Constant Cell Disruptor followed by ultracentrifugation at  $235000\ g$  and washing. Membrane vesicles were resuspended in  $100\ \text{mM}$  KPi buffer pH7.5, and the amount of protein was determined by the Peterson protein assay<sup>41</sup>. For the differential radial capillary action of ligand assay (DRaCALA), the protocol of Roelofs *et al.*<sup>28</sup> was followed.  $^3\text{H-L-histidine}$  (final concentration  $1.35\ \mu\text{M}$ ,  $37\ \text{Ci mmol}^{-1}$ ) was added to the pre-incubated membrane vesicles containing  $27\ \text{mg mL}^{-1}$  total protein, and samples were incubated at  $25\ ^\circ\text{C}$  for 10 min. Five  $\mu\text{l}$  aliquots were subsequently pipetted onto dry nitrocellulose (GE Healthcare) in triplicates. The nitrocellulose was exposed to a Storage Tritium Screen, and a Typhoon Trio Imager (Amersham Biosciences) was used for detection of radioactivity. Analysis of the resulting image was performed with ImageJ.

**Protein purification.** Genes encoding CbrA, CbrA $\Delta$ SLC5, CbrA $\Delta$ SLC5-H766N, CbrA-PAS, or CbrB were expressed from plasmid pET21a in *E. coli* BL21 or C43. For this purpose, an over day preculture was used to inoculate a  $100\ \text{ml}$  overnight culture, which in turn was used to inoculate a  $1\ \text{l}$  culture. Gene expression was induced by adding  $0.5\ \text{mM}$  IPTG at  $\text{OD}_{420} = 1$ . Cells were harvested, washed ( $0.1\ \text{M}$  KPi pH7.5) and the pellets stored at  $-80\ ^\circ\text{C}$  after freezing in liquid nitrogen. All following steps were carried out at  $4\ ^\circ\text{C}$  or on ice. The cells were resuspended in the respective purification buffer ( $0.2\ \text{g mL}^{-1}$ ) and disrupted with high pressure ( $1.35\ \text{kbar}$ ) in a Constant Cell Disruptor. For purification of soluble proteins, the cell lysates were centrifuged first at low speed ( $4500\ g$ ) to remove cell debris and then at high speed to remove the membrane fraction ( $235000\ g$ ). The cytosolic fraction was applied to a HisTrap column on an Äkta system, thoroughly washed with a  $10$ – $50\ \text{mM}$  imidazole gradient and eluted with  $250\ \text{mM}$  imidazole. Alternatively, the same steps were carried out manually on a chromatography column. The purity of the proteins was estimated via Coomassie-stained SDS-PAGE and the identity by Western Blot with a  $\alpha$ -PentaHis Antibody. The protein concentration was measured by the NanoDrop or via Bradford protein assay<sup>42</sup>. The buffer for the cytosolic domain (CbrA $\Delta$ SLC5) contained  $100\ \text{mM}$  Tris-HCl pH7.5,  $100\ \text{mM}$  KCl and  $10\%$  glycerol. The buffer for the PAS domain contained  $100\ \text{mM}$  Tris-HCl pH7.5,  $100\ \text{mM}$  KCl and  $10\%$  glycerol for NanoDSF assays or  $100\ \text{mM}$  KPi buffer pH7.5 and  $20\%$  glycerol for thermal shift assays with SYPRO Orange. The buffer for CbrB contained  $50\ \text{mM}$  Tris-HCl pH7.5,  $100\ \text{mM}$  NaCl and  $5\%$  glycerol.

To isolate wild type CbrA, cell lysates in  $50\ \text{mM}$  Tris-HCl pH7.5,  $300\ \text{mM}$  KCl,  $10\%$  glycerol were centrifuged first at low speed ( $4500\ g$ ) to remove cell debris and then at high speed to ( $235000\ g$ ) at  $4\ ^\circ\text{C}$  to obtain the membranes. The membrane pellet was washed, resuspended in a small volume of  $50\ \text{mM}$  Tris-HCl pH7.5,  $300\ \text{mM}$  KCl,  $10\%$  glycerol and if required stored in aliquots at  $-80\ ^\circ\text{C}$  after shock freezing in liquid nitrogen. The protein amount in the membranes was determined via Peterson Protein assay<sup>41</sup>. The membrane proteins ( $5\ \text{mg mL}^{-1}$  total membrane protein) were solubilized by adding  $1.5\%$  n-dodecyl  $\beta$ -D-maltoside during stirring for 30 min. The membranes were removed by ultracentrifugation ( $113000\ g$ ). The solubilized proteins were mixed with Ni-NTA resin for 45 minutes and packed onto a chromatography column. After washing with imidazole ( $10$  and  $40\ \text{mM}$ ) CbrA was eluted with  $400\ \text{mM}$  imidazole. Purity and concentration were estimated and measured as for soluble proteins. The buffer for CbrA contained  $50\ \text{mM}$  Tris-HCl pH7.5,  $300\ \text{mM}$  KCl,  $10\%$  glycerol and  $0.04\%$  n-dodecyl  $\beta$ -D-maltoside. Imidazole was removed from the purified proteins either via gel filtration or dialysis. Purified CbrA was reconstituted into liposomes prepared from Avanti *E. coli* polar lipid extract at a lipid to protein ratio (w/w) of 50 to 1. Reconstitution was carried out as previously described for *E. coli* PutP<sup>43</sup>.

**Determination of protein melting temperature.** Two separate methods were used to measure the melting temperature ( $T_m$ ) of the purified PAS domain. One method was based on Nano differential scanning

fluorimetry (NanoDSF)<sup>44</sup> and used the Prometheus system from Nanotemper. The latter system recorded the intrinsic tryptophan and tyrosine fluorescence. The ratio of the fluorescence intensities at 350 nm and 330 nm was determined while the temperature was steadily increased from 20 to 95 °C which results in a melting curve. The inflection point of the melting curve is considered as the  $T_m$ . Ligand binding was analyzed by determining the impact of potential ligands on the  $T_m$  value. As a second method, the fluorescent dye SYPRO orange was added to the protein and the fluorescent signal was measured in a real-time PCR instrument (Bio-Rad iCycler5) while the temperature was steadily increased from 10 to 80 °C. The dye binds preferentially to hydrophobic regions resulting in an increase in fluorescence emission while the protein unfolds and hydrophobic parts become exposed<sup>45,46</sup>. The  $\Delta T_m$  is calculated by comparing the  $T_m$  of the respective sample to a control without ligand.

**Autokinase and phosphotransfer activity assays.** Nucleotide sequences encoding CbrA and its variants were heterologously expressed in *E. coli* TKR2000 ( $F_0F_1$  ATPase inactivated)<sup>29</sup> from pBAD24, and membrane vesicles were prepared and suspended in 50 mM Tris-HCl, pH7.5 supplemented with 2 mM DTT, 10 mM  $MgCl_2$ , and 360 mM KCl to yield a final protein concentration of 150–200  $\mu g\ ml^{-1}$ . If indicated, L-histidine was added to a final concentration of 1 mM. Phosphorylation was initiated by adding 20  $\mu M$   $\gamma$ -<sup>32</sup>P-ATP (4760 Ci mol<sup>-1</sup>), 100  $\mu M$   $\gamma$ -<sup>32</sup>P-ATP (956 Ci mol<sup>-1</sup>) or 0.05  $\mu M$   $\gamma$ -<sup>32</sup>P-ATP (3640 Ci mmol<sup>-1</sup>) (Amersham, Bioscience). The samples were incubated at 30 °C and after given periods of time stopped by mixing with 5x SDS-loading dye solution. For the transfer onto the response regulator, purified CbrB (500  $\mu g\ ml^{-1}$ ) was added after 45 s of the incubation of CbrA with  $\gamma$ -<sup>32</sup>P-ATP. All samples were loaded onto a 10% SDS gel and run at 100 V for 3 h. Gels were dried on Whatman paper, wrapped in sticky foil and exposed to a phosphor screen (GE Healthcare) overnight. The screen was scanned in a Typhoon scanner.

**Phosphatase activity assay.** <sup>32</sup>P-ACP was synthesized from <sup>32</sup>P-orthophosphate (Hartmann Analytic) with 2 mCi activity on the reference day (10 mCi ml<sup>-1</sup>). The synthesis was performed as described by Stadtmann (1957)<sup>47</sup>. The amount was measured using the assay by Lipmann and Tuttle<sup>48</sup> and found to be approximately 140  $\mu mol$  in total. The yield was calculated by measuring the CPM of the starting material and the product in a scintillation counter, which enabled us to estimate the specific radioactivity with approximately 12 Ci mol<sup>-1</sup>.

To phosphorylate CbrB, the purified protein was mixed with <sup>32</sup>P-ACP in 50 mM Tris-HCl, pH7.5, 100 mM KCl, 10% glycerol, 20 mM  $MgCl_2$  and incubated at 30 °C. The phosphorylation reaction was terminated at a given time point (usually 60 minutes) by changing the buffer in a desalting column (HiTrap, GE Healthcare) equilibrated with 50 mM Tris-HCl, pH7.5, 360 mM KCl, 2 mM DTT, 10 mM  $MgCl_2$  to remove excess <sup>32</sup>P-ACP. This dilutes the protein 2fold resulting in a final protein amount of ~0.4 mg ml<sup>-1</sup>.

To test the capability to dephosphorylate CbrB~P, CbrA in TKR200 membrane vesicles (3 mg ml<sup>-1</sup>) or purified CbrA $\Delta$ SLC5 (0.38 mg ml<sup>-1</sup>) was added to the CbrB~P solution (0.4 mg ml<sup>-1</sup>) in 50 mM Tris-HCl, pH7.5, 360 mM KCl, 2 mM DTT, 10 mM  $MgCl_2$ . If required 1 mM L-histidine was added to the buffer. The samples were incubated at 30 °C and the reaction terminated by adding 5x SDS loading dye solution. For the control, buffer was added instead of CbrA to test the stability of phosphorylation. The samples were further treated as for the kinase assay.

### Data availability

The data that support the findings of this study are available from the corresponding author upon reasonable request.

Received: 22 January 2020; Accepted: 10 March 2020;

Published online: 25 March 2020

### References

1. Västermark, A. & Saier, M. H. Jr. The involvement of transport proteins in transcriptional and metabolic regulation. *Curr. Opin. Microbiol.* **18**, 8–15, <https://doi.org/10.1016/j.mib.2014.01.002> (2014).
2. Tetsch, L. & Jung, K. The regulatory interplay between membrane-integrated sensors and transport proteins in bacteria. *Mol. Microbiol.* **73**, 982–991, <https://doi.org/10.1111/j.1365-2958.2009.06847.x> (2009).
3. Tetsch, L., Koller, C., Haneburger, I. & Jung, K. The membrane-integrated transcriptional activator CadC of *Escherichia coli* senses lysine indirectly via the interaction with the lysine permease LysP. *Mol. Microbiol.* **67**, 570–583, <https://doi.org/10.1111/j.1365-2958.2007.06070.x> (2008).
4. Unden, G., Wörner, S. & Monzel, C. Cooperation of secondary transporters and sensor kinases in transmembrane signalling: the DctA/DcuS and DcuB/DcuS sensor complexes of *Escherichia coli*. *Adv. Microb. Physiol.* **68**, 139–167, <https://doi.org/10.1016/bb.amps.2016.02.003> (2016).
5. Jung, H. The sodium/substrate symporter family: structural and functional features. *FEBS Lett.* **529**, 73–77 (2002).
6. Reizer, J., Reizer, A. & Saier, M. H. Jr. A functional superfamily of sodium/solute symporters. *Biochim. Biophys. Acta* **1197**, 133–166 (1994).
7. Jung, H., Hilger, D. & Raba, M. The Na<sup>+</sup>/L-proline transporter PutP. *Front. Biosci.* **17**, 745–759, doi:10.2741/ (2012).
8. Ghezzi, C., Loo, D. D. F. & Wright, E. M. Physiology of renal glucose handling via SGLT1, SGLT2 and GLUT2. *Diabetologia* **61**, 2087–2097, <https://doi.org/10.1007/s00125-018-4656-5> (2018).
9. Abramson, J. & Wright, E. M. Structure and function of Na<sup>+</sup>-symporters with inverted repeats. *Curr. Opin. Struct. Biol.* **19**, 425–432 (2009).
10. Quick, M. & Shi, L. In *Vitamins & Hormones* Vol. Volume 98 (ed Litwack Gerald) 63–100 (Academic Press, 2015).
11. Ravera, S., Reyna-Neyra, A., Ferrandino, G., Amzel, L. M. & Carrasco, N. The sodium/Iodide symporter (NIS): molecular physiology and preclinical and clinical applications. *Annu. Rev. Physiol.* **79**, 261–289, <https://doi.org/10.1146/annurev-physiol-022516-034125> (2017).
12. Korycinski, M. *et al.* STAC—a new domain associated with transmembrane solute transport and two-component signal transduction systems. *J. Mol. Biol.* **427**, 3327–3339, <https://doi.org/10.1016/j.jmb.2015.08.017> (2015).
13. Sepulveda, E. & Lupas, A. N. Characterization of the CrbS/R two-component system in *Pseudomonas fluorescens* reveals a new set of genes under its control and a DNA motif required for CrbR-mediated transcriptional activation. *Front. Microbiol.* **8**, 2287, <https://doi.org/10.3389/fmicb.2017.02287> (2017).

14. Monteagudo-Cascales, E., Garcia-Maurino, S. M., Santero, E. & Canosa, I. Unraveling the role of the CbrA histidine kinase in the signal transduction of the CbrAB two-component system in *Pseudomonas putida*. *Sci. Rep.* **9**, 9110, <https://doi.org/10.1038/s41598-019-45554-9> (2019).
15. Valentini, M. *et al.* Hierarchical management of carbon sources is regulated similarly by the CbrA/B systems in *Pseudomonas aeruginosa* and *Pseudomonas putida*. *Microbiology* **160**, 2243–2252, <https://doi.org/10.1099/mic.0.078873-0> (2014).
16. Nishijyo, T., Haas, D. & Itoh, Y. The CbrA-CbrB two-component regulatory system controls the utilization of multiple carbon and nitrogen sources in *Pseudomonas aeruginosa*. *Mol. Microbiol.* **40**, 917–931, <https://doi.org/10.1046/j.1365-2958.2001.02435.x> (2001).
17. Amador, C. I., Canosa, I., Govantes, F. & Santero, E. Lack of CbrB in *Pseudomonas putida* affects not only amino acids metabolism but also different stress responses and biofilm development. *Environ. Microbiol.* **12**, 1748–1761, <https://doi.org/10.1111/j.1462-2920.2010.02254.x> (2010).
18. Zhang, X. X. & Rainey, P. B. Dual involvement of CbrAB and NtrBC in the regulation of histidine utilization in *Pseudomonas fluorescens* SBW25. *Genetics* **178**, 185–195 (2008).
19. Bender, R. A. Regulation of the histidine utilization (*hut*) system in bacteria. *Microbiol. Mol. Biol. Rev.* **76**, 565–584, <https://doi.org/10.1128/MMBR.00014-12> (2012).
20. Filiatrault, M. J. *et al.* CrcZ and CrcX regulate carbon source utilization in *Pseudomonas syringae* pathovar tomato strain DC3000. *RNA Biol.* **10**, 245–255, <https://doi.org/10.4161/rna.23019> (2013).
21. Moreno, R., Fonseca, P. & Rojo, F. Two small RNAs, CrcY and CrcZ, act in concert to sequester the Crc global regulator in *Pseudomonas putida*, modulating catabolite repression. *Mol. Microbiol.* **83**, 24–40, <https://doi.org/10.1111/j.1365-2958.2011.07912.x> (2012).
22. Abdou, L., Chou, H. T., Haas, D. & Lu, C. D. Promoter recognition and activation by the global response regulator CbrB in *Pseudomonas aeruginosa*. *J. Bacteriol.* **193**, 2784–2792, <https://doi.org/10.1128/JB.00164-11> (2011).
23. Sonnleitner, E. & Haas, D. Small RNAs as regulators of primary and secondary metabolism in *Pseudomonas* species. *Appl. Microbiol. Biotechnol.* **91**, 63–79, <https://doi.org/10.1007/s00253-011-3332-1> (2011).
24. Garcia-Maurino, S. M., Perez-Martinez, I., Amador, C. I., Canosa, I. & Santero, E. Transcriptional activation of the CrcZ and CrcY regulatory RNAs by the CbrB response regulator in *Pseudomonas putida*. *Mol. Microbiol.* **89**, 189–205, <https://doi.org/10.1111/mmi.12270> (2013).
25. Belda, E. *et al.* The revisited genome of *Pseudomonas putida* KT2440 enlightens its value as a robust metabolic chassis. *Environ. Microbiol.* **18**, 3403–3424, <https://doi.org/10.1111/1462-2920.13230> (2016).
26. Zhang, X. X., Gauntlett, J. C., Oldenburg, D. G., Cook, G. M. & Rainey, P. B. Role of the transporter-like sensor kinase CbrA in histidine uptake and signal transduction. *J. Bacteriol.* **197**, 2867–2878, <https://doi.org/10.1128/JB.00361-15> (2015).
27. Lassak, J., Henche, A. L., Binnenkade, L. & Thormann, K. M. ArcS, the cognate sensor kinase in an atypical Arc system of *Shewanella oneidensis* MR-1. *Appl. Environ. Microbiol.* **76**, 3263–3274, <https://doi.org/10.1128/AEM.00512-10> (2010).
28. Roelofs, K. G., Wang, J., Sintim, H. O. & Lee, V. T. Differential radial capillary action of ligand assay for high-throughput detection of protein-metabolite interactions. *Proc. Natl. Acad. Sci. USA* **108**, 15528–15533, <https://doi.org/10.1073/pnas.1018949108> (2011).
29. Kollmann, R. & Altendorf, K. ATP-driven potassium transport in right-side-out membrane vesicles via the Kdp system of *Escherichia coli*. *Biochim. Biophys. Acta* **1143**, 62–66, [https://doi.org/10.1016/0005-2728\(93\)90216-3](https://doi.org/10.1016/0005-2728(93)90216-3) (1993).
30. Moscoso, J. A. *et al.* Binding of cyclic di-AMP to the *Staphylococcus aureus* sensor kinase KdpD occurs via the universal stress protein domain and downregulates the expression of the Kdp potassium transporter. *J. Bacteriol.* **198**, 98–110, <https://doi.org/10.1128/JB.00480-15> (2016).
31. Gao, R., Bouillet, S. & Stock, A. M. Structural basis of response regulator function. *Annu. Rev. Microbiol.* **73**, 175–197, <https://doi.org/10.1146/annurev-micro-020518-115931> (2019).
32. Lukat, G. S., McCleary, W. R., Stock, A. M. & Stock, J. B. Phosphorylation of bacterial response regulator proteins by low molecular weight phospho-donors. *Proc. Natl. Acad. Sci. USA* **89**, 718–722, <https://doi.org/10.1073/pnas.89.2.718> (1992).
33. Godeke, J., Heun, M., Bubendorfer, S., Paul, K. & Thormann, K. M. Roles of two *Shewanella oneidensis* MR-1 extracellular endonucleases. *Appl. Environ. Microbiol.* **77**, 5342–5351, <https://doi.org/10.1128/AEM.00643-11> (2011).
34. Sarker, M. R. & Cornelis, G. R. An improved version of suicide vector pKNG101 for gene replacement in gram-negative bacteria. *Mol. Microbiol.* **23**, 410–411, <https://doi.org/10.1046/j.1365-2958.1997.t01-1-00190.x> (1997).
35. Barroso, R. *et al.* The CbrB regulon: Promoter dissection reveals novel insights into the CbrAB expression network in *Pseudomonas putida*. *PLoS One* **13**, e0209191, <https://doi.org/10.1371/journal.pone.0209191> (2018).
36. Hilger, D., Böhm, M., Hackmann, A. & Jung, H. Role of Ser-340 and Thr-341 in transmembrane domain IX of the Na<sup>+</sup>/proline transporter PutP of *Escherichia coli* in ligand binding and transport. *J. Biol. Chem.* **283**, 4921–4929 (2008).
37. Zhang, X. X. *et al.* Variation in transport explains polymorphism of histidine and urocanate utilization in a natural *Pseudomonas* population. *Environ. Microbiol.* **14**, 1941–1951, <https://doi.org/10.1111/j.1462-2920.2011.02692.x> (2012).
38. Janausch, I. G., Zientz, E., Tran, Q. H., Kroger, A. & Unden, G. C4-dicarboxylate carriers and sensors in bacteria. *Biochim. Biophys. Acta* **1553**, 39–56 (2002).
39. Schwoppe, C., Winkler, H. H. & Neuhaus, H. E. Connection of transport and sensing by UhpC, the sensor for external glucose-6-phosphate in *Escherichia coli*. *Eur. J. Biochem.* **270**, 1450–1457 (2003).
40. Jacob, K. *et al.* Regulation of acetyl-CoA synthetase transcription by the CbrS/R two-component system is conserved in genetically diverse environmental pathogens. *PLoS One* **12**, e0177825, <https://doi.org/10.1371/journal.pone.0177825> (2017).
41. Peterson, G. L. A simplification of the protein assay method of Lowry *et al.* which is more generally applicable. *Anal. Biochem.* **83**, 346–356 (1977).
42. Bradford, M. M. A rapid and sensitive method for the quantitation of microgram quantities of protein utilizing the principle of protein-dye binding. *Anal. Biochem.* **72**, 248–254 (1976).
43. Jung, H., Tebbe, S., Schmid, R. & Jung, K. Unidirectional reconstitution and characterization of purified Na<sup>+</sup>/proline transporter of *Escherichia coli*. *Biochemistry* **37**, 11083–11088 (1998).
44. Wen, J., Lord, H., Knutson, N. & Wikström, M. Nano differential scanning fluorimetry for comparability studies of therapeutic proteins. *Anal. Biochem.* **593**, 113583, <https://doi.org/10.1016/j.ab.2020.113581> (2020).
45. Ericsson, U. B., Hallberg, B. M., DeTitta, G. T., Dekker, N. & Nordlund, P. Thermofluor-based high-throughput stability optimization of proteins for structural studies. *Anal. Biochem.* **357**, 289–298, <https://doi.org/10.1016/j.ab.2006.07.027> (2006).
46. Niesen, F. H., Berglund, H. & Vedadi, M. The use of differential scanning fluorimetry to detect ligand interactions that promote protein stability. *Nat. Prot.* **2**, 2212–2221, <https://doi.org/10.1038/nprot.2007.321> (2007).
47. Stadtman, E. R. Preparation and assay of acetyl phosphate. *Methods Enzymol.* **3**, 228–231, [https://doi.org/10.1016/S0076-6879\(57\)03379-0](https://doi.org/10.1016/S0076-6879(57)03379-0) (1957).
48. Lipmann, F. & Tuttle, L. C. The detection of activated carboxyl groups with hydroxylamine as interceptor. *J. Biol. Chem.* **161**, 415 (1945).

## Acknowledgements

Research was supported by the Deutsche Forschungsgemeinschaft, project JU 333/5-2. We thank the former students Heiner Brookmann, Iris Lade and Simon Krauß for their contribution during Bachelor and Diploma thesis projects or research courses.

**Author contributions**

L.W., M.E., S.R. and K.S. generated the strains and plasmids; L.W. and M.E. performed growth curves and reporter assays; L.W. and M.E. performed transport measurements; L.W. performed the DRaCALA; L.W. purified the proteins; L.W. performed thermal shift assays; H.J. and L.W. synthesized the P<sup>32</sup>-ACP; K. S. S. R., L.W. and M.E. performed phosphorylation assays; L.W. and H.J. planned and supervised the experiments; L.W. and H.J. wrote the manuscript. All authors reviewed the results and approved the final version of the manuscript.

**Competing interests**

The authors declare no competing interests.

**Additional information**

**Supplementary information** is available for this paper at <https://doi.org/10.1038/s41598-020-62337-9>.

**Correspondence** and requests for materials should be addressed to H.J.

**Reprints and permissions information** is available at [www.nature.com/reprints](http://www.nature.com/reprints).

**Publisher's note** Springer Nature remains neutral with regard to jurisdictional claims in published maps and institutional affiliations.



**Open Access** This article is licensed under a Creative Commons Attribution 4.0 International License, which permits use, sharing, adaptation, distribution and reproduction in any medium or format, as long as you give appropriate credit to the original author(s) and the source, provide a link to the Creative Commons license, and indicate if changes were made. The images or other third party material in this article are included in the article's Creative Commons license, unless indicated otherwise in a credit line to the material. If material is not included in the article's Creative Commons license and your intended use is not permitted by statutory regulation or exceeds the permitted use, you will need to obtain permission directly from the copyright holder. To view a copy of this license, visit <http://creativecommons.org/licenses/by/4.0/>.

© The Author(s) 2020

## Supplementary Information

### Transport and kinase activities of CbrA of *Pseudomonas putida* KT2440

Larissa Wirtz<sup>1</sup>, Michelle Eder<sup>1</sup>, Kerstin Schipper<sup>1\*</sup>, Stefanie Rohrer<sup>1\*\*</sup> and Heinrich Jung<sup>1‡</sup>

<sup>1</sup>Division of Microbiology, Department of Biology 1, Ludwig Maximilians University  
Munich, D-82152 Martinsried, Germany

‡Correspondence and requests for materials can be addressed to Heinrich Jung,  
[hjung@lmu.de](mailto:hjung@lmu.de)

\*Current address: Institute of Microbiology, Department of Biology, Heinrich-Heine-  
University, D-40225 Düsseldorf, Germany

\*\* Current address: Technical University of Munich, D-80333 Munich, Germany

#### Materials included:

Table S1. Strains used in this investigation.

Table S2. Plasmids used in this investigation.

Table S3. Oligonucleotides used in this investigation.

Figure S1. SDS-PAGE analysis of the courses of purification of CbrA domains and CbrB

Figure S2. Determination of the melting temperature ( $T_m$ ) of CbrA-PAS via nanoDSF.

Figure S3. Determination of the melting temperature ( $T_m$ ) of CbrA-PAS via SYPRO Orange.

Figure S4. Phosphorylation of CbrA and phosphotransfer onto CbrB (complete gels)

Figure S5. Phosphorylation of CbrAΔSLC5 and phosphotransfer onto CbrB (complete gels)

Figure S6. Phosphorylation of CbrB and CbrB-D52N by acetyl phosphate.

Figure S7. Test of a possible CbrA-dependent dephosphorylation of CbrB-<sup>32</sup>P.

Supplementary References

**Table S1.** Strains used in this investigation

Strain	Description	Reference
<i>Escherichia coli</i> BL21(DE3)	<i>E. coli</i> B <i>dcm ompT hsdS(rB-mB) gal</i>	Novagen
<i>Escherichia coli</i> BL21(DE3) pLysS	<i>E. coli</i> B <i>dcm ompT hsdS(rB-mB) gal pLysS Cm<sup>R</sup></i>	Novagen
<i>Escherichia coli</i> C41	<i>E. coli</i> B F <sup>-</sup> <i>ompT gal dcm hsdSB(rB- mB-)(DE3)</i>	Lucigen
<i>Escherichia coli</i> C43	<i>E. coli</i> F <sup>-</sup> <i>ompT gal dcm hsdSB(rB- mB-)(DE3)</i>	Lucigen
<i>Escherichia coli</i> TKR2000	$\Delta kdpFABCDE thi rha lacZ nagA trkA405 trkD1 atp706$	1,2
<i>Pseudomonas putida</i> KT2440	<i>rmo- mod+</i>	<sup>3,4</sup> DSMZ 6125, ATCC 47054
<i>Pseudomonas putida</i> KT2440 $\Delta cbrA$	$\Delta cbrA$	This work
<i>Pseudomonas putida</i> KT2440 $\Delta cbrB$	$\Delta cbrB$	This work
<i>Pseudomonas putida</i> KT2440 LW1	$\Delta cbrA \Delta hutT \Delta hutH \Delta 3558 \Delta 3559$	This work

**Table S2.** Plasmids used in this investigation

Plasmid	Description	Reference
pMRS101	<i>LMBP 3654</i> , suicide vector; <i>ApR, SmR, sacB</i>	<sup>5</sup>
pFLP2	<i>ApR; Flp recombinase, sacB</i>	<sup>6</sup>
pNPTS138-R6KT	<i>mobRP4<sup>+</sup> ori-R6K sacB</i> ; suicide plasmid for in-frame deletions; Km <sup>r</sup> ( <i>npt1</i> )	<sup>7</sup>
pUCP- <i>NdeI</i>	pUCP19 with <i>NdeI</i> restriction enzyme cloning site, Amp <sup>R</sup>	<sup>8</sup>
pUCP- <i>NdeI</i> -Tc <sup>R</sup>	<i>tet</i> in pUCP- <i>NdeI</i> via <i>SspI</i> , Amp <sup>R</sup> , Tc <sup>R</sup>	This work
pUCP <i>cbrB</i> -6his-Tc <sup>R</sup>	<i>cbrB</i> , in pUCP- <i>NdeI</i> -Tc <sup>R</sup> , 6-his-tag, Amp <sup>R</sup> , Tc <sup>R</sup>	This work
pUCP <i>cbrA</i> -6his-Tc <sup>R</sup>	<i>cbrA</i> ( $\Delta 1-6$ ) in pUCP- <i>NdeI</i> -Tc <sup>R</sup> , 6-his-tag, Amp <sup>R</sup> , Tc <sup>R</sup>	This work
pUCP <i>cbrA</i> -SLC5-6his-Tc <sup>R</sup>	<i>cbrA</i> -SLC5 ( $\Delta 1-6, \Delta 1633-2976$ ) in pUCP- <i>NdeI</i> -Tc <sup>R</sup> , 6His tag, Amp <sup>R</sup> , Tc <sup>R</sup>	This work
pUCP <i>cbrA</i> - $\Delta$ SLC5-6his-Tc <sup>R</sup>	<i>cbrA</i> - $\Delta$ SLC5 ( $\Delta 1-1509$ ) in pUCP- <i>NdeI</i> -Tc <sup>R</sup> , 6His tag, Amp <sup>R</sup> , Tc <sup>R</sup>	This work

pUCP <i>cbrA</i> -H766N-6his-Tc <sup>R</sup>	<i>cbrA</i> -H766N ( $\Delta$ 1-6, H766N) in pUCP- <i>Nde</i> I-Tc <sup>R</sup> , 6His tag, Amp <sup>R</sup> , Tc <sup>R</sup>	This work
pUCP-SA-6his-Tc <sup>R</sup>	<i>crbS</i> (1-1598) + <i>cbrA</i> (1539-2976) in pUCP- <i>Nde</i> I-Tc <sup>R</sup> , 6His tag, Amp <sup>R</sup> , Tc <sup>R</sup>	This work
pUCP <i>cbrA</i> - $\Delta$ STAC-6his-Tc <sup>R</sup>	<i>cbrA</i> - $\Delta$ SLC5 ( $\Delta$ 1-6, $\Delta$ 1588-1770) in pUCP- <i>Nde</i> I-Tc <sup>R</sup> , 6His tag, Amp <sup>R</sup> , Tc <sup>R</sup>	This work
pUCP <i>cbrA</i> - $\Delta$ PAS-6his-Tc <sup>R</sup>	<i>cbrA</i> - $\Delta$ SLC5 ( $\Delta$ 1-6, $\Delta$ 1894-2211) in pUCP- <i>Nde</i> I-Tc <sup>R</sup> , 6His tag, Amp <sup>R</sup> , Tc <sup>R</sup>	This work
pET21a	N-terminal T7-tag, C-terminal His-tag, Amp/Carb <sup>R</sup> , lacI	Novagen
p <i>EcbrA</i> -2-12His	<i>cbrA</i> -2 ( $\Delta$ 1-6) in pET21a, C-terminal 12His tag	This work
p <i>EcbrA</i> -2-SLC5-12His	<i>cbrA</i> -2-SLC5 ( $\Delta$ 1-6, $\Delta$ 1632-2976) in pET21a, C-terminal 12His tag	This work
p <i>EcbrA</i> -PAS-12His	<i>cbrA</i> -PAS (1840-2235) in pET21a, C-terminal 12His tag	This work
p <i>EcbrA</i> - $\Delta$ SLC5-12His	<i>cbrA</i> - $\Delta$ SLC5 (1840-2976) in pET21a, C-terminal 12His tag	This work
p <i>EcbrA</i> - $\Delta$ SLC5-12His-H766N	<i>cbrA</i> - $\Delta$ SLC5 (1840-2976, H766N) in pET21a, C-terminal 12His tag	This work
p <i>EcbrB</i> -6His	<i>cbrB</i> in pET21a, C-terminal 6-his-tag	This work
p <i>EcbrB</i> -D52N-6His	<i>cbrB</i> in pET21a (D52N), C-terminal 6His tag	This work
pBAD24	Amp <sup>R</sup> , <i>araC</i> promoter	<sup>9</sup>
p <i>BcbrA</i> -12his	<i>cbrA</i> in pBAD24, 12His tag	This work
pBBR1-MSC5 <i>luxCDABE</i>	<i>luxCDABE</i> and terminators lambda T0 rrnB1 T1 cloned into pBBR1-MCS5 for plasmid-based transcriptional fusions; Gmr	<sup>10,11</sup>
pBBR1- <i>lux</i> -P <sub><i>crcZ</i></sub>	<i>luxCDABE</i> under the control of the <i>crcZ</i> promoter	This work

**Table S3.** Oligonucleotides used in this investigation. Nucleotides marked in red are restriction sites.

Oligonucleotide	Sequence (5'->3')
Del4695A1s	TTACCTGCAGAATT <b>TCGGGCCCC</b> CGTGCAGCCGGA
Del4695A2as	CACCATGAG <b>GGATCC</b> GGCGCTGATCAG
Del4695B1s	CCGAAGACAG <b>TCGACT</b> CATCGAAAGCC
Del4695B2as	TGATCGGGT <b>AAGCTTACTAGT</b> GGGCCACGCCGG

delcbrBA1s	GCCTGCCGAATTCGGGCCCTGCGCGAGGAAC
delcbrBA2as	GACGATGGTACCGTGCGGCATTGA
delcbrBB1s	CRACTGCACGTCGACGCCCTGAAGCTG
delcbrBB2as	TACGGCGGAAAGCTTACTAGTCAGATTTTTACG
Del5031A_s	TTCTGGTGGAATTCGGTGGGGTCAAC
del5032_Bas	TTCCAGGGCGAATTCGCACGTATCTGC
delhutTH_Aas	GCCTGGCACCCCGGTAGCGGAGCCGGCCGAGCTG
delHutTH_Bs	CCGCTACCGGGGTGCCAGGCTTGAGGGTGAGTTCGG
del35589_As_BamHI	GCGCACTCAGGATCCGGTGAAGAAAC
del3558-9_Aas_OL	GCAACGAGGGGTCGACAAAATGGATAGGCG
del3558-9_Bs_OL	CGCCTATCCATTTTGTGACCCCTCGTTGC
del35589_Bas_NheI	TCATAGGCAGCTAGCAGGCTTTCGGCG
PP4696 s	GTCGAGAGAGGATCCCATATGCCGCACATTCTG
PP4696 as	GGCGTGCGAAGCTTAGCTCGAGGCTTCGCTGGTAGCGTT
1935 as	CAGGCAACTATGGATGAACGA
SDcbrBs	GTCCCCGGATCCTCGAGACCGTCGAGAGAATTGAACATATGCC GCACATTC
4695-2 s	ATAGATATGCATATGAGCTTTAGC
4695_6800as	GCGCAGTGCTTGCTCGACTTC
4695_SSF3as	CAGTGCTTGCTCGAGTTCCTTTTGCGC
pE4695_XhoIchange_ as	ATGATGATGGCTCGAGGCATTCTCTCGACG
SSF3 XhoI3	ATGATGGATGGCTCGAGACTTCCTTTTGCGC
CS-long_s_NdeI	GAAGAGGTCCATATGGCCGAAGCCTG
pp4695cs_XhoI_as	ATGATGATGCTCGAGATTCTCTCGACG
pp4695 cs ndeI_s	TCGAAAGCCATATGGAAGACTACCACT
pp4695_PAS_as	CTTGTCCTCGAGTGCCTGGGTTC
4695_H766N_as	GCCGATCTCGTTGGCCACGCCGGC
4695_H766N_s	CGGCGTGGCCAACGAGATCGGCAAC

CrbS_OL_as2	CTCTCGGCGCTGTGGACGTGCACTGGTCTG
cbrA_OL_s2	CAGACCAGTGCACGTCCACAGCGCCGAGAG
PcrcZ_BamHI_s	AGCGAATAAGGATCCTACGCACCGCAC
PcrcZ_EcoRI_as	TGTACCAAGAATTCAGCAGGTGCCGTG

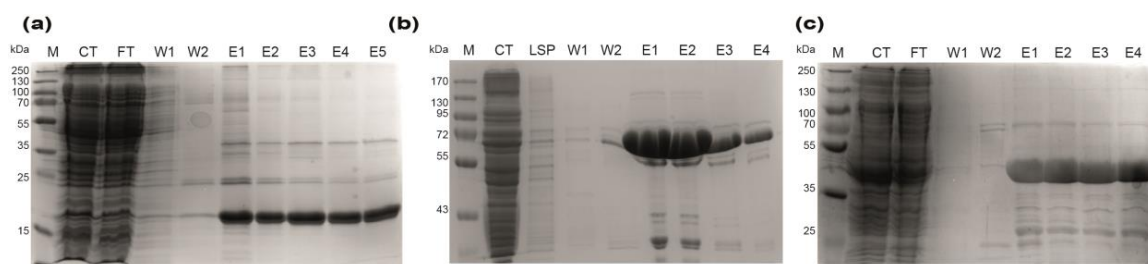


**Figure S1.** SDS-PAGE analysis of the courses of purification of CbrA domains and CbrB. Genes were expressed from plasmid pET21a in given *E. coli* strains. Cells were grown in three liters LB medium, disrupted by high pressure treatment, and His-tagged proteins were isolated by Ni-NTA affinity chromatography. Aliquots of the fractions were subjected to SDS-PAGE and stained with Coomassie. (a) The PAS domain of CbrA (17 kDa including C-terminal 12His tag) was purified from *E. coli* BL21 (DE3) cells via HisTrap. (b) CbrB (54 kDa including C-terminal 6His tag) was purified from *E. coli* BL21 (DE3) plysS via HisTrap. (c) The cytosolic domain of CbrA (44 kDa including C-terminal 12His tag) was purified from *E. coli* C41 cells via HisTrap. M, marker/protein ladder; CT, cytosolic fraction; FT, column flow through; LSP, low speed centrifugation pellet; W1, wash buffer 1 with 10 mM imidazole; W2, wash buffer 2 with 30-50 mM imidazole; E, elution fractions with 250 mM imidazole.

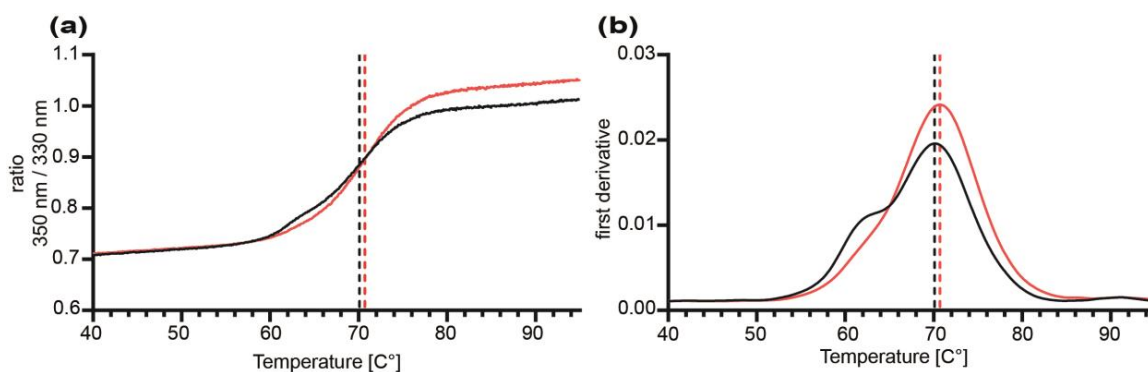


**Figure S2.** Determination of the melting temperature ( $T_m$ ) of CbrA-PAS via Nano differential scanning fluorimetry in a Prometheus (Nanotemper). **(a)** The ratio 350 nm / 330 nm results in a melting curve. **(b)** The peak of the first derivative shows the inflection point of the ratio curve (dotted line) which reflects the  $T_m$ . Exemplary melting curves of the PAS domain without ligand (black) and with 1.0 mM L-histidine (red) are shown (mean of a technical triplicate). The addition of L-histidine leads to a red shift of the fluorescence signal.

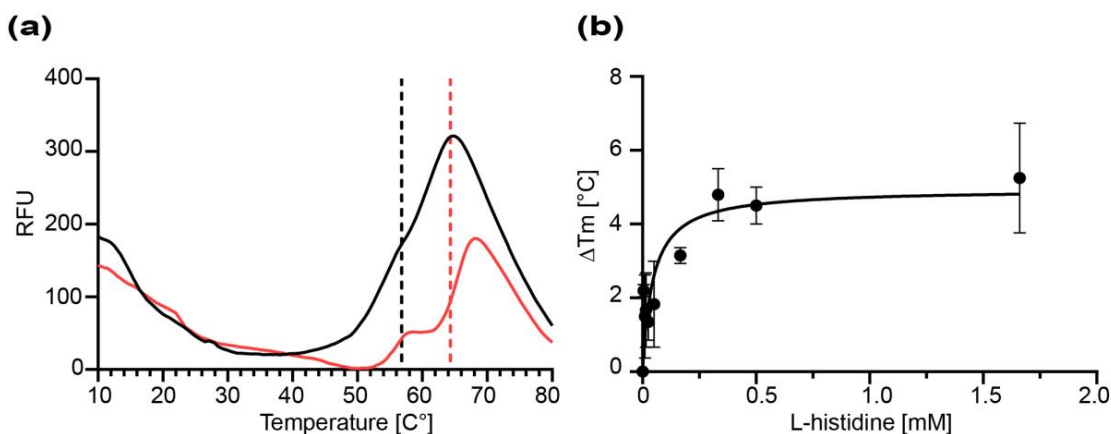


**Figure S3.** Determination of the melting temperature ( $T_m$ ) of CbrA-PAS via SYPRO Orange. The relative fluorescent units (RFU) were recorded in a real-time PCR instrument while the temperature was steadily increased from 10 to 80°C. The dye binds to hydrophobic regions of the protein that are exposed while it unfolds. **(a)** Exemplary melting curves of the PAS domain without ligand (black) and with 1.66 mM L-histidine (red) are shown. The inflection point of the melting curve represents the  $T_m$ . **(b)** The  $\Delta T_m$  was plotted against the ligand concentration and a Michaelis-Menten fit applied. The  $k_d$  value for L-histidine determined with this method was  $46 \pm 17$   $\mu$ M.

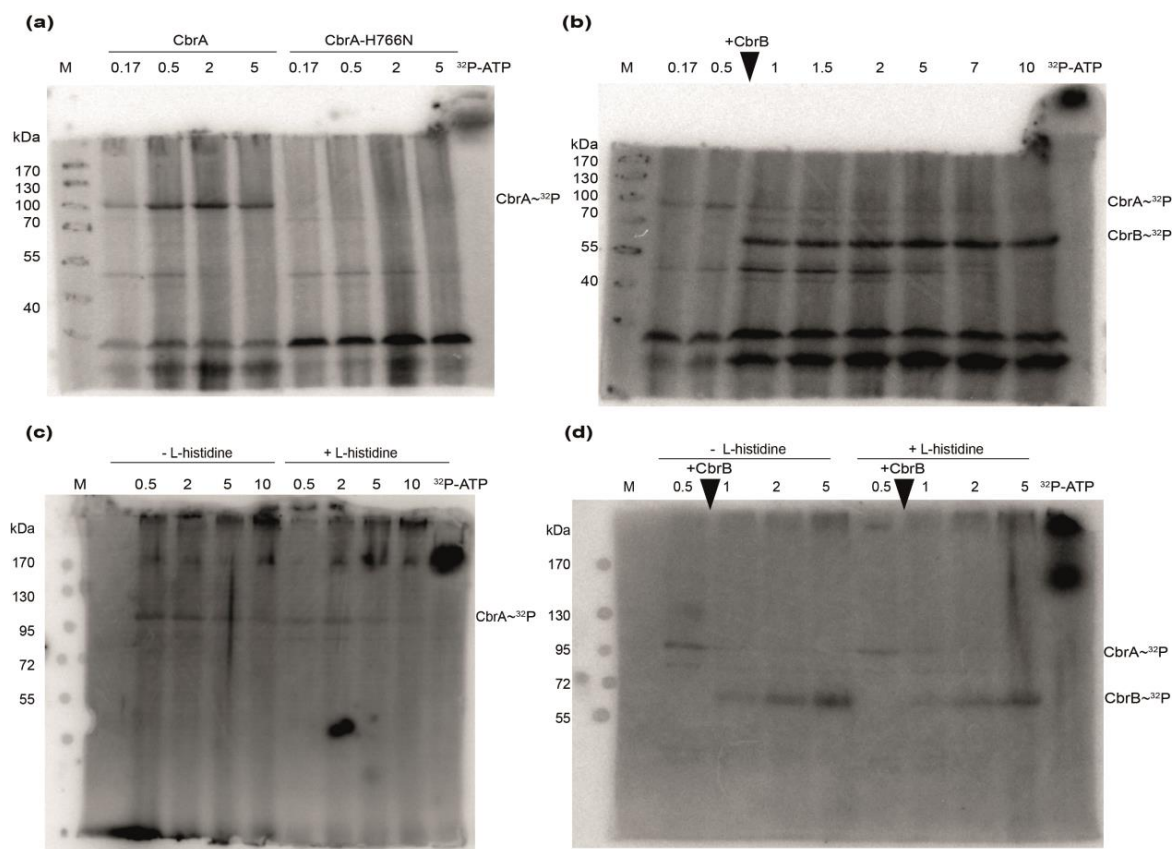


**Figure S4.** Phosphorylation of CbrA and phosphotransfer onto CbrB (complete gels accompanying Fig. 5). **(a)** *E. coli* TKR2000 membrane vesicles containing either CbrA or CbrA-H766N (in 50 mM Tris-HCl, pH7.5, 10% glycerol, 10 mM  $\text{MgCl}_2$ , 2 mM dithiothreitol, 360 mM KCl) were incubated with  $\gamma$ - $^{32}\text{P}$ -ATP. The reaction was stopped at given time points (min), and proteins were separated by SDS-PAGE. Radioactive protein bands were visualized using a phosphor screen. **(b)** Transfer of the phosphoryl group onto purified CbrB that was added after 45 s of incubation of CbrA in membrane vesicles with  $\gamma$ - $^{32}\text{P}$ -ATP. CbrA has a predicted size of 109 kDa and CbrB of 54 kDa. **(c)** *E. coli* TKR2000 membrane vesicles containing either CbrA (in 50 mM Tris-HCl, pH7.5, 10% glycerol, 10 mM  $\text{MgCl}_2$ , 2 mM dithiothreitol, 360 mM KCl) were incubated with  $\gamma$ - $^{32}\text{P}$ -ATP either without or with the addition of 1 mM L-histidine. **(d)** Transfer of the phosphoryl group onto purified CbrB. CbrB was added after 45 s of incubation of CbrA in membrane vesicles with  $\gamma$ - $^{32}\text{P}$ -ATP either without or with the addition of 1 mM L-histidine.  $^{32}\text{P}$ -ATP,  $\gamma$ - $^{32}\text{P}$ -ATP standard for quantification of radioactivity.

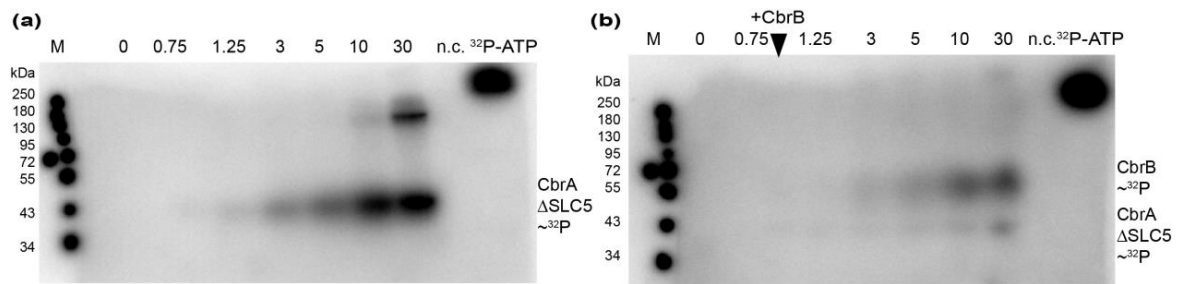


**Figure S5.** Phosphorylation of CbrA $\Delta$ SLC5 and phosphotransfer onto CbrB (complete gels accompanying Fig. 6). **(a)** Purified CbrA $\Delta$ SLC5 (in 50 mM Tris-HCl, pH7.5, 10% glycerol, 10 mM MgCl<sub>2</sub>, 2 mM dithiothreitol, 360 mM KCl) was incubated with  $\gamma$ -<sup>32</sup>P-ATP. The reaction was stopped after given periods of incubation (min), and the protein was separated by SDS-PAGE. Radioactive protein bands were visualized using a phosphor screen. **(b)** Transfer of the phosphoryl group from CbrA $\Delta$ SLC5 to purified CbrB that was added after 45 s of incubation with  $\gamma$ -<sup>32</sup>P-ATP. Purified CbrA $\Delta$ SLC5-H766N incubated with CbrB under the same conditions for 10 min served as negative control (n.c.). CbrA $\Delta$ SLC5 has a predicted size of 44 kDa and CbrB of 54 kDa. <sup>32</sup>P-ATP,  $\gamma$ -<sup>32</sup>P-ATP standard for quantification of radioactivity.

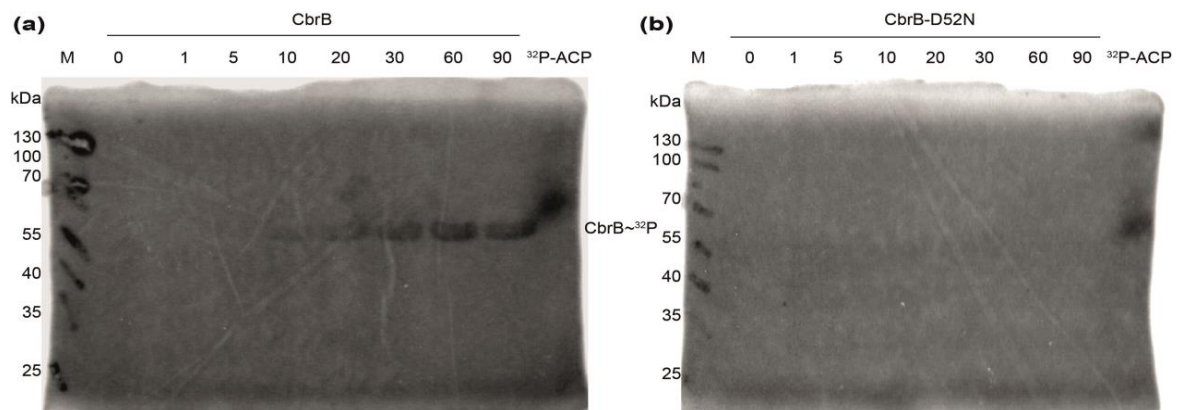


**Figure S6.** Phosphorylation of CbrB by acetylphosphate (ACP). **(a)** Purified CbrB and **(b)** CbrB-D52N (predicted site of phosphorylation replaced) were chemically phosphorylated with <sup>32</sup>P-ACP in 50 mM Tris-HCl, pH7.5, 100 mM KCl, 10% glycerol, 20 mM MgCl<sub>2</sub> and incubated at 30°C. Samples were taken after given periods of incubation (min) and applied to SDS-PAGE. Radioactive protein bands were visualized using a phosphor screen. <sup>32</sup>P-ACP, <sup>32</sup>P-ACP standard for quantification of radioactivity.

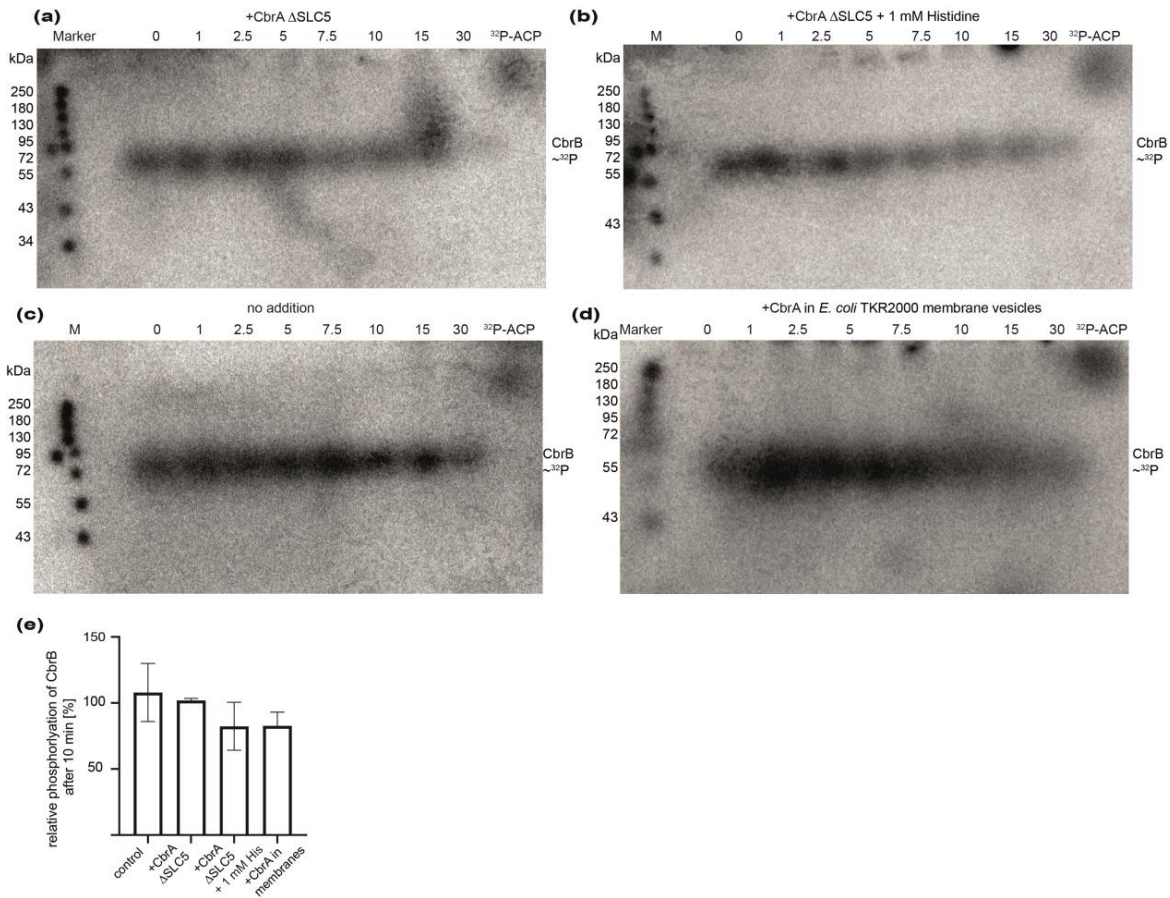


**Figure S7.** Test of a possible CbrA-dependent dephosphorylation of CbrB~<sup>32</sup>P. Purified CbrB was chemically phosphorylated with <sup>32</sup>P-ACP as shown in Fig. S4. Given CbrA variants were added as indicated, and samples were taken after given periods of incubation (min) and applied to SDS-PAGE. Radioactive protein bands were visualized using a phosphor screen. **(a)** CbrB~<sup>32</sup>P was incubated with purified CbrAΔSLC5 (in 50 mM Tris-HCl, pH7.5, 360 mM KCl, 2 mM DTT, 10 mM MgCl<sub>2</sub>) **(b)** CbrB~<sup>32</sup>P was incubated as in (a) with the addition of 1 mM L-histidine. **(c)** Purified CbrB~<sup>32</sup>P was incubated with no CbrA added. **(d)** CbrB~<sup>32</sup>P was incubated with full length CbrA contained in *E. coli* TKR2000 membranes. **(e)** The band intensity of the 10 min time point was measured and compared to the intensity at 0 min. Incubation of CbrB~<sup>32</sup>P without a CbrA variant served as control (cp. also Fig. S5c). The relative quantification is based on three replicates. CbrB has a predicted size of 54 kDa. Complete gels of representative experiments are shown.; <sup>32</sup>P-ACP, <sup>32</sup>P-ACP standard for quantification of radioactivity.

## Supplementary References

- 1 Kollmann, R. & Altendorf, K. ATP-driven potassium transport in right-side-out membrane vesicles via the Kdp system of *Escherichia coli*. *Biochim. Biophys. Acta* **1143**, 62-66, doi:[https://doi.org/10.1016/0005-2728\(93\)90216-3](https://doi.org/10.1016/0005-2728(93)90216-3) (1993).
- 2 Siebers, A. & Altendorf, K. The K<sup>+</sup>-translocating Kdp-ATPase from *Escherichia coli*. *Eur. J. Biochem.* **178**, 131-140, doi:10.1111/j.1432-1033.1988.tb14438.x (1988).
- 3 Regenhardt, D. *et al.* Pedigree and taxonomic credentials of *Pseudomonas putida* strain KT2440. *Environ. Microbiol.* **4**, 912-915, doi:10.1046/j.1462-2920.2002.00368.x (2002).
- 4 Bagdasarian, M. *et al.* Specific-purpose plasmid cloning vectors II. Broad host range, high copy number, RSF 1010-derived vectors, and a host-vector system for gene cloning in *Pseudomonas*. *Gene* **16**, 237-247, doi:[http://dx.doi.org/10.1016/0378-1119\(81\)90080-9](http://dx.doi.org/10.1016/0378-1119(81)90080-9) (1981).
- 5 Sarker, M. R. & Cornelis, G. R. An improved version of suicide vector pKNG101 for gene replacement in Gram-negative bacteria. *Mol. Microbiol.* **23**, 410-411, doi:10.1046/j.1365-2958.1997.t01-1-00190.x (1997).
- 6 Hoang, T. T., Karkhoff-Schweizer, R. R., Kutchma, A. J. & Schweizer, H. P. A broad-host-range Flp-FRT recombination system for site-specific excision of chromosomally-located DNA sequences: application for isolation of unmarked *Pseudomonas aeruginosa* mutants. *Gene* **212**, 77-86, doi:[https://doi.org/10.1016/S0378-1119\(98\)00130-9](https://doi.org/10.1016/S0378-1119(98)00130-9) (1998).
- 7 Lassak, J., Henche, A.-L., Binnenkade, L. & Thormann, K. M. ArcS, the cognate sensor kinase in an atypical Arc system of *Shewanella oneidensis* MR-1. *Appl. Environ. Microbiol.* **76**, 3263-3274, doi:10.1128/AEM.00512-10 (2010).
- 8 Cronin, C. N. & McIntire, W. S. pUCP-Nco and pUCP-Nde: *Escherichia-Pseudomonas* Shuttle Vectors for Recombinant Protein Expression in *Pseudomonas*. *Anal. Biochem.* **272**, 112-115, doi:<http://dx.doi.org/10.1006/abio.1999.4160> (1999).
- 9 Guzman, L. M., Belin, D., Carson, M. J. & Beckwith, J. Tight regulation, modulation, and high-level expression by vectors containing the arabinose PBAD promoter. *J. Bacteriol.* **177**, 4121-4130 (1995).
- 10 Gödeke, J., Heun, M., Bubendorfer, S., Paul, K. & Thormann, K. M. Roles of two *Shewanella oneidensis* MR-1 extracellular endonucleases. *Appl. Environ. Microbiol.* **77**, 5342-5351, doi:10.1128/AEM.00643-11 (2011).
- 11 Kovach, M. E. *et al.* Four new derivatives of the broad-host-range cloning vector pBBR1MCS, carrying different antibiotic-resistance cassettes. *Gene* **166**, 175-176, doi:[https://doi.org/10.1016/0378-1119\(95\)00584-1](https://doi.org/10.1016/0378-1119(95)00584-1) (1995).

# HutT functions as the main L-Histidine transporter in *Pseudomonas putida* KT2440

This research was originally published in *FEBS Letters* in July 2021.

**Larissa Wirtz**, **Michelle Eder**, **Anna-Katharina Brand** and **Heinrich Jung** HutT functions as the main L-Histidine transporter in *Pseudomonas putida* KT2440. *FEBS LETT*, Volume 595, Issue 16, p. 2113-2126.

<https://doi.org/10.1002/1873-3468.14159>

## HutT functions as the major L-histidine transporter in *Pseudomonas putida* KT2440

Larissa Wirtz , Michelle Eder, Anna-Katharina Brand and Heinrich Jung 

Division of Microbiology, Department of Biology 1, Ludwig Maximilians University Munich, Martinsried, Germany

### Correspondence

H. Jung, Division of Microbiology,  
Department of Biology 1, Ludwig  
Maximilians University Munich, D-82152  
Martinsried, Germany  
Tel: +49-89-2180-74630  
E-mail: hjung@lmu.de

(Received 6 May 2021, revised 1 July 2021,  
accepted 6 July 2021)

doi:10.1002/1873-3468.14159

Edited by Stuart Ferguson

**Histidine is an important carbon and nitrogen source of  $\gamma$ -proteobacteria and can affect bacteria–host interactions. The mechanisms of histidine uptake are only partly understood. Here, we analyze functional properties of the putative histidine transporter HutT of the soil bacterium *Pseudomonas putida*. The *hutT* gene is part of the histidine utilization operon, and the gene product belongs to the amino acid-polyamine-organocation (APC) family of secondary transporters. Deletion of *hutT* severely impairs growth of *P. putida* on histidine, suggesting that the encoded transporter is the major histidine uptake system of *P. putida*. Transport experiments with cells and purified and reconstituted protein indicate that HutT functions as a high-affinity histidine : proton symporter with high specificity for the amino acid. Substitution analyses identified amino acids crucial for HutT function.**

**Keywords:** APC transporter; histidine; HutT; secondary transport

The amino acid histidine can be used by many bacteria as a source of carbon, nitrogen, and/or energy. For this purpose, histidine is converted into glutamate and a one-carbon compound (formate or formamide) in a four- or five-step enzymatic process [1]. Respective genes are organized in *hut* (histidine utilization) gene clusters, which are widely distributed not only in bacteria but also in archaea and eukaryotes [1,2]. Histidine uptake and degradation are known to affect bacteria–host interactions. For example, the amino acid can be detected extracellularly in a mouse infection model and is suggested to represent a crucial nitrogen source during infection with *Acinetobacter baumannii* thereby promoting colonization of the lung [3]. Furthermore, histidine and the product of the first step of its degradation, urocanate, play an important role in host recognition by *Pseudomonas aeruginosa* and the expression of genes of virulence factors [4,5]. Histidine is also part of plant exudates and can

be utilized by root-colonizing bacteria such as *Pseudomonas putida* and *Pseudomonas fluorescens* [6–9].

The positively charged histidine is hardly membrane permeable and requires a transporter for efficient uptake into cells. In fact, individual bacteria may employ several transport systems with varying specificity and affinity for histidine [10]. In *Salmonella enterica* serovar typhimurium and other enterobacteria, the well-studied ABC transport system HisJQMP is mainly responsible for the uptake of histidine and other basic amino acids [11, 12]. HisJ is a periplasmic binding protein that delivers histidine to the membrane-bound transport complex HisQMP, with HisP acting as an ATPase. Furthermore, the lysine-arginine-ornithine binding protein ArgT can deliver histidine to the HisQMP complex albeit its affinity for histidine is 100fold lower than the one of HisJ [12]. In addition to the ABC system, *S. enterica* and other enterobacteria may take up histidine by secondary

### Abbreviations

3AT, 3-amino-1,2,4-triazole; APC family, amino acid-polyamine-organocation family; CCCP, m-chlorophenyl hydrazine; DNP, 2,4-dinitrophenol; Imi, imidazole; NEM, N-ethylmaleimide; pmf, proton motive force; smf, sodium motive force; TM, transmembrane segment; Tra, 1,2,4-triazolyl-3-alanine.

transport systems including the aromatic amino acids transporter AroP as well as two other putative secondary transporters [10,13].

Also in *Pseudomonas* species, primary (ABC-type) and secondary transport systems have been proposed to contribute to histidine uptake [2,14]. Here, a gene frequently annotated as *proY* is part of the *hut* gene cluster and represents a candidate for a secondary histidine transporter. Assignment of the function 'proline-specific permease' (ProY) in various bacteria including *Pseudomonas* species is based on similarity to the product of a cryptic gene (hereafter referred to as *proY*) of *Salmonella typhimurium*, overexpression of which restores growth on proline in a mutant unable to take up proline [15]. However, deletion of the homologous gene (PA5097) in *P. aeruginosa* inhibited growth of the bacterium on histidine. Therefore, the gene product was proposed to function as a histidine transporter and renamed HutT [5]. First direct experimental evidence for a function of HutT in histidine transport comes from growth and  $^3\text{H}$ -histidine uptake measurements with *P. fluorescens* SBW25 [10]. The latter strain has two genes annotated as *hutT<sub>h</sub>* (Pfl0368) and *hutT<sub>u</sub>* (Pfl0362). Deletion of the *hutT<sub>h</sub>* compromised growth of the strain on histidine and reduced the rate of  $^3\text{H}$ -histidine uptake to 30% of the value of the wild type [10]. The second gene, *hutT<sub>u</sub>*, did not prove to be important for histidine uptake but was required for growth on urocanate, the product of the first step of histidine degradation [10]. Not all *Pseudomonas* strains encode a specific urocanate transporter, but those that do might use urocanate excreted by fungi as a carbon or nitrogen source [10]. Furthermore, deletion of genes coding for a putative histidine transport system of the ABC type (*hutXWV*, Pfl0363-0365 in *P. fluorescens* SBW25) did not affect histidine uptake. However, simultaneous deletion of *hutXWV* and *hutT<sub>h</sub>* further reduced growth on histidine compared to the effect of the individual deletion of *hutT<sub>h</sub>*, suggesting that *hutXWV* is also involved in histidine uptake [10]. Surprisingly, a mutant of *P. fluorescens* SBW25, devoid of all these histidine uptake systems, was still able to grow on histidine. The protein responsible for histidine transport in the latter mutant turned out to be the sensor kinase CbrA (Pfl5236) [14]. CbrA does in fact contain an N-terminal domain that is homologous to members of the solute/sodium symporter family (TC 2.A.21) [14, 16, 17]. The capability to bind and transport histidine was confirmed for CbrA (PP\_4695) of *P. putida* KT2440 [18].

The histidine transporter HutT of *Pseudomonas* species belongs, within the amino acid-polyamine-organocation (APC) superfamily (TC 2.A.3), to the

amino acid transporter (AAT) family (TC 2.A.3.1) [19]. The APC superfamily entails 18 different protein families and is, after the major facilitator superfamily (MFS) (TC 2.A.1), the second largest family of secondary transport systems [20,21]. Members of the APC superfamily function as solute/cation symporters or solute/solute antiporters [20]. The transport proteins share the LeuT fold that is characterized by a core of ten transmembrane segments (TMs), arranged in a five plus five inverted repeat with an antiparallel orientation and a pseudosymmetry axis in the membrane plane, and operate via an alternating access mechanism [22,23].

The soil bacterium *P. putida* KT2440 is predicted to contain only one *hutT*-like gene (PP\_5031) [24,25]. The gene product shares 60% sequence identity with ProY of *S. typhimurium*. The function of the gene (gene product) in *P. putida* has not been analyzed so far. We set out here to obtain information on the role of the gene in *P. putida* and to gain more detailed insights into the functional properties of HutT in general. To demonstrate that the *hutT* gene (HutT) of *P. putida* is indeed sufficient for histidine uptake, we used *E. coli* and *P. putida* strains lacking all known histidine uptake systems and expressed *hutT* from a plasmid. We also purified HutT and reconstituted it into proteoliposomes. Cells, membranes, and/or proteoliposomes were used for  $^3\text{H}$ -histidine binding and transport measurements to elucidate the kinetic properties, specificity, and energetic requirements of HutT. The results indicate that HutT catalyzes active histidine transport with high substrate affinity and specificity, most likely acting as an L-histidine:proton symporter. In addition, preliminary amino acid substitution analyses led to the identification of amino acids crucial for HutT function.

## Material & Methods

### Cultivation

All strains of *P. putida* and *E. coli* and all plasmids used in this investigation are listed in Tables S1 and S2. Cells were cultivated aerobically at 30°C and 37°C, respectively. When cells were transformed with plasmids, antibiotics were added at the following concentrations: ampicillin/carbenicillin (100  $\mu\text{g mL}^{-1}$ ) or kanamycin (50  $\mu\text{g mL}^{-1}$ ). For standard cultivation and precultures, LB medium was used (1% tryptone/peptone, 1% NaCl, 0.5% yeast extract). For plates, the medium was supplemented with 1.5% agar and poured into petri dishes. As minimal medium, a M9 salt solution containing 33.7 mM  $\text{Na}_2\text{HPO}_4$ , 22 mM

$\text{KH}_2\text{PO}_4$ , 8.5 mM NaCl, 18.7 mM  $\text{NH}_4\text{Cl}$ , 0.2 mM  $\text{CaCl}_2$ , 2 mM  $\text{MgSO}_4$ , 2 mM thiamin, and 20 mM of the appropriate carbon source was used. Additionally, the following trace elements were added: 134  $\mu\text{M}$   $\text{Na}_2\text{-EDTA}$ , 31  $\mu\text{M}$   $\text{FeCl}_3$ , 6.2  $\mu\text{M}$   $\text{ZnCl}_2$ , 0.76  $\mu\text{M}$   $\text{CuCl}_2$ , 0.42  $\mu\text{M}$   $\text{CoCl}_2$ , 1.62  $\mu\text{M}$   $\text{H}_3\text{BO}_3$ , and 81 nM  $\text{MnCl}_2$ .

The *hutT* gene of *P. putida* KT2440 was deleted by cloning the flanking regions of the gene into the suicide vector pNPTS138-R6KT [26] followed by double homologous recombination for insertion into the bacterial chromosomal genome. The LW1 mutant  $\Delta\text{cbrA}$   $\Delta\text{hutTH}$   $\Delta\text{hutWX}$  was used as described in Wirtz *et al.* [18]. *E. coli* JW2306  $\Delta\text{hisJ}$  was inoculated from the commercially available Keio Collection [27]. For transport assays with *E. coli*, the *hutT* gene of *P. putida* together with a sequence encoding a 6His tag was cloned into plasmid pT7-5 yielding plasmid pT7-5-*hutT6H*. For overproduction and purification of HutT, *hutT* was cloned into pET21a yielding plasmid pET21a-*hutT6H*. For transport assays and growth measurements with *P. putida*, *hutT* together with a sequence encoding a 6His tag was cloned into pUCP20-ANT2-MCS [28] yielding plasmid pUCP20-ANT2-*hutT6H*. Cloning was achieved by performing PCRs with the primers listed in Table S3, and restriction of amplicons and plasmid vectors with enzymes *Bam*HI, *Xho*I, or *Nde*I followed by ligation with T4 ligase and transformation of *E. coli* DH5 $\alpha$ . For DNA extraction from agarose gels and purification of PCR products, the HiYield® PCR Clean-up/Gel Extraction Kit (SLG® Sued-Laborbedarf, Gauting, Germany) was used. Plasmid extraction from 3 mL overnight cultures in LB medium was performed with the HiYield® Plasmid Mini Kit (SLG® Sued-Laborbedarf).

### Protein purification

HutT was expressed from plasmid pET21a-*hutT6H* in *E. coli* BL21 pLysS. For this purpose, an over day preculture was used to inoculate a 100 mL overnight culture in LB medium, which in turn was used to inoculate a 1 L culture. Gene expression was induced by adding 0.5 mM IPTG at  $\text{OD}_{600} = 0.7$  and cultivation continued for 3 h. Cells were harvested and washed (0.1 M  $\text{KP}_i$  pH 7.5), and the pellets were frozen in liquid nitrogen and were stored at  $-80^\circ\text{C}$ . All following steps were carried out at  $4^\circ\text{C}$  or on ice. The cells were resuspended in 0.1 M  $\text{KP}_i$  pH 7.5 buffer (0.2 g  $\text{mL}^{-1}$ ) and disrupted with high pressure (1.35 kbar) in a Constant Cell Disruptor. To isolate HutT, cell lysates in 0.1 M  $\text{KP}_i$  pH 7.5 were centrifuged first at low speed (4500  $\times g$ ) to remove cell debris and then at high speed to (235 000  $\times g$ ) at  $4^\circ\text{C}$  for 1.5 h to obtain the

membranes. The membrane pellet was washed, resuspended in a small volume of 50 mM Tris/HCl pH 7.5, 300 mM KCl, 10% glycerol and if required stored in aliquots at  $-80^\circ\text{C}$  after shock freezing in liquid nitrogen. The protein amount in the membranes was determined *via* the Peterson protein assay [29]. The membrane proteins (5 mg  $\text{mL}^{-1}$  total membrane protein) were solubilized by adding 1% n-dodecyl- $\beta$ -maltoside (DDM) during stirring for 30 min. The membranes were removed by ultracentrifugation (113 000  $\times g$ ) for 20 min. The solubilized proteins were mixed with Ni-NTA resin (1 mL agarose beads) for 45 min and packed onto a chromatography column. After washing with 50 mL buffer (50 mM Tris/HCl pH 7.5, 300 mM KCl, 10% glycerol, 0.04% DDM) with 10 mM imidazole followed by 15 mL buffer with 40 mM imidazole, HutT was eluted with 200 mM imidazole in the same buffer in six fractions of 600  $\mu\text{L}$  each. Purity was estimated *via* Coomassie stained SDS/PAGE and the identity by western blot analysis with an  $\alpha$ -PentaHis Antibody (Qiagen, Hilden, Germany). The protein concentration was measured by NanoDrop™.

### Reconstitution

For reconstitution of purified HutT, liposomes (Avanti *E. coli* polar lipids in 0.1 M  $\text{KP}_i$ , pH 7.5) were prepared by extruding through 400 nm pore size polycarbonate membranes and destabilized by addition of 0.3% Triton X-100 (partial solubilization of lipids). The liposomes were mixed with HutT protein in a ratio of 50:1. The detergent was removed in three steps at room temperature and later  $4^\circ\text{C}$  by the addition of Bio-Beads SM-2 (Bio-Rad, Feldkirchen, Germany). Next, the liposomes were washed by dilution with buffer (0.1 M  $\text{KP}_i$  pH 7.5 with 2 mM  $\beta$ -mercaptoethanol) and concentrated at 235 000  $\times g$  in an ultracentrifuge. The liposomes were finally formed by extruding and concentrated again at 113 000  $\times g$ . Afterwards, they were suspended in buffer containing 0.1 M  $\text{KP}_i$  pH 7.5 and 5 mM  $\text{MgSO}_4$ .

### Transport assay

Whole cell transport assays were performed as described by Wirtz *et al.* (2020) *via* rapid filtration assay [18]. In brief, cells expressing *hutT* were harvested, washed, and resuspended in 100 mM Tris/MES buffer, pH 6.0 ( $\text{OD}_{600} = 5$ ). Prior to transport, cells were incubated with 20 mM D-lactate for 5 min. Transport was initiated by the addition of  $^3\text{H}$ -L-histidine (500 Ci  $\text{mol}^{-1}$ ) at a final concentration of

1  $\mu\text{M}$  (or a given range of concentrations for kinetic measurements) and incubated at 20°C. At given time points uptake was stopped, the suspension was rapidly filtered and radioactivity associated with the filter was quantified with a  $\beta$ -counter.

For measurements in proteoliposomes, the protocol of Jung *et al.* (1998) was used [30]. To initiate transport, 2  $\mu\text{L}$  aliquots of the proteoliposome suspension (0.9 mg protein/mL) were diluted 200fold into 400  $\mu\text{L}$  of given transport buffers all containing 0.2  $\mu\text{M}$  valinomycin and 1  $\mu\text{M}$   $^3\text{H}$ -L-histidine (500 Ci  $\text{mol}^{-1}$ ) (or a given range of concentrations for kinetic measurements). Transport was stopped after 30 s, proteoliposomes were collected and washed by rapid filtration, and radioactivity was determined with a  $\beta$ -counter.

### DRaCALA

HutT containing membrane vesicles were prepared from *E. coli* C43 (DE3) heterologously expressing *hutT6H* from plasmid pET21a-*hutT6H* upon induction by 0.5 mM IPTG. Cells transformed with plasmid pET21a without *hutT* served for the preparation of the negative control. The cells, resuspended in 0.1 M  $\text{KPi}$  pH 7.5 buffer (0.2 g  $\text{mL}^{-1}$ ), were disrupted with high pressure (1.35 kbar) in a Constant Cell Disruptor followed by ultracentrifugation at 235 000  $\times g$  and washing. Membrane vesicles were resuspended in 100 mM  $\text{KPi}$  buffer pH 7.5, and the amount of protein was determined by the Peterson protein assay [29]. For the differential radial capillary action of ligand assay (DRaCALA), the protocol from Roelofs *et al.* was followed [31].  $^3\text{H}$ -L-histidine (final concentration 1.35  $\mu\text{M}$ , 37 Ci  $\text{mmol}^{-1}$ ) was added to the membrane vesicles containing 27 mg  $\text{mL}^{-1}$  total protein, and samples were incubated at 25°C for 10 min. Five  $\mu\text{L}$  aliquots were subsequently pipetted onto dry nitrocellulose membrane (0.45  $\mu\text{m}$ , GE Healthcare, Solingen, Germany) in triplicates. The nitrocellulose was exposed to a Storage Tritium Screen, and a Typhoon Trio Imager (Amersham Biosciences acquired by GE Healthcare, Chicago, IL, USA) was used for the detection of radioactivity. Analysis of the resulting image was performed with IMAGEJ.

## Results

### Physiological significance of *hutT* of *P. putida* KT2440

The genetic arrangement of the *hut* gene cluster of *P. putida* KT2440 is shown in Fig. 1A. Genes *hutU*, *hutH*, *hutI*, *hutG*, and *hutF* encode enzymes that

convert histidine into glutamate, formate, and two  $\text{NH}_3$ . *In silico* hydropathy profile and secondary structure analyses of the product of the *hutT* gene predicted the existence of twelve mostly hydrophobic,  $\alpha$ -helical domains expected to traverse the cytoplasmic membrane in a zigzag fashion and connected by hydrophilic loops (Fig. 1B). Sequence alignments of HutT with members of the APC family and homology modeling suggested that transmembrane segments (TMs) 1 to 10 constitute the core equivalent to the core formed by TMs 1 to 10 of LeuT (Fig. 1C).

To obtain information on the function of HutT in *P. putida* KT2440, growth of the wild-type strain, the  $\Delta hutT$  mutant, and the complemented  $\Delta hutT$  mutant was analyzed in different media. In LB complex media and in M9 minimal medium supplemented with succinate and  $\text{NH}_4\text{Cl}$  as sources of carbon and nitrogen, respectively, there was no significant difference in growth dynamics between the three strains (Fig. 2). However, in M9 minimal medium supplemented with histidine and  $\text{NH}_4\text{Cl}$  as sources of carbon and nitrogen, respectively, growth of the  $\Delta hutT$  strain was strongly impaired compared to wild-type. Expression of *hutT* from plasmid pUCP20-ANT2-*hutT6H* stimulated growth of the  $\Delta hutT$  strain compared to the  $\Delta hutT$  strain transformed with the empty plasmid [28]. However, wild-type growth behavior was only partially restored (Fig. 2). The latter observation may at least partially be explained by toxic effects of the overproduction of the integral membrane protein HutT. The idea is supported by the observation that the described stimulation of growth of the  $\Delta hutT$  strain was measured only when very low inducer concentration (e.g., 3  $\mu\text{M}$ ) was used for the expression of plasmid-encoded *hutT* in minimal medium. Higher inducer concentrations did not lead to a stimulation of growth but inhibited growth even when succinate was used as carbon source (Fig. S1). Nevertheless, the growth experiments show that *hutT* is required for efficient growth of *P. putida* KT2440 on histidine as carbon source.

### HutT-catalyzed L-histidine transport in whole cells

To obtain more information on the function of HutT, the activity of protein was tested first in intact cells of *P. putida* LW1. The strain was previously derived from *P. putida* KT2440 by deleting all genes known or predicted to encode histidine uptake systems (*hutT*, *cbrA*, *hutXW*) and *hutH* encoding the enzyme of the first step of histidine degradation [18]. Strain LW1 was transformed with plasmid pUCP20-ANT2-*hutT6H* (contains the *hutT* gene plus six codons encoding a

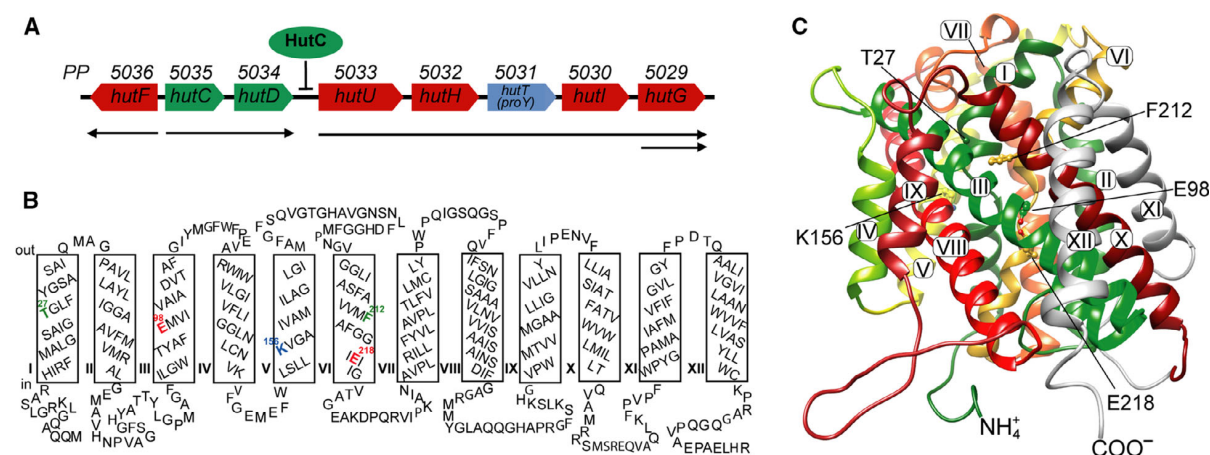


**Fig. 1.** Genomic organization of the *hut* genes and structural predictions for HutT. (A) Genetic arrangement of the *hut* gene cluster of *P. putida* KT2440 (based on [1,53]). Genes highlighted in red code for enzymes that convert histidine into glutamate, formate and two NH<sub>3</sub>. Genes colored in green play a role in regulation of the expression of the *hut* gene cluster. Arrows under the gene clusters indicate transcription units. (B) Model of the membrane topology of the putative transporter HutT. Potentially important residues are colored: positively charged residues (blue), acidic residues (red), putative substrate binding site (green). Predictions were made using Octopus [54]. (C) Structural model of HutT. The homology model was generated using the structure of the APC family member GkApC [34]. The template was identified and the model was generated by Phyre2 [55].

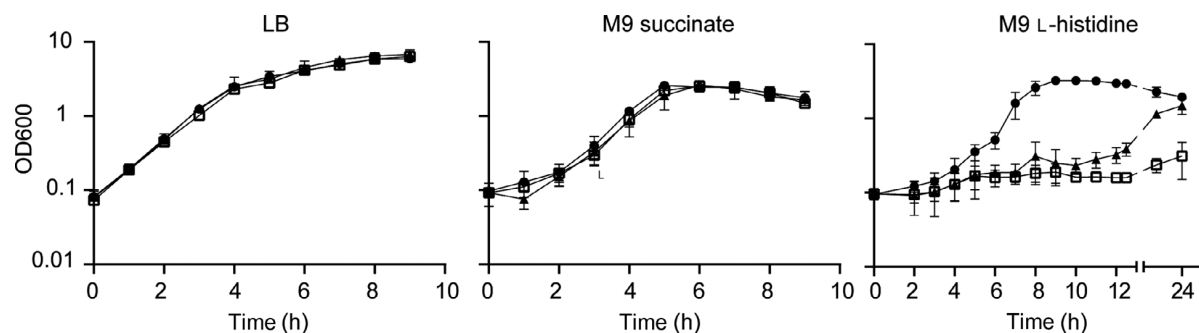


**Fig. 2.** Growth curves of *P. putida* KT2440 wild-type harboring pUCP20-ANT2-MCS (filled circles) and derived  $\Delta$ *hutT* strain harboring either pUCP20-ANT2-MCS (empty squares) or in pUCP20-ANT2-*hut6H* (filled triangles) in LB complex medium, M9 medium plus 20 mM succinate and 18.7 mM NH<sub>4</sub>Cl, and M9 plus 20 mM L-histidine and 18.7 mM NH<sub>4</sub>Cl. Expression of the *hutT* gene from the *antA* promoter in pUCP20-ANT2-*hut6H* was induced with 3  $\mu$ M anthranilic acid. Growth was analyzed in shaking liquid cultures by measuring the optical density (OD) at 600 nm. Shown are mean values and standard deviations calculated from at least three independent experiments.

6His tag) or pUCP20-ANT2-MCS (negative control). Gene expression in complex medium (LB) was optimal upon induction with 1 mM anthranilic acid for 2 h. To record times courses of transport, cell suspensions were prepared, and aliquots of the suspension were incubated with <sup>3</sup>H-L-histidine for different periods of time. Uptake was stopped by rapid filtration. The time courses of <sup>3</sup>H-L-histidine uptake into *P. putida* LW1 revealed that expression of *hutT* stimulated the initial rate of uptake ( $v$ ) significantly ( $v = 0.74 \pm 0.09$  nmol min<sup>-1</sup> mg<sup>-1</sup>) compared to the negative control ( $v = 0.04 \pm 0.01$  nmol min<sup>-1</sup> mg<sup>-1</sup>) (Fig. 3A).

The maximum level of <sup>3</sup>H-L-histidine accumulation in cells expressing *hutT* was reached after one minute, while in the negative control accumulation of <sup>3</sup>H-L-histidine increased linearly with time over a period of 10 min (Fig. 3A).

To obtain more detailed information on the kinetics of <sup>3</sup>H-L-histidine uptake catalyzed by HutT, initial rates were determined at substrate concentrations ranging from 0.1 to 25  $\mu$ M. Values were corrected for background activity determined with the negative control. The resulting transport rates are saturated with increasing substrate concentration as expected for a

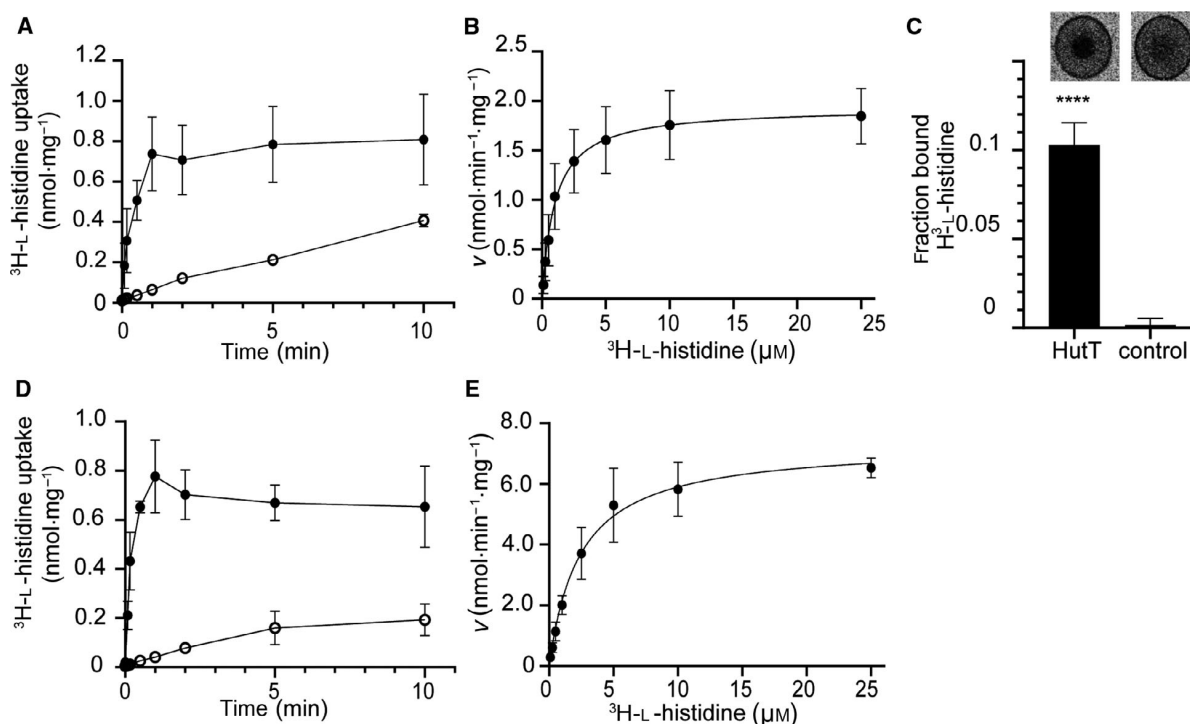


**Fig. 3.** Kinetics of  $^3\text{H}$ -L-histidine uptake into *P. putida* LW1. (A) Time course of  $^3\text{H}$ -L-histidine uptake into *P. putida* LW1 transformed with either pUCP20-ANT2-MCS (empty symbols) or pUCP20-ANT2-*hutT6H* (filled symbols). Expression of *hutT* was induced with 1 mM anthranilic acid for 2 h. Resulting cells were washed and suspended in 100 mM Tris/MES buffer, pH 6.0 ( $\text{OD}_{600} = 5$ ). Prior to transport, cells were incubated with 20 mM D-lactate for 5 min. Transport was initiated by the addition of  $^3\text{H}$ -L-histidine at a final concentration of 1  $\mu\text{M}$ . At given time points uptake was stopped, the suspension was rapidly filtered, and radioactivity associated with the filter was quantified with a  $\beta$ -counter. (B) Michaelis-Menten kinetics of  $^3\text{H}$ -L-histidine uptake by HutT in *P. putida* LW1. Initial rates of transport were measured under the conditions described in (A) with  $^3\text{H}$ -L-histidine concentrations ranging from 0.1 to 25  $\mu\text{M}$ . The initial rate of transport (10 s) determined at each substrate concentration was corrected for background activity (rate without HutT). Data were fitted and kinetic parameters were determined using GRAPHPAD Prism. For all experiments, mean values and standard deviations were calculated from minimum three independent experiments. (C) Binding of L-histidine to HutT in membranes of *E. coli* C43 containing HutT. Membranes without HutT served as control. Membrane vesicles were mixed with 1.35  $\mu\text{M}$   $^3\text{H}$ -L-histidine (37 Ci  $\text{mmol}^{-1}$ ) and spotted on nitrocellulose membranes. Diffusion of radioactivity in the resulting spots was visualized using a tritium screen and a Typhoon scanner (representative spots in upper image). The spots were quantified using ImageJ and the bound fraction of  $^3\text{H}$ -L-histidine was calculated according to Roelofs et al. [31] (graph below the image). (D) Time course of  $^3\text{H}$ -L-histidine uptake into *E. coli* JW2306 cells harboring pT7-5 (empty symbols) or pT7-5-*hutT6H* (filled symbols) over 10 min. Cells were treated and transport was measured as described in (A). (E) Michaelis-Menten kinetics of  $^3\text{H}$ -L-histidine uptake by HutT in *E. coli* JW2306. Transport was measured as described in (A) with substrate concentrations ranging from 0.1 to 25  $\mu\text{M}$ . Kinetic parameters were calculated as described in (B). For all experiments, mean values and standard deviations were calculated from minimum three independent experiments (error bars). Student's t-test was applied for statistical analysis. \*\*\*\*= $P \leq 0.0001$ .

transporter-dependent process (Fig. 3B). Analysis of the data according to Michaelis and Menten yielded a maximum rate of  $^3\text{H}$ -L-histidine uptake ( $V_{max}$ ) of  $1.93 \pm 0.11 \text{ nmol mg}^{-1} \text{ min}^{-1}$ . The histidine concentration at which the uptake proceeded at half-maximal speed (apparent  $K_M$ ) was determined to be  $0.99 \pm 0.23 \mu\text{M}$ .

In addition to the measurements with *P. putida* LW1, function of HutT was analyzed in *E. coli* JW2306 from the Keio collection [27]. The strain is unable to metabolize histidine, and the ABC-type

histidine transporter HisPMQJ is inactivated due to the deletion of *hisJ* encoding the histidine binding protein. For transport measurements, *E. coli* JW2306 was transformed either with plasmid pT7-5-*hutT6H* or pT7-5. Expression of *hutT* from the *lac* promoter in pT7-5 was induced with 0.5 mM IPTG for 2 h. Transport experiments were performed as described above for *P. putida* LW1. The resulting time courses of  $^3\text{H}$ -L-histidine uptake were similar to the one obtained with *P. putida* LW1 (Fig. 3D). The Michaelis-Menten parameters deviated with

$V_{max} = 7.30 \pm 0.37 \text{ nmol mg}^{-1} \text{ min}^{-1}$  and apparent  $K_M = 2.4 \pm 0.38 \text{ }\mu\text{M}$  only slightly from the values determined for HutT in strain LW1 (Fig. 3E). The slight deviations may be explained by differences in gene expression ( $V_{max}$ ) and composition of the cytoplasmic membranes (apparent  $K_M$ ).

To obtain independent evidence for an interaction between HutT and histidine, a qualitative DRaCALA assay [31] was performed. For this purpose, membranes were prepared from *E. coli* C43 expressing *hutT* from plasmid pET21a-*hutT6H*. The membranes were mixed with  $1.35 \text{ }\mu\text{M}$   $^3\text{H-L-histidine}$  ( $37 \text{ Ci mmol}^{-1}$ ) and spotted on nitrocellulose membranes. Diffusion of radioactivity in the resulting spots was visualized using a tritium screen and a Typhoon scanner (Fig. 3C). The observed retention of radioactivity in the center of the spot relative to the negative control (membranes without HutT) was taken as evidence for binding of  $^3\text{H-L-histidine}$  to HutT (Fig. 3C).

Taken together, the results suggest that HutT of *P. putida* KT2440 is able to bind and catalyze uptake of histidine. The relatively low apparent  $K_M$  of histidine transport may be considered as a hint on a relatively high affinity of HutT for histidine.

### Energetics and specificity of HutT-dependent transport

Energetic requirements of the HutT-dependent transport were analyzed by measuring  $^3\text{H-L-histidine}$  uptake into *E. coli* JW2306 expressing *hutT* from plasmid pT7-5-*hutT6H* in the presence of different ionophores (Fig. 4A). Since the ionophores were dissolved in DMSO, cell suspensions supplemented with DMSO without inhibitors were used for comparison. Cells incubated with the ionophores valinomycin (potassium), nigericin (proton/potassium antiport), nonactin (ammonium, potassium, sodium) showed  $^3\text{H-L-histidine}$  uptake rates comparable to the DMSO control (Fig. 4A). However, cells treated with the proton ionophores carbonyl cyanide *m*-chlorophenyl hydrazine (CCCP) or 2,4-dinitrophenol (DNP) were not able to accumulate detectable amounts of  $^3\text{H-L-histidine}$  (Fig. 4A). The results suggest that transport catalyzed by HutT is an energy-dependent process that seems to depend on an (electro)chemical proton gradient. Besides ionophores, the effect of the sulfhydryl reagent *N*-ethylmaleimide (NEM) on HutT activity was analyzed. Addition of NEM reduced the initial rate of  $^3\text{H-L-histidine}$  uptake to about 30% of the values obtained for the control (Fig. 4A). The result can be interpreted as an indication that at least one of the three native cysteine residues [Cys140 (TM 4), Cys262

(TM 7), Cys456 (C-terminal region) of HutT is located at or near a site critical for function. However, none of these cysteine residues are conserved within the APC superfamily.

The substrate specificity of HutT was tested by recording  $^3\text{H-L-histidine}$  uptake into *E. coli* JW2306 transformed with plasmid pT7-5-*hutT6H* in the presence of a 100fold molar excess of potential substrates (Fig. 4B and Fig. S4). While the addition of nonradioactive L-histidine competed with the uptake of the  $^3\text{H}$ -labeled compound and inhibited transport strongly, the presence of the positively charged amino acids arginine and lysine as well as of cyclic proline did not significantly affect the uptake of  $^3\text{H-L-histidine}$  (Fig. 4B). Furthermore, compounds structurally related to histidine such as imidazole (Imi), 3-amino-1,2,4-triazole (3AT), and urocanate (Uro) did not have significant effects on  $^3\text{H-L-histidine}$  uptake. Only 1,2,4-triazolyl-3-alanine (TRA) reduced the rate of  $^3\text{H-L-histidine}$  uptake significantly (Fig. 4B). We concluded from these results that HutT is highly specific for histidine, thereby imidazole ring, amino, and carboxyl group are crucial for binding.

### Purification and reconstitution of HutT

To unequivocally test the function of HutT, the membrane protein was purified and reconstituted in proteoliposomes. For this purpose, *hutT* was cloned into plasmid pET21a and expressed in *E. coli* BL21 pLysS. Membranes containing the resulting protein with a C-terminal 6His tag were prepared, solubilized with 1% (w/v) *n*-dodecyl- $\beta$ -maltoside (DDM), and purified by Ni-NTA affinity chromatography followed by size exclusion chromatography with a Superdex200 column. The resulting protein was about 90% pure but had a high tendency to aggregate as shown by SDS/PAGE and size exclusion chromatography (Fig. 5). The main peak in the size exclusion chromatogram (11.8 mL elution volume) corresponded to an apparent molecular weight ( $M_r$ ) of about 250 kDa (HutT monomer: 50 kDa). This observation is reminiscent of the structurally well-characterized HutT homolog AdiC of *Escherichia coli* (AdiC monomer: 47 kDa), which is known to be homodimeric and yields in complex with DDM and adhering phospholipids a  $M_r$  of 257 kDa in size exclusion chromatography [32,33]. Higher state oligomers observed here with HutT were probably the result of unspecific aggregation (Fig. 5).

For reconstitution, preformed liposomes prepared from *E. coli* polar lipid extract were destabilized with 0.3% (w/v) Triton X-100 and mixed with purified HutT at a lipid to protein ratio of 50 to 1 (w/w). The

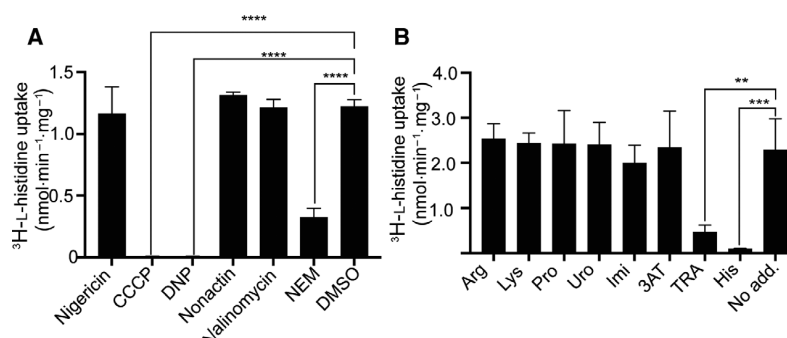


**Fig. 4.** Properties of the HutT-dependent transport of <sup>3</sup>H-L-histidine. (A) Effect of ionophores and the sulfhydryl reagent N-ethylmaleimide (NEM) on the initial rate of <sup>3</sup>H-L-histidine uptake into *E. coli* JW2306 cells expressing *hutT* from plasmid pT7-5-*hutT6H*. Cells transformed with pT7-5 served as negative control. Transport was measured as described in the legend of Fig. 3A except that cells were not preincubated with D-lactate but with the ionophores nigericin (6 μM), m-chlorophenyl hydrazine (CCCP, 20 μM), 2,4-dinitrophenol (DNP, 2 mM), nonactin (10 μM), valinomycin (2 μM), or NEM (2 mM) for 30 min. Since ionophores were dissolved in dimethyl sulfoxide (DMSO), cell suspensions supplemented with DMSO without inhibitors were used for comparison. (B) Impact of amino acids and compounds structurally related to histidine on the initial rates of HutT-dependent <sup>3</sup>H-L-histidine uptake into *E. coli* JW2306 cells. Transport was measured as described in Fig. 3A in the presence of a 100fold molar excess (100 μM) of amino acids (arginine, lysine, proline), urocanate (Uro), imidazole (Imi), 3-amino-1,2,4-triazole (3AT) or 1,2,4-triazolyl-3-alanine (TRA) (cp. structures in Fig. S3). For all experiments, standard deviations were calculated from minimum three independent experiments. Student's t-test was applied for statistical analyses. \*=*P* ≤ 0.05, \*\*=*P* ≤ 0.01, \*\*\*=*P* ≤ 0.001, \*\*\*\*=*P* ≤ 0.0001.

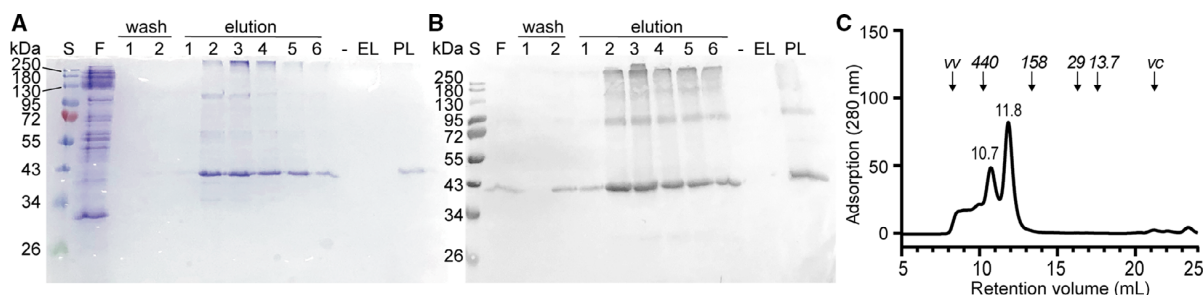


**Fig. 5.** Purification of HutT. The *hutT* gene was expressed in *E. coli* BL21 pLysS from plasmid pET21a-*hutT6H*. HutT was solubilized with 1% DDM from membranes of the strain and purified by Ni-NTA affinity chromatography (A) Coomassie stained SDS-PAGE gel of steps of the purification protocol. (B) Western blot analysis of the steps of the purification protocol shown in (A). Detection was performed with anti-PentaHis antibody and α-mouse antibody with alkaline phosphatase. S, protein standard; F, Ni-NTA flow through; wash, fractions of column wash; elution, elution fractions; EL, liposomes without HutT; PL, proteoliposomes containing HutT. (C) Size exclusion chromatography of the elution fraction 2 of the Ni-NTA affinity chromatography. Shown is the elution profile of a Superdex200 column. The arrows represent the position of Blue dextran (vv, void volume), ferritin (440 kDa), aldolase (158 kDa), carbonic anhydrase (29 kDa), ribonuclease A (13.7 kDa), acetone (vc, geometric column volume).

reconstitution process was completed by stepwise adsorption of detergents on polystyrene beads followed by washing of the resulting proteoliposomes with buffer. The presence of HutT in the proteoliposome preparations was confirmed by SDS/PAGE and western blot analyses (Fig. 5A and B).

### Transport in proteoliposomes

To test the functionality of reconstituted HutT, uptake of <sup>3</sup>H-L-histidine into HutT containing

proteoliposomes was analyzed in the presence of different driving forces. Proteoliposomes were loaded with 0.1 M KP<sub>i</sub> pH 7.5. A membrane potential (Δψ, negative inside) and desired ion gradients were imposed across the proteoliposome membrane by creating an outwardly directed diffusion gradient of potassium ions with valinomycin and changing the ionic composition and/or pH of the buffer into which the proteoliposomes were diluted. We found that the imposition of an inwardly directed electrochemical proton gradient (Δψ + ΔpH) stimulated the rate of

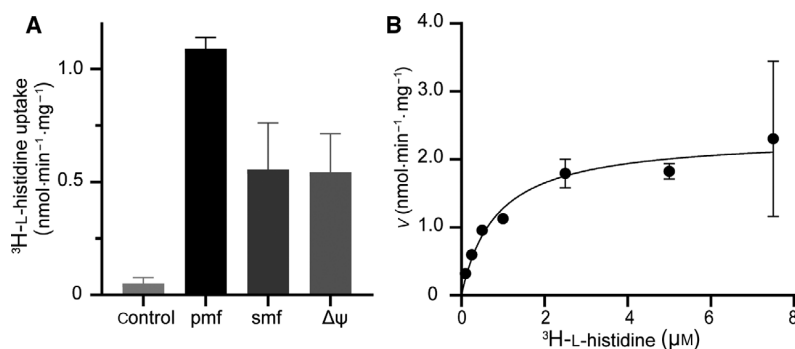


**Fig. 6.** HutT-catalyzed uptake of <sup>3</sup>H-L-histidine into proteoliposomes. (A) Initial rates of <sup>3</sup>H-L-histidine uptake in the presence of different driving forces. Proteoliposomes reconstituted with purified HutT were resuspended in 100 mM KPi pH 7.5, 5 mM MgSO<sub>4</sub>, 2 mM β-mercaptoethanol and extruded through filters with a 400 nm pore diameter. To initiate transport, 2 μL aliquots of the proteoliposome suspension (0.9 mg protein/mL) were diluted 200fold into 400 μL of given transport buffers all containing 0.2 μM valinomycin and 1 μM <sup>3</sup>H-L-histidine (500 Ci mol<sup>-1</sup>). Transport was stopped after 30 s, proteoliposomes were collected and washed by rapid filtration, and radioactivity was determined with a β-counter. Selected driving forces were established by dilution into the following transport buffers: 100 mM Tris/MES pH 7.5 (Δψ), 100 mM Tris/MES pH 6.0 (proton motive force, pmf), 100 mM Tris/MES pH 7.5 + 50 mM NaCl (sodium motive force, smf), or 100 mM KPi pH 7.5 (facilitated diffusion/unspecific binding, control). (B) Michaelis-Menten kinetics of <sup>3</sup>H-L-histidine uptake into proteoliposomes. Initial rates of transport were measured under the conditions described in (A) with <sup>3</sup>H-L-histidine concentrations ranging from 0.1 to 7.5 μM, and kinetic parameters were calculated with GRAPHPAD Prism. For all experiments, standard deviations were calculated from three experiments.

<sup>3</sup>H-L-histidine uptake into the proteoliposomes 21fold compared to measurements in the absence of both ion gradient and Δψ (control) (Fig. 6A). Imposition of only Δψ or of an inwardly directed electrochemical sodium ion gradient (Δψ + Δ[Na<sup>+</sup>]) stimulated the uptake of <sup>3</sup>H-L-histidine 10 to 11fold (Fig. 6A). The results indicated that HutT catalyzes an active transport process and provide further evidence that <sup>3</sup>H-L-histidine transport is driven by an electrochemical proton gradient.

Next the kinetics of <sup>3</sup>H-L-histidine uptake into proteoliposomes were analyzed according to Michaelis and Menten. For this purpose, initial rates of uptake were determined at <sup>3</sup>H-L-histidine concentrations between 0.1 and 7.5 μM in the presence of an inwardly directed electrochemical proton gradient (Fig. 6B). The analysis yielded a saturation curve with a maximum rate of <sup>3</sup>H-L-histidine uptake ( $V_{max}$ ) of  $2.34 \pm 0.23$  nmol mg<sup>-1</sup> min<sup>-1</sup>. The histidine concentration at which the uptake proceeded at half-maximal speed (apparent  $K_M$ ) was determined to be  $0.83 \pm 0.25$  μM. These parameters were in good agreement with those obtained with intact cells (Fig. 3B).

### Amino acids important for HutT function

To get a first idea on amino acids potentially important for HutT function, the amino acid sequence was aligned with the sequences of members of the APC

superfamily including transporters of the AAT family (TC 2.A.3.1) as well as two members of the archaeal/bacterial transporter (ABT) family (TC 2.A.3.6), the cationic amino acid transporters of *Methanococcus jannaschii* (MjApcT) and *Geobacillus kaustophilus* (GkApcT) (Fig. S4). MjApcT (apo state) and GkApcT (with bound alanine) were previously crystallized [34,35]. Based on conservation and functional significance in other members of the family, five amino acids (Thr27, Glu98, Lys156, Phe212, and Glu218) of HutT of *P. putida* KT2440 were selected for replacement analysis (Table 1).

With the exception of Glu98, all amino acids were found to be important for HutT function (Fig. 7A). In more detail, replacement of Thr27 by alanine, serine, or asparagine reduced the HutT-dependent initial rate of <sup>3</sup>H-L-histidine uptake into *E. coli* JW2306 to values between 20 and 60% of the wild-type activity. Substitution of Lys156 by alanine or glutamine reduced transport to less than 10%, and by arginine to about 40% of the wild-type value suggesting that a positive charge at this site is important for function. Replacement of Phe212 with alanine or glutamine, or of Glu218 with alanine or glutamine reduced the transport activity below the detection limit. However, HutT with tyrosine at the position of Phe212 was as active as the wild type indicating that an aromatic amino acid is required for function at this position. Similarly, HutT with aspartate at the position of Glu218

**Table 1.** Possible functions of amino acids replaced in HutT of *P. putida* KT2440. The information is based on amino acid sequence alignment (Fig. S4) and comparison with structural and functional data from other members of the APC family. aa, amino acid; GkApcT, ApcT of *G. kaustophilus*; MjApcT, ApcT of *M. jannaschii*; EcLysP, LysP of *E. coli*.

aa in HutT of <i>P. putida</i>	Related aa (APC transporter)	Proposed function of aa in transport cycle	References
Thr27 (TM 1)	Thr43 (GkApcT)	Part of a gate sealing the binding site from the extracellular side of the membrane	[34]
Glu98 (TM 3)	Glu115 (GkApcT)	Coupling of proton and substrate transport	[34]
Lys156 (TM 5)	Lys191 (GkApcT)	Substitute for Na <sup>+</sup> in the Na2 site of sodium ion-dependent transporters	[34]
	Lys168 (MjApcT)		[35]
	Lys163 (EcLysP)		[40]
Phe212 (TM 6)	Phe231 (GkApcT)	Part of a gate sealing the binding site from the extracellular side of the membrane	[34]
Glu218 (TM 6)	Asp237 (GkApcT) & Glu222 (EcPutP)	Coupling of proton and substrate transport	[34]
			[40]

catalyzed <sup>3</sup>H-L-histidine uptake with about 70% of the rate of wild type indicating that a negative charge is imported at this position (Fig. 7A).

To test whether the mutations and the resulting amino acid substitutions affected the amount of HutT in the membrane, cells of the transport experiment were disrupted and membranes were prepared. The amount of HutT in the membranes was detected by SDS/PAGE and western blotting. By this means, it was shown that all HutT variants were present in the membrane in amounts comparable to wild-type HutT (Fig. 7B and Fig. S3).

In conclusion, transport defects observed upon given amino acid substitutions were not due to reduced amounts of HutT in the membrane but to defects in the transport cycle. Comparing these results with those published on GkApcT [34], we speculate that Thr27 and Phe212 of HutT are located at or close to the histidine binding site and participate in substrate binding and/or the gating mechanism. Furthermore, the positive charge of Lys156 may mimic a sodium ion localized in the Na2 site of sodium-dependent transporters with a LeuT fold, while Glu218 may play a role in proton coupling.

### Discussion

The putative histidine transporter HutT of *P. putida* KT2440 was functionally characterized. Transport measurements with intact cells and the purified and reconstituted transporter demonstrated that HutT is able to catalyze the uptake of L-histidine. The pattern of the effect of ionophores and of different potential driving forces on the uptake suggest that L-histidine transport is driven by a proton motive force. The low apparent  $K_M$  for L-histidine (about 1 μM) hints at a

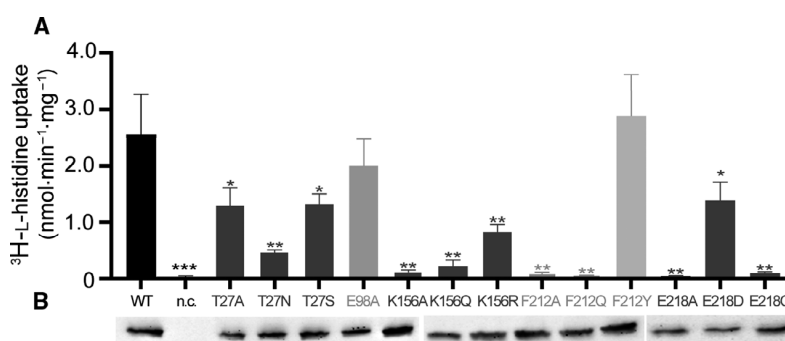


**Fig. 7.** Effects of individual amino acid substitutions on the initial rate of uptake of <sup>3</sup>H-L-histidine into in *E. coli* JW2306 transformed with pT7-5-*hutT6H* encoding HutT with given amino acid substitutions. (A) Transport was measured as described in the legend of Fig. 3A. Transport was initiated by addition of <sup>3</sup>H-L-histidine at a final concentration of 1 μM. Shown are mean values and standard deviations of the initial rates (10 s) of transport calculated from three independent experiments. Student's t-test was applied for statistical analyses. \*= $P \leq 0.05$ , \*\*= $P \leq 0.01$ , \*\*\*= $P \leq 0.001$ , \*\*\*\*= $P \leq 0.0001$ . (B) Representative western blot analysis of HutT6H and its variants in membranes prepared from cells used for the transport experiments presented in Fig. 7A. Fifty μg total membrane protein were applied per lane. HutT6H was detected with anti-6His antibody and α-mouse antibody coupled to horse radish peroxidase. All HutT variants were compared to wild-type HutT. Membranes without HutT served as negative control (n.c.). Complete western blots are shown in Fig. S2.

high affinity of the transporter for the amino acid. A similar  $K_M$  value was previously determined for HutT<sub>h</sub> of *P. fluorescens* SBW25 [10]. Furthermore, we found that HutT is highly specific for L-histidine. The ring structure, amino, and carboxyl group proved crucial for competition with L-histidine in transport measurements. Only a modification of the ring (triazole instead of imidazole) is tolerated by HutT.

A proton-coupled amino acid uptake has also been proposed for other members of the APC family including, for example, PheP and AroP of *E. coli*, MjApcT, and GkApcT [34–37] while other members of the family function as solute : solute antiporters [38]. The amino acid : proton symporters of the APC family differ significantly in substrate specificity. HutT (histidine) is like LysP (lysine) and PheP (phenylalanine) specific for one amino acid, while AroP (aromatic amino acids), MjApcT (broad spectrum of amino acids) and GkApcT (preferentially small hydrophobic and polar amino acids) exhibit a much broader substrate specificity [34,35,39–41].

The observation that a proton gradient but not a sodium ion gradient stimulates the uptake of L-histidine by HutT is in agreement with the lack of conserved binding sites for sodium ions as proposed for sodium ion-dependent transporters with a LeuT folding motif [42–45]. Instead, we find that a positively charged amino acid [lysine (native) or arginine] at position 156 in TM 5 of HutT is of particular importance for histidine uptake. The lysine residue is highly conserved within the APC family and was previously shown to be of functional significance also for MjApcT (K158), GkApcT (K191), and LysP (K163) [34,35,40] (Fig. S4). A structural alignment of MjApcT with sodium ion-dependent transporters with a LeuT folding motif located the lysine residue in a position equivalent to the sodium ion in the Na2 site of LeuT and suggested that the positively charged amino group of the side chain of lysine fulfills similar functions as a sodium ion at the corresponding site of a sodium ion-dependent transport system [35]. Our results with HutT further extend the idea that these transporters use common mechanistic principles for function.

Previous analyses of GkApcT implicate the functionally important acidic amino acids Glu115 and Asp237 in proton coupling, thereby Glu115 is suggested to directly participate in proton translocation [34]. However, replacement of the amino acid corresponding to Glu115 in HutT (Glu98 in TM 3) has only little impact on L-histidine transport indicating that the residue does not play a key role in proton coupling in HutT (Fig. 7). On the contrary, a negative charge at position 218 [glutamate (native) or aspartate]

in TM 6 seems to be essential for transport. The precise role of Glu218 in HutT and the corresponding Asp237 in GkApcT in the transport cycle remains enigmatic since the acidic residue is conserved also in transporters that are not proton coupled [34].

Furthermore, we speculate that the functionally important amino acids Thr27 (TM 1) and Phe212 (TM 6) of HutT function as gating residues that seal the substrate-binding site from the extracellular side of the membrane similar as proposed for Thr43 and Phe231 of GkApcT [34]. The results are in good agreement with the pivotal role of core TMs 1 and 6 in substrate binding and translocation described for transporters with a LeuT like folding motif [42,45–48].

While none of the native cysteine residues in well-characterized secondary transporters such as, for example, LacY, PutP, and CaiT proved to be essential for transport, modification of sulfhydryl groups by alkylating reagents like NEM can inhibit transport [49–52]. HutT is also inhibited by NEM, probably by modification of one or more of the native cysteine residues (Cys140, Cys262, Cys456). We speculate that this modification could block functionally important conformational changes and/or access to the ligand-binding site. Indeed, Cys456 is located in TM 7 near a conserved tyrosine residue that contributes to substrate binding in ABT transporters [34]. To find out which cysteines of HutT are functionally important, individual amino acid exchanges are required.

Finally, our growth experiments confirm the significance of HutT as an uptake system for L-histidine. The severe growth defect observed upon deletion of the *hutT* gene suggests that HutT is the main L-histidine transporter of *P. putida* KT2440. Neither the sensor kinase CbrA with its previously described L-histidine specific transport activity [18] nor other not yet characterized putative histidine transporters can compensate for the loss of HutT function.

## Acknowledgment

Research in the group of HJ is supported by the Deutsche Forschungsgemeinschaft, projects JU333/5-2 and JU333/6-1, and the Faculty of Biology, LMU Munich. We thank Prof. Thomas Brüser, Leibniz University Hannover, Germany, for kindly providing plasmid pUCP20-ANT2-MCS.

## Data accessibility

The data that support the findings of this study are available from the corresponding authors upon reasonable request.

### Author contribution

LW and HJ planned and supervised the experiments; LW and ME generated the strains and plasmids; LW performed the growth analysis; A-KB and ME performed transport measurements; LW purified and reconstituted protein; LW and ME performed the DRaCALA; HJ performed bioinformatic analysis; LW and HJ wrote the manuscript; All authors reviewed the results and approved the final version of the manuscript.

### References

- 1 Bender RA (2012) Regulation of the histidine utilization (Hut) system in bacteria. *Microbiol Mol Bio Rev* **76**, 565–584.
- 2 Itoh Y, Nishijyo T and Nakada Y (2007) In Histidine catabolism and catabolite regulation in *Pseudomonas*: A Model System in Biology (Ramos J-L and Filloux A, eds), pp. 371–395. Springer, Netherlands, Dordrecht.
- 3 Lonergan ZR, Palmer LD and Skaar EP (2020) Histidine utilization is a critical determinant of *Acinetobacter* pathogenesis. *Infect Immun* **88**, e00118–e120.
- 4 Zhang XX, Ritchie SR and Rainey PB (2014) Urocanate as a potential signaling molecule for bacterial recognition of eukaryotic hosts. *Cell Mol Life Sci* **71**, 541–547.
- 5 Rietsch A, Wolfgang MC and Mekalanos JJ (2004) Effect of metabolic imbalance on expression of type III secretion genes in *Pseudomonas aeruginosa*. *Infect Immun* **72**, 1383–1390.
- 6 Bais HP, Weir TL, Perry LG, Gilroy S and Vivanco JM (2006) The role of root exudates in rhizosphere interactions with plants and other organisms. *Annu Rev Biophys* **57**, 233–266.
- 7 Phillips DA, Fox TC, King MD, Bhuvaneshwari TV and Teuber LR (2004) Microbial products trigger amino acid exudation from plant roots. *Plant Physiol* **136**, 2887–2894.
- 8 Bacilio-Jiménez M, Aguilar-Flores S, Ventura-Zapata E, Pérez-Campos E, Bouquelet S and Zenteno E (2003) Chemical characterization of root exudates from rice (*Oryza sativa*) and their effects on the chemotactic response of endophytic bacteria. *Plant Soil* **249**, 271–277.
- 9 Zhang XX, George A, Bailey MJ and Rainey PB (2006) The histidine utilization (*hut*) genes of *Pseudomonas fluorescens* SBW25 are active on plant surfaces, but are not required for competitive colonization of sugar beet seedlings. *Microbiology* **152**, 1867–1875.
- 10 Zhang XX, Chang H, Tran SL, Gauntlett JC, Cook GM and Rainey PB (2012) Variation in transport explains polymorphism of histidine and urocanate utilization in a natural *Pseudomonas* population. *Enviro Microbiol* **14**, 1941–1951.
- 11 Ardeshir F and Ames GF-L (1980) Cloning of the histidine transport genes from *Salmonella typhimurium* and characterization of an analogous transport system in *Escherichia coli*. *J Supramol Struct* **13**, 117–130.
- 12 Ames GF-L (1985) The histidine transport system of *Salmonella typhimurium*. *Curr Top Membr Trans* **23**, 103–119.
- 13 Ames GF and Roth JR (1968) Histidine and aromatic permeases of *Salmonella typhimurim*. *J Bacteriol* **96**, 1742–1749.
- 14 Zhang X-X, Gauntlett JC, Oldenburg DG, Cook GM and Rainey PB (2015) Role of the transporter-like sensor kinase CbrA in histidine uptake and signal transduction. *J Bacteriol* **197**, 2867–2878.
- 15 Liao MK, Gort S and Maloy S (1997) A cryptic proline permease in *Salmonella typhimurium*. *Microbiology* **143**, 2903–2911.
- 16 Jung H (2002) The sodium/substrate symporter family: structural and functional features. *FEBS Lett* **529**, 73–77.
- 17 Reizer J, Reizer A and Saier MH Jr (1994) A functional superfamily of sodium/solute symporters. *Biochim Biophys Acta* **1197**, 133–166.
- 18 Wirtz L, Eder M, Schipper K, Rohrer S and Jung H (2020) Transport and kinase activities of CbrA of *Pseudomonas putida* KT2440. *Sci Rep* **10**, 5400.
- 19 Jack DL, Paulsen IT and Saier MH (2000) The amino acid/polyamine/organocation (APC) superfamily of transporters specific for amino acids, polyamines and organocations. *Microbiology* **146**, 1797–1814.
- 20 Wong FH, Chen JS, Reddy V, Day JL, Shlykov MA, Wakabayashi ST and Saier JMH (2012) The amino acid-polyamine-organocation superfamily. *J Mol Microb Biotech* **22**, 105–113.
- 21 Vastermark A, Wollwage S, Houle ME, Rio R and Saier MH Jr (2014) Expansion of the APC superfamily of secondary carriers. *Proteins* **82**, 2797–2811.
- 22 Shi Y (2013) Common folds and transport mechanisms of secondary active transporters. *Annu Rev Biophys* **42**, 51–72.
- 23 Penmatsa A and Gouaux E (2014) How LeuT shapes our understanding of the mechanisms of sodium-coupled neurotransmitter transporters. *J Physiol* **592**, 863–869.
- 24 Nelson KE, Weinel C, Paulsen IT, Dodson RJ, Hilbert H, Martins dos Santos VA, Fouts DE, Gill SR, Pop M, Holmes M et al. (2002) Complete genome sequence and comparative analysis of the metabolically versatile *Pseudomonas putida* KT2440. *Environ Microbiol* **4**, 799–808.
- 25 Belda E, van Heck RG, Jose Lopez-Sanchez M, Cruveiller S, Barbe V, Fraser C, Klenk HP, Petersen J, Morgat A, Nikel PI et al. (2016) The revisited genome

- of *Pseudomonas putida* KT2440 enlightens its value as a robust metabolic chassis. *Environ Microbiol* **18**, 3403–3424.
- 26 Lassak J, Henche AL, Binnenkade L and Thormann KM (2010) ArcS, the cognate sensor kinase in an atypical Arc system of *Shewanella oneidensis* MR-1. *Appl Environ Microbiol* **76**, 3263–3274.
  - 27 Baba T, Ara T, Hasegawa M, Takai Y, Okumura Y, Baba M, Datsenko KA, Tomita M, Wanner BL and Mori H (2006) Construction of *Escherichia coli* K-12 in-frame, single-gene knockout mutants: the Keio collection. *Mol Syst Biol* **2**, 2006.0008–2006.0008.
  - 28 Hoffmann L, Sugue MF and Bruser T (2021) A tunable anthranilate-inducible gene expression system for *Pseudomonas* species. *Appl Microbiol Biotechnol* **105**, 247–258.
  - 29 Peterson GL (1977) A simplification of the protein assay method of Lowry which is more generally applicable. *Anal Biochem* **83**, 346–356.
  - 30 Jung H, Tebbe S, Schmid R and Jung K (1998) Unidirectional reconstitution and characterization of purified Na<sup>+</sup>/proline transporter of *Escherichia coli*. *Biochemistry* **37**, 11083–11088.
  - 31 Roelofs KG, Wang J, Sintim HO and Lee VT (2011) Differential radial capillary action of ligand assay for high-throughput detection of protein-metabolite interactions. *Proc Natl Acad Sci USA* **108**, 15528–15533.
  - 32 Ilgu H, Jeckelmann JM, Gachet MS, Boggavarapu R, Ucurum Z, Gertsch J and Fotiadis D (2014) Variation of the detergent-binding capacity and phospholipid content of membrane proteins when purified in different detergents. *Biophys J* **106**, 1660–1670.
  - 33 Fang Y, Kolmakova-Partensky L and Miller C (2007) A bacterial arginine-agsmatine exchange transporter involved in extreme acid resistance. *J Biol Chem* **282**, 176–182.
  - 34 Jungnickel KEJ, Parker JL and Newstead S (2018) Structural basis for amino acid transport by the CAT family of SLC7 transporters. *Nat Commun* **9**, 550–550.
  - 35 Shaffer PL, Goehring A, Shankaranarayanan A and Gouaux E (2009) Structure and mechanism of a Na<sup>+</sup>-independent amino acid transporter. *Science* **325**, 1010–1014.
  - 36 Pi J, Wookey PJ and Pittard AJ (1993) Site-directed mutagenesis reveals the importance of conserved charged residues for the transport activity of the PheP permease of *Escherichia coli*. *J Bacteriol* **175**, 7500–7504.
  - 37 Cosgriff AJ and Pittard AJ (1997) A topological model for the general aromatic amino acid permease, AroP, of *Escherichia coli*. *J Bacteriol* **179**, 3317–3323.
  - 38 Wong FH, Chen JS, Reddy V, Day JL, Shlykov MA, Wakabayashi ST and Saier MH Jr (2012) The amino acid-polyamine-organocation superfamily. *J Mol Microbiol Biotechnol* **22**, 105–113.
  - 39 Pi J, Wookey PJ and Pittard AJ (1991) Cloning and sequencing of the *pheP* gene, which encodes the phenylalanine-specific transport system of *Escherichia coli*. *J Bacteriol* **173**, 3622–3629.
  - 40 Rauschmeier M, Schuppel V, Tetsch L and Jung K (2014) New insights into the interplay between the lysine transporter LysP and the pH sensor CadC in *Escherichia coli*. *J Mol Biol* **426**, 215–229.
  - 41 Trip H, Mulder NL and Lolkema JS (2013) Cloning, expression, and functional characterization of secondary amino acid transporters of *Lactococcus lactis*. *J Bacteriol* **195**, 340–350.
  - 42 Yamashita A, Singh SK, Kawate T, Jin Y and Gouaux E (2005) Crystal structure of a bacterial homologue of Na<sup>+</sup>/Cl<sup>-</sup>-dependent neurotransmitter transporters. *Nature* **437**, 215–223.
  - 43 Wahlgren WY, Dunevall E, North RA, Paz A, Scalise M, Bisignano P, Bengtsson-Palme J, Goyal P, Claesson E, Caing-Carlsson R *et al.* (2018) Substrate-bound outward-open structure of a Na<sup>+</sup>-coupled sialic acid symporter reveals a new Na<sup>+</sup> site. *Nat Commun* **9**, 1753.
  - 44 Henriquez T, Wirtz L, Su D and Jung H (2021) Prokaryotic solute/sodium symporters: versatile functions and mechanisms of a transporter family. *Int J Mol Sci* **22**, 1880.
  - 45 Forrest LR, Kramer R and Ziegler C (2011) The structural basis of secondary active transport mechanisms. *Biochim Biophys Acta* **1807**, 167–188.
  - 46 Pirch T, Landmeier S and Jung H (2003) Transmembrane domain II of the Na<sup>+</sup>/proline transporter PutP of *Escherichia coli* forms part of a conformationally flexible, cytoplasmic exposed aqueous cavity within the membrane. *J Biol Chem* **278**, 42942–42949.
  - 47 Bracher S, Schmidt CC, Dittmer SI and Jung H (2016) Core transmembrane domain 6 plays a pivotal role in the transport cycle of the sodium/proline symporter PutP. *J Biol Chem* **291**, 26208–26215.
  - 48 Faham S, Watanabe A, Besserer GM, Cascio D, Specht A, Hirayama BA, Wright EM and Abramson J (2008) The crystal structure of a sodium galactose transporter reveals mechanistic insights into Na<sup>+</sup>/sugar symport. *Science* **321**, 810–814.
  - 49 Bracher S, Hilger D, Guerin K, Polyhach Y, Jeschke G, Krafczyk R, Giacomelli G and Jung H (2019) Comparison of the functional properties of trimeric and monomeric CaiT of *Escherichia coli*. *Sci Rep* **9**, 3787.
  - 50 Jung H, Rübenhagen R, Tebbe S, Leifker K, Tholema N, Quick M and Schmid R (1998) Topology of the Na<sup>+</sup>/proline transporter of *Escherichia coli*. *J Biol Chem* **273**, 26400–26407.
  - 51 van Iwaarden PR, Pastore JC, Konings WN and Kaback HR (1991) Construction of a functional lactose

- permease devoid of cysteine residues. *Biochemistry* **30**, 9595–9600.
- 52 Kaback HR (2021) It's better to be lucky than smart. *Annu Rev Biochem* **90**, 1–29.
- 53 Hu L and Phillips AT (1988) Organization and multiple regulation of histidine utilization genes in *Pseudomonas putida*. *J Bacteriol* **170**, 4272–4279.
- 54 Viklund H and Elofsson A (2008) OCTOPUS: improving topology prediction by two-track ANN-based preference scores and an extended topological grammar. *Bioinformatics* **24**, 1662–1668.
- 55 Kelley LA, Mezulis S, Yates CM, Wass MN and Sternberg MJ (2015) The Phyre2 web portal for protein modeling, prediction and analysis. *Nat Protoc* **10**, 845–858.
- Table S1.** Strains used in this investigation.
- Table S2.** Plasmids used in this investigation.
- Table S3.** Oligonucleotides used in this investigation.
- Fig. S1.** Impact of the concentration of the inducer anthranilic acid on growth of *P. putida* KT2440  $\Delta hutT$  harboring plasmid pUCP20-ANT2-*hutT6H*.
- Fig. S2.** Complete Western Blots of the HutT variants shown in Fig. 7B.
- Fig. S3.** Molecular structures of compounds used to test the substrate specificity of HutT (Fig. 4B).
- Fig. S4.** Alignment of amino acid sequences of HutT of *P. putida* KT2440 and other transporters of the APC family.

## Supporting information

Additional supporting information may be found online in the Supporting Information section at the end of the article.

## Supplementary Information

### Functional characterization of the putative histidine transporter HutT of *Pseudomonas putida* KT2440

Larissa Wirtz<sup>1</sup>, Michelle Eder<sup>1</sup>, Anna-Katharina Brand<sup>1</sup> and Heinrich Jung<sup>1†</sup>

<sup>1</sup>Division of Microbiology, Department of Biology 1, Ludwig Maximilians University Munich,  
D-82152 Martinsried, Germany

Materials included:

**Table S1.** Strains used in this investigation.

**Table S2.** Plasmids used in this investigation.

**Table S3.** Oligonucleotides used in this investigation.

**Fig. S1.** Impact of the concentration of the inducer anthranilic acid on growth of *P. putida* KT2440  $\Delta hutT$  harboring plasmid pUCP20-ANT2-*hutT6H*.

**Fig. S2.** Complete Western Blots of the HutT variants shown in Fig. 7B.

**Fig. S3.** Molecular structures of compounds used to test the substrate specificity of HutT (Fig. 4B).

**Fig. S4.** Alignment of amino acid sequences of HutT of *P. putida* KT2440 and other transporters of the APC family.

**Supplementary References**

**Table S1.** Strains used in this investigation.

Strain	Description	Source/Reference
<i>Escherichia coli</i> DH5 $\alpha$	F <sup>-</sup> endA1 glnV44 thi-1 recA1 relA1 gyrA96 deoR nupG $\Phi$ 80dlacZ $\Delta$ M15 $\Delta$ (lacZYA-argF)U169, hsdR17(r <sub>K</sub> <sup>-</sup> m <sub>K</sub> <sup>+</sup> ), $\lambda$ -	[1]
<i>Escherichia coli</i> DH5 $\alpha$ $\lambda$ pir	endA1 hsdR17 glnV44 (= supE44) thi-1 recA1 gyrA96 relA1 $\phi$ 80dlac $\Delta$ (lacZ)M15 $\Delta$ (lacZYA-argF)U169 zdg-232::Tn10 uidA::pir+	[2]
<i>Escherichia coli</i> WM3064	thrB1004 pro thi rpsL hsdS lacZ $\Delta$ M15 RP4-1360 $\Delta$ (araBAD)567 $\Delta$ dapA1341::[erm pir]	[3]
<i>Escherichia coli</i> BL21 (DE3) pLysS	<i>E. coli</i> B dcm ompT hsdS(rB-mB) gal pLysS, Cm <sup>R</sup>	Novagen
<i>Escherichia coli</i> K12 JW2306	$\Delta$ hisJ Kan <sup>R</sup>	[4]
<i>Escherichia coli</i> C43 (DE3)	<i>E. coli</i> B F <sup>-</sup> ompT gal dcm hsdSB(rab- mB-)(DE3)	Lucigen
<i>Pseudomonas putida</i> KT2440		[5, 6]
<i>Pseudomonas putida</i> KT2440 LW1	$\Delta$ cbrA $\Delta$ hutT $\Delta$ hutH $\Delta$ PP_3558 $\Delta$ PP_3559	[7]
<i>Pseudomonas putida</i> KT2440 $\Delta$ hutT	$\Delta$ hutT (PP_5031)	This work

**Table S2.** Plasmids used in this investigation.

Plasmid	Description	Source/Reference
pNPTS138-R6KT	mobRP4 <sup>+</sup> ori-R6K sacB; suicide plasmid for in-frame deletions; Kan <sup>R</sup> (npt1)	[8]
pET21a	N-terminal T7-tag, C-terminal 6His tag, Amp/Carb <sup>R</sup> , lacI, T7 promoter	Novagen

pET21a- <i>hutT6H</i>	<i>hutT</i> in pET21a	This work
pT7-5	<i>lac</i> promoter, Amp/Carb <sup>R</sup>	[9]
pT7-5- <i>hutT6H</i>	<i>hutT</i> in pT7-5, C-terminal 6His tag	This work
pUCP20-ANT2-MCS	pUCP20 with <i>antA</i> promoter, Kan <sup>R</sup>	[10]
pUCP20-ANT2- <i>hutT6H</i>	<i>hutT</i> in pUCP20-ANT2-MCS, C-terminal 6His tag	This work

**Table S3.** Oligonucleotides used in this investigation. Restriction sites are marked in red, overlapping regions for overlap PCR are marked in grey.

Oligonucleotides	Sequence (5'→3')
hutT_s_NdeI	CAATTCAAGGACGTcAtATGCAACAAGCTC
hutT_as_XhoI	AATCTCCTTctcgAGCGGTGCAGC
pET21a_s2	CGATCCCGCGAAATTAATACG
pet21as	CTAGTTATTGCTCAGCGG
hutT_BamHI_delXhoI_s	ATTCAAGGAgGatcCATGCAACAAGCTCAAGGTCTgAAaCGCGGGCTAAGTG
hutT_XhoI3_as	CACAATCTaCTcgaggcGCGGTGCAGC
hutTseq359s	AGGTAGCCCGCTGGATCTGG
hutTseq869s	TCGTGGTGATTTCCGCTGCCATC
hutTseq1262s	TCGGTTACTTCCCGGACACC
1935 as	CAGGCAACTATGGATGAACGA
pUC19510as	CTCCGGCTCGTATGTTGTGT
Lac_P_60_s	AACTTAATCGCCTTGCAGCAC
DelhutTA_s	TTCCTGGTGGAAATTCGGTGGGGTCAAC
DelhutTA_as	CCGCTACCGGACCTTGAGCTTGTTCATGTC
DelhutTB_as	CGCCGGCCAAGATCCGCAACATCTCGTC
DelhutTB_s	AGCTCAAGGTCCGGTAGCGGAGCCGGCCGAGCTG
5031_checkBs	TTCGGCATGCAGCTTGACCGG
5031_checkAas	CCGAAATCGGCTCGCTCAGCG
bla_as	CAGGCAACTATGGATGAACGA
T27A sense	CATCGGCGCAGGCCTTTTC
T27A antisense	GAAAAGGCCTGCGCCGATG
E98A sense	CTACGCTTTCGCTATGGTCATC
E98A antisense	GATGACCATAGCGAAAGCGTAG
K156A sense	CTGCTCGCAGTCGGCGCCATC
K156A antisense	GATGGCGCCGACTGCGAGCAG
F212A sense	GTGGTGATGGCTGCCTTCGGC
F212A antisense	GCCGAAGGCAGCCATCACCAC

E218A sense	GGCGGTATCGCTATCATCGGCG
E218A antisense	CGCCGATGATAGCGATACCGCC
T27N sense	CATCGGCAaCGGCCTTTTC
T27N antisense	GAAAAGGCCGtTGCCGATG
T27S sense	CATCGGcTCCGGCCTTTTC
T27S antisense	GAAAAGGCCGgGACCGATG
K156R sense	CTGCTCAgGGTCGGCGCCATC
K156R antisense	GATGGCGCCGACCtGAGCAG
K156Q sense	CTGCTCcaGGTCGGCGCCATC
K156Q antisense	GATGGCGCCGACctgGAGCAG
F212Y sense	GTGGTGATGTatGCCTTCGGC
F212Y antisense	GCCGAAGGCatACATCACCAC
F212Q sense	GTGGTGATGcaaGCCTTCGG
F212Q antisense	CCGAAGGcttgCATCACCAC
E218D sense	GGCGGTATCGAtATCATCGGCG
E218D antisense	CGCCGATGATaTCGATACCGCC
E218Q sense	GGCGGTATCcAGATCATCGG
E218Q antisense	CCGATGATCTgGATACCGCC

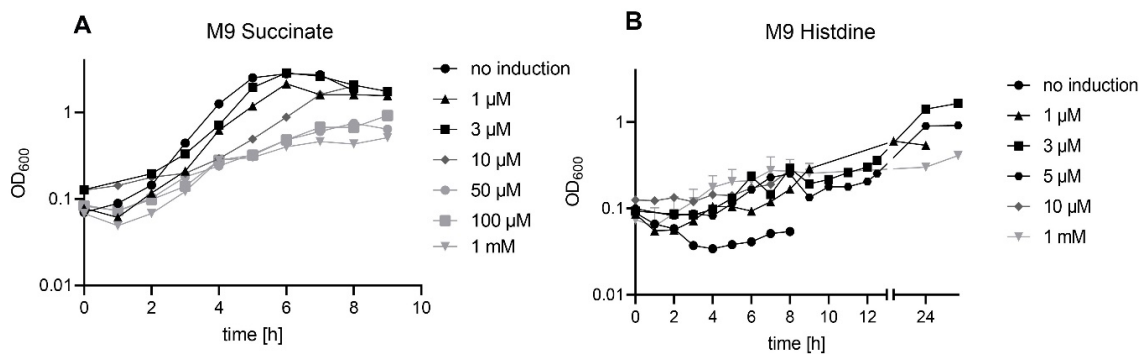


**Fig. S1.** Impact of the concentration of the inducer anthranilic acid on growth of *P. putida* KT2440  $\Delta hutT$  harboring plasmid pUCP20-ANT2-*hutT6H* (A) in M9 medium with succinate or (B) L-histidine as carbon source. Growth was measured by determining the optical density at 600 nm ( $OD_{600}$ ).

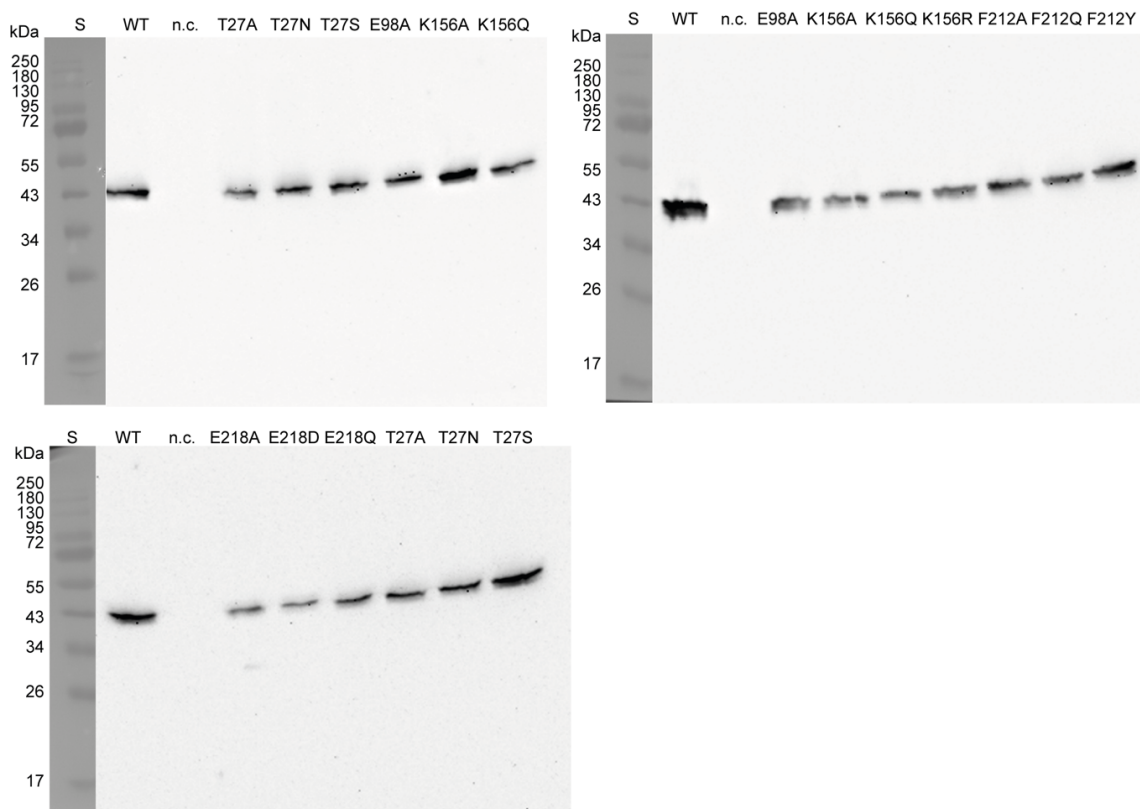


**Fig. S2.** Complete western blots of HutT variants shown in Fig. 7B. HutT was detected via a C-terminal 6His tag with anti-6His antibody and secondary  $\alpha$ -mouse antibody coupled to horse radish peroxidase in membranes prepared from *E. coli* JW2306 expressing given *hutT* variants from plasmid pT7-5-*hutT6H*. Fifty  $\mu$ g total membrane protein were applied per lane. n.c., negative control without HutT.

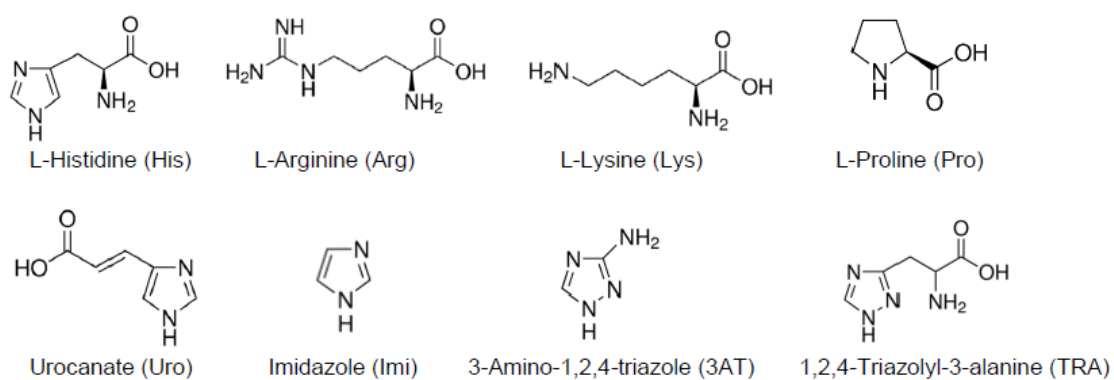


**Fig. S3.** Molecular structures of compounds used to test the substrate specificity of HutT (Fig. 4B).



(P25527); GABP\_BACSU, GabP of *Bacillus subtilis* (P46349); ApcT\_METJA, ApcT of *Methanocaldococcus jannaschii* (Q58026); ApcT\_GEOKA, ApcT of *Geobacillus kaustophilus* (Q5L1G5). The alignment was performed with Clustal Omega [11]. TMDs predicted for HutT of *P. putida* are indicated by a black line and the TMD number above the line. Amino acids highlighted in red are implicated in coupling proton and substrate transport, the amino acid highlighted in blue may function as a substitute for a sodium ion in the Na<sup>2</sup> site of sodium ion-dependent transporters and amino acids highlighted in green may seal the substrate binding site in the extracellular side of the membrane. Other conserved amino acids are highlighted in grey. Amino acids highlighted in bold have been shown experimentally to be important for transporter function. Information was taken from the following sources: HutT of *P. putida*, this work; LysP of *E. coli* [12]; ApcT of *M. jannaschii* [13]; ApcT of *G. kaustophilus* [14].

## Supplementary References

1. Chen, J., Li, Y., Zhang, K. & Wang, H. (2018) Whole-genome sequence of phage-resistant strain *Escherichia coli* DH5alpha. *Genome Announc* **6**.
2. Platt, R., Drescher, C., Park, S. K. & Phillips, G. J. (2000) Genetic system for reversible integration of DNA constructs and *lacZ* gene fusions into the *Escherichia coli* chromosome. *Plasmid* **43**, 12-23.
3. Dehio, C. & Meyer, M. (1997) Maintenance of broad-host-range incompatibility group P and group Q plasmids and transposition of Tn5 in *Bartonella henselae* following conjugal plasmid transfer from *Escherichia coli*. *J Bacteriol* **179**, 538-40.
4. Baba, T., Ara, T., Hasegawa, M., Takai, Y., Okumura, Y., Baba, M., Datsenko, K. A., Tomita, M., Wanner, B. L. & Mori, H. (2006) Construction of *Escherichia coli* K-12 in-frame, single-gene knockout mutants: the Keio collection. *Mol Syst Biol* **2**, 2006.0008-2006.0008.
5. Bagdasarian, M., Lurz, R., Ruckert, B., Franklin, F. C., Bagdasarian, M. M., Frey, J. & Timmis, K. N. (1981) Specific-purpose plasmid cloning vectors. II. Broad host range, high copy number, RSF1010-derived vectors, and a host-vector system for gene cloning in *Pseudomonas*. *Gene* **16**, 237-47.
6. Nelson, K. E., Weinel, C., Paulsen, I. T., Dodson, R. J., Hilbert, H., Martins dos Santos, V. A., Fouts, D. E., Gill, S. R., Pop, M., Holmes, M., Brinkac, L., Beanan, M., DeBoy, R. T., Daugherty, S., Kolonay, J., Madupu, R., Nelson, W., White, O., Peterson, J., Khouri, H., Hance, I., Chris Lee, P., Holtzapple, E., Scanlan, D., Tran, K., Moazzez, A., Utterback, T., Rizzo, M., Lee, K., Kosack, D., Moestl, D., Wedler, H., Lauber, J., Stjepandic, D., Hoheisel, J., Straetz, M., Heim, S., Kiewitz, C., Eisen, J. A., Timmis, K. N., Dusterhoft, A., Tumbler, B. & Fraser, C. M. (2002) Complete genome sequence and comparative analysis of the metabolically versatile *Pseudomonas putida* KT2440. *Environ Microbiol* **4**, 799-808.
7. Wirtz, L., Eder, M., Schipper, K., Rohrer, S. & Jung, H. (2020) Transport and kinase activities of CbrA of *Pseudomonas putida* KT2440. *Sci Rep* **10**, 5400.
8. Lassak, J., Henche, A.-L., Binnenkade, L. & Thormann, K. M. (2010) ArcS, the cognate sensor kinase in an atypical Arc system of *Shewanella oneidensis* MR-1. *Appl Environ Microbiol* **76**, 3263-3274.
9. Tabor, S. & Richardson, C. C. (1985) A bacteriophage T7 RNA polymerase/promoter system for controlled exclusive expression of specific genes. *Proc Natl Acad Sci U S A* **82**, 1074-1078.
10. Hoffmann, L., Sugue, M. F. & Bruser, T. (2021) A tunable anthranilate-inducible gene expression system for *Pseudomonas* species. *Appl Microbiol Biotechnol* **105**, 247-258.
11. Madeira, F., Park, Y. m., Lee, J., Buso, N., Gur, T., Madhusoodanan, N., Basutkar, P., Tivey, A. R. N., Potter, S. C., Finn, R. D. & Lopez, R. (2019) The EMBL-EBI search and sequence analysis tools APIs in 2019. *Nucleic Acids Research* **47**, W636-W641.
12. Rauschmeier, M., Schuppel, V., Tetsch, L. & Jung, K. (2014) New insights into the interplay between the lysine transporter LysP and the pH sensor CadC in *Escherichia coli*. *J Mol Biol* **426**, 215-29.
13. Shaffer, P. L., Goehring, A., Shankaranarayanan, A. & Gouaux, E. (2009) Structure and mechanism of a Na<sup>+</sup>-independent amino acid transporter. *Science* **325**, 1010-1014.

14. Jungnickel, K. E. J., Parker, J. L. & Newstead, S. (2018) Structural basis for amino acid transport by the CAT family of SLC7 transporters. *Nat Commun* **9**, 550-550.

# Prokaryotic solute/sodium symporters: versatile functions of a transporter family

This review was originally published in *International Journal of Molecular Sciences* in February 2021.

**Tania Henriquez, Larissa Wirtz, Dan Su and Heinrich Jung** Prokaryotic solute/sodium symporters: versatile functions of a transporter family. *Int. J. Mol. Sci.* 2021, 22(4).  
<https://doi.org/10.3390/ijms22041880>



Review

# Prokaryotic Solute/Sodium Symporters: Versatile Functions and Mechanisms of a Transporter Family †

Tania Henriquez <sup>1</sup>, Larissa Wirtz <sup>1</sup>, Dan Su <sup>1</sup> and Heinrich Jung <sup>1,\*</sup>

Microbiology, Department Biology 1, Ludwig Maximilians University Munich, D-82152 Martinsried, Germany; T.Henriquez@bio.lmu.de (T.H.); larissa.wirtz@biologie.uni-muenchen.de (L.W.); D.Su@biologie.uni-muenchen.de (D.S.)

\* Correspondence: hjung@lmu.de; Tel.: +49-89-218074630

† This article is dedicated to the memory of Ron Kaback, an exceptional scientist and great mentor.

**Abstract:** The solute/sodium symporter family (SSS family; TC 2.A.21; SLC5) consists of integral membrane proteins that use an existing sodium gradient to drive the uphill transport of various solutes, such as sugars, amino acids, vitamins, or ions across the membrane. This large family has representatives in all three kingdoms of life. The human sodium/iodide symporter (NIS) and the sodium/glucose transporter (SGLT1) are involved in diseases such as iodide transport defect or glucose-galactose malabsorption. Moreover, the bacterial sodium/proline symporter PutP and the sodium/sialic acid symporter SiaT play important roles in bacteria–host interactions. This review focuses on the physiological significance and structural and functional features of prokaryotic members of the SSS family. Special emphasis will be given to the roles and properties of proteins containing an SSS family domain fused to domains typically found in bacterial sensor kinases.

**Keywords:** secondary transport; solute/sodium symport; SLC5; PutP; signal transduction; bacterial two-component systems; bacterial sensor kinase



**Citation:** Henriquez, T.; Wirtz, L.; Su, D.; Jung, H. Prokaryotic Solute/Sodium Symporters: Versatile Functions and Mechanisms of a Transporter Family †. *Int. J. Mol. Sci.* **2021**, *22*, 1880. <https://doi.org/10.3390/ijms22041880>

Academic Editors: Stathis Frillingos and Maria Botou

Received: 23 December 2020

Accepted: 10 February 2021

Published: 13 February 2021

**Publisher's Note:** MDPI stays neutral with regard to jurisdictional claims in published maps and institutional affiliations.



**Copyright:** © 2021 by the authors. Licensee MDPI, Basel, Switzerland. This article is an open access article distributed under the terms and conditions of the Creative Commons Attribution (CC BY) license (<https://creativecommons.org/licenses/by/4.0/>).

## 1. Introduction

Inwardly directed electrochemical sodium ion gradients are important parts of bioenergetic circuits in pro- and eukaryotic cells. The idea that these gradients play a role in the active transport of solutes originally came from Robert K. Crane. He proposed at a Symposium on Membrane Transport and Metabolism in Prague in 1960 that the transport of sodium ions and glucose are coupled (Na<sup>+</sup>/glucose cotransport hypothesis) [1–3]. Peter Mitchel later generalized the idea of ion-coupled substrate transport and coined the term *symport* for processes in which coupling ion and substrate are transported in the same direction across the membrane [4].

In prokaryotes, the sodium ion gradients are established by primary sodium pumps (for example, sodium pumping complexes of the respiratory chain [5,6], membrane-integrated decarboxylases [7], sodium-translocating ATPases [8], and sodium/proton antiporters [9]). The electrochemical sodium ion gradients can be used by secondary transporters to drive the transport of solutes across membranes. These transporters are classified into families based on sequence similarities and common functional features. The glycoside-pentoside-hexuronide (GPH)/cation symporter family (TC2.A.2), the betaine-choline-carnitine-choline transporter (BCCT) family (TC2.A.15), the solute/sodium symporter (SSS) family (TC2.A.21), the neurotransmitter/sodium symporter (NSS) family (TC2.A.22), the dicarboxylate-amino acid-cation symporter (DAACS) family (TC2.A.23), and the glutamate/sodium symporter (ESS) family (TC2.A.27) are examples for families containing well-characterized sodium-dependent transporters of prokaryotic origin (<http://www.tcdb.org>, accessed on 30 November 2020) [10].

In recent years, crystallization-based structural analyses revealed important insights into the three-dimensional structures of various transporters including sodium-dependent

systems. The analyses led to the discovery of common structural folds (for example, MFS fold, LeuT fold) [11,12]. Thereby, common core structures are shared even by transporters that do not have a significant sequence similarity or fulfill different functions (for example, sodium or proton-coupled solute uptake or solute antiport). In some cases, relatively small changes (for example, a positively charged amino acid in place of a site of sodium binding) can lead to a fundamental change in the coupling mechanism [13]. The structural insights led to a reclassification of the transporters. For example, the BCCT, SSS, and NSS families share, together with the amino acid-polyamine-organocation (APC) family and other transporter families, the LeuT fold and are now grouped together to constitute the APC superfamily [14,15]. Furthermore, transporters sharing a common core structure were eventually crystallized in different conformations. Comparison of these conformations provided insights into different conformational states underlying the respective transport cycle [16–18]. Analyses of conformational dynamics of transporters were further advanced by site-directed labeling combined with fluorescence or electron paramagnetic resonance (EPR) spectroscopic approaches [19–23]. More recently, single-molecule Förster resonance energy transfer (smFRET) and simulations of molecular dynamics were used to probe conformational dynamics of transporters under biologically relevant conditions [18,24,25]. These and other investigations of structure-function relationships in transporters greatly advanced our understanding of molecular details of solute transport across membranes.

Here, we briefly summarize information on the physiological significance, structure, and molecular mechanisms of function of transporters of the SSS family focusing on the prokaryotic part of the family. In addition to transport proteins, members of the SSS family show a distant similarity to the N-terminal domains of some sensor kinases of bacterial two component signal transduction pathways [26,27]. Initially it was not clear whether the SSS domain of the sensor kinases controls the kinase activity (for example, whether it is required for signal perception and transduction of the signal to other domains of the protein) and/or also functions as a solute transporter. In recent years, some of these sensor kinases and the functionally associated response regulators were characterized. Here, special emphasis will be given to the distribution, physiological significance, and functional properties of these prokaryotic two-component systems.

## 2. Functional Properties and Physiological Significance of Prokaryotic Transporters of the SSS Family

Transporters of the SSS family are responsible for the supply of cells with nutrients (for example, monosaccharides and amino acids), vitamins, and anions [26]. For eukaryotic SSS family members, the role in the development of diseases has been intensively investigated. For example, mutations in genes of human sodium/glucose transporters (SGLTs) cause the rare diseases glucose-galactose malabsorption and familial renal glucosuria [28]. Substrates of the sodium/multivitamin transporter (SMVT) play central roles in the cellular metabolism, and transporter defects can lead to growth retardation, dermatological disorders, and neurological disorders [29]. The human sodium/iodide symporter (NIS) is required for hormone synthesis in the thyroid and used for diagnostics and therapy of thyroid cancer [30]. Prokaryotic SSS family members catalyze the uptake of organic compounds as carbon, nitrogen and energy sources, and contribute to the adaptation of cells to environmental stresses such as osmotic stress and oxidative stress. Some of the SSS-related proteins perform important functions in regulating the metabolism of bacteria. Fulfilling these transport and regulatory functions, the SSS family members contribute also to the virulence of a variety of human pathogens. Selected examples are discussed in the following subsections.

### 2.1. PutP-Mediated Nutrient Supply and Osmoadaptation

The SSS family transporter PutP catalyzes the sodium ion-dependent uptake of the amino acid proline in cells [31]. Similar to SGLT, both sodium ions and a membrane potential are crucial for substrate accumulation by PutP [2,32]. PutP has a high affinity for proline and is highly specific for the amino acid [32,33] (Table 1). The transporter is

widespread in the prokaryotic world and can be found in archaea (for example, in the orders Methanococcales, Archaeoglobales, Thermococcales, Halobacteriales) as well as in Gram-positive and Gram-negative bacteria [26]. In *Enterobacteriaceae*, PutP is associated with PutA, a multifunctional proline dehydrogenase that oxidizes proline via  $\Delta^1$ -pyrroline-5-carboxylate and L-glutamate- $\gamma$ -semialdehyde to glutamate [34]. The latter amino acid is central to the carbon and nitrogen metabolism and is further converted for catabolic and anabolic purposes (Figure 1). For example, amino transferases can transfer the amino group from glutamate to  $\alpha$ -ketoacids, yielding other amino acids, and the citric acid cycle intermediate  $\alpha$ -ketoglutarate, or glutamate, can be oxidized by glutamate dehydrogenase to yield  $\alpha$ -ketoglutarate and ammonia. Other bacteria and archaea possess similar degradation pathways, although regulation and enzymatic basis of proline oxidation varies between organisms [35–39]. Proline accumulation via PutP can also play a role in the adaptation of cells to osmotic stress. For example, transcription of the gene encoding the PutP ortholog OpuE in *Bacillus subtilis* is upregulated by means of sigma A- and sigma B-dependent stress-responsive promoters [40,41]. However, contrary to other proline and betaine transporters such as ProP (major facilitator superfamily [42]) and BetP (betaine/carnitine/choline transporter family [43]), the activity of PutP and its orthologs is not stimulated at the protein level [44].

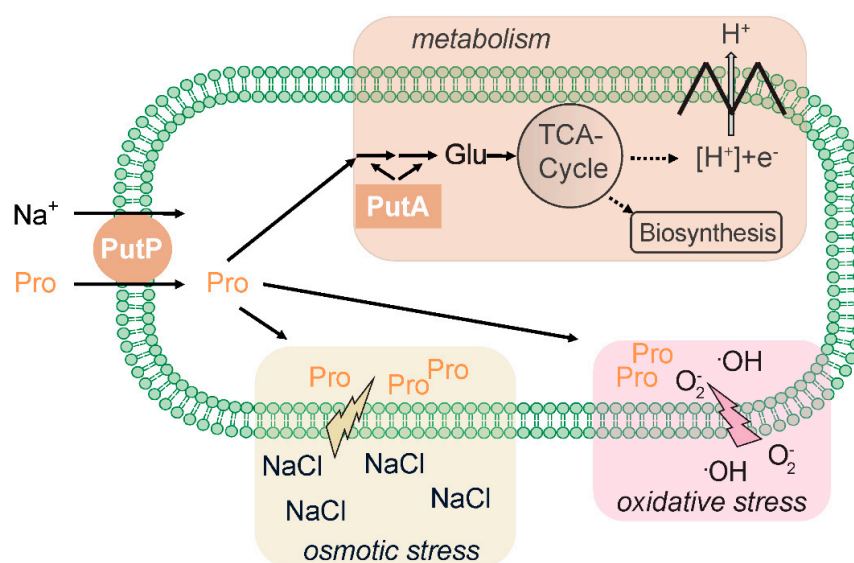


**Figure 1.** Possible roles of PutP in the proline metabolism of prokaryotes.

Furthermore, intracellular accumulation of L-proline can protect mammals, plants, fungi, yeast, and bacteria from damage by reactive oxygen species (for example,  $\cdot\text{OH}$ ,  $^1\text{O}_2$ ) [45]. The protective effect may rely on the unique chemical properties of L-proline (for example, secondary amine of the pyrrolidine ring and low ionization potential) and involve the chemical modification of L-proline by reactive oxygen species [46,47]. On the other hand, up-regulation of *putA* may lead to the generation of reactive oxygen species, thereby decreasing oxidative resistance of bacteria and other organisms [45,48].

The amino acid proline plays an important role in interactions between pathogens and hosts [49]. In fact, disruption of PutP-dependent proline uptake attenuates the virulence of different pathogens [31]. For example, proline transport is vital for the survival and growth of *Staphylococcus aureus* upon human infection [50]. In this context, the *putP* gene is transcriptionally activated by low-proline and high osmotic environments in murine and human clinical specimens [51]. PutP is thought to particularly stimulate the early stages of the infection process by helping the pathogen to adapt to high osmolarity conditions in the host [50–52]. In addition, since many *S. aureus* strains are proline auxotrophs, PutP

is required to supply the bacterium with the proteinogenic amino acid [51]. Despite the high similarity to *E. coli* PutP and the conservation of amino acids known to be involved in sodium binding in solute/sodium symporters, the activity of *S. aureus* PutP was not stimulated by NaCl [53,54]. Therefore, it has been suggested that under high osmolarity conditions, PutP-mediated proline uptake in *S. aureus* might be driven by a proton motive force instead of a sodium motive force [50]. More investigations at the biochemical level are necessary to test the coupling mechanism.

*Helicobacter pylori*, a causative agent of stomach inflammation and cancer [55], needs PutP for the successful colonization of the stomach of Mongolian gerbils [56]. Since the *putP* gene is associated with *putA* encoding proline dehydrogenase [49], the supply of the bacterium with proline as a carbon, nitrogen, and/or energy source seems to be of particular significance under the conditions in the stomach. This idea is supported by the observation that proline is the predominant amino acid in the gastric juice of humans infected with *H. pylori* [57]. Whether PutP contributes also to adaptation to high osmolarity conditions (for example in the mucus layer of the stomach) requires further investigations. *H. pylori* PutP is sodium-dependent, and its functional properties are almost identical to the *E. coli* ortholog [58].

Furthermore, proline is known to be involved in regulating alternative lifestyles of *Photobacterium luminescens*, a  $\gamma$ -proteobacterium that lives in symbiosis with nematodes and is a lethal pathogen of insects [59]. By accumulating proline in the cells, PutP contributes to an enhanced production of selected secondary metabolites known to be involved in antibiosis, insect virulence, and nematode mutualism [60]. Finally, PutP was shown to affect pulmonary and systematic infections of mice by the Gram-negative bacterium *Francisella novicida* [61], and facilitates the colonization of the plant rhizosphere by *Pseudomonas putida* [39].

**Table 1.** Functional properties of PutP, vSGLT, and SiaT.

Property	PutP [32,62]	vSGLT [63]	SiaT [64]
Substrate and apparent $k_M$	L-proline 2 $\mu$ M	Galactose 158 $\mu$ M	N-acetylneuraminic acid 16 $\mu$ M
Apparent $k_{\text{sodium}}$	31 $\mu$ M	129 mM	n.d.
Sodium: substrate stoichiometry	1:1	1:1	2:1

## 2.2. Sugar Uptake via SSS Family Transporters

Glucose is an important carbon and energy source for pro- and eukaryotic cells. While in mammalian cells, glucose is coupled to sodium ions and catalyzed by SSS family transporters of the SGLT group [2], many bacteria take up glucose via a phosphotransferase system (PTS) which transports and modifies glucose to glucose-6-phosphate [65]. However, bacteria need to adapt to rapidly changing environments, and therefore often employ several transporters of different families (ABC, MFS, SSS, PTS) for the same substrate [65]. For example, the marine bacterium *Vibrio parahaemolyticus* can take up glucose (galactose) via a PTS and by vSGLT (SglS), a sodium-dependent SSS family protein [66] (Table 1). Proteins similar to SGLT are predicted based on genome analyses also for other bacteria including, for example, the marine bacterium *Rhodospirillum rubrum*, the Gram-positive soil bacterium *Streptomyces coelicolor*, the gut bacterium *Bacteroides plebeius*, and the Gram-negative bacterium *Teredinibacter turnerae* that lives in symbiosis with mollusks (string-db.org). Similar to glucose (galactose), the monosaccharide mannose can be taken up by a phosphotransferase system (ManP<sup>I</sup>) and by an SSS transporter, the putative sodium/mannose transporter (ManP<sup>II</sup>) as suggested for the marine bacteria of the genus *Shewanella* [67]. Whether this and other related proteins indeed catalyze the sodium-coupled uptake of the respective monosaccharide still has to be tested biochemically. In any case, in the fight against bacterial multidrug resistance, vSGLT was recently discussed to represent a drug target [68].

SSS proteins also play an important role for the uptake of sialic acids, a family of 9-carbon sugar acids found predominantly on the cell-surface glycans of humans and other animals [69]. Mammalian commensals and pathogenic bacteria that colonize sialic acid rich tissues, such as the respiratory or gastrointestinal tract, have evolved mechanisms to use host-derived sialic acids [70]. Bacteria can employ different types of transporters for the uptake of the sugar acids. One of these transporters is the SSS protein SiaT (sometimes also termed NanT, which should not be confused with the MFS transporter NanT of *Escherichia coli* and its orthologs) (Table 1). Orthologs of SiaT are found, for example, in *Vibrio fischeri* and *Lactobacillus sakei*, and in the human pathogens *Salmonella enterica* serovar Typhimurium, *S. aureus*, and *Clostridium difficile* [69]. In the case of the latter two pathogens, SiaT (NanT) proved to be important for the colonization of the mouse intestine after treatment with antibiotics [71].

### 2.3. Uptake of Short Chain Organic Acids via SSS Family Transporters

Short organic acids are produced and secreted by pro- and eukaryotes and play important roles in bacteria–host interactions and interactions within bacterial communities, for example, in a process called cross-feeding [72–74]. SSS transporters such as ActP (sodium/acetate symporter) [75], MctC (proton/pyruvate, propionate, acetate symporter) [76] and MctP (cation/lactate, pyruvate, propionate, butyrate symporter) [77] contribute to the dynamics of these interactions by catalyzing the uptake of the respective short chain organic acid from the environment. ActP is found in many bacteria, including *Enterobacteriaceae* and *Pseudomonadaceae*. Interestingly, acetate uptake and metabolism in *Pseudomonadaceae* and other  $\gamma$ -Proteobacteria are controlled by a two-component signal transduction system with a sensor kinase containing an SSS family domain (see below). In addition to acetate transport, ActP has been shown to catalyze the uptake of toxic tellurite [78].

## 3. Structural Basis of Transport

SSS transporters are composed of about 500 to 700 amino acids that form 13 (bacterial PutP, ActP, SiaT, MctP; human NIS and SMVT), 14 (bacterial and human SGLT), or 15 (bacterial ManP<sup>II</sup>) transmembrane domains (TMDs) and hydrophilic loops connecting the TMDs on both sites of the membrane ([www.uniprot.org](http://www.uniprot.org), accessed on 1 February 2020). The N terminus of the transporters is located on the outer site of the membrane [79–82]. Crystal structures are available for SGLT of *V. parahaemolyticus* (vSGLT) [83,84] and SiaT of *Proteus mirabilis* (PmSiaT) [64]. The structural analyses revealed that SSS proteins share the same structural fold with the sodium-dependent leucine transporter LeuT of the thermophilic marine bacterium *Aquifex aeolicus* (AaLeuT, neurotransmitter/sodium symporter family, NSS, TC 2.A.22) [12,85]. The fold is characterized by a core of ten TMDs (cTMDs) that are arranged in five + five inverted repeats (in SSS transporters TMDs 2 to 6 and 7 to 12) with an antiparallel orientation and a pseudosymmetry axis in the membrane plane. To avoid confusion, TMD 1 of SSS transporters is counted as TMD -1 followed by the cTMDs 1 to 10 and more non-core TMDs in the C-terminal region of the transporters (Figure 2A). The TMDs are intertwined with cTMDs 1, 2, 3, 6, 7, 8 and 10 forming the central sites of substrate and sodium binding [12] (Figure 2B). Furthermore, cTMDs 1 and 6 contain unwound regions that are crucial for ligand binding and conformational alteration underlying the transport cycle. For the NSS transporter LeuT [86,87] and the SSS transporter PutP [20,88], features of the structural fold were confirmed by comprehensive electron paramagnetic resonance (EPR) spectroscopic analyses.

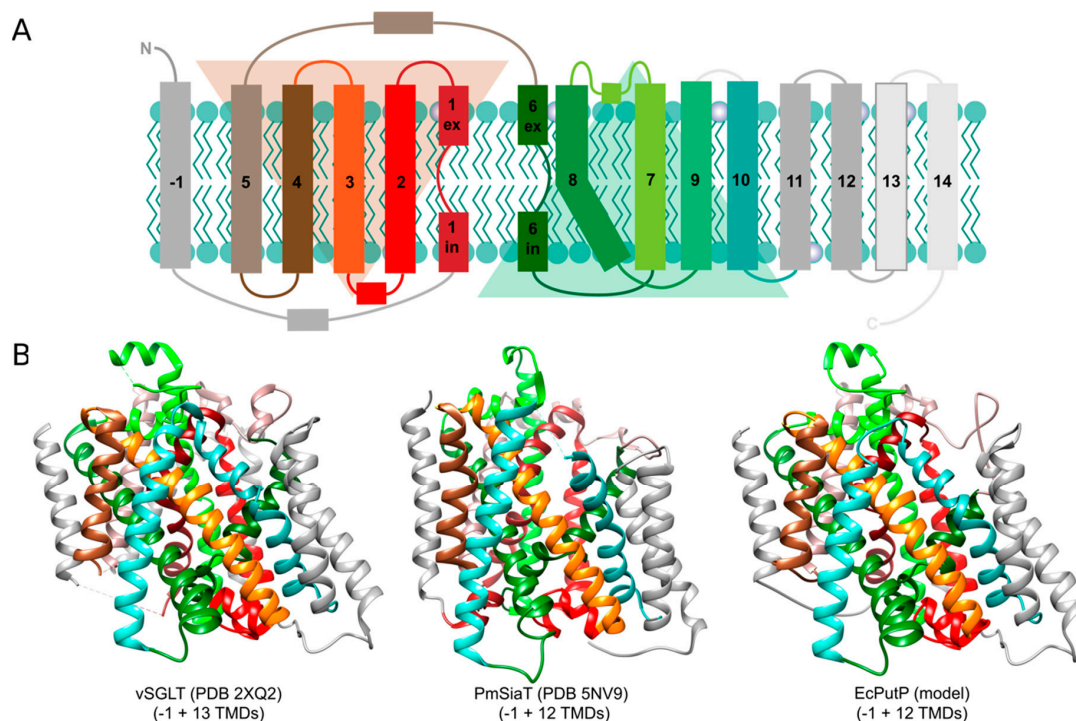


**Figure 2.** (A) Membrane topology of solute/sodium symporter (SSS) family transporters. SSS transporters are composed of 13 to 15 transmembrane domains (TMDs) connected by hydrophilic loops. The N terminus of the transporters is located on the outer site of the membrane. The transporters share the LeuT-type structural fold that is characterized by a core of ten TMDs that are arranged in five + five inverted repeats with an antiparallel orientation and a pseudosymmetry axis in the membrane plane [89]. The core domain starts at TMD 2 of SSS transporters (TMD 1 of SSS transporters is counted as TMD -1). (B) Ribbon representation of the three-dimensional structures of vSGLT, PmSiaT and EcPutP. The structures of vSGLT [84] and PmSiaT [64] are the result of X-ray analyses of respective crystals. The structure of EcPutP is based on homology modeling and experimental distance restraints obtained by site-directed spin labeling and EPR spectroscopy [90]. The figures were generated using UCSF Chimera. Chimera is developed by the Resource for Biocomputing, Visualization, and Informatics at the University of California, San Francisco [91]. (A) was taken and modified from Jung et al., 2012 [31].

#### 4. Molecular Mechanism of Transport

##### 4.1. Sites of Substrate and Sodium Ion Binding

Sites of sodium ion binding in transporters were modeled based on the available crystal structures in combinations with amino acid substitution analyses. By this means, two putative sodium ion binding sites were identified in LeuT, Na1 and Na2 [85]. The central site of sodium ion binding (Na2) is highly conserved between transporters belonging to the structural class of proteins with a LeuT fold including SSS family transporters. It is located about half-way in the membrane between cTMDs 1 and 8 including the unwound region in cTMD1 (Figure 3A). Thereby, the sodium ion is coordinated by the main-chain carboxyl oxygen atoms of three nonpolar, aliphatic amino acids (two in cTMD1 and one in cTMD8) and the hydroxyl groups of two serine (or threonine) residues in cTMD8 [31,64,84] (Figure 3B and Table S1). In LeuT, a second sodium binding site (termed Na1 site) was suggested. The sodium ion at this site is proposed to participate directly in coordinating the substrate leucine [85].

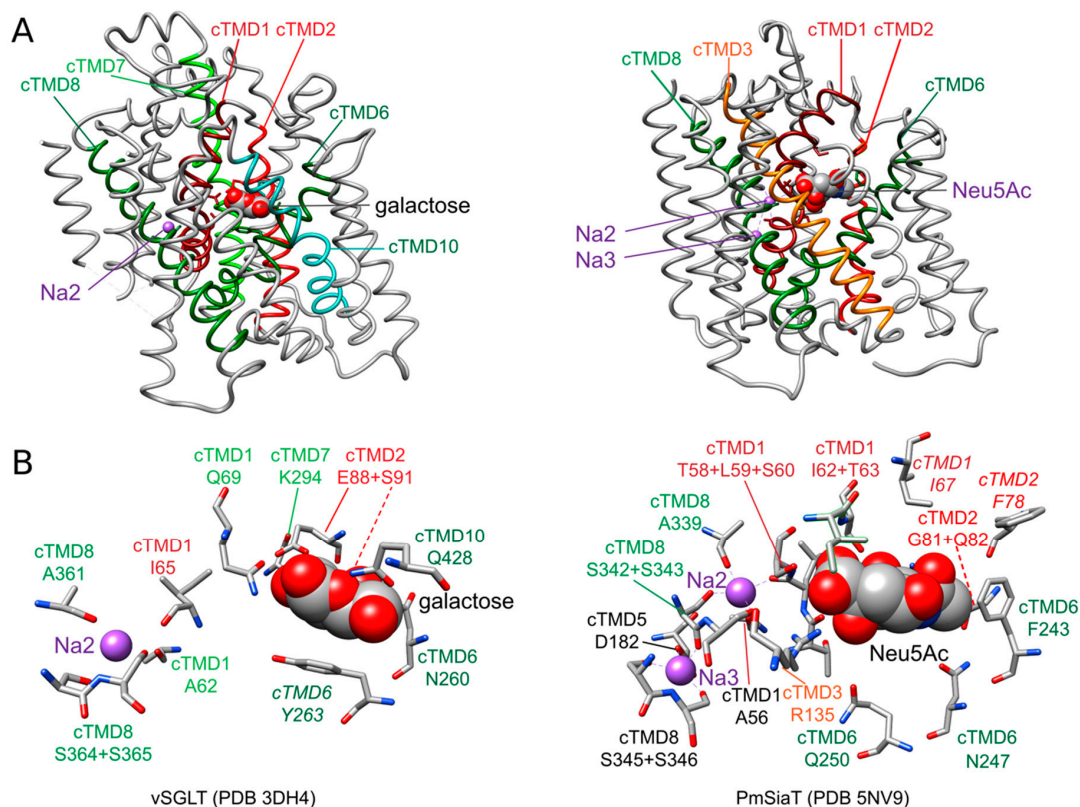


**Figure 3.** Sodium ion and substrate binding sites of vSGLT and PmSiaT. **(A)** Sideview of vSGLT and PmSiaT in the membrane plane. Core transmembrane domains (cTMDs) that coordinate with sodium ions and substrate are depicted in color, while the remaining TMDs are colored in grey. Substrates are shown as grey spheres colored by heteroatom and sodium ions are shown in purple. **(B)** Amino acids coordinating sodium ions or substrate. Amino acids are presented as grey sticks colored by heteroatom and substrates are presented as in **(A)**. Amino acids positions highlighted in *italics* are considered to function as thin gates. Images were generated based on the crystal structures of vSGLT (3DH4) and PmSiaT (PDB 5NV9) using UCSF Chimera. Chimera is developed by the Resource for Biocomputing, Visualization, and Informatics at the University of California, San Francisco [91]. Neu5Ac, *N*-acetylneuraminic acid.

A site corresponding to Na1 of LeuT has so far not been detected in SSS family members. However, the crystal structure of SiaT suggests a third site for sodium binding (termed Na3 site) that is located more towards the cytoplasmic side of the transporter, 0.65 nm away from the Na2 site. Here, the sodium ion is proposed to be coordinated by the carboxyl group of an acidic amino acid of cTMD5, a main-chain carbonyl oxygen and the hydroxyl groups of two serine of cTMD8 (Figure 3 and Table S1). While substitutions of amino acids of the putative Na2 site are highly deleterious for the function of all transporters investigated, substitutions at the proposed Na3 site are more nuanced. It has been suggested that sodium at this site plays a more modulatory role and helps to further pre-organize the substrate binding site by stabilizing the transporter in an outward-facing conformation [64]. The authors of the latter article suggested that SSS family transporters with a sodium: substrate stoichiometry of 2:1 (SiaT, human SGLT1) contain the Na2 and Na3 sites, while transporters with a 1:1 stoichiometry (PutP, vSGLT) harbor only the Na2 site. Nevertheless, an alignment of the amino acid sequences revealed that the Na3 site is in part conserved also in PutP (Figure S1). Substitution of respective amino acids in PutP (compare Table S1) affected transport properties similarly to as observed for SiaT [64,92–94]. Without a crystal structure at the time, the functional results obtained with PutP led to the conclusion that these amino acids are important for sodium release on the cytoplasmic side

of PutP. In view of the new insights into the structure and function of SiaT, the role of the respective amino acids in PutP needs to be revisited.

Due to the chemical diversity of the substrates of SSS family proteins, substrate binding sites are much less conserved and more complex compared to sodium binding sites (Figure S1). Among different TMDs of the core structural motif participating in substrate binding, there are always amino acids of the unwound regions of cTMDs 1 and 6 that contribute to coordinating the substrate (Table S1). For example, binding of *N*-acetylneuraminic acid to SiaT is achieved by interactions with eight amino acids of cTMDs 1, 2, 3, and 6 and via seven water molecules. A hydration layer lies between the substrate and cTMDs 5 and 6 with hydrogen bonds to water and water-mediated interactions with side chains in cTMDs 2 and 6 [64] (Figure 3B).

There has been controversy regarding the existence of a second binding site (termed S2 site) in the NSS family protein LeuT located more externally above the central substrate binding site (termed S1) [95,96]. Substrate binding, flux analyses and computational studies suggest that the S2 site constitutes a high-affinity ligand binding site that is crucial for the transport cycle [95,97]. It has been hypothesized that the S2 site could allosterically modulate substrate release both positively and negatively. For example, binding of a second substrate molecule in S2 induces the release of the substrate bound to S1, whereas inhibitor binding prevents the release of substrate from S1 [98]. Based on the results with LeuT, the SSS family proteins vSGLT and PutP were examined for the existence of a second substrate binding site [99]. Radiolabeled galactose and proline saturation binding experiments indicated that both vSGLT and PutP can simultaneously bind two substrate molecules (Table S1). Amino acid substitutions in S1 or S2 reduced the binding capacity from two substrate molecules to one substrate molecule per transporter and impaired transport [99]. Furthermore, for vSGLT, the computational analyses suggest that the second binding site aligns to the S1 site of LeuT, while the amino acid coordinating galactose on the crystal structure [83] forms the more external binding site (S2) [99]. However, emerging evidence suggests that SGLT, like the lactose permease LacY (major facilitator family), may contain only one sugar binding site [21,100,101]. In any case, more computational and functional analyses are necessary to elucidate the existence and precise functional role of a possible second substrate binding site in SSS family transporters.

#### 4.2. Transport by Alternating Access

Transporters have been proposed to function following an alternating access mechanism. Thereby, a centrally located substrate binding site is accessible either from the outside or from the inside [102–104]. The elucidation of the 3D structures of transporters of different (super)families in different conformational states over the last fifteen years has confirmed the correctness of the alternating access mechanism and revealed detailed mechanistic insights. The location of hydrophilic pathways (cavities) connecting the substrate binding site with either the outer environment or the cytosol, and of structural elements capable of blocking one pathway or the other (referred to as gates) were discovered. In addition to outward and inward open conformations, occluded states and intermediate states of gate opening and closure were identified (Figure 4). The alternating access mechanisms vary in detail depending on structural fold, substrate specificity, and mechanism of energization [105].

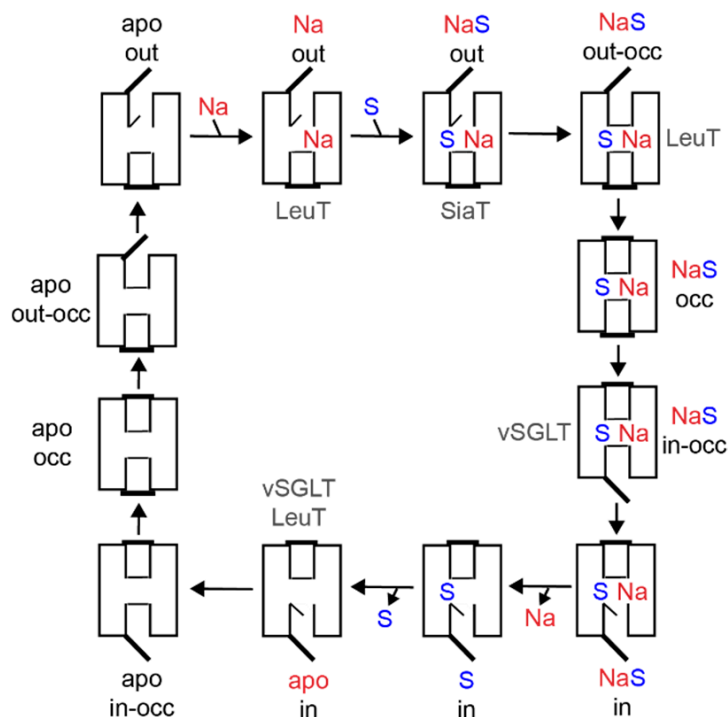


**Figure 4.** Model of conformational states underlying the alternating access mechanism of SSS family transporters and other transporters with a LeuT-type structural fold. The conformational states observed in crystal structures of vSGLT, PmSiaT and AaLeuT are indicated. Comprehensive kinetic analyses particularly with SGLT [2] and to some extent with PutP [106] propose an ordered binding mechanism. Sodium ions bind first to the transporter in the outward-open apo state inducing a conformational alteration that facilitates substrate binding. The ion-substrate-protein complex undergoes further conformational alterations that lead, via an occluded state, to an opening of the ion and substrate binding sites towards the inside of the cell, and finally, to the release of both ligands into the cytosol. The resulting inwardly oriented apo state of the transporters changes to the outward-open conformation to allow for a new transport cycle. Reciprocal opening and closing of inwardly and outwardly oriented cavities may involve movement of thin gates (vSGLT: Y263; PmSiaT: I67, F78; AaLeuT: Y108, F253), rearrangements of interactions between TMDs as well as between TMDs and inner and outer loops (for example the loop connecting TMDs 7 and 8 [11,64,84]. out: outward-open conformation, occ: occluded conformation, in: inward-open conformation.

The SSS family transporter vSGLT has been crystallized in two conformations: (1) inward-occluded state with galactose bound to the center of the core domain (vSGLT-wild type, PDB: 3DH4) and (2) inward-open apo-state (vSGLT-K294A, PDB: 2XQ2) [83,84]. The pathway to the outside is blocked by a hydrophobic “thin” gate formed by M73 (cTMD1), Y87 (cTMD2) and F424 (outer end of cTMD10) and located directly above the central substrate binding site. In addition, interactions between the outer halves of cTMDs 1, 2, 6 and 10 and the loops connecting cTMDs 1 and 2, 7 and 8, and 9 and 10 (“thick” gate) prevent access to the central binding site. The hydrophilic pathway from the central substrate binding site to the cytoplasmic side of the transporter is (partially) open and lined by the inner portions of cTMDs 1, 2, 3, 6, and 8 [83,84]. In the inward-occluded state, access to the central substrate binding site is blocked by Y263 (cTMD6) that appears to function as an inner “thin” gate (Figure 3B). Comparison of the crystal structures, molecular dynamics simulation, and functional biochemical analyses led to the hypothesis that the transition from the outward- to the inward-occluded state of vSGLT alters the coordination of sodium at the Na2 leading finally to the release of sodium on the inner side of the transporter. Subsequent conformational changes including a movement of cTMD1 disrupt a hydrogen bond between

N64 (cTMD1) and Y263 (cTMD6), allowing the side chain of Y263 to reorient and to open a pathway to the intracellular space. Additional rigid body movements then widen the inner pathway leading to substrate release into the cytosol [84].

PmSiaT has been crystallized in an outward-open conformation in complex with *N*-acetylneuraminic acid and two sodium ions (pdb: 5NV9) [64]. The open outer cavity is lined by cTMDs 1, 2, 3, 6, 8 and 10. The closed inner gate is stabilized by interactions between the inner portions of cTMDs 1, 6, 8 and 9 and the loops connecting cTMDs -1 and 1, and 4 and 5. Generation of an inward-open conformation based on vSGLT and morphing of both states suggest that the closing of the outer gate involves movements of the outer portion of cTMD10 towards cTMDs 1 and 2, cTMD9 towards cTMD2, and the outer loop connecting cTMDs 7 and 8 towards cTMD1. During the closing process, a “thin” gate is formed above the substrate binding site by the hydrophobic amino acids I67 (cTMD1), F78 (cTMD2) and W404 (outer end of cTMD10) [64] (Figure 3B). The amino acids align with the amino acids of the outer “thin” gate of vSGLT. To open the inner gate, interactions between the above listed inner portions of cTMDs and inner loops are disrupted. At the same time, cTMDs 8 and 9 move readily away from the inner pathway axis thereby providing access from the central binding site to the cytosol [64].

For PutP, comprehensive cysteine accessibility, fluorescence, and EPR spectroscopic analyses suggest that the transporter adopts an inward-open conformation in the absence of substrate (and a membrane potential) [80,88,94,107,108]. The inner portions of cTMDs 1, 6, and 8 have been suggested to line the inwardly-oriented hydrophilic pathway. Cysteine placed at various site in the inner cTMD portions were readily modified by sulfhydryl reagents, and modification was blocked by the addition of a substrate in the presence of sodium. These results suggest that the inner portions of cTMDs 1, 6, and 8 participate in the inner gating mechanism [88,94,107]. Furthermore, D55 (cTMD1) and Y248 (cTMD6) proved crucial for PutP function. Since the amino acids align with N64 (cTMD1) and Y263 (cTMD6) of vSGLT, it was speculated that D55 and Y248 participate in the formation of an inner gate in PutP [94,109]. Out of the amino acids of PutP (L64, cTMD1; T83, cTMD2; and W405, outer end of cTMD10) that align with the three amino acids forming the outer “thin” gate in vSGLT [83], L64 and W405 proved to be crucial for proline transport and may participate in forming the outer gate in PutP (T83 was not investigated) [90,107]. Furthermore, the complete spin-labeling site scan of the extracellular loop connecting cTMDs 7 and 8 revealed that the loop participates in the closure of the outer pathway also in PutP [20]. The results suggest that F314 of the loop anchors the loop by means of hydrophobic contacts to cTMD1 close to the ligand binding sites. In addition, E311 at the tip of the loop, and various amino acids around the outer end of TM10', proved particularly important for PutP functions, thereby interactions of E311 with the peptide backbone of cTMD10 might also stabilize the closed state [90].

The comparison of the gating mechanisms underlying alternating access in the different transporters reveals conserved feature and diverse differences. In all proteins investigated, cTMDs 1 and 6, and the flexibility of the unwound regions of the cTMDs, play a decisive role. In addition, the external loop connecting cTMDs 7 and 8 plays an important role in closing the outwardly-directed pathway. Interactions of the loop with cTMDs 1 and 10 stabilize the transporters in a conformational state that is closed to the outside. Finally, the participation of a hydrophobic “thin” gate above the central substrate binding side seems to be a common feature of SSS family transporters and other proteins with a LeuT structural motif.

## 5. SSS Domain-Dependent Sensor Kinases

### 5.1. Occurrence, Significance and Targets of SSS Domain-Dependent Signal Transduction Systems

Sensor kinases containing an SSS domain were first described in 2001 [110]. This domain is distantly related, but homologous to the PutP transporter of *E. coli* [26,111]. The predicted role of these proteins would be to act as sensors of membrane-associated stimuli such as ligand binding, turgor or mechanical stress of the membrane, and ion or

electrochemical gradients and transport processes, among others [112]. However, to this day, the specific stimuli and roles of the SSS domain in sensor kinases are enigmatic. In this section, we provide an overview on the information available about the occurrence and distribution of the SSS domain in connection to other protein domains (such as in sensor kinases), and summarize the current knowledge on the biological role and target genes of the associated two-component system.

#### 5.1.1. Distribution in Prokaryotes

Since the initial description of SSS domain-dependent sensor kinases, only a few dozen publications have appeared on this topic. In this context, most of the research has been published in Proteobacteria, specifically  $\gamma$ -Proteobacteria (such as *Vibrio* spp. or *Pseudomonas* spp.). However, the analysis of the SMART database (a Simple Modular Architecture Research Tool) [113–115] revealed a wide distribution through the Bacteria domain, including Proteobacteria, FCB group (Bacteroidetes), PVC group (Verrucomicrobia), and Nitrospirae and Terrabacteria groups (Deinococcus) (Figure 5). Surprisingly, even some Archaea are predicted to contain SSS domains in putative kinases (Figure 5).

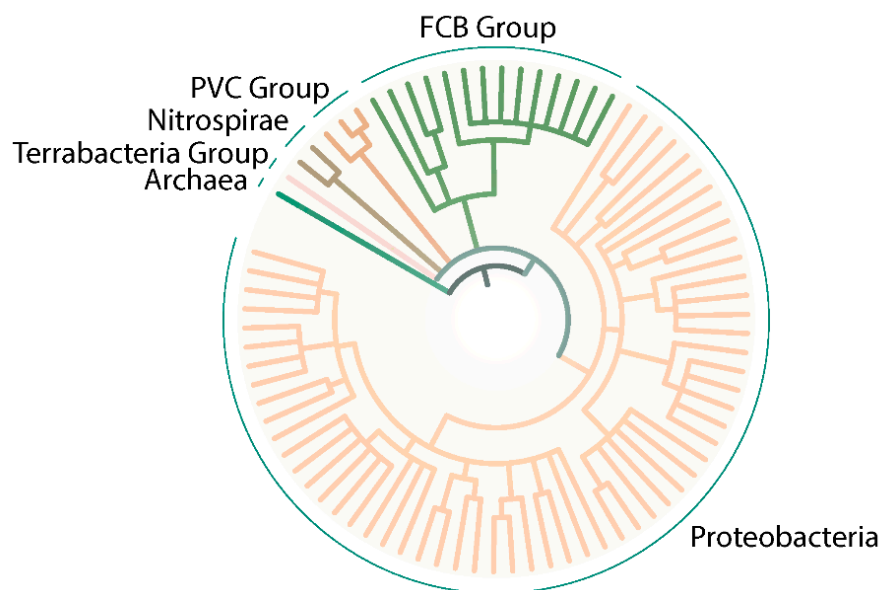


**Figure 5.** Prediction of organisms containing SSS family in association with HisKa domain. SMART was used to identify proteins containing Pfam:ssf (SSS) and HisKa domains. After selection of representative organisms to be displayed for each group, a Newick formatted tree based on NCBI taxonomy was generated. The tree was visualized and modified using iTOL (Intreactive Tree Of Life) [116,117] tool and Adobe Illustrator.

At a first glance, the analysis indicated the absence of proteins containing Pfam:ssf (SSS) and HisKa domains in Gram-positive bacteria. Since the crystal structure of several sensor kinases revealed the importance of two different domains for their function: the ATPase domain, also called HATPase in Pfam (that binds ATP and transfer the  $\gamma$ -phosphate to the second domain), and the dimerization/phosphorylation domain, also called HisKA in Pfam (involved in phosphotransfer from the kinase to the response regulator) [118], a second analysis to identify proteins including SSS and HATPase\_c (Histidine kinase-like ATPases) domains was performed. The results indicate the presence of proteins containing these domains in Actinobacteria (Figure 6). In this case, the proteins contained additional domains such as GAF and PP2C\_SIG (Sigma factor PP2C-like phosphatases), which are also involved in signaling. These findings suggest the SSS family domain as a component

of proteins involved in signal transduction in different groups of organisms, which would not always be linked to histidine kinase domain.

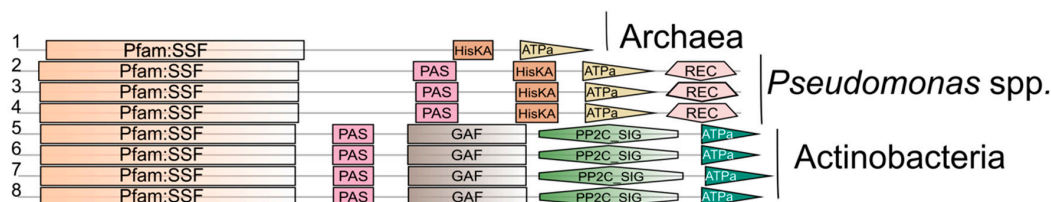


**Figure 6.** Gram-positive organisms containing SSS family domain associated to HATPase\_c. SMART database was used to identify proteins containing Pfam:ssf and HATPase\_c (presented in the figure as “ATPa”) domains. Four isolates of Actinobacteria (5: *Actinospica acidiphila*, 6: *Streptomyces griseorubens*, 7: *Streptomyces albus*, 8: *Streptomyces gilvosporeus*) were selected and, as a comparison, three *Pseudomonas* spp. (2: *Pseudomonas stutzeri*, 3: *Pseudomonas fluorescens* Q2-87, 4: *Pseudomonas corrugata*) and one Archaea were also analyzed (1: *Candidatus Nitrosocaldus cavascurensis*). The ID of the isolates (SMART database) can be found in Table S2.

### 5.1.2. Biological Significance and Targets of Two-Component Systems Containing SSS Domains

Microorganisms can live in extremely different and fluctuating environments, since they have developed numerous features to sense and respond to these conditions [119]. These mechanisms include the one-/two-/multi-component systems, which are named according to the number of proteins involved in the transduction process. In the following, information on the physiological role of recently characterized two-component systems with an SSS domain containing sensor kinase and a response regulator is summarized.

The CbrA/CbrB two-component system was originally described in 2001 in a variant of *Pseudomonas aeruginosa* PAO1 that could not utilize selected amino acids (such as histidine, arginine and proline), polyamines and agmatine as sole carbon or nitrogen source [110]. The gene encoding the sensor kinase of the system was designated as *cbrA*, for catabolite regulation, due to the pleiotropic effects produced by its interruption [110]. Further analyses revealed an involvement of the CbrA/CbrB system in carbon catabolite repression (CCR) [120,121]. Homologs of the system in *Pseudomonas fluorescens* [122] and *P. putida* [123,124] have similar functions in histidine metabolism and CCR. Additionally, the involvement of the system in virulence and antibiotic resistance was reported in *P. aeruginosa* [125,126]. CbrA/CbrB was also recently described in *Azotobacter vinelandii*, where it would be involved in glucose uptake (through the regulation of the GluP transporter) and alginate production [127,128].

Another well-described system in  $\gamma$ -Proteobacteria is CrbS/CrbR, also called MxtR/ErdR in *P. aeruginosa*. It has been linked to acetate metabolism based on analyses of the regulation of the *acs* gene and the growth behavior on acetate in *V. cholerae* [129–131], *P. aeruginosa* [130,132], *P. fluorescens* [133] and *P. entomophila* [130]. Several elements were reported to be regulated by this system, which range from other genes possibly involved in acetate metabolism, such as *actP* (encoding an acetate permease) or Pflu0110 (putative hydrolase) in *P. fluorescens* [133], to genes related to antibiotic resistance [132]. The involvement of this system in pathogenicity was studied in *V. cholerae*, where the expression of *crbS* or *acs-1* was linked to the consumption of host intestinal acetate by the bacteria, which deactivated the insulin signaling and lipid accumulation in enterocytes. This mechanism led to the death of the host, *Drosophila melanogaster* [129]. In *Pseudomonas* spp., a role in virulence was suggested by Zaoui and colleagues in 2011 [132]. In their study, the authors described the expression of important elements for bacterial virulence such as quorum sensing molecules, pyoverdine and pyocyanin, among others, were affected by the presence of the sensor kinase MxtR [132]. However, to date, there are no in vivo results to quantify the importance of the system in pathogenicity.

In addition to the findings in other  $\gamma$ -Proteobacteria associated to CbrA/CbrB and MxtR/ErdR, Rodríguez-Moya and coworkers described in 2010 the presence of a two-component system in the obligately halophilic *Chromohalobacter salexigens*, which would be involved in osmoadaptation [134]. This system is composed of a response regulator (EupR) and a multi-sensor hybrid histidine kinase (the product of the gene *csal869* that includes a PutP/Pfam SSF domain). In the study, the authors reported the involvement of the system in the regulation of the utilization of ectoines as a carbon source and compatible solutes in this halophilic bacterium [135]. However, it is still unknown whether this system has a more general function regulating also other processes (in a similar way to CbrA/CbrB and MxtR/ErdR in virulence).

Additionally, a recent report described a two-component system, PrlS/PrlR, in *Brucella melitensis* ( $\alpha$ -Proteobacteria) that would be important for bacterial adaptation to ionic strength and persistence in mice [136]. The sensor kinase of the system, PrlS, is a hybrid histidine kinase with an SSS N-terminal domain, while the response regulator, PrlR, belongs to the LuxR family. According to the authors, the signal sensed by this two-component system would be ionic strength [136]. In this context, it is interesting to notice that PrlS proteins from other organisms, such as *Aeromonas hydrophila*, were previously predicted to contain an SSS domain [26], which would suggest a role in *A. hydrophila* similar to the one in *B. melitensis*.

## 5.2. Structure-Functions Relationships in SSS Domain-Dependent Sensor Kinases

### 5.2.1. General Characteristics of SSS-Containing Sensor Kinases

From the biochemical point of view, there are only two well-studied SSS-containing sensor kinases in  $\gamma$ -Proteobacteria: CbrA and MxtR (also known as CrbS), that were analyzed in *P. putida*, *P. fluorescens*, *P. aeruginosa*, *V. cholerae*, and *A. vine-landii* [110,123,124,127,128,130,133]. In both CbrA and MxtR, the N-terminal domain is predicted to form 13 TMDs resembling the topology of a member of the SSS family (Figure 7). Transport activity has only been shown so far for the SSS domain of CbrA, with the substrate being L-histidine [124,137]. Connected to this transporter protein is a STAC domain, that was only recently described as a new protein domain. The STAC domain could serve as a linker between the transporter and the C-terminal domains, that are typically found in histidine sensor kinases [133,138]. Following the STAC domain, a Per-Arnt-Sim (PAS) domain, a histidine phosphotransfer (DHp) domain, and a catalytic ATP-binding (CA) domain are present [124,133]. The only difference in domain structure between CbrA and MxtR is that MxtR carries at its C terminus a REC (receiver) domain that CbrA lacks, which implies that MxtR is a hybrid kinase that functions via a phosphorelay mechanism [139].

### 5.2.2. Transport Activity of SSS Family-Containing Sensor Kinase CbrA

The transport activity of CbrA was analyzed in *P. fluorescens* [137] and *P. putida* [124]. CbrA was identified as a possible histidine uptake system in *P. fluorescens* SBW25, because a mutant lacking known histidine transporters was still able to survive with histidine as the sole C and N source, indicating the presence of another transporter. A transposon screen selecting for growth on histidine led to the identification of *cbrA*. Uptake of  $^3\text{H}$ -histidine by wild type cells and mutants confirmed that CbrA functions as a constitutive histidine transporter [137]. The role of the SSS domain in histidine uptake was further explored in a *P. putida* KT2440 mutant [124]. CbrA takes up L-histidine with a  $k_m$  of 0.7  $\mu\text{M}$ , similar to PutP of *E. coli* (Table 1). The maximum uptake rate is relatively low (0.27  $\text{nmol min}^{-1} \text{mg}^{-1}$  of total cell protein). Interestingly, even though CbrA belongs to the sodium solute symporter family [10,26], not a sodium but a proton electrochemical gradient appears to stimulate transport. Amino acids that are involved in sodium binding (Na2 site) in PutP are not conserved in CbrA [124]. It was shown also that a mutant lacking the cytosolic domains of CbrA (SSS domain only) or a mutant that has no kinase activity (CbrA-H766N) transport histidine with the same efficiency, suggesting that the sensor kinase domain is not required for the transport function [124]. The specificity for

histidine is high, and neither other amino acids nor histidine analogues affected the uptake of  $^3\text{H}$ -L-histidine in competition experiments [124].

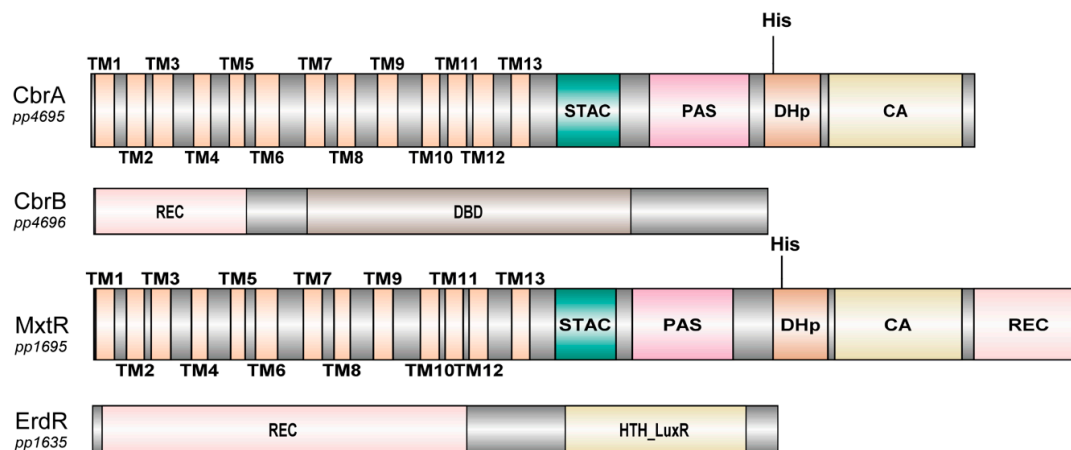


**Figure 7.** Domain structure of CbrA and MxtR as typical SSS-dependent sensor kinases with the according response regulators. The N-terminal portion of the sensor kinases forms 13 TMDs that resemble the topology of an SSS family member, while the C-terminal portions contains domains typically found in sensor kinases. TM, also called TMD, transmembrane domain; STAC, SLC and TCST-Associated Component; PAS, Per-Arnt-Sim; DHp, histidine phosphotransfer domain, also referred to as HisKA; CA, catalytic ATP-binding domain, also referred to as HATpase\_c; REC, receiver; DBD, DNA binding domain (for “sigma-54 interaction domain” predicted by ScanProsite; HTH, helix-turn-helix. Images created with DOG 2.0 illustrator [140]. Domain prediction relies on SMART [113,114] and [133].

### 5.2.3. Properties of Domains Associated with SSS Domain-Containing Sensor Kinases

In prokaryotes, mostly dimeric histidine kinases autophosphorylate at a conserved histidine residue using ATP as a phosphate donor [141]. The H box, with the histidine residue that is the phosphorylation target in the DHp domain, as well as the N-, D- and G- boxes in the CA domain are highly conserved between different SSS domain-containing sensor kinases from different species. It was shown that CbrA contained in *E. coli* TKR2000 membranes can autophosphorylate upon the addition of radioactively labeled  $\gamma$ - $^{32}\text{P}$ -ATP [124]. The histidine residue that is phosphorylated is H766 at the beginning of the DHp domain. The CbrA variant H766N did not show phosphorylation. The protein could also be purified without the SSS domain (CbrA $\Delta$ SSS). The remaining soluble sensor kinase was still phosphorylated at H766. In addition, a reporter assay showed that soluble CbrA $\Delta$ SSS can activate expression of the downstream target gene *crcZ* [124]. In addition, in *P. fluorescens*, a chimeric construct consisting of the SSS domain of CbrS and the kinase domain of CbrA could be used to complement a  $\Delta$ *cbrA*  $\Delta$ *crbS* mutant and support growth on histidine [133]. The results were confirmed in *P. putida* [124]. In conclusion, it seems that the SSS domain is not necessary for the kinase function of CbrA. Even though physical interaction between the two protein domains seems not to be essential for transport and signal transduction, the SSS domain modulates the auto kinase kinetics. This is corroborated by the fact that a target gene can be activated by a soluble CbrA variant (CbrA $\Delta$ SSS) missing the TMDs, but only when it is expressed on a high level [123]. It was also shown that the phosphate can be transferred from CbrA to Asp52 in the REC domain of purified CbrB [124]. Phosphatase activity of CbrA, i.e., dephosphorylation of CbrB-P<sub>i</sub>, has not been observed so far.

The STAC domain was recently described either as a separate protein or embedded within proteins that combine SSS domains with sensor kinase domains [138]. The vast majority of STAC domains occurs between N-terminal SSS domains and C-terminal sensor kinase domains, but so far, the role of the STAC domain remains elusive. A CbrA $\Delta$ STAC

variant had no visible phenotype in *P. fluorescens* [133], but the expression of target gene *crcZ* was decreased in *P. putida* by the deletion of the STAC domain [124].

The structure of PAS domains is broadly conserved and comprises a five-stranded antiparallel  $\beta$ -sheet and several  $\alpha$ -helices, even though the sequence identity is below 20% on average [142]. Almost half of the described PAS containing proteins are histidine kinases, but effector domains include serine/threonine kinases, guanylate cyclases, phosphodiesterases, methyl-accepting chemotaxis proteins and more, that play a role in signal transduction [143]. Typically, the PAS domain is linked N-terminally to the effector domain, like in the case of CbrA or MxtR (CrbS), but there are also examples where the PAS domain is located C-terminally, e.g., in the Sim protein, which contains the first described PAS domain [144]. The PAS domain evolved to bind a huge variety of ligands and cofactors, which can serve as a direct signal or be a step-in sensing signals like gases, redox potential or light [143]. The range of ligands that can bind PAS domains is broad and includes hemes, flavins, amino acids, divalent metal cations, coumaric acid, and fatty acids. Described SSS domain-dependent kinases carry a conserved PAS domain between the STAC and DHP domain in the cytosolic part of the protein. The fact that a CbrA $\Delta$ SSS variant can still function as a kinase and induce signal transduction makes it likely that the sensed signal is intracellular [123,124]. The PAS domain is a likely candidate for a yet to be identified signal. The idea is confirmed by the observation that a CbrA $\Delta$ PAS variant was not able to induce expression of one of its target genes [123].

MxtR (CrbS) of *P. aeruginosa* was cloned as a truncated version without TMDs and used in auto phosphorylation assays. The phosphorylation was inhibited in vitro by ubiquinone, the central electron carrier of respiration, indicating a possible role of MxtR (CrbS) in sensing the redox state of the cell [132]. As mentioned before, the only obvious difference between these sensor kinases is related to the REC domain. A REC (receiver) domain is usually found in response regulators, which is the case for CbrB and ErdR, next to one or several effector domains [112]. Its role is to receive the phosphate from the histidine kinase on an aspartate residue and through a neighboring effector domain leading to a cellular response, usually a change in transcription of target genes. If a REC domain occurs in a hybrid sensor kinase, like MxtR (CrbS), this is called a phosphorelay mechanism. These systems provide greater versatility in signaling strategies and occur often in eukaryotes, while prokaryotes mostly use simpler schemes [139]. So far, the role of MxtR's REC domain is unknown.

## 6. Conclusions

The crystal structures of SGLT of *V. parahaemolyticus* and SiaT of *P. mirabilis* show that the SSS family transporters also share the structural fold of the NSS transporter LeuT, despite the lack of similarity at the amino acid sequence level. Clearly, 3D structures of non-sugar transporters such as the amino acid transporter PutP or vitamin transporters would complete the picture. Numerous structure-function analyses have provided important insights into the details of the transport cycle of SSS family proteins, including the location of sites of sodium and substrate binding, and conformational changes associated with the alternating access mechanism of transport. Future research should focus on more detailed information on physiological relevant intermediate states of transporters, the kinetics of the transitions between these states, the precise stoichiometry of coupling ion and substrate translocated per transporter molecule, and the role of proposed secondary ligand binding sites. This aim can be achieved by combining structure determination, spectroscopic approaches including single molecule analyses, kinetic measurements, and computational simulations. In fact, recent computational analyses of vSGLT suggested, for example, a previously unknown proofreading/editing mechanism enabling the bacteria to discriminate between glucose and potentially toxic analogs [145]. To better understand the role of SSS domains in sensor kinases of regulatory two-component systems, high resolution structures and more precise information on the functions of individual domains (for example, identification of ligands and of the functional consequences of ligand binding

and potentially transport) and on interactions between these domains are required. In addition, more effort is necessary to explore the physiological relevance of these systems in microorganisms. Finally, the knowledge on the structure, functions, and dynamics of the transporters and transporter-related signal transduction systems will provide tools to modulate transporter activities for therapeutic purposes and biotechnological applications.

**Supplementary Materials:** Supplementary materials can be found at <https://www.mdpi.com/1422-0067/22/4/1880/s1>. Figure S1: Amino acid sequence alignment of the SSS family transporters SGLT of *V. parahaemolyticus* (vSGLT), SiaT of *P. mirabilis* (PmSiaT) and PutP of *E. coli* (EcPutP), Table S1: Amino acids involved in sodium and substrate binding in PutP, vSGLT and SiaT, Table S2: Information of the isolates from the SMART database used for Figure 5.

**Funding:** This research and the APC were funded by the Deutsche Forschungsgemeinschaft through grants JU333/5-1, 2 (SPP1617) and JU333/6-1.

**Institutional Review Board Statement:** Not applicable.

**Informed Consent Statement:** Not applicable.

**Data Availability Statement:** Data sharing not applicable.

**Conflicts of Interest:** The authors declare no conflict of interest. The funders had no role in the design of the study; in the collection, analyses, or interpretation of data; in the writing of the manuscript, or in the decision to publish the results.

## References

1. Crane, R.; Miller, D.; Bihler, I. The restrictions on possible mechanisms of intestinal transport of sugars. In *Membrane Transport and Metabolism, Proceedings of a Symposium held in Prague, August 22–27, 1960*; Kleinzeller, A., Kotyk, A., Eds.; ISRC 11795501; Czech Academy of Sciences: Prague, Czech Republic, 1961; pp. 439–449.
2. Wright, E.M.; Loo, D.D.; Hirayama, B.A. Biology of human sodium glucose transporters. *Physiol. Rev.* **2011**, *91*, 733–794. [[CrossRef](#)] [[PubMed](#)]
3. Kleinzeller, A.; Kotyk, A. *Membrane Transport and Metabolism: Proceedings of a Symposium, Prague, Czechia, 22–27 August 1960*; Academic Press: London, UK, 1961.
4. Mitchell, P. Molecule, group and electron translocation through natural membranes. *Biochem. Soc. Symp.* **1962**, *22*, 142–169.
5. Schmidt, S.; Biegel, E.; Müller, V. The ins and outs of Na<sup>+</sup> bioenergetics in *Acetobacterium woodii*. *Biochim. Biophys. Acta (BBA)-Bioenerg.* **2009**, *1787*, 691–696. [[CrossRef](#)]
6. Steffen, W.; Steuber, J. Cation transport by the respiratory NADH:quinone oxidoreductase (complex I): Facts and hypotheses. *Biochem Soc. Trans.* **2013**, *41*, 1280–1287. [[CrossRef](#)]
7. Dimroth, P.; von Ballmoos, C. ATP synthesis by decarboxylation phosphorylation. *Results Probl. Cell Differ.* **2008**, *45*, 153–184. [[CrossRef](#)] [[PubMed](#)]
8. Häse, C.C.; Fedorova, N.D.; Galperin, M.Y.; Dibrov, P.A. Sodium ion cycle in bacterial pathogens: Evidence from cross-genome comparisons. *Microbiol. Mol. Biol. Rev. MMBR* **2001**, *65*, 353–370. [[CrossRef](#)]
9. Padan, E.; Landau, M. Sodium-Proton (Na<sup>+</sup>/H<sup>+</sup>) Antiporters: Properties and roles in health and disease. *Metal. Ions Life Sci.* **2016**, *16*, 391–458.
10. Saier, M.H., Jr.; Reddy, V.S.; Tamang, D.G.; Västermark, Å. The Transporter Classification Database. *Nucleic Acids Res.* **2013**, *42*, D251–D258. [[CrossRef](#)]
11. Krishnamurthy, H.; Piscitelli, C.L.; Gouaux, E. Unlocking the molecular secrets of sodium-coupled transporters. *Nature* **2009**, *459*, 347–355. [[CrossRef](#)] [[PubMed](#)]
12. Abramson, J.; Wright, E.M. Structure and function of Na<sup>+</sup>-symporters with inverted repeats. *Curr. Opin. Struct. Biol.* **2009**, *19*, 425–432. [[CrossRef](#)] [[PubMed](#)]
13. Kalayil, S.; Schulze, S.; Kühlbrandt, W. Arginine oscillation explains Na<sup>+</sup> independence in the substrate/product antiporter CaiT. *Proc. Natl. Acad. Sci. USA* **2013**, *110*, 17296–17301. [[CrossRef](#)] [[PubMed](#)]
14. Shi, Y. Common folds and transport mechanisms of secondary active transporters. *Annu. Rev. Biophys.* **2013**, *42*, 51–72. [[CrossRef](#)]
15. Västermark, Å.; Saier, M.H., Jr. Evolutionary relationship between 5+5 and 7+7 inverted repeat folds within the amino acid-polyamine-organocation superfamily. *Proteins* **2014**, *82*, 336–346. [[CrossRef](#)]
16. Krishnamurthy, H.; Gouaux, E. X-ray structures of LeuT in substrate-free outward-open and apo inward-open states. *Nature* **2012**, *481*, 469–474. [[CrossRef](#)] [[PubMed](#)]
17. Forrest, L.R.; Krämer, R.; Ziegler, C. The structural basis of secondary active transport mechanisms. *Biochim. Biophys. Acta* **2011**, *1807*, 167–188. [[CrossRef](#)]

18. Gottfryd, K.; Boesen, T.; Mortensen, J.S.; Khelashvili, G.; Quick, M.; Terry, D.S.; Missel, J.W.; LeVine, M.V.; Gourdon, P.; Blanchard, S.C.; et al. X-ray structure of LeuT in an inward-facing occluded conformation reveals mechanism of substrate release. *Nat. Commun.* **2020**, *11*, 1005. [[CrossRef](#)]
19. McHaurab, H.S.; Steed, P.R.; Kazmier, K. Toward the fourth dimension of membrane protein structure: Insight into dynamics from spin-labeling EPR spectroscopy. *Structure* **2011**, *19*, 1549–1561. [[CrossRef](#)] [[PubMed](#)]
20. Raba, M.; Dunkel, S.; Hilger, D.; Lipiszko, K.; Polyhach, Y.; Jeschke, G.; Bracher, S.; Klare, J.P.; Quick, M.; Jung, H.; et al. Extracellular loop 4 of the proline transporter PutP controls the periplasmic entrance to ligand binding sites. *Structure* **2014**, *22*, 769–780. [[CrossRef](#)] [[PubMed](#)]
21. Kaback, H.R.; Guan, L. It takes two to tango: The dance of the permease. *J. Gen. Physiol.* **2019**, *151*, 878–886. [[CrossRef](#)]
22. Hilger, D.; Jung, H. *Protein Chemical and Electron Paramagnetic Resonance Spectroscopic Approaches to Monitor Membrane Protein Structure and Dynamics—Methods Chapter*; Wiley-Blackwell: Weinheim, Germany, 2010; pp. 247–263.
23. Hubbell, W.L.; Cafiso, D.S.; Altenbach, C. Identifying conformational changes with site-directed spin labeling. *Nat. Struct. Biol.* **2000**, *7*, 735–739. [[CrossRef](#)]
24. Lerner, E.; Cordes, T.; Ingargiola, A.; Alhadid, Y.; Chung, S.; Michalet, X.; Weiss, S. Toward dynamic structural biology: Two decades of single-molecule Förster resonance energy transfer. *Science* **2018**, *359*. [[CrossRef](#)] [[PubMed](#)]
25. Zhao, Y.; Terry, D.; Shi, L.; Weinstein, H.; Blanchard, S.C.; Javitch, J.A. Single-molecule dynamics of gating in a neurotransmitter transporter homologue. *Nature* **2010**, *465*, 188–193. [[CrossRef](#)] [[PubMed](#)]
26. Jung, H. The sodium/substrate symporter family: Structural and functional features. *FEBS Lett.* **2002**, *529*, 73–77. [[CrossRef](#)]
27. Saier, M.H., Jr.; Reddy, V.S.; Tsu, B.V.; Ahmed, M.S.; Li, C.; Moreno-Hagelsieb, G. The Transporter Classification Database (TCDB): Recent advances. *Nucleic Acids Res.* **2016**, *44*, D372–D379. [[CrossRef](#)] [[PubMed](#)]
28. Wright, E.M.; Ghezzi, C.; Loo, D.D.F. Novel and unexpected functions of SGLTs. *Physiology* **2017**, *32*, 435–443. [[CrossRef](#)]
29. Quick, M.; Shi, L. The sodium/multivitamin transporter: A multipotent system with therapeutic implications. *Vitam. Horm.* **2015**, *98*, 63–100. [[CrossRef](#)]
30. Ravera, S.; Reyna-Neyra, A.; Ferrandino, G.; Amzel, L.M.; Carrasco, N. The sodium/iodide symporter (NIS): Molecular physiology and preclinical and clinical applications. *Annu. Rev. Physiol.* **2017**, *79*, 261–289. [[CrossRef](#)]
31. Jung, H.; Hilger, D.; Raba, M. The Na<sup>+</sup>/L-proline transporter PutP. *Front. Biosci.* **2012**, *17*, 745–759. [[CrossRef](#)]
32. Jung, H.; Tebbe, S.; Schmid, R.; Jung, K. Unidirectional reconstitution and characterization of purified Na<sup>+</sup>/proline transporter of *Escherichia coli*. *Biochemistry* **1998**, *37*, 11083–11088. [[CrossRef](#)]
33. Liao, M.K.; Maloy, S. Substrate recognition by proline permease in *Salmonella*. *Amino Acids* **2001**, *21*, 161–174. [[CrossRef](#)]
34. Tanner, J.J. Structural biology of proline catabolic enzymes. *Antioxid. Redox Signal.* **2019**, *30*, 650–673. [[CrossRef](#)] [[PubMed](#)]
35. Moses, S.; Sinner, T.; Zapras, A.; Stöveken, N.; Hoffmann, T.; Belitsky, B.R.; Sonenshein, A.L.; Bremer, E. Proline utilization by *Bacillus subtilis*: Uptake and catabolism. *J. Bacteriol.* **2012**, *194*, 745–758. [[CrossRef](#)] [[PubMed](#)]
36. Köcher, S.; Tausendschön, M.; Thompson, M.; Saum, S.H.; Müller, V. Proline metabolism in the moderately halophilic bacterium *Halobacillus halophilus*: Differential regulation of isogenes in proline utilization. *Environ. Microbiol. Rep.* **2011**, *3*, 443–448. [[CrossRef](#)] [[PubMed](#)]
37. Lee, J.H.; Park, N.Y.; Lee, M.H.; Choi, S.H. Characterization of the *Vibrio vulnificus putAP* operon, encoding proline dehydrogenase and proline permease, and its differential expression in response to osmotic stress. *J. Bacteriol.* **2003**, *185*, 3842–3852. [[CrossRef](#)] [[PubMed](#)]
38. Nakada, Y.; Nishijyo, T.; Itoh, Y. Divergent structure and regulatory mechanism of proline catabolic systems: Characterization of the *putAP* proline catabolic operon of *Pseudomonas aeruginosa* PAO1 and its regulation by PruR, an AraC/XylS family protein. *J. Bacteriol.* **2002**, *184*, 5633–5640. [[CrossRef](#)]
39. Vilchez, S.; Molina, L.; Ramos, C.; Ramos, J.L. Proline catabolism by *Pseudomonas putida*: Cloning, characterization, and expression of the put genes in the presence of root exudates. *J. Bacteriol.* **2000**, *182*, 91–99. [[CrossRef](#)] [[PubMed](#)]
40. Spiegelhalter, F.; Bremer, E. Osmoregulation of the *opuE* proline transport gene from *Bacillus subtilis*: Contributions of the sigma A- and sigma B-dependent stress-responsive promoters. *Mol. Microbiol.* **1998**, *29*, 285–296. [[CrossRef](#)]
41. Von Blohn, C.; Kempf, B.; Kappes, R.M.; Bremer, E. Osmostress response in *Bacillus subtilis*: Characterization of a proline uptake system (OpuE) regulated by high osmolarity and the alternative transcription factor sigma B. *Mol. Microbiol.* **1997**, *25*, 175–187. [[CrossRef](#)]
42. Ozturk, T.N.; Culham, D.E.; Tempelhagen, L.; Wood, J.M.; Lamoureux, G. Salt-dependent interactions between the C-terminal domain of osmoregulatory transporter ProP of *Escherichia coli* and the lipid membrane. *J. Phys. Chem. B* **2020**, *124*, 8209–8220. [[CrossRef](#)]
43. Ziegler, C.; Bremer, E.; Krämer, R. The BCCT family of carriers: From physiology to crystal structure. *Mol. Microbiol.* **2010**, *78*, 13–34. [[CrossRef](#)] [[PubMed](#)]
44. Racher, K.I.; Voegelé, R.T.; Marshall, E.V.; Culham, D.E.; Wood, J.M.; Jung, H.; Bacon, M.; Cairns, M.T.; Ferguson, S.M.; Liang, W.J.; et al. Purification and reconstitution of an osmosensor: Transporter ProP of *Escherichia coli* senses and responds to osmotic shifts. *Biochemistry* **1999**, *38*, 1676–1684. [[CrossRef](#)] [[PubMed](#)]
45. Krishnan, N.; Doster, A.R.; Duhamel, G.E.; Becker, D.F. Characterization of a *Helicobacter hepaticus putA* mutant strain in host colonization and oxidative stress. *Infect. Immun.* **2008**, *76*, 3037. [[CrossRef](#)]
46. Available, N.A.N.; Mohanty, P.; Matysik, J. Effect of proline on the production of singlet oxygen. *Amino Acids* **2001**, *21*, 195–200. [[CrossRef](#)] [[PubMed](#)]

47. Smirnov, N.; Cumbes, Q.J. Hydroxyl radical scavenging activity of compatible solutes. *Phytochemistry* **1989**, *28*, 1057–1060. [[CrossRef](#)]
48. Krishnan, N.; Becker, D.F. Oxygen reactivity of PutA from *Helicobacter* species and proline-linked oxidative stress. *J. Bacteriol.* **2006**, *188*, 1227. [[CrossRef](#)] [[PubMed](#)]
49. Christgen, S.L.; Becker, D.F. Role of proline in pathogen and host interactions. *Antioxid. Redox Signal.* **2019**, *30*, 683–709. [[CrossRef](#)]
50. Schwan, W.R.; Wetzel, K.J. Osmolyte transport in *Staphylococcus aureus* and the role in pathogenesis. *World J. Clin. Infect. Dis.* **2016**, *6*, 22–27. [[CrossRef](#)]
51. Schwan, W.R.; Lehmann, L.; McCormick, J. Transcriptional activation of the *Staphylococcus aureus* *putP* gene by low-proline-high osmotic conditions and during infection of murine and human tissues. *Infect. Immun.* **2006**, *74*, 399–409. [[CrossRef](#)]
52. Schwan, W.R.; Wetzel, K.J.; Gomez, T.S.; Stiles, M.A.; Beitlich, B.D.; Grunwald, S. Low-proline environments impair growth, proline transport and in vivo survival of *Staphylococcus aureus* strain-specific *putP* mutants. *Microbiology* **2004**, *150*, 1055–1061. [[CrossRef](#)] [[PubMed](#)]
53. Bae, J.H.; Miller, K.J. Identification of two proline transport systems in *Staphylococcus aureus* and their possible roles in osmoregulation. *Appl. Environ. Microbiol.* **1992**, *58*, 471–475. [[CrossRef](#)]
54. Miller, K.J.; Zelt, S.C.; Bae, J.-H. Glycine betaine and proline are the principal compatible solutes of *Staphylococcus aureus*. *Curr. Microbiol.* **1991**, *23*, 131–137. [[CrossRef](#)]
55. Suerbaum, S.; Josenhans, C. *Helicobacter pylori* evolution and phenotypic diversification in a changing host. *Nat. Rev. Microbiol.* **2007**, *5*, 441–452. [[CrossRef](#)]
56. Kavermann, H.; Burns, B.P.; Angermuller, K.; Odenbreit, S.; Fischer, W.; Melchers, K.; Haas, R. Identification and characterization of *Helicobacter pylori* genes essential for gastric colonization. *J. Exp. Med.* **2003**, *197*, 813–822. [[CrossRef](#)]
57. Nakajima, K.; Inatsu, S.; Mizote, T.; Nagata, Y.; Aoyama, K.; Fukuda, Y.; Nagata, K. Possible involvement of *putA* gene in *Helicobacter pylori* colonization in the stomach and motility. *Biomed. Res.* **2008**, *29*, 9–18. [[CrossRef](#)]
58. Rivera-Ordaz, A.; Bracher, S.; Sarrach, S.; Li, Z.; Shi, L.; Quick, M.; Hilger, D.; Haas, R.; Jung, H. The sodium/proline transporter PutP of *Helicobacter pylori*. *PLoS ONE* **2013**, *8*, e83576. [[CrossRef](#)] [[PubMed](#)]
59. Park, H.B.; Sampathkumar, P.; Perez, C.E.; Lee, J.H.; Tran, J.; Bonanno, J.B.; Hallem, E.A.; Almo, S.C.; Crawford, J.M. Stilbene epoxidation and detoxification in a *Photobacterium luminescens*-nematode symbiosis. *J. Biol. Chem.* **2017**, *292*, 6680–6694. [[CrossRef](#)]
60. Kontnik, R.; Crawford, J.M.; Clardy, J. Exploiting a global regulator for small molecule discovery in *Photobacterium luminescens*. *ACS Chem. Biol.* **2010**, *5*, 659–665. [[CrossRef](#)]
61. Kraemer, P.S.; Mitchell, A.; Pelletier, M.R.; Gallagher, L.A.; Wasnick, M.; Rohmer, L.; Brittnacher, M.J.; Manoilo, C.; Skerrett, S.J.; Salama, N.R. Genome-wide screen in *Francisella novicida* for genes required for pulmonary and systemic infection in mice. *Infect. Immun.* **2009**, *77*, 232–244. [[CrossRef](#)]
62. Wilson, T.H.; Ding, P.Z. Sodium-substrate cotransport in bacteria. *Biochim. Biophys. Acta* **2001**, *1505*, 121–130. [[CrossRef](#)]
63. Turk, E.; Kim, O.; le Coutre, J.; Whitelegge, J.P.; Eskandari, S.; Lam, J.T.; Kremann, M.; Zampighi, G.; Faull, K.F.; Wright, E.M. Molecular characterization of *Vibrio parahaemolyticus* vSGLT: A model for sodium-coupled sugar cotransporters. *J. Biol. Chem.* **2000**, *275*, 25711–25716. [[CrossRef](#)] [[PubMed](#)]
64. Wahlgren, W.Y.; Dunevall, E.; North, R.A.; Paz, A.; Scalise, M.; Bisignano, P.; Bengtsson-Palme, J.; Goyal, P.; Claesson, E.; Caing-Carlsson, R.; et al. Substrate-bound outward-open structure of a Na<sup>+</sup>-coupled sialic acid symporter reveals a new Na<sup>+</sup> site. *Nat. Commun.* **2018**, *9*, 1753. [[CrossRef](#)] [[PubMed](#)]
65. Jeckelmann, J.M.; Erni, B. Transporters of glucose and other carbohydrates in bacteria. *Pflügers Arch.* **2020**, *472*, 1129–1153. [[CrossRef](#)]
66. Sarker, R.I.; Ogawa, W.; Tsuda, M.; Tanaka, S.; Tsuchiya, T. Characterization of a glucose transport system in *Vibrio parahaemolyticus*. *J. Bacteriol.* **1994**, *176*, 7378–7382. [[CrossRef](#)]
67. Rodionov, D.A.; Yang, C.; Li, X.; Rodionova, I.A.; Wang, Y.; Obratsova, A.Y.; Zagnitko, O.P.; Overbeek, R.; Romine, M.F.; Reed, S.; et al. Genomic encyclopedia of sugar utilization pathways in the *Shewanella* genus. *BMC Genom.* **2010**, *11*, 494. [[CrossRef](#)] [[PubMed](#)]
68. Wiczew, D.; Borowska, A.; Szkaradek, K.; Biegus, T.; Wozniak, K.; Pyclik, M.; Sitarska, M.; Jaszewski, L.; Radosinski, L.; Hanus-Lorenz, B.; et al. Molecular mechanism of vSGLT inhibition by gneyulin reveals antiseptic properties against multidrug-resistant Gram-negative bacteria. *J. Mol. Model.* **2019**, *25*, 186. [[CrossRef](#)] [[PubMed](#)]
69. Thomas, G.H. Sialic acid acquisition in bacteria—one substrate, many transporters. *Biochem. Soc. Trans.* **2016**, *44*, 760–765. [[CrossRef](#)]
70. North, R.A.; Wahlgren, W.Y.; Remus, D.M.; Scalise, M.; Kessans, S.A.; Dunevall, E.; Claesson, E.; Soares da Costa, T.P.; Perugini, M.A.; Ramaswamy, S.; et al. The sodium sialic acid symporter from *Staphylococcus aureus* has altered substrate specificity. *Front. Chem.* **2018**, *6*, 233. [[CrossRef](#)]
71. Ng, K.M.; Ferreyra, J.A.; Higginbottom, S.K.; Lynch, J.B.; Kashyap, P.C.; Gopinath, S.; Naidu, N.; Choudhury, B.; Weimer, B.C.; Monack, D.M.; et al. Microbiota-liberated host sugars facilitate post-antibiotic expansion of enteric pathogens. *Nature* **2013**, *502*, 96–99. [[CrossRef](#)]
72. Morrison, D.J.; Preston, T. Formation of short chain fatty acids by the gut microbiota and their impact on human metabolism. *Gut Microbes* **2016**, *7*, 189–200. [[CrossRef](#)]
73. Vives-Peris, V.; de Ollas, C.; Gómez-Cadenas, A.; Pérez-Clemente, R.M. Root exudates: From plant to rhizosphere and beyond. *Plant Cell Rep.* **2020**, *39*, 3–17. [[CrossRef](#)]
74. D'Souza, G.; Shitut, S.; Preussger, D.; Yousif, G.; Waschina, S.; Kost, C. Ecology and evolution of metabolic cross-feeding interactions in bacteria. *Nat. Prod. Rep.* **2018**, *35*, 455–488. [[CrossRef](#)]

75. Gimenez, R.; Nuñez, M.F.; Badia, J.; Aguilar, J.; Baldoma, L. The gene *yjcG*, cotranscribed with the gene *acs*, encodes an acetate permease in *Escherichia coli*. *J. Bacteriol.* **2003**, *185*, 6448–6455. [[CrossRef](#)]
76. Jolkver, E.; Emer, D.; Ballan, S.; Krämer, R.; Eikmanns, B.J.; Marin, K. Identification and characterization of a bacterial transport system for the uptake of pyruvate, propionate, and acetate in *Corynebacterium glutamicum*. *J. Bacteriol.* **2009**, *191*, 940–948. [[CrossRef](#)]
77. Hosie, A.H.; Allaway, D.; Poole, P.S. A monocarboxylate permease of *Rhizobium leguminosarum* is the first member of a new subfamily of transporters. *J. Bacteriol.* **2002**, *184*, 5436–5448. [[CrossRef](#)]
78. Borghese, R.; Zannoni, D. Acetate permease (ActP) is responsible for tellurite ( $\text{TeO}_3^{2-}$ ) uptake and resistance in cells of the facultative phototroph *Rhodobacter capsulatus*. *Appl. Environ. Microbiol.* **2010**, *76*, 942–944. [[CrossRef](#)] [[PubMed](#)]
79. Jung, H.; Rübenhagen, R.; Tebbe, S.; Leifker, K.; Tholema, N.; Quick, M.; Schmid, R. Topology of the  $\text{Na}^+$ /proline transporter of *Escherichia coli*. *J. Biol. Chem.* **1998**, *273*, 26400–26407. [[CrossRef](#)]
80. Wegener, C.; Tebbe, S.; Steinhoff, H.-J.; Jung, H. Spin labeling analysis of structure and dynamics of the  $\text{Na}^+$ /proline transporter of *Escherichia coli*. *Biochemistry* **2000**, *39*, 4831–4837. [[CrossRef](#)] [[PubMed](#)]
81. Turk, E.; Wright, E.M. Membrane topology motifs in the SGLT cotransporter family. *J. Membr. Biol.* **1997**, *159*, 1–20. [[CrossRef](#)] [[PubMed](#)]
82. Hediger, M.A.; Turk, E.; Wright, E.M. Homology of the human intestinal  $\text{Na}^+$ /glucose and *Escherichia coli*  $\text{Na}^+$ /proline cotransporters. *Proc. Natl. Acad. Sci. USA* **1989**, *86*, 5748. [[CrossRef](#)]
83. Faham, S.; Watanabe, A.; Besserer, G.M.; Cascio, D.; Specht, A.; Hirayama, B.A.; Wright, E.M.; Abramson, J. The crystal structure of a sodium galactose transporter reveals mechanistic insights into  $\text{Na}^+$ /sugar symport. *Science* **2008**, *321*, 810–814. [[CrossRef](#)] [[PubMed](#)]
84. Watanabe, A.; Choe, S.; Chaptal, V.; Rosenberg, J.M.; Wright, E.M.; Grabe, M.; Abramson, J. The mechanism of sodium and substrate release from the binding pocket of vSGLT. *Nature* **2010**, *468*, 988–991. [[CrossRef](#)]
85. Yamashita, A.; Singh, S.K.; Kawate, T.; Jin, Y.; Gouaux, E. Crystal structure of a bacterial homologue of  $\text{Na}^+$ /Cl<sup>-</sup>-dependent neurotransmitter transporters. *Nature* **2005**, *437*, 215–223. [[CrossRef](#)]
86. Claxton, D.P.; Quick, M.; Shi, L.; de Carvalho, F.D.; Weinstein, H.; Javitch, J.A.; McHaourab, H.S. Ion/substrate-dependent conformational dynamics of a bacterial homolog of neurotransmitter:sodium symporters. *Nat. Struct. Mol. Biol.* **2010**, *17*, 822–829. [[CrossRef](#)]
87. Kazmier, K.; Claxton, D.P.; McHaourab, H.S. Alternating access mechanisms of LeuT-fold transporters: Trailblazing towards the promised energy landscapes. *Curr. Opin. Struct. Biol.* **2017**, *45*, 100–108. [[CrossRef](#)] [[PubMed](#)]
88. Bracher, S.; Schmidt, C.C.; Dittmer, S.I.; Jung, H. Core transmembrane domain 6 plays a pivotal role in the transport cycle of the sodium/proline symporter PutP. *J. Biol. Chem.* **2016**, *291*, 26208–26215. [[CrossRef](#)]
89. Penmatsa, A.; Gouaux, E. How LeuT shapes our understanding of the mechanisms of sodium-coupled neurotransmitter transporters. *J. Physiol.* **2014**, *592*, 863–869. [[CrossRef](#)]
90. Bracher, S.; Guérin, K.; Polyhach, Y.; Jeschke, G.; Dittmer, S.; Frey, S.; Böhm, M.; Jung, H. Glu-311 in external loop 4 of the sodium/proline transporter PutP is crucial for external gate closure. *J. Biol. Chem.* **2016**, *291*, 4998–5008. [[CrossRef](#)] [[PubMed](#)]
91. Pettersen, E.F.; Goddard, T.D.; Huang, C.C.; Couch, G.S.; Greenblatt, D.M.; Meng, E.C.; Ferrin, T.E. UCSF Chimera—A visualization system for exploratory research and analysis. *J. Comput. Chem.* **2004**, *25*, 1605–1612. [[CrossRef](#)]
92. Hilger, D.; Böhm, M.; Hackmann, A.; Jung, H. Role of Ser-340 and Thr-341 in transmembrane domain IX of the  $\text{Na}^+$ /proline transporter PutP of *Escherichia coli* in ligand binding and transport. *J. Biol. Chem.* **2008**, *283*, 4921–4929. [[CrossRef](#)] [[PubMed](#)]
93. Quick, M.; Jung, H. A conserved aspartate residue, Asp187, is important for  $\text{Na}^+$ -dependent proline binding and transport by the  $\text{Na}^+$ /proline transporter of *Escherichia coli*. *Biochemistry* **1998**, *37*, 13800–13806. [[CrossRef](#)]
94. Raba, M.; Baumgartner, T.; Hilger, D.; Klempahn, K.; Härtel, T.; Jung, K.; Jung, H. Function of transmembrane domain IX in the  $\text{Na}^+$ /proline transporter PutP. *J. Mol. Biol.* **2008**, *382*, 884–893. [[CrossRef](#)] [[PubMed](#)]
95. Quick, M.; Shi, L.; Zehnpfennig, B.; Weinstein, H.; Javitch, J.A. Experimental conditions can obscure the second high-affinity site in LeuT. *Nat. Struct. Mol. Biol.* **2012**, *19*, 207–211. [[CrossRef](#)]
96. Wang, H.; Elferich, J.; Gouaux, E. Structures of LeuT in bicelles define conformation and substrate binding in a membrane-like context. *Nat. Struct. Mol. Biol.* **2012**, *19*, 212–219. [[CrossRef](#)]
97. Shi, L.; Quick, M.; Zhao, Y.; Weinstein, H.; Javitch, J.A. The mechanism of a neurotransmitter:sodium symporter—inward release of  $\text{Na}^+$  and substrate is triggered by substrate in a second binding site. *Mol. Cell* **2008**, *30*, 667–677. [[CrossRef](#)] [[PubMed](#)]
98. LeVine, M.V.; Cuendet, M.A.; Khelashvili, G.; Weinstein, H. Allosteric mechanisms of molecular machines at the membrane: Transport by sodium-coupled symporters. *Chem. Rev.* **2016**, *116*, 6552–6587. [[CrossRef](#)] [[PubMed](#)]
99. Li, Z.; Lee, A.S.; Bracher, S.; Jung, H.; Paz, A.; Kumar, J.P.; Abramson, J.; Quick, M.; Shi, L. Identification of a second substrate-binding site in solute-sodium symporters. *J. Biol. Chem.* **2015**, *290*, 127–141. [[CrossRef](#)] [[PubMed](#)]
100. Paz, A.; Claxton, D.P.; Kumar, J.P.; Kazmier, K.; Bisignano, P.; Sharma, S.; Nolte, S.A.; Liwag, T.M.; Nayak, V.; Wright, E.M.; et al. Conformational transitions of the sodium-dependent sugar transporter, vSGLT. *Proc. Natl. Acad. Sci. USA* **2018**, *115*, E2742. [[CrossRef](#)] [[PubMed](#)]
101. Bisignano, P.; Ghezzi, C.; Jo, H.; Polizzi, N.F.; Althoff, T.; Kalyanaraman, C.; Friemann, R.; Jacobson, M.P.; Wright, E.M.; Grabe, M. Inhibitor binding mode and allosteric regulation of  $\text{Na}^+$ -glucose symporters. *Nat. Commun.* **2018**, *9*, 5245. [[CrossRef](#)] [[PubMed](#)]
102. Jardetzky, O. Simple allosteric model for membrane pumps. *Nature* **1966**, *211*, 969–970. [[CrossRef](#)] [[PubMed](#)]
103. Vidaver, G.A. Inhibition of parallel flux and augmentation of counter flux shown by transport models not involving a mobile carrier. *J. Theor. Biol.* **1966**, *10*, 301–306. [[CrossRef](#)]

104. Widdas, W.F. Inability of diffusion to account for placental glucose transfer in the sheep and consideration of the kinetics of a possible carrier transfer. *J. Physiol.* **1952**, *118*, 23–39. [[CrossRef](#)]
105. Bai, X.; Moraes, T.F.; Reithmeier, R.A.F. Structural biology of solute carrier (SLC) membrane transport proteins. *Mol. Membr. Biol.* **2017**, *34*, 1–32. [[CrossRef](#)] [[PubMed](#)]
106. Zhou, A.; Wozniak, A.; Meyer-Lipp, K.; Nietschke, M.; Jung, H.; Fendler, K. Charge translocation during cosubstrate binding in the Na<sup>+</sup>/proline transporter of *E. coli*. *J. Mol. Biol.* **2004**, *343*, 931–942. [[CrossRef](#)] [[PubMed](#)]
107. Pirch, T.; Landmeier, S.; Jung, H. Transmembrane domain II of the Na<sup>+</sup>/proline transporter PutP of *Escherichia coli* forms part of a conformationally flexible, cytoplasmic exposed aqueous cavity within the membrane. *J. Biol. Chem.* **2003**, *278*, 42942–42949. [[CrossRef](#)] [[PubMed](#)]
108. Olkhova, E.; Raba, M.; Bracher, S.; Hilger, D.; Jung, H. Homology model of the Na<sup>+</sup>/proline transporter PutP of *Escherichia coli* and its functional implications. *J. Mol. Biol.* **2011**, *406*, 59–74. [[CrossRef](#)]
109. Quick, M.; Jung, H. Aspartate 55 in the Na<sup>+</sup>/proline permease of *Escherichia coli* is essential for Na<sup>+</sup>-coupled proline uptake. *Biochemistry* **1997**, *36*, 4631–4636. [[CrossRef](#)]
110. Nishijyo, T.; Haas, D.; Itoh, Y. The CbrA–CbrB two-component regulatory system controls the utilization of multiple carbon and nitrogen sources in *Pseudomonas aeruginosa*. *Mol. Microbiol.* **2001**, *40*, 917–931. [[CrossRef](#)]
111. Jung, H. Towards the molecular mechanism of Na<sup>+</sup>/solute symport in prokaryotes. *Biochim. Biophys. Acta (BBA)-Bioenerg.* **2001**, *1505*, 131–143. [[CrossRef](#)]
112. Mascher, T.; Helmman, J.D.; Uden, G. Stimulus perception in bacterial signal-transducing histidine kinases. *Microbiol. Mol. Biol. Rev.* **2006**, *70*, 910–938. [[CrossRef](#)] [[PubMed](#)]
113. Letunic, I.; Doerks, T.; Bork, P. SMART: Recent updates, new developments and status in 2015. *Nucleic Acids Res.* **2015**, *43*, D257–D260. [[CrossRef](#)]
114. Letunic, I.; Bork, P. 20 years of the SMART protein domain annotation resource. *Nucleic Acids Res.* **2017**, *46*, D493–D496. [[CrossRef](#)]
115. Schultz, J.; Milpetz, F.; Bork, P.; Ponting, C.P. SMART, a simple modular architecture research tool: Identification of signaling domains. *Proc. Natl. Acad. Sci. USA* **1998**, *95*, 5857–5864. [[CrossRef](#)] [[PubMed](#)]
116. Letunic, I.; Bork, P. Interactive Tree of Life (iTOL) v4: Recent updates and new developments. *Nucleic Acids Res.* **2019**, *47*, W256–W259. [[CrossRef](#)]
117. Letunic, I.; Bork, P. Interactive Tree of Life (iTOL): An online tool for phylogenetic tree display and annotation. *Bioinformatics* **2007**, *23*, 127–128. [[CrossRef](#)] [[PubMed](#)]
118. Galperin, M. Sensory transduction in bacteria. *Encycl. Microbiol.* **2009**, 447–463. [[CrossRef](#)]
119. Tiwari, S.; Jamal, S.B.; Hassan, S.S.; Carvalho, P.V.S.D.; Almeida, S.; Barh, D.; Ghosh, P.; Silva, A.; Castro, T.L.P.; Azevedo, V. Two-component signal transduction systems of pathogenic bacteria as targets for antimicrobial therapy: An Overview. *Front. Microbiol.* **2017**, *8*, 1878. [[CrossRef](#)]
120. Valentini, M.; García-Mauriño, S.M.; Pérez-Martínez, I.; Santero, E.; Canosa, I.; Lapouge, K. Hierarchical management of carbon sources is regulated similarly by the CbrA/B systems in *Pseudomonas aeruginosa* and *Pseudomonas putida*. *Microbiology* **2014**, *160*, 2243–2252. [[CrossRef](#)] [[PubMed](#)]
121. Moreno, R.; Fonseca, P.; Rojo, F. Two small RNAs, CrcY and CrcZ, act in concert to sequester the Crc global regulator in *Pseudomonas putida*, modulating catabolite repression. *Mol. Microbiol.* **2012**, *83*, 24–40. [[CrossRef](#)]
122. Zhang, X.-X.; Rainey, P.B. Genetic analysis of the histidine utilization (*hut*) genes in *Pseudomonas fluorescens* SBW25. *Genetics* **2007**, *176*, 2165–2176. [[CrossRef](#)]
123. Monteagudo-Cascales, E.; García-Mauriño, S.M.; Santero, E.; Canosa, I. Unraveling the role of the CbrA histidine kinase in the signal transduction of the CbrAB two-component system in *Pseudomonas putida*. *Sci. Rep.* **2019**, *9*, 9110. [[CrossRef](#)]
124. Wirtz, L.; Eder, M.; Schipper, K.; Rohrer, S.; Jung, H. Transport and kinase activities of CbrA of *Pseudomonas putida* KT2440. *Sci. Rep.* **2020**, *10*, 5400. [[CrossRef](#)]
125. Yeung, A.T.Y.; Janot, L.; Pena, O.M.; Neidig, A.; Kukavica-Ibrulj, I.; Hilchie, A.; Levesque, R.C.; Overhage, J.; Hancock, R.E.W. Requirement of the *Pseudomonas aeruginosa* CbrA sensor kinase for full virulence in a murine acute lung infection model. *Infect. Immun.* **2014**, *82*, 1256–1267. [[CrossRef](#)]
126. Yeung, A.T.Y.; Bains, M.; Hancock, R.E.W. The sensor kinase CbrA is a global regulator that modulates metabolism, virulence, and antibiotic resistance in *Pseudomonas aeruginosa*. *J. Bacteriol.* **2011**, *193*, 918–931. [[CrossRef](#)]
127. Quiroz-Rocha, E.; Bonilla-Badía, F.; García-Aguilar, V.; López-Pliego, L.; Serrano-Román, J.; Cocotl-Yañez, M.; Guzmán, J.; Ahumada-Manuel, C.L.; Muriel-Millán, L.F.; Castañeda, M.; et al. Two-component system CbrA/CbrB controls alginate production in *Azotobacter vinelandii*. *Microbiology* **2017**, *163*, 1105–1115. [[CrossRef](#)]
128. Quiroz-Rocha, E.; Moreno, R.; Hernández-Ortíz, A.; Fragoso-Jiménez, J.C.; Muriel-Millán, L.F.; Guzmán, J.; Espín, G.; Rojo, F.; Núñez, C. Glucose uptake in *Azotobacter vinelandii* occurs through a GluP transporter that is under the control of the CbrA/CbrB and Hfq-Crc systems. *Sci. Rep.* **2017**, *7*, 858. [[CrossRef](#)]
129. Hang, S.; Purdy, A.E.; Robins, W.P.; Wang, Z.; Mandal, M.; Chang, S.; Mekalanos, J.J.; Watnick, P.I. The acetate switch of an intestinal pathogen disrupts host insulin signaling and lipid metabolism. *Cell Host Microbe* **2014**, *16*, 592–604. [[CrossRef](#)] [[PubMed](#)]
130. Jacob, K.; Rasmussen, A.; Tyler, P.; Servos, M.M.; Sylla, M.; Prado, C.; Daniele, E.; Sharp, J.S.; Purdy, A.E. Regulation of acetyl-CoA synthetase transcription by the CbrS/R two-component system is conserved in genetically diverse environmental pathogens. *PLoS ONE* **2017**, *12*, e0177825. [[CrossRef](#)] [[PubMed](#)]

131. Muzhingi, I.; Prado, C.; Sylla, M.; Diehl, F.F.; Nguyen, D.K.; Servos, M.M.; Flores Ramos, S.; Purdy, A.E. Modulation of CrbS-dependent activation of the acetate switch in *Vibrio cholerae*. *J. Bacteriol.* **2018**, *200*. [[CrossRef](#)] [[PubMed](#)]
132. Zaoui, C.; Overhage, J.; Löns, D.; Zimmermann, A.; Müsken, M.; Bielecki, P.; Pustelny, C.; Becker, T.; Nimtz, M.; Häussler, S. An torphan sensor kinase controls quinolone signal production via MexT in *Pseudomonas aeruginosa*. *Mol. Microbiol.* **2012**, *83*, 536–547. [[CrossRef](#)] [[PubMed](#)]
133. Sepulveda, E.; Lupas, A.N. Characterization of the CrbS/R two-component system in *Pseudomonas fluorescens* reveals a new set of genes under its control and a DNA motif required for CrbR-mediated transcriptional activation. *Front. Microbiol.* **2017**, *8*. [[CrossRef](#)] [[PubMed](#)]
134. Rodríguez-Moya, J.; Argandoña, M.; Reina-Bueno, M.; Nieto, J.J.; Iglesias-Guerra, F.; Jebbar, M.; Vargas, C. Involvement of EupR, a response regulator of the NarL/FixJ family, in the control of the uptake of the compatible solutes ectoines by the halophilic bacterium *Chromohalobacter salexigens*. *BMC Microbiol.* **2010**, *10*, 256. [[CrossRef](#)]
135. Silva-Rocha, R.; Martínez-García, E.; Calles, B.; Chavarria, M.; Arce-Rodríguez, A.; de Las Heras, A.; Paez-Espino, A.D.; Durante-Rodríguez, G.; Kim, J.; Nikel, P.I.; et al. The Standard European Vector Architecture (SEVA): A coherent platform for the analysis and deployment of complex prokaryotic phenotypes. *Nucleic Acids Res.* **2013**, *41*, D666–D675. [[CrossRef](#)]
136. Mirabella, A.; Villanueva, R.-M.Y.; Delrue, R.-M.; Uzureau, S.; Zygmunt, M.S.; Cloeckaert, A.; De Bolle, X.; Letesson, J.-J. The two-component system PrlS/PrIR of *Brucella melitensis* is required for persistence in mice and appears to respond to ionic strength. *Microbiology* **2012**, *158*, 2642–2651. [[CrossRef](#)]
137. Zhang, X.-X.; Gauntlett, J.C.; Oldenburg, D.G.; Cook, G.M.; Rainey, P.B. Role of the transporter-like sensor kinase CbrA in histidine uptake and signal transduction. *J. Bacteriol.* **2015**, *197*, 2867–2878. [[CrossRef](#)]
138. Korycynski, M.; Albrecht, R.; Ursinus, A.; Hartmann, M.D.; Coles, M.; Martin, J.; Dunin-Horkawicz, S.; Lupas, A.N. STAC—A new domain associated with transmembrane solute transport and two-component signal transduction systems. *J. Mol. Biol.* **2015**, *427*, 3327–3339. [[CrossRef](#)] [[PubMed](#)]
139. West, A.H.; Stock, A.M. Histidine kinases and response regulator proteins in two-component signaling systems. *Trends Biochem. Sci.* **2001**, *26*, 369–376. [[CrossRef](#)]
140. Ren, J.; Wen, L.; Gao, X.; Jin, C.; Xue, Y.; Yao, X. DOG 1.0: Illustrator of protein domain structures. *Cell Res.* **2009**, *19*, 271–273. [[CrossRef](#)] [[PubMed](#)]
141. Wolanin, P.M.; Thomason, P.A.; Stock, J.B. Histidine protein kinases: Key signal transducers outside the animal kingdom. *Genome Biol.* **2002**, *3*, REVIEWS3013. [[CrossRef](#)]
142. Möglich, A.; Ayers, R.A.; Moffat, K. Structure and signaling mechanism of Per-ARNT-Sim domains. *Structure* **2009**, *17*, 1282–1294. [[CrossRef](#)]
143. Henry, J.T.; Crosson, S. Ligand-binding PAS domains in a genomic, cellular, and structural context. *Annu. Rev. Microbiol.* **2011**, *65*, 261–286. [[CrossRef](#)]
144. Nambu, J.R.; Lewis, J.O.; Wharton, K.A.; Crews, S.T. The *Drosophila* single-minded gene encodes a helix-loop-helix protein that acts as a master regulator of CNS midline development. *Cell* **1991**, *67*, 1157–1167. [[CrossRef](#)]
145. Bisignano, P.; Lee, M.A.; George, A.; Zuckerman, D.M.; Grabe, M.; Rosenberg, J.M. A kinetic mechanism for enhanced selectivity of membrane transport. *PLoS Comput. Biol.* **2020**, *16*, e1007789. [[CrossRef](#)] [[PubMed](#)]

Supplementary Information

**Prokaryotic solute/sodium symporters: versatile functions and mechanisms of a transporter family**

Tania Henriquez <sup>1</sup>, Larissa Wirtz <sup>1</sup>, Dan Su <sup>1</sup> and Heinrich Jung <sup>1,\*</sup>

<sup>1</sup> Microbiology, Dept. Biology 1, Ludwig Maximilians University Munich, D-82152 Martinsried, Germany

\* Correspondence: [hjung@lmu.de](mailto:hjung@lmu.de); Tel.: +49-89-218074630



**Supplementary Figure S1.** Amino acid sequence alignment of the SSS family transporters SGLT of *V. parahaemolyticus* (vSGLT), SiaT of *P. mirabilis* (PmSiaT) and PutP of *E. coli* (EcPutP). The alignment was performed with Clustal Omega [1]. Amino acid sequences forming TMDs are underlined. TMDs are numbered as described in Figure 2a. Amino acids highlighted in **red** coordinate sodium at the Na2 site, while amino acids in **orange** belong to the recently described Na3 site of PmSiaT. Amino acids labeled in **blue** constitute the central substrate binding site. Amino acids highlighted in **blue** and *italic* interact with the substrate via water molecules. Amino acids highlighted in **brown** form the outer “thin” hydrophobic gate. For PutP, amino acids of particular functional significance are highlighted in **bold** (compare also Table 2). Information was taken from the following references: vSGLT [2,3], PmSiaT [4], EcPutP [5-9].

**Supplementary Table S1. Amino acids involved in sodium and substrate binding in PutP, vSGLT and SiaT<sup>a</sup>**

Function	PutP	vSGLT	SiaT
Na <sub>2</sub> site	cTMD1: A53, M56 cTMD8: A337, S340, T341	cTMD1: A62, I65 cTMD8: A361, S364, S365	cTMD1: A56, L59 cTMD8: A339, S342, S343
Na <sub>3</sub> site	cTMD5: D187 (?) cTMD8: S340 (?), C344 (?), Q345 (?)	no experimental evidence	cTMD5: D182 cTMD8: S342, S345 S346
central substrate binding site	cTMD1: S54, S57 (?) cTMD6: Y248, P252 (?) cTMD8: C344, M369 (?)	cTMD1: Q69 cTMD2: E88, S91 cTMD6: N260 cTMD7: K294 cTMD10: Q428	cTMD1: T58, S60, T63 cTMD2: F78, Q82 cTMD3: R135 cTMD6: N247, Q250
2 <sup>nd</sup> substrate binding site <sup>b</sup>	cTMD1: S57, W59 (?) cTMD6: W244, Y248 (?) cTMD10: L398, S402 (?)	cTMD1: S66 (?) cTMD6: Y269, R273 (?) cTMD8: S365, S368 (?)	no experimental evidence

<sup>a</sup>The data of the sodium and the central substrate binding sites of vSGLT and PmSiaT were taken from the analyses of respective crystal structures [4,10]. For PutP, the amino acids proposed to be involved in sodium and substrate binding were identified by amino acid replacements in combination with comprehensive analyses of transport kinetics, ligand affinities and site directed labeling approaches [5-8]. The location of a 2<sup>nd</sup> substrate binding site in PutP and vSGLT was predicted based on computational analyses in combination with amino acid replacements, substrate binding and transport studies [11].

<sup>b</sup>Of note: Structural alignments between LeuT and vSGLT revealed that the crystallographically identified galactose-binding site in vSGLT [10] is located in a more extracellular location relative to the central substrate-binding site in LeuT. Therefore, the existence of an additional galactose-binding site in vSGLT was suggested and experimentally tested that aligns to the central binding site of LeuT [11]. Following this logic, the amino acids of vSGLT listed in the table under "2<sup>nd</sup> substrate binding site" constitute the central binding site while the amino acids listed under "central binding site" form a more external binding site.

Supplementary Table S2. Information of the isolates from the SMART database used for Figure 5.

Number in Figure 5	Isolates (Organisms/SMART ID)
1	<i>Candidatus Nitrosocaldus cavascurens</i> / <a href="#">A0A2K5ARA0_9ARCH</a> (A0A2K5ARA0)
2	<i>Pseudomonas stutzeri</i> / <a href="#">A0A0H3Z2P6_PSEST</a> (A0A0H3Z2P6)
3	<i>Pseudomonas fluorescens</i> Q2-87/ <a href="#">J2EGW4_PSEFL</a> (J2EGW4)
4	<i>Pseudomonas corrugata</i> / <a href="#">A0A1B3C9J6_9PSED</a> (A0A1B3C9J6)
5	<i>Actinospica acidiphila</i> / <a href="#">UPI00052494D7</a>
6	<i>Streptomyces griseorubens</i> / <a href="#">UPI00056BF26D</a>
7	<i>Streptomyces albus</i> / <a href="#">UPI000689E04F</a>
8	<i>Streptomyces gilvosporeus</i> / <a href="#">A0A1V0TJU0_9ACTN</a> (A0A1V0TJU0)

## References

- Madeira, F.; Park, Y.m.; Lee, J.; Buso, N.; Gur, T.; Madhusoodanan, N.; Basutkar, P.; Tivey, A.R.N.; Potter, S.C.; Finn, R.D., et al. The EMBL-EBI search and sequence analysis tools APIs in 2019. *Nucleic Acids Research* **2019**, *47*, W636-W641, doi:10.1093/nar/gkz268.
- Watanabe, A.; Choe, S.; Chaptal, V.; Rosenberg, J.M.; Wright, E.M.; Grabe, M.; Abramson, J. The mechanism of sodium and substrate release from the binding pocket of vSGLT. *Nature* **2010**, *468*, 988-991, doi:10.1038/nature09580.
- Faham, S.; Watanabe, A.; Besserer, G.M.; Cascio, D.; Specht, A.; Hirayama, B.A.; Wright, E.M.; Abramson, J. The crystal structure of a sodium galactose transporter reveals mechanistic insights into Na<sup>+</sup>/sugar symport. *Science* **2008**, *321*, 810-814, doi:10.1126/science.1160406.
- Wahlgren, W.Y.; Dunevall, E.; North, R.A.; Paz, A.; Scalise, M.; Bisignano, P.; Bengtsson-Palme, J.; Goyal, P.; Claesson, E.; Caing-Carlsson, R., et al. Substrate-bound outward-open structure of a Na<sup>+</sup>-coupled sialic acid symporter reveals a new Na<sup>+</sup> site. *Nat Commun* **2018**, *9*, 1753, doi:10.1038/s41467-018-04045-7.
- Hilger, D.; Böhm, M.; Hackmann, A.; Jung, H. Role of Ser-340 and Thr-341 in transmembrane domain IX of the Na<sup>+</sup>/proline transporter PutP of *Escherichia coli* in ligand binding and transport. *Journal of Biological Chemistry* **2008**, *283*, 4921-4929, doi:10.1074/jbc.M706741200.
- Quick, M.; Jung, H. A conserved aspartate residue, Asp187, is important for Na<sup>+</sup>-dependent proline binding and transport by the Na<sup>+</sup>/proline transporter of *Escherichia coli*. *Biochemistry* **1998**, *37*, 13800-13806, doi:10.1021/bi980562j.
- Pirch, T.; Quick, M.; Nietschke, M.; Langkamp, M.; Jung, H. Sites important for Na<sup>+</sup> and substrate binding in the Na<sup>+</sup>/proline transporter of *Escherichia coli*, a member of the Na<sup>+</sup>/solute symporter family. *J Biol Chem* **2002**, *277*, 8790-8796, doi:10.1074/jbc.M111008200.
- Olkhova, E.; Raba, M.; Bracher, S.; Hilger, D.; Jung, H. Homology model of the Na<sup>+</sup>/proline transporter PutP of *Escherichia coli* and its functional implications. *J Mol Biol* **2011**, *406*, 59-74, doi:10.1016/j.jmb.2010.11.045.

9. Bracher, S.; Schmidt, C.C.; Dittmer, S.I.; Jung, H. Core transmembrane domain 6 plays a pivotal role in the transport cycle of the sodium/proline symporter PutP. *The Journal of biological chemistry* **2016**, *291*, 26208-26215, doi:10.1074/jbc.M116.753103.
10. Faham, S.; Watanabe, A.; Besserer, G.M.; Cascio, D.; Specht, A.; Hirayama, B.A.; Wright, E.M.; Abramson, J. The crystal structure of a sodium galactose transporter reveals mechanistic insights into Na<sup>+</sup>/sugar symport. *Science* **2008**, *321*, 810-814.
11. Li, Z.; Lee, A.S.; Bracher, S.; Jung, H.; Paz, A.; Kumar, J.P.; Abramson, J.; Quick, M.; Shi, L. Identification of a second substrate-binding site in solute-sodium symporters. *J Biol Chem* **2015**, *290*, 127-141, doi:10.1074/jbc.M114.584383.

## Discussion

This thesis deals with the functional characterization of two membrane proteins, CbrA and HutT, which are both transporters for L-histidine in *P. putida* KT2440. Despite fulfilling different functions in the cell, they are connected at the regulatory level, since CbrA is not only a transporter but also a sensor kinase. The role of CbrA as a transporter and, together with CbrB, as an important cellular regulator and HutT as the main histidine transporter, were analyzed in detail in this thesis. Genetic and biochemical methods were applied to gain insight into the physiological role of these proteins.

### 5.1 Histidine uptake and utilization in *P. putida* KT2440

Histidine can be used by *P. putida* KT2440 as the single source of carbon and nitrogen [Clarke, 1982]. In other organisms e.g., *S. enterica* serovar Typhimurium, histidine is transported into the cytoplasm by active transport via ABC-transporters such as the HisJQMP complex under the consumption of ATP [Reitzer, 2005]. In *P. putida* KT2440, however, it is exclusively taken up by secondary transporters.

Two membrane proteins were identified that catalyze the uptake of histidine in this organism. It was shown in this thesis that CbrA, besides its function as a sensor kinase (chapter 2), has a high affinity for histidine but a low overall uptake rate. This was demonstrated in the *P. putida* KT2440 LW1 strain, devoid of all known and suspected histidine transporters and the first gene required for histidine degradation ( $\Delta cbrA \Delta hutTH \Delta hutWX$ ) but expressing *cbrA* from a plasmid. Interestingly, cells expressing of *cbrA-SSSF* (referred to as *cbrA-SLC5* (sodium solute symporter family 5) in chapter 2), a variant lacking the sensor kinase moiety of the protein, could catalyze histidine uptake on the same level as cells containing full-length CbrA, indicating that the transport function is independent of the kinase activity. The uptake could not be shown in *E. coli*, as possibly the native phospholipid composition of *P. putida* is required for the transport function of CbrA. Probably due to the low uptake rates and the fact that *E. coli* phospholipids were used, the transport could not be successfully shown with purified protein reconstituted into proteoliposomes, even though a purification protocol was successfully established for full-length CbrA as well as only the SSSF domain. The binding of membrane-bound CbrA to histidine was shown independently with differential radial capillary action of ligand assay (DRaCALA) [Roelofs et al., 2011]. It was proven that CbrA requires a proton motive force for transport and is therefore a secondary transporter. Radioactively labeled  $^3\text{H}$ -L-histidine was used for all transport and binding assays. None of the substances used in a competition assay had any effect on  $^3\text{H}$ -L-histidine uptake, except non-radioactive histidine, illustrating CbrA's high specificity for histidine.

HutT's only role known so far is the uptake of L-histidine with high affinity, specificity and much higher uptake rates than CbrA (chapter 3). This was shown in the same *P. putida* KT2440 LW1 strain that was used for CbrA, but *hutT* was expressed from a plasmid instead. In case of HutT, however, it was also possible to measure uptake in *E. coli* JW2306. A strain with a deletion of *hisJ*, encoding the histidine periplasmic binding protein, was used to avoid uptake by *E. coli*'s native histidine transport system HisJQMP. Furthermore, histidine uptake was catalyzed in proteoliposomes made of *E. coli* phospholipids and purified HutT. However, the transport kinetics were slightly different in *E. coli* with the  $K_M$  and  $V_{max}$  both being higher than in *P. putida*. These differences could suggest that binding is more specific for protein contained within the native phospholipid composition and that the overexpression system for HutT was more efficient in *E. coli*, so that more protein was available, leading to higher maximum rates. The binding of membrane-bound HutT to histidine was proven via DRaCALA as well. The only substance found to compete with histidine as transport substrate was 1,2,4-triazolyl-3-alanine (TRA) (see chapter 3, Fig. 4). TRA is very similar to histidine; only the ring structure is a triazole instead of imidazole (molecular structures provided in appendix, Fig. S3 Supplementary information for chapter 3). This illustrates the high specificity of HutT for histidine since TRA was provided in 100x fold concentration and has only a slight effect on histidine uptake, while the addition of 100x fold non-radioactive histidine almost completely inhibited uptake of  $^3\text{H}$ -L-histidine as expected. None of the other histidine analogs or amino acids tested had any effect.

After histidine is taken up either by CbrA or HutT, it is usually degraded via the histidine utilization pathway, starting with the elimination of ammonia resulting in urocanate by the histidase HutH as described in chapter 1.2.3 [Bender, 2012]. This is why *hutH* was also deleted in the *P. putida* strain used for transport assays so that the radioactive  $^3\text{H}$ -L-histidine could accumulate in the cell and not be excreted again during the experiment as part of a degradation product. *E. coli* lacks enzymes for histidine degradation and can therefore only use the amino acid as a building block in proteins that remain in the cell [Reitzer, 2005, Bowser Revel and Magasanik, 1958].

### 5.1.1 CbrA and HutT as members of the APC superfamily

Both CbrA and HutT belong to the APC superfamily of secondary transporters based on overall structural homology [Västermark et al., 2014]. Most members of the APC superfamily have a five-plus-five inverted repeat structure, with ten transmembrane segments that are folded along a symmetry axis [Västermark and Saier, 2014, Shi, 2013]. The superfamily was extended to include some proteins that have a seven-plus-seven repeat unit topology like the SulP and NCS2 family [Västermark and Saier, 2014]. Within the APC superfamily, HutT belongs to the APC (amino acid-polyamine-organocation) family (TCDB 2.A.3) [Jack et al., 2000] that contains solute:cation symporters and solute:solute antiporters [Schweikhard and Ziegler, 2012]. HutT appears to be, like many other APC transporters, a proton-coupled

transporter since the addition of DNP and CCCP had inhibiting effects on the uptake (chapter 3). This was further proven by experiments with HutT containing proteoliposomes. Here a sodium gradient ( $\Delta\text{Na}^+$ ) had no effect, compared to solute imposition of membrane potential ( $\Delta\psi$ ), while a potassium gradient ( $\Delta\text{pH}$ ) doubled the initial uptake rate.

CbrA, however, is included in the sodium solute symporter family (SSSF, TCDB 2.A.21), leading to the conclusion that it probably requires sodium coupling for transport (smf), like PutP of *E. coli* [Jung et al., 2012]. Instead it also relies on a proton gradient (pmf), which was proven by adding ionophores during transport assays (chapter 2). Only DNP reduced uptake significantly and CCCP caused a strong trend, while potassium or sodium specific ionophores valinomycin, nonactin and nigericin did not affect transport. The  $\text{Na}^+$ -binding sites known from other transporters in the SSS-family were also not found to be conserved in a CbrA sequence alignment performed by Prof. H Jung.

The structurally analyzed ApcT from *Methanocaldococcus jannaschii* functions with proton motive force as well [Shaffer et al., 2009]. It was revealed that protonation of a lysine in TM5 fulfills the same role as  $\text{Na}^+$  binding to  $\text{Na}^+$  binding site 2 in sodium-coupled transporters [Shaffer et al., 2009]. This lysin is strongly conserved in APC transporters and mutating it in HutT (Lys156Ala, Lys156Gln) abolished its function (chapter 3). Only another positively charged amino acid (Lys156Arg) could restore the transport partially. Apparently, a positive charge is required instead of binding of  $\text{Na}^+$  at this position in APC transporters. In *Geobacillus kaustophilus* ApcT, the hydroxyl group of Tyr268 in TM7 has the same position as the sodium ion in the Na1 site in LeuT [Jungnickel et al., 2018, Yamashita et al., 2005]. This tyrosin is also strongly conserved in all proteins used for an alignment, including HutT. The fact that  $\text{Na}^+$  ions were observed to be replaced by strongly conserved amino acids at both  $\text{Na}^+$ -binding sites in proton-coupled APC transporters, demonstrates similar principles in proton- and sodium-coupled transport.

CbrA is a very atypical APC transporter since a sensor kinase is fused C-terminally. CbrA is, so far, the only SSS-containing sensor kinase with characterized transport activity (chapter 4). In contrast to what was suggested for CbrA of *P. fluorescens* [Zhang et al., 2015], the transport does not depend on signal transduction. We could prove that CbrA was still functional when His766 was mutated, or when the whole SSSF domain was deleted, and no signal transduction could take place.

### 5.1.2 Comparison of transport activity between CbrA and HutT

CbrA is not only a transport protein but also a sensor kinase and part of a two-component system together with CbrB [Zhang et al., 2015, Nishijyo et al., 2001]. It is a major regulator of carbon catabolite repression and a transporter with a relatively low uptake rate for histidine. The maximal uptake rate  $V_{\text{max}}$  was determined as  $0.27 \pm 0.02 \text{ nmol mg}^{-1} \text{ min}^{-1}$ . However, the affinity for histidine is high ( $K_M = 0.7 \pm 0.2 \mu\text{M}$ ) and the transporter appears very specific (Table 1). HutT, on the other hand, is the main transporter for histidine with a much higher

maximal uptake rate ( $V_{\max} = 1.93 \pm 0.11 \text{ nmol mg}^{-1} \text{ min}^{-1}$ ), but similar affinity as CbrA ( $K_M = 0.99 \pm 0.23 \mu\text{M}$  (measured in LW1), but has no kinase domain or regulatory function (Table 1).

Table 1: Comparison of parameters between L-histidine transporters CbrA and HutT of *P. putida* KT2440. Kinetic parameters were all determined in *P. putida* LW1. [Wirtz et al., 2020, Wirtz et al., 2021, Zhang et al., 2015, Sepulveda and Lupas, 2017, Saier et al., 2013].

Parameter	CbrA	HutT
<b>protein superfamily</b>	APC	APC
<b>protein family</b>	SSSF, TCDB 2.A.21	APC, TCDB 2.A.3
<b>TMs</b>	13	12
<b><math>K_M</math></b>	$0.7 \pm 0.2 \mu\text{M}$	$0.99 \pm 0.23 \mu\text{M}$
<b><math>V_{\max}</math></b>	$0.27 \pm 0.02 \text{ nmol mg}^{-1} \text{ min}^{-1}$	$1.93 \pm 0.11 \text{ nmol mg}^{-1} \text{ min}^{-1}$
<b>inhibited by</b>	CCCP, DNP,	CCCP, DNP
<b>energetics</b>	pmf	pmf
<b>specificity for histidine</b>	high	high
<b>promoter type</b>	constitutive	inducible
<b>contains sensor kinase</b>	yes	no

The results obtained in this thesis suggest that CbrA mostly acts as a regulatory sensor kinase, phosphorylating CbrB and causing a cellular response on the transcriptional or, through Crc, the translational level (chapter 5.2).

CbrA appears to be transcribed from a constitutive promoter and does not require induction by histidine [Zhang et al., 2015]. Opposite to that, it has been known for a long time that expression of the *hut* genes, including *hutT*, is inducible by urocanate [Leidigh and Wheelis, 1973, Lessie and Neidhardt, 1967], the first degradation product of histidine, which is required for HutC to cease blocking the promoter [Zhang and Rainey, 2007].

### 5.1.3 Differences in histidine transport between *Pseudomonas* species

HutT was confirmed as the major histidine transporter in *P. putida* in this thesis. Since a  $\Delta\text{hutT}$  strain was not able to grow on histidine as a single carbon source, the amount of histidine transported by CbrA when it is expressed from its native promoter appears not to be sufficient to sustain growth. Contrary to these findings in *P. putida*, *P. fluorescens* was described as being able to grow on histidine when *hutT* was deleted [Zhang et al., 2015]. This finding might be explained by differences between the two *Pseudomonas* strains. *P. fluorescens*

contains an additional permease in the *hut* gene cluster (*hutT<sub>u</sub>*), specific for urocanate, the first degradation product of histidine, that might also account for some low unspecific uptake of histidine. There is no annotation for this urocanate transporter in the *P. putida hut* cluster. There are also the *hutXWV* genes in the *hut* genes of *P. fluorescens* that have a small role as an ABC transporter for histidine [Zhang et al., 2015]. In the genome of *P. putida*, genes homologous to *hutXWV* can be found, but they are located elsewhere in the genome (pp\_3558-pp\_3560) and can't sustain growth on histidine when *hutT* is deleted. Possibly they evolved to encode an ABC transporter for a different substrate but were not investigated further in this thesis. For purposes of transport measurement of histidine in *P. putida*, they were still deleted from the genome via homologous recombination to avoid any potential background effects of histidine uptake. In contrast to *P. putida*, *P. fluorescens* has enough options for histidine uptake without HutT. A study reveals the polymorphism of histidine and urocanate uptake between *Pseudomonas* populations [Zhang et al., 2012]. In a genome comparison, *P. putida* was predicted to have only one histidine permease (*hutT*), while *P. aeruginosa* has eight putative transporter genes and *P. stutzeri* A1501 has none [Zhang et al., 2012]. As mentioned in chapter 1, *P. putida* and *P. aeruginosa* share 85% of predicted coding regions, but *P. putida* is missing key virulence factors [Nelson et al., 2002]. Maybe histidine uptake is a virulence factor for *P. aeruginosa* as well like it was shown for *Acinetobacter baumannii* in lung infections [Lonergan et al., 2020].

## 5.2 CbrA's regulatory role

CbrA is a transporter for histidine in *P. fluorescens* [Zhang et al., 2015] and in *P. putida*, as shown in chapter 5.1. Even though the affinity for histidine is high and binding to membrane-bound protein was shown, the uptake is not very efficient, especially in comparison to the inducible transporter HutT. However, besides catalyzing histidine uptake on a low level, CbrA plays a very important role as a regulator in the cell and, together with CbrB, forms a classic TCS. CbrA auto-phosphorylates under ATP consumption and transfers the phosphate to CbrB, which was shown by kinase studies using  $^{32}\text{P}$ -ATP (chapter 2). The phosphorylation of CbrA was achieved with full-length CbrA contained in *E. coli* TKR2000 membrane vesicles and with purified CbrA $\Delta$ SSSF (referred to as CbrA $\Delta$ SLC5 in chapter 2). Unambiguously, a histidine at position 766 is the site of phosphorylation since a His766Asn mutant could not be phosphorylated when treated the same way as the wild type. By adding purified CbrB to the experiment, the transfer of phosphate from CbrA to Asp52 of CbrB could be observed. Of special interest was the fact that autophosphorylation and the phosphotransfer worked with full-length membrane-bound CbrA but also with soluble purified protein without any transmembrane domains (CbrA $\Delta$ SSSF). Protein lacking the SSSF-transporter domain still acts as a histidine kinase, proving that the transporter domain is not required for phosphorylation. However, comparing the time courses of the phosphorylation assays, the kinase activity appears to be lower when the SSSF domain is missing. It might not be essential for phosphorylation, but maybe the SSSF domain does relay a signal that increases the kinase activity. The option that CbrA could also dephosphorylate CbrB upon signal recognition was rejected since no significant decrease of phosphorylation was observed when CbrA was added to CbrB previously phosphorylated with  $^{32}\text{P}$ -ACP.

### 5.2.1 CbrA regulates carbon catabolite repression

CbrA's role as a sensor kinase was described in several publications [Nishijyo et al., 2001, Zhang et al., 2015, Monteagudo-Cascales et al., 2019, Barroso et al., 2018, García-Mauriño et al., 2013, Valentini et al., 2014], however, the biochemical phosphorylation, as described above, was never shown before. The CbrA/B TCS has an important role in regulating the cell's ability to use different substrates as carbon sources (CCR). In *P. putida* metabolic pathways for less preferred carbon sources are blocked by mRNA binding protein Crc inhibiting translation [Hester et al., 2000]. This blockage needs to be removed when preferred carbon sources e.g., succinate, are not available. CbrB induces expression of *crcZ* and *crcY* as a transcription factor [García-Mauriño et al., 2013]. The small RNAs CrcZ and CrcY can then sequester Crc and therefore, the enzymes required for other pathways can be translated [Sonnleitner et al., 2009]. The preference of *P. putida* for a substrate can be measured in a reporter assay by fusing the *luxCDABE*-operon of *Photobacterium luminescens* to the promoter region of *crcZ* on a plasmid [Gödeke et al., 2011]. The luminescence signal in *P. putida*  $\Delta$ *cbrA* transformed

with two plasmids (pBBR1- $P_{crcZ}::luxCDABE$  and pUCP-Tc-*cbrA*) was used as a measure of preference for a substrate (chapter 2). Oxalo-acetate, arginine and histidine gave the highest signal, indicating strong induction of *crcZ* transcription. When the cells were grown in LB or with succinate as the carbon source, the signal was much lower since no carbon catabolite repression had to be overcome. The same assay was used to test the ability of CbrA variants to function as sensor kinases and activate *crcZ* transcription. Deletion of CbrA and CbrB, naturally, did not lead to a signal. A mutation of His766 (CbrA-His766N) was no longer functional, just as a variant lacking the whole sensor kinase domain (CbrA-SSSF). Interestingly, deletion of the SSSF domain, which results in a soluble protein, was still able to activate target gene expression. This reporter assay confirmed the biochemical results obtained by using  $^{32}\text{P}$ -ATP, described in the previous section. Here, CbrA and the CbrA $\Delta$ SSSF variant both reached the maximum level of luminescence and differences, like those found in the phosphorylation time course, could not be observed in this type of reporter assay.

### 5.2.2 CbrA regulates expression of *hut* genes

CbrA/B has many known target genes, like *crcZ* and *crcY*, as described above, but the TCS can also directly activate gene expression without the CCR cascade [Barroso et al., 2018, Abdou et al., 2011]. Barroso *et al.* performed a ChIP-Seq analysis to find other target genes of CbrB in *P. putida*, that revealed many potential binding sites [Barroso et al., 2018]. Some of these genes were validated as being upregulated by CbrB by RT-qPCR or their promoter sequences were shown to bind CbrB in an EMSA (electrophoretic mobility shift assay). A consensus binding sequence was suggested that is very similar to another sequence suggested before and found in different *Pseudomonads* [Abdou et al., 2011, Bender, 2012, Itoh et al., 2007]. The *hut* genes were not among the genes found in the screen in *P. putida* [Barroso et al., 2018], even though in *P. aeruginosa* and *P. fluorescens*, the conserved binding sequence can be found in the promoter region of *hutUHTIG*. The question arises if CbrB also binds the *hut* promoter in *P. putida*, even though there is no obvious binding site.

The luminescence reporter assay was performed, as described before, but with the *luxCDABE* genes fused to the promoter of *hutU*. This experiment revealed that in the presence of a preferred carbon source like succinate, the *hut* genes are not expressed, but when histidine is the only carbon source, the expression is induced (data not shown). A control sequence instead of  $P_{hutU}$  does not have the same effect and when CbrB is deleted and not complemented, the expression remains on a lower basic level. The promoter site could be narrowed down to between -90 and -60 bp upstream of the *hutU* gene start +1 by varying the gene sequence used for the reporter fusion. Apparently, CbrB binds the *hut* promoter in *P. putida* as well, but this could never have been revealed in the ChIP-Seq screen [Barroso et al., 2018] since it is only relevant when histidine is used as a carbon source, while in the screen, OAA was provided instead. Knowledge of the exact binding site could lead to the discovery of other unknown targets that are only required in certain situations like specific nutrient limitations

and cannot be found in a general screen.

### 5.2.3 Role of CbrA's domains

CbrA is a large protein containing several subdomains. The first half is the SSSF-transporter responsible for histidine uptake, as described above in more detail. The SSSF (SLC5 is used analogously in chapter 2) domain can apparently function independently from the rest of the protein since CbrA-SSSF alone had very similar uptake rates as full-length CbrA in *P. putida* LW1.

Connected to this SSSF moiety is the STAC (SLC and TCST-Associated Component) domain, which was only recently annotated as a protein domain [Korycinski et al., 2015, Sepulveda and Lupas, 2017]. The majority of STAC domains is found between N-terminal SSSF-like membrane domains and C-terminal signal transduction domains like in the case of CbrA and CrbS (chapter 4), but it can also constitute a smaller protein as in the exemplary case of Af1503 from the archaea *Archaeoglobus fulgidus*, where it is connected only to a HAMP (helical linker domain of receptor histidine kinase and methyl-accepting proteins) domain [Korycinski et al., 2015, Aravind and Ponting, 1999]. Korycinski *et al.* conclude that the association between SLC5 and STAC domains led to the emergence of a protein family which couples solute uptake to the generation of an intracellular signal [Korycinski et al., 2015]. Surprisingly, in *P. fluorescens* the deletion of the STAC domain of either CbrA or CrbS proteins had no obvious effect on growth under the tested conditions [Sepulveda and Lupas, 2017]. CrbS $\Delta$ STAC had no disadvantage compared to the wild type in acetate utilization, regulation of which is the best-described role of CrbS [Sepulveda and Lupas, 2017]. The deletion of this domain (CbrA $\Delta$ STAC) in *P. putida* resulted in reduced signal transduction in a transcriptional reporter assay, where the *luxCDABE* genes were fused to the *crcZ* promoter sequence, compared to the wild type CbrA (chapter 2). However, the expression of the target gene was not completely abolished. The STAC domain might relay interaction between the two protein moieties since kinase activity is reduced when it is deleted. This finding might corroborate the fact that CbrA $\Delta$ SSSF showed slower autophosphorylation and phosphotransfer than full-length membrane-bound CbrA, as described above.

The PAS (Per-Arnt-Sim) domain is known to typically be a ligand-binding domain or signal sensing domain in sensor kinases [Henry and Crosson, 2011] (chapter 4). Surprisingly, the deletion of the PAS domain did not significantly reduce the expression of the target gene *crcZ* in a *lux* reporter assay (chapter 2). Our finding is contrary to what was described by Monteagudo-Cascales *et al.* [Monteagudo-Cascales et al., 2019]. In this study, a reporter fusion of the newly found CbrA target gene pp2810 to the *lacZ* gene was generated and expression analyzed for CbrA variants [Monteagudo-Cascales et al., 2019]. Here, CbrA $\Delta$ TM and CbrA $\Delta$ PAS showed strongly reduced expression of the target gene when the CbrA variants were transcribed from the native CbrA promoter and integrated chromosomally via transposon miniTn7 [Monteagudo-Cascales et al., 2019]. When a stronger *tac* promoter was used instead

of the native one, CbrA $\Delta$ TM could activate the expression of the target gene on a low level. Growth on citrate and histidine as sole carbon sources could also only be restored when CbrA $\Delta$ TM was overexpressed [Monteagudo-Cascales et al., 2019]. The authors conclude that CbrA should respond to an intracellular signal, probably through its PAS domain.

In the *creZ-luxCDABE* reporter assay, the variants CbrA, CbrA $\Delta$ SSSF and CbrSA (a mutant with the SSSF domain of CrbS instead of CbrA) were expressed from a high-copy plasmid with an inducible *lac* promoter and all reached maximum levels of luminescence, while CbrA $\Delta$ PAS had a lower level of luminescence, but was not significantly reduced. Possibly, the differences in signal transduction ability of the CbrA variants observed by Monteagudo-Cascales cannot be shown in an overexpression plasmid-based system. Additionally, the differences could partly be explained by the use of different CbrA target genes as reporters.

The PAS domain was also analyzed for its ligand-binding abilities in two different melting temperature assays (chapter 2). The purified PAS domain was able to bind L-histidine with a  $K_D$  of  $43 \pm 13 \mu\text{M}$  (and  $46 \pm 17 \mu\text{M}$  for the other method), thus further confirming its suggested role as the signal recognition domain in CbrA and pointing towards L-histidine as the intracellularly recognized signal.

After the STAC and the PAS domains, CbrA has the typical features required for a histidine sensor kinase, a DHP, (histidine phosphotransfer domain) and CA (catalytic ATP-binding domain) [Henrquez et al., 2021]. The H box is conserved among SSSF-containing sensor kinases and includes the phosphorylation residue His766, which was confirmed by reporter and phosphorylation assays.

#### 5.2.4 Transporters as information transmitters

Transporters can be transmitters of information to cytoplasmic components, in addition to actually delivering substrate [Tetsch and Jung, 2009b]. In eukaryotes, proteins with the dual role of receptor and transporter have been named transceptors [Holsbeeks et al., 2004, Kriel et al., 2011], but this designation is not commonly used for prokaryotes. They have to sense the extracellular availability of their substrate, sometimes in very low concentrations, which is illustrated by the following examples.

The lysine transporter LysP of *E. coli* acts as a co-sensor for the lysine-cadaverine antiporter CadC, combined with the sensing of low pH [Rauschmeier et al., 2014]. The nature and consequences of the interactions between transporters and sensor kinases are diverse. Interactions between LysP and CadC are stable and permanent. In the absence of its substrate, LysP inhibits a pH-induced activation of CadC. Binding and/or transport of lysine by LysP then allows activation of CadC [Rauschmeier et al., 2014, Brameyer et al., 2019]. The two proteins interact via the transmembrane and periplasmic domains.

On the contrary, the C4-dicarboxylate transporter DctA has a structural role in the DctA/DcuS complex, rather than in substrate or flux sensing [Stopp et al., 2021]. Binding of DctA transfers DcuS from a permanent "ON" state into an "OFF" state. Activation of DcuS then occurs by

binding of the C4-dicarboxylate to a PAS domain of the sensor kinase [Stopp et al., 2021]. DcuS and the according response regulator DcuR then regulate the expression of *dctA* and *dcuB* encoding the aerobic and the anaerobic C4DC transporters DctA and DcuB [Kleefeld et al., 2009, Davies et al., 1999]. CbrA probably is activated by binding of substrate to the PAS domain as well, which in turn leads to expression of downstream target genes, e.g. *crcz* and the *hut* genes. CbrA's SSSF domain might also play structural role required for signal recognition, since we found in phosphorylation experiments that it might modulate kinase activity.

In the described examples, transporter proteins deliver sensory information to a regulatory system, a one-component system in case of CadC and a TCS in case of DcuS/R. This illustrates that transporters and sensor kinases are sometimes required to closely interact when they are not transcribed in one polypeptide like CbrA. Other secondary transporters, for example, UhpC, have lost most of their transport function in favor of sensing [Tetsch and Jung, 2009a]. UhpC senses the availability of glucose-6-phosphate in *E. coli* and stimulates phosphorylation of the TCS UhpB/A, but has no transport activity. In turn, UhpA induces expression of the main Glucose-6-phosphate transporter UhpT, a homolog to UhpC [Wright and Kadner, 2001]. The sensing component can also be part of ABC transporter complexes, like in MalE, the maltose-binding protein of *E. coli* [Tetsch and Jung, 2009a]. It works with transporters MalG and MalF and ATPase MalK to transport maltose across the cytoplasmic membrane but can also interact with the chemoreceptor Tar and therefore possesses regulatory function [Manson et al., 1985, Hazelbauer, 1975].

In 2009, CbrA's SSSF domain was suggested to be a sensory domain for the sensor kinase and, back then, its substrate as well as whether it retained transport function was unclear [Tetsch and Jung, 2009a]. In this case, the sensory transporter domain and the TCS are combined in one large bifunctional polypeptide. Noticeably, the SSSF domain does retain transport function (chapter 2) and can even function independently from the sensor kinase domain. However, the transport rates are not very high, even though there is a strong affinity for the substrate histidine, which is likely sensed intracellularly via the PAS domain in the sensor kinase half of the protein. In conclusion, CbrA's SSSF domain might play the role of transporting enough substrate inside the cell to be sensed and to induce autophosphorylation of the sensor kinase, similar to LysP internalizing lysine to be sensed by CadC [Brameyer et al., 2019]. However, the histidine transport is not very efficient and additionally expression of the main histidine transporter HutT is induced via the response regulator CbrB, among other targets.

### 5.3 Model of CbrA and HutT functions

The transporter and TCS CbrA/B and the transporter HutT were thoroughly analyzed in this thesis and a model of their functions and interaction in *Pseudomonas putida* is presented here (Fig. 7).

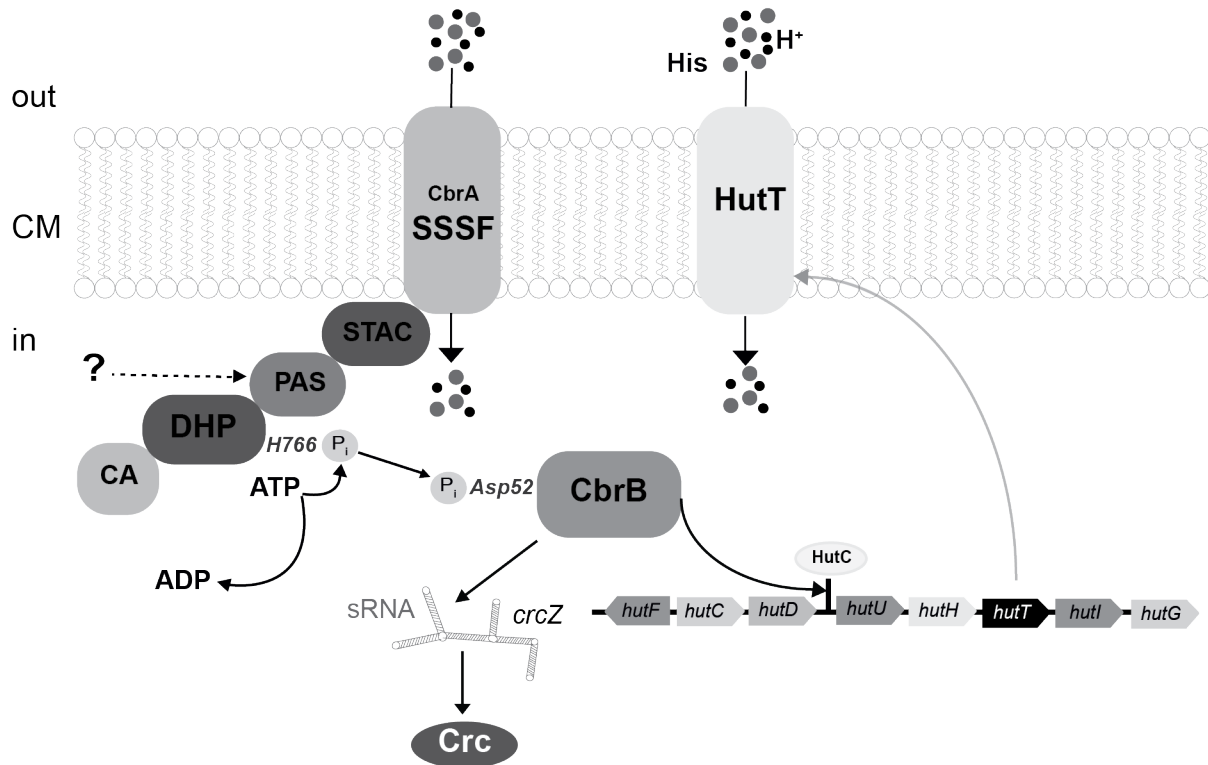


Figure 7: Uptake of histidine in *P. putida* via CbrA and HutT, which both function via an electrochemical proton gradient. CbrA autophosphorylates at H766 and subsequently phosphorylates CbrB at Asp52. CbrB, in turn, regulates the expression of the *hut*-operon and therefore *hutT* among other target genes. Another important function of CbrB is the transcription initiation of small RNAs CrcZ and CrcY that can sequester Crc, which then no longer can block pathways for less preferred carbon sources. Figure based on [Wirtz et al., 2020, Wirtz et al., 2021, Bender, 2012, Zhang and Rainey, 2007, Zhang et al., 2015, Sepulveda and Lupas, 2017, Sonnleitner et al., 2009, Henríquez et al., 2021]. ADP, adenosine diphosphate; ATP, adenosine triphosphate; CA, catalytic ATP-binding domain; CM, cytosolic membrane; DHP, histidine phosphotransfer domain; H<sup>+</sup>, proton; P<sub>i</sub>, orthophosphate; PAS, Per-Arndt-Sim; sRNA, small RNA; SSSF, sodium solute symporter family domain; STAC, SLC and TCST-Associated Component

CbrA's SSSF domain catalyzes the uptake of histidine into the cytosol with high affinity but low rates via an electrochemical proton gradient. The STAC domain connects the sensor kinase to the transporter and might be important for interaction between the two protein moieties. Like a typical sensor kinase, the protein has a DHP domain that contains the site of phosphorylation His766 and a catalytic CA domain. Additionally, it has a PAS

domain that is most likely involved in signal recognition, probably binding histidine. Upon autophosphorylation under ATP consumption, the phosphate is transferred to Asp52 of the response regulator CbrB (chapter 2). CbrB is a transcription factor that can induce transcription of various genes, especially *crcZ* and *crcY* encoding the small RNAs that can sequester Crc and unlock catabolic pathways for less preferred carbon sources [Sonnleitner et al., 2009]. CbrB also induces expression of the *hut* genes by binding to the promoter in front of *hutUHTIG*. At the same time, urocanate is required to release the blocking by HutC to enable transcription [Leidigh and Wheelis, 1973, Lessie and Neidhardt, 1967, Zhang and Rainey, 2007]. Together with the other enzymes required for histidine degradation, HutT, the main histidine transporter, is expressed. It transports histidine with similar affinity but at higher rates as CbrA and also requires proton motive force (chapter 3).

All the results obtained in this thesis are in agreement with this model, however, there are some limitations. There is no obvious reason why histidine is the only transport substrate and ligand of the PAS domain since CbrA has a global role in the cell as a major regulator of carbon catabolite repression. CbrB has many more target genes and through Crc, the whole cell metabolism is affected. One explanation might be that histidine serves as a sort of trigger molecule when the cell no longer has more preferred carbon sources available and induces the switch to derepressing several catabolic pathways. The binding of histidine to the PAS domain was observed in melting temperature assays, but conversely, no influence of histidine on the phosphorylation of the sensor kinase was observed in-vitro. This opens up the question whether the binding of histidine to the PAS domain really is a signal for the sensor kinase or if it just could not be observed under the experimental conditions. Possibly, histidine is not the only substrate of the PAS and SSSF domains, even though no other molecule tested showed any binding or transport activity.

## 5.4 Outlook

Even though a lot of information was gathered about the two membrane proteins CbrA and HutT that act as histidine transporters, still some open questions remain. Both proteins share the LeuT fold that many secondary transporters have, even though they are not very conserved on the amino acid level. Several of these proteins' structures were successfully resolved [Shaffer et al., 2009, Jungnickel et al., 2018], but not HutT and CbrA. CbrA stands out especially since it is not only a member of the SSS family but also a sensor kinase. A protein with this unique dual function has not been structurally resolved until today. Autophosphorylation and transfer of phosphate onto CbrB were shown radioactively, confirming that His766 of CbrA is the site of phosphorylation and Asp52 the receiver site of CbrB. The structure of this membrane protein might also reliably reveal the binding ligand or signal that induces autophosphorylation of CbrA and confirm or disprove histidine as the ligand.

It is known that CbrB directly activates the expression of HutT and other genes by binding to the promoter region in front of the *hut* gene cluster (unpublished data), like it does for some other genes [Monteagudo-Cascales et al., 2019] and not via Crc [Moreno et al., 2009]. However, the binding site is not conserved in *P. putida* KT2440, unlike in *P. aeruginosa* KT2440 and *P. fluorescens* KT2440, where it is very similar to the binding site in front of *crcZ*. The identification of this binding site might lead in turn to the discovery of unknown targets of CbrA/B.

## Bibliography

- [Abdou et al., 2011] Abdou, L., Chou, H.-T., Haas, D., and Lu, C.-D. (2011). Promoter recognition and activation by the global response regulator CbrB in *Pseudomonas aeruginosa*. *J Bacteriol*, 193(11):2784–2792.
- [Abramson and Wright, 2009] Abramson, J. and Wright, E. M. (2009). Structure and function of Na<sup>+</sup>-symporters with inverted repeats. *Curr Opin Struct Biol*, 19(4):425–432.
- [Abramson and Wright, 2021] Abramson, J. and Wright, E. M. (2021). Function trumps form in two sugar symporters, LacY and vSGLT. *Int J Mol Sci*, 22(7):3572.
- [Akashi and Gojobori, 2002] Akashi, H. and Gojobori, T. (2002). Metabolic efficiency and amino acid composition in the proteomes of *Escherichia coli* and *Bacillus subtilis*. *Proc Natl Acad Sci USA*, 99(6):3695–3700.
- [Allison and Phillips, 1990] Allison, S. L. and Phillips, A. T. (1990). Nucleotide sequence of the gene encoding the repressor for the histidine utilization genes of *Pseudomonas putida*. *J Bacteriol*, 172(9):5470–5476.
- [Amador et al., 2010] Amador, C. I., Canosa, I., Govantes, F., and Santero, E. (2010). Lack of CbrB in *Pseudomonas putida* affects not only amino acids metabolism but also different stress responses and biofilm development. *Environ Microbiol*, 12(6):1748–1761.
- [Ames, 1964] Ames, G. F. (1964). Uptake of amino acids by *Salmonella typhimurium*. *Arch Biochem Biophys*, 104(1):1–18.
- [Ames and Lever, 1970] Ames, G. F. and Lever, J. (1970). Components of histidine transport: histidine-binding proteins and (hisp) protein. *Proc Natl Acad Sci USA*, 66(4):1096–1103.
- [Ames and Lever, 1972] Ames, G. F.-L. and Lever, J. E. (1972). The histidine-binding protein j is a component of histidine transport: Identification of its structural gene, *hisJ*. *J Biol Chem*, 247(13):4309–4316.
- [Aravind and Ponting, 1999] Aravind, L. and Ponting, C. P. (1999). The cytoplasmic helical linker domain of receptor histidine kinase and methyl-accepting proteins is common to many prokaryotic signalling proteins. *FEMS Microbiol Lett*, 176(1):111–116.
- [Bacilio-Jiménez et al., 2003] Bacilio-Jiménez, M., Aguilar-Flores, S., Ventura-Zapata, E., Pérez-Campos, E., Bouquelet, S., and Zenteno, E. (2003). Chemical characterization of root exudates from rice (*Oryza sativa*) and their effects on the chemotactic response of endophytic bacteria. *Plant Soil*, 249(2):271–277.

- [Bagdasarian et al., 1981] Bagdasarian, M., Lurz, R., Rückert, B., Franklin, F. C. H., Bagdasarian, M. M., Frey, J., and Timmis, K. N. (1981). Specific-purpose plasmid cloning vectors ii. broad host range, high copy number, rsf 1010-derived vectors, and a host-vector system for gene cloning in *Pseudomonas*. *Gene*, 16(1):237–247.
- [Barroso et al., 2018] Barroso, R., García-Mauriño, S. M., Tomás-Gallardo, L., Andújar, E., Pérez-Alegre, M., Santero, E., and Canosa, I. (2018). The CbrB regulon: Promoter dissection reveals novel insights into the CbrAB expression network in *Pseudomonas putida*. *PLOS ONE*, 13(12):e0209191.
- [Belda et al., 2016] Belda, E., van Heck, R. G. A., José Lopez-Sanchez, M., Cruveiller, S., Barbe, V., Fraser, C., Klenk, H.-P., Petersen, J., Morgat, A., Nikel, P. I., Vallenet, D., Rouy, Z., Sekowska, A., Martins dos Santos, V. A. P., de Lorenzo, V., Danchin, A., and Médigue, C. (2016). The revisited genome of *Pseudomonas putida* KT2440 enlightens its value as a robust metabolic chassis. *Environ Microbiol*, 18(10):3403–3424.
- [Bender, 2012] Bender, R. A. (2012). Regulation of the histidine utilization (Hut) system in bacteria. *Microbiol Mol Biol Rev*, 76(3):565–584.
- [Bodey et al., 1983] Bodey, G. P., Ricardo, B., Victor, F., and Leena, J. (1983). Infections caused by *Pseudomonas aeruginosa*. *Rev Infect Dis*, 5(2):279–313.
- [Bowser Revel and Magasanik, 1958] Bowser Revel, H. R. and Magasanik, B. (1958). Utilization of the imidazole carbon 2 of histidine for the biosynthesis of purines in bacteria. *J Biol Chem*, 233(2):439–443.
- [Bracher et al., 2019] Bracher, S., Hilger, D., Guérin, K., Polyhach, Y., Jeschke, G., Krafczyk, R., Giacomelli, G., and Jung, H. (2019). Comparison of the functional properties of trimeric and monomeric cait of *Escherichia coli*. *Sci Rep*, 9(1):3787.
- [Brameyer et al., 2019] Brameyer, S., Rösch, T. C., El Andari, J., Hoyer, E., Schwarz, J., Graumann, P. L., and Jung, K. (2019). Dna-binding directs the localization of a membrane-integrated receptor of the toxR family. *Commun Biol*, 2:4–4.
- [Bramley and Kornberg, 1987] Bramley, H. F. and Kornberg, H. L. (1987). Sequence homologies between proteins of bacterial phosphoenolpyruvate-dependent sugar phosphotransferase systems: identification of possible phosphate-carrying histidine residues. *Proc Natl Acad Sci USA*, 84(14):4777–4780.
- [Bretl et al., 2011] Bretl, D. J., Demetriadou, C., and Zahrt, T. C. (2011). Adaptation to environmental stimuli within the host: Two-component signal transduction systems of *Mycobacterium tuberculosis*. *Microbiol Mol Biol Rev*, 75(4):566–582.

- [Brodey et al., 1991] Brodey, C. L., Rainey, P., Tester, M., and Johnstone, K. (1991). Bacterial blotch disease of the cultivated mushroom is caused by an ion channel forming lipodepsipeptide toxin. *Mol Plant-microbe Interact*, 4:407–411.
- [Brückner and Titgemeyer, 2002] Brückner, R. and Titgemeyer, F. (2002). Carbon catabolite repression in bacteria: choice of the carbon source and autoregulatory limitation of sugar utilization. *FEMS Microbiol Lett*, 209(2):141–148.
- [Burkovski and Krämer, 2002] Burkovski, A. and Krämer, R. (2002). Bacterial amino acid transport proteins: occurrence, functions, and significance for biotechnological applications. *Appl Microbiol Biotechnol*, 58(3):265–274.
- [Busch et al., 2007] Busch, A., Lacal, J., Martos, A., Ramos, J. L., and Krell, T. (2007). Bacterial sensor kinase TodS interacts with agonistic and antagonistic signals. *Proc Natl Acad Sci USA*, 104(34):13774–13779.
- [Clarke, 1982] Clarke, P. H. (1982). The metabolic versatility of *pseudomonads*. *Antonie van Leeuwenhoek*, 48(2):105–130.
- [Cock and Whitworth, 2007] Cock, P. J. A. and Whitworth, D. E. (2007). Evolution of prokaryotic two-component system signaling pathways: Gene fusions and fissions. *Mol Biol Evol*, 24(11):2355–2357.
- [Copeland, 2005] Copeland, P. R. (2005). Making sense of nonsense: the evolution of selenocysteine usage in proteins. *Genome Biol*, 6(6):221.
- [Davies et al., 1999] Davies, S. J., Golby, P., Omrani, D., Broad, S. A., Harrington, V. L., Guest, J. R., Kelly, D. J., and Andrews, S. C. (1999). Inactivation and regulation of the aerobic c<sub>4</sub>-dicarboxylate transport *dctA* gene of *Escherichia coli*. *J Bacteriol*, 181(18):5624–5635.
- [den Dooren de Jong, 1926] den Dooren de Jong, L. (1926). *Bijdragetot de kennis van het mineralisatieproces*. Thesis.
- [Dyer et al., 2002] Dyer, J., Wood, I. S., Palejwala, A., Ellis, A., and Shirazi-Beechey, S. P. (2002). Expression of monosaccharide transporters in intestine of diabetic humans. *Am J Physiol Gastrointest Liver Physiol*, 282(2):G241–8.
- [Díaz-Pérez et al., 2018] Díaz-Pérez, A. L., Núñez, C., Meza Carmen, V., and Campos-García, J. (2018). The expression of the genes involved in leucine catabolism of *Pseudomonas aeruginosa* is controlled by the transcriptional regulator LiuR and by the CbrAB/Crc system. *Res Microbiol*, 169(6):324–334.

- [Espinosa-Urgel et al., 2002] Espinosa-Urgel, M. ., Kolter, R. ., and Ramos, J.-L. . (2002). Root colonization by *Pseudomonas putida*: love at first sight. *Microbiology*, 148(2):341–343.
- [Faham et al., 2008] Faham, S., Watanabe, A., Besserer, G. M., Cascio, D., Specht, A., Hirayama, B. A., Wright, E. M., and Abramson, J. (2008). The crystal structure of a sodium galactose transporter reveals mechanistic insights into Na<sup>+</sup>sugar symport. *Science*, 321(5890):810–814.
- [Fang et al., 2009] Fang, Y., Jayaram, H., Shane, T., Kolmakova-Partensky, L., Wu, F., Williams, C., Xiong, Y., and Miller, C. (2009). Structure of a prokaryotic virtual proton pump at 3.2 Å resolution. *Nature*, 460(7258):1040–1043.
- [Forrest et al., 2011] Forrest, L. R., Krämer, R., and Ziegler, C. (2011). The structural basis of secondary active transport mechanisms. *Biochim Biophys Acta Bioenerg*, 1807(2):167–188.
- [Gao et al., 2009] Gao, X., Lu, F., Zhou, L., Dang, S., Sun, L., Li, X., Wang, J., and Shi, Y. (2009). Structure and mechanism of an amino acid antiporter. *Science*, 324(5934):1565–1568.
- [García-Mauriño et al., 2013] García-Mauriño, S. M., Pérez-Martínez, I., Amador, C. I., Canosa, I., and Santero, E. (2013). Transcriptional activation of the CrcZ and CrcY regulatory RNAs by the CbrB response regulator in *Pseudomonas putida*. *Mol Microbiol*, 89(1):189–205.
- [Gerth et al., 2017] Gerth, M., Liu, Y., Jiao, W., Zhang, X.-X., Baker, E., Lott, J., Rainey, P., and Johnston, J. (2017). Crystal structure of a bicupin protein HutD involved in histidine utilization in *Pseudomonas*. *Proteins*, 85(8):1580–1588.
- [Gödeke et al., 2011] Gödeke, J., Heun, M., Bubendorfer, S., Paul, K., and Thormann, K. M. (2011). Roles of two *Shewanella oneidensis* mr-1 extracellular endonucleases. *Appl Environ Microbiol*, 77(15):5342–5351.
- [Hazelbauer, 1975] Hazelbauer, G. L. (1975). Maltose chemoreceptor of *Escherichia coli*. *J Bacteriol*, 122(1):206–14.
- [Henry and Crosson, 2011] Henry, J. T. and Crosson, S. (2011). Ligand-binding PAS domains in a genomic, cellular, and structural context. *Annu Rev Microbiol*, 65:261–286.
- [Henríquez et al., 2019] Henríquez, T., Stein, N. V., and Jung, H. (2019). PvdRT-OpmQ and MdtABC-OpmB efflux systems are involved in pyoverdine secretion in *Pseudomonas putida* kt2440. *Environ Microbiol Rep*, 11(2):98–106.
- [Henríquez et al., 2021] Henríquez, T., Wirtz, L., Su, D., and Jung, H. (2021). Prokaryotic solute/sodium symporters: Versatile functions and mechanisms of a transporter family. *Int J Mol Sci*, 22(4):1880.

- [Hester et al., 2000] Hester, K. L., Lehman, J., Najjar, F., Song, L., Roe, B. A., MacGregor, C. H., Hager, P. W., Phibbs, P. V., and Sokatch, J. R. (2000). Crc is involved in catabolite repression control of the *bkd* operons of *Pseudomonas putida* and *Pseudomonas aeruginosa*. *J Bacteriol*, 182(4):1144–1149.
- [Holsbeeks et al., 2004] Holsbeeks, I., Lagatie, O., Van Nuland, A., Van de Velde, S., and Thevelein, J. M. (2004). The eukaryotic plasma membrane as a nutrient-sensing device. *Trends Biochem Sci*, 29(10):556–64.
- [Hu et al., 1989] Hu, L., Allison, S. L., and Phillips, A. T. (1989). Identification of multiple repressor recognition sites in the *hut* system of *Pseudomonas putida*. *J Bacteriol*, 171(8):4189–4195.
- [Hu and Phillips, 1988a] Hu, L. and Phillips, A. T. (1988a). Organization and multiple regulation of histidine utilization genes in *Pseudomonas putida*. *J Bacteriol*, 170(9):4272–9.
- [Hu and Phillips, 1988b] Hu, L. and Phillips, A. T. (1988b). Organization and multiple regulation of histidine utilization genes in *Pseudomonas putida*. *J Bacteriol*, 170(9):4272–4279.
- [Inada et al., 1996] Inada, T., Kimata, K., and Aiba, H. (1996). Mechanism responsible for glucose–lactose diauxie in *Escherichia coli*: challenge to the camp model. *Genes to Cells*, 1(3):293–301.
- [Itoh et al., 2007] Itoh, Y., Nishijyo, T., and Nakada, Y. (2007). *Histidine Catabolism and Catabolite Regulation*, pages 371–395. Springer Netherlands, Dordrecht.
- [Jack et al., 2000] Jack, D. L., Paulsen, I. T., and Saier, M. H. (2000). The amino acid/polyamine/organocation (APC) superfamily of transporters specific for amino acids, polyamines and organocations. *Microbiology*, 146(8):1797–1814.
- [Jardetzky, 1966] Jardetzky, O. (1966). Simple allosteric model for membrane pumps. *Nature*, 211(5052):969–970.
- [Jung, 2002] Jung, H. (2002). The sodium/substrate symporter family: structural and functional features. *FEBS Letters*, 529(1):73–77.
- [Jung et al., 2012] Jung, H., Hilger, D., and Raba, M. (2012). The  $\text{Na}^+$ /L-proline transporter PutP. *Front Biosci (Landmark Ed)*, 17:745–59.
- [Jungnickel et al., 2018] Jungnickel, K. E. J., Parker, J. L., and Newstead, S. (2018). Structural basis for amino acid transport by the CAT family of SLC7 transporters. *Nat. Commun.*, 9(1):550–550.

- [Kaspar et al., 1999] Kaspar, S., Perozzo, R., Reinelt, S., Meyer, M., Pfister, K., Scapozza, L., and Bott, M. (1999). The periplasmic domain of the histidine autokinase CitA functions as a highly specific citrate receptor. *Mol Microbiol*, 33(4):858–872.
- [Kendrick and Wheelis, 1982] Kendrick, K. E. and Wheelis, M. L. (1982). Histidine dissimilation in *Streptomyces coelicolor*. *Microbiology*, 128(9):2029–2040.
- [Kleefeld et al., 2009] Kleefeld, A., Ackermann, B., Bauer, J., Krämer, J., and Unden, G. (2009). The fumarate/succinate antiporter dcub of *Escherichia coli* is a bifunctional protein with sites for regulation of dcus-dependent gene expression. *J Biol Chem*, 284(1):265–275.
- [Korycinski et al., 2015] Korycinski, M., Albrecht, R., Ursinus, A., Hartmann, M. D., Coles, M., Martin, J., Dunin-Horkawicz, S., and Lupas, A. N. (2015). STAC - a new domain associated with transmembrane solute transport and two-component signal transduction systems. *J Mol Biol*, 427(20):3327–3339.
- [Krell et al., 2010] Krell, T., Lacal, J., Busch, A., Silva-Jiménez, H., Guazzaroni, M.-E., and Ramos, J. L. (2010). Bacterial sensor kinases: Diversity in the recognition of environmental signals. *Annu Rev Microbiol*, 64(1):539–559.
- [Kriel et al., 2011] Kriel, J., Haesendonckx, S., Rubio-Teixeira, M., Van Zeebroeck, G., and Thevelein, J. M. (2011). From transporter to transeptor: signaling from transporters provokes re-evaluation of complex trafficking and regulatory controls. *Bioessays*, 33(11):870–9.
- [Leidigh and Wheelis, 1973] Leidigh, B. J. and Wheelis, M. L. (1973). Genetic control of the histidine dissimilatory pathway in *Pseudomonas putida*. *Mol Gen Genet*, 120(3):201–210.
- [Lessie and Neidhardt, 1967] Lessie, T. G. and Neidhardt, F. C. (1967). Formation and operation of the histidine-degrading pathway in *pseudomonas aeruginosa*. *J Bacteriol*, 93(6):1800–10.
- [Letunic and Bork, 2017] Letunic, I. and Bork, P. (2017). 20 years of the smart protein domain annotation resource. *Nucleic Acids Res*, 46(D1):D493–D496.
- [Letunic et al., 2014] Letunic, I., Doerks, T., and Bork, P. (2014). Smart: recent updates, new developments and status in 2015. *Nucleic Acids Res*, 43(D1):D257–D260.
- [Li and Lu, 2007] Li, W. and Lu, C.-D. (2007). Regulation of carbon and nitrogen utilization by CbrAB and NtrBC two-component systems in *Pseudomonas aeruginosa*. *J Bacteriol*, 189(15):5413–5420.
- [Li et al., 2015a] Li, Z., Lee, A. S. E., Bracher, S., Jung, H., Paz, A., Kumar, J. P., Abramson, J., Quick, M., and Shi, L. (2015a). Identification of a second substrate-binding site in solute-sodium symporters. *J Biol Chem*, 290(1):127–141.

- [Li et al., 2015b] Li, Z., Lee, A. S. E., Bracher, S., Jung, H., Paz, A., Kumar, J. P., Abramson, J., Quick, M., and Shi, L. (2015b). Identification of a second substrate-binding site in solute-sodium symporters. *J Biol Chem*, 290(1):127–141.
- [Liao et al., 1997] Liao, M. K., Gort, S., and Maloy, S. (1997). A cryptic proline permease in *Salmonella typhimurium*. *Microbiology*, 143 ( Pt 9):2903–2911.
- [Loeschcke and Thies, 2015] Loeschcke, A. and Thies, S. (2015). *Pseudomonas putida* -a versatile host for the production of natural products. *Appl Microbiol and Biotechnol*, 99(15):6197–6214.
- [Lolkema et al., 1994] Lolkema, J. S., Speelmans, G., and Konings, W. N. (1994). Na<sup>+</sup>-coupled versus H<sup>+</sup>-coupled energy transduction in bacteria. *Biochim Biophys Acta Bioenerg*, 1187(2):211–215.
- [Lonergan et al., 2020] Lonergan, Z. R., Palmer, L. D., and Skaar, E. P. (2020). Histidine utilization is a critical determinant of acinetobacter pathogenesis. *Infect Immun*, 88(7):e00118–20.
- [Ma et al., 2012] Ma, D., Lu, P., Yan, C., Fan, C., Yin, P., Wang, J., and Shi, Y. (2012). Structure and mechanism of a glutamate–GABA antiporter. *Nature*, 483(7391):632–636.
- [Manson et al., 1985] Manson, M. D., Boos, W., Bassford, P. J., J., and Rasmussen, B. A. (1985). Dependence of maltose transport and chemotaxis on the amount of maltose-binding protein. *J Biol Chem*, 260(17):9727–33.
- [Mascher et al., 2006] Mascher, T., Helmann, J. D., and Uden, G. (2006). Stimulus perception in bacterial signal-transducing histidine kinases. *Microbiol Mol Biol Rev*, 70(4):910–938.
- [Melin and Meeuwisse, 1969] Melin, K. and Meeuwisse, G. W. (1969). Glucose-galactose malabsorption. *Acta Paediatrica*, 58(S188):19–24.
- [Migula, 1894] Migula, W. (1894). *Über ein neues System der Bakterien*. Arb. Bakteriolog. Inst. Karlsruhe.
- [Mitchell, 1991] Mitchell, P. (1991). Foundations of vectorial metabolism and osmochemistry. *Biosci Rep*, 11(6):297–346.
- [Monteagudo-Cascales et al., 2019] Monteagudo-Cascales, E., García-Mauriño, S. M., Santero, E., and Canosa, I. (2019). Unraveling the role of the CbrA histidine kinase in the signal transduction of the CbrAB two-component system in *Pseudomonas putida*. *Sci Rep*, 9(1):9110–9110.

- [Moore et al., 2006] Moore, E. R., Tindall, B. J., Martins Dos Santos, V., Pieper, D. H., Ramos, J.-L., and Palleroni, N. J. (2006). Nonmedical: pseudomonas. *Prokaryotes*, 6:646–703.
- [Moreno et al., 2009] Moreno, R., Martínez-Gomariz, M., Yuste, L., Gil, C., and Rojo, F. (2009). The *Pseudomonas putida* Crc global regulator controls the hierarchical assimilation of amino acids in a complete medium: Evidence from proteomic and genomic analyses. *Proteomics*, 9(11):2910–2928.
- [Moreno et al., 2007] Moreno, R., Ruiz-Manzano, A., Yuste, L., and Rojo, F. (2007). The *Pseudomonas putida* Crc global regulator is an rna binding protein that inhibits translation of the AlkS transcriptional regulator. *Mol Microbiol*, 64(3):665–675.
- [Naren and Zhang, 2020] Naren, N. and Zhang, X.-X. (2020). Global regulatory roles of the histidine-responsive transcriptional repressor HutC in *Pseudomonas fluorescens* SBW25. *J Bacteriol*, 202(13):e00792–19.
- [Nelson et al., 2002] Nelson, K. E., Weinell, C., Paulsen, I. T., Dodson, R. J., Hilbert, H., Martins dos Santos, V. A. P., Fouts, D. E., Gill, S. R., Pop, M., Holmes, M., Brinkac, L., Beanan, M., DeBoy, R. T., Daugherty, S., Kolonay, J., Madupu, R., Nelson, W., White, O., Peterson, J., Khouri, H., Hance, I., Lee, P. C., Holtzapple, E., Scanlan, D., Tran, K., Moazzez, A., Utterback, T., Rizzo, M., Lee, K., Kosack, D., Moestl, D., Wedler, H., Lauber, J., Stjepandic, D., Hoheisel, J., Straetz, M., Heim, S., Kiewitz, C., Eisen, J., Timmis, K. N., Dusterhöft, A., Tümmler, B., and Fraser, C. M. (2002). Complete genome sequence and comparative analysis of the metabolically versatile *Pseudomonas putida* KT2440. *Environ Microbiol*, 4(12):799–808.
- [Nishijyo et al., 2001] Nishijyo, T., Haas, D., and Itoh, Y. (2001). The CbrA–CbrB two-component regulatory system controls the utilization of multiple carbon and nitrogen sources in *Pseudomonas aeruginosa*. *Mol Microbiol*, 40(4):917–931.
- [Palleroni, 2010] Palleroni, N. J. (2010). The pseudomonas story. *Environ Microbiol*, 12(6):1377–1383.
- [Parkinson, 1993] Parkinson, J. S. (1993). Signal transduction schemes of bacteria. *Cell*, 73(5):857–871.
- [Phillips et al., 2004] Phillips, D. A., Fox, T. C., King, M. D., Bhuvaneshwari, T. V., and Teuber, L. R. (2004). Microbial products trigger amino acid exudation from plant roots. *Plant Physiol*, 136(1):2887–2894.
- [Quiroz-Rocha et al., 2017a] Quiroz-Rocha, E., Bonilla-Badía, F., García-Aguilar, V., López-Pliego, L., Serrano-Román, J., Cocotl-Yañez, M., Guzmán, J., Ahumada-Manuel, C. L.,

- Muriel-Millán, L. F., Castañeda, M., Espín, G., and Nuñez, C. (2017a). Two-component system CbrA/CbrB controls alginate production in *Azotobacter vinelandii*. *Microbiology*, 163(7):1105–1115.
- [Quiroz-Rocha et al., 2017b] Quiroz-Rocha, E., Moreno, R., Hernández-Ortíz, A., Fragoso-Jiménez, J. C., Muriel-Millán, L. F., Guzmán, J., Espín, G., Rojo, F., and Núñez, C. (2017b). Glucose uptake in *Azotobacter vinelandii* occurs through a GluP transporter that is under the control of the CbrA/CbrB and Hfq-Crc systems. *Sci Rep*, 7(1):858–858.
- [Rauschmeier et al., 2014] Rauschmeier, M., Schüppel, V., Tetsch, L., and Jung, K. (2014). New insights into the interplay between the lysine transporter *lysp* and the pH sensor *cadC* in *Escherichia coli*. *J Mol Biol*, 426(1):215–229.
- [Regaiolo et al., 2020] Regaiolo, A., Dominelli, N., Andresen, K., Heermann, R., and Schaffner, D. W. (2020). The biocontrol agent and insect pathogen *Photorhabdus luminescens* interacts with plant roots. *Appl Environ Microbiol*, 86(17):e00891–20.
- [Regenhardt et al., 2002] Regenhardt, D., Heuer, H., Heim, S., Fernandez, D. U., Strömpl, C., Moore, E. R. B., and Timmis, K. N. (2002). Pedigree and taxonomic credentials of *Pseudomonas putida* strain KT2440. *Environ Microbiol*, 4(12):912–915.
- [Reitzer, 2005] Reitzer, L. (2005). Catabolism of amino acids and related compounds. *EcoSal Plus*.
- [Ren et al., 2009] Ren, J., Wen, L., Gao, X., Jin, C., Xue, Y., and Yao, X. (2009). Dog 1.0: illustrator of protein domain structures. *Cell Res*, 19(2):271–273.
- [Ren and Paulsen, 2007] Ren, Q. and Paulsen, I. T. (2007). Large-scale comparative genomic analyses of cytoplasmic membrane transport systems in prokaryotes. *J Mol Microbiol Biotechnol*, 12(3-4):165–179.
- [Rietsch et al., 2004] Rietsch, A., Wolfgang, M. C., and Mekalanos, J. J. (2004). Effect of metabolic imbalance on expression of type III secretion genes in *Pseudomonas aeruginosa*. *Infect Immun*, 72(3):1383–1390.
- [Rodrigue et al., 2000] Rodrigue, A., Quentin, Y., Lazdunski, A., Méjean, V., and Foglino, M. (2000). Cell signalling by oligosaccharides. two-component systems in *Pseudomonas aeruginosa*: why so many? *Trends Microbiol*, 8(11):498–504.
- [Roelofs et al., 2011] Roelofs, K. G., Wang, J., Sintim, H. O., and Lee, V. T. (2011). Differential radial capillary action of ligand assay for high-throughput detection of protein-metabolite interactions. *Proc Natl Acad Sci USA*, 108(37):15528–33.

- [Rojo, 2010] Rojo, F. (2010). Carbon catabolite repression in *Pseudomonas*: optimizing metabolic versatility and interactions with the environment. *FEMS Microbiol Rev*, 34(5):658–684.
- [Saier, 2000] Saier, M. H., J. (2000). A functional-phylogenetic classification system for transmembrane solute transporters. *Microbiol Mol Biol Rev*, 64(2):354–411.
- [Saier et al., 2006] Saier, M. H., J., Tran, C. V., and Barabote, R. D. (2006). TCDB: the transporter classification database for membrane transport protein analyses and information. *Nucleic Acids Res*, 34(Database issue):D181–6.
- [Saier, 2015] Saier, Milton H., J. (2015). The bacterial phosphotransferase system: New frontiers 50 years after its discovery. *J Mol Microbiol*, 25(2-3):73–78.
- [Saier et al., 2013] Saier, Milton H., J., Reddy, V. S., Tamang, D. G., and Västermark, A. (2013). The transporter classification database. *Nucleic Acids Res*, 42(D1):D251–D258.
- [Savada et al., 2011] Savada, D., Hills, D. M., Heller, H. C., and Berenbaum, M. R. (2011). *Purves Biologie*. Jürgen Markl, Springer Spektrum, 9 edition.
- [Schweikhard and Ziegler, 2012] Schweikhard, E. S. and Ziegler, C. M. (2012). *Chapter One - Amino Acid Secondary Transporters: Toward a Common Transport Mechanism*, volume 70, pages 1–28. Academic Press.
- [Sepulveda and Lupas, 2017] Sepulveda, E. and Lupas, A. N. (2017). Characterization of the CrbS/R two-component system in *Pseudomonas fluorescens* reveals a new set of genes under its control and a dna motif required for CrbR-mediated transcriptional activation. *Front Microbiol*, 8(2287).
- [Shaffer et al., 2009] Shaffer, P. L., Goehring, A., Shankaranarayanan, A., and Gouaux, E. (2009). Structure and mechanism of a Na<sup>+</sup>-independent amino acid transporter. *Science*, 325(5943):1010–1014.
- [Shi, 2013] Shi, Y. (2013). Common folds and transport mechanisms of secondary active transporters. *Annu. Rev. Biophys.*, 42(1):51–72.
- [Silby et al., 2011] Silby, M. W., Winstanley, C., Godfrey, S. A., Levy, S. B., and Jackson, R. W. (2011). *Pseudomonas* genomes: diverse and adaptable. *FEMS Microbiol Rev*, 35(4):652–680.
- [Sonnleitner et al., 2009] Sonnleitner, E., Abdou, L., and Haas, D. (2009). Small RNA as global regulator of carbon catabolite repression in *Pseudomonas aeruginosa*. *Proc Natl Acad Sci USA*, 106(51):21866–21871.

- [Sonnleitner and Bläsi, 2014] Sonnleitner, E. and Bläsi, U. (2014). Regulation of Hfq by the RNA CrcZ in *Pseudomonas aeruginosa* carbon catabolite repression. *PLOS Genetics*, 10(6):e1004440.
- [Sonnleitner and Haas, 2011] Sonnleitner, E. and Haas, D. (2011). Small RNAs as regulators of primary and secondary metabolism in *Pseudomonas* species. *Appl Microbiol Biotechnol*, 91(1):63–79.
- [Stopp et al., 2021] Stopp, M., Schubert, C., and Unden, G. (2021). Conversion of the sensor kinase dcus to the fumarate sensitive state by interaction of the bifunctional transporter dcta at the tm2/pas(c)-linker region. *Microorganisms*, 9(7):1397.
- [Tabor and Hayaishi, 1952] Tabor, H. and Hayaishi, O. (1952). The enzymatic conversion of histidine to glutamic acid. *J Biol Chem*, 194(1):171–175.
- [Tetsch and Jung, 2009a] Tetsch, L. and Jung, K. (2009a). How are signals transduced across the cytoplasmic membrane? Transport proteins as transmitter of information. *Amino Acids*, 37(3):467–477.
- [Tetsch and Jung, 2009b] Tetsch, L. and Jung, K. (2009b). The regulatory interplay between membrane-integrated sensors and transport proteins in bacteria. *Mol Microbiol*, 73(6):982–991.
- [Timmis, 2002] Timmis, K. N. (2002). *Pseudomonas putida*: a cosmopolitan opportunist par excellence. *Environ Microbiol*, 4(12):779–781.
- [Valentini et al., 2014] Valentini, M., García-Mauriño, S. M., Pérez-Martínez, I., Santero, E., Canosa, I., and Lapouge, K. (2014). Hierarchical management of carbon sources is regulated similarly by the CbrA/B systems in *Pseudomonas aeruginosa* and *Pseudomonas putida*. *Microbiology*, 160(10):2243–2252.
- [Vinothkumar and Henderson, 2010] Vinothkumar, K. R. and Henderson, R. (2010). Structures of membrane proteins. *Q Rev Biophys*, 43(1):65–158.
- [Västermark and Saier, 2014] Västermark, A. and Saier, M. H., J. (2014). Evolutionary relationship between 5+5 and 7+7 inverted repeat folds within the amino acid-polyamine-organocation superfamily. *Proteins*, 82(2):336–46.
- [Västermark et al., 2014] Västermark, A., Wollwage, S., Houle, M. E., Rio, R., and Saier, M. H., J. (2014). Expansion of the APC superfamily of secondary carriers. *Proteins*, 82(10):2797–811.
- [Watanabe et al., 2010] Watanabe, A., Choe, S., Chaptal, V., Rosenberg, J. M., Wright, E. M., Grabe, M., and Abramson, J. (2010). The mechanism of sodium and substrate release from the binding pocket of vSGLT. *Nature*, 468(7326):988–991.

- [Weyand et al., 2008] Weyand, S., Shimamura, T., Yajima, S., Suzuki, S., Mirza, O., Krusong, K., Carpenter, E. P., Rutherford, N. G., Hadden, J. M., O'Reilly, J., Ma, P., Saidijam, M., Patching, S. G., Hope, R. J., Norbertczak, H. T., Roach, P. C. J., Iwata, S., Henderson, P. J. F., and Cameron, A. D. (2008). Structure and molecular mechanism of a nucleobase–cation–symport-1 family transporter. *Science*, 322(5902):709–713.
- [Wirtz et al., 2021] Wirtz, L., Eder, M., Brand, A. K., and Jung, H. (2021). HutT functions as the major L-histidine transporter in *Pseudomonas putida* KT2440. *FEBS Lett*, 595(16):2113–2126.
- [Wirtz et al., 2020] Wirtz, L., Eder, M., Schipper, K., Rohrer, S., and Jung, H. (2020). Transport and kinase activities of CbrA of *Pseudomonas putida* KT2440. *Sci Rep*, 10(1):5400.
- [Wolf et al., 1995] Wolf, B. F., Sabine, H., Michael, U., and Olaf, N. (1995). Seed and vascular expression of a high-affinity transporter for cationic amino acids in arabidopsis. *Proc Natl Acad Sci USA*, 92(26):12036–12040.
- [Wong et al., 2012] Wong, F. H., Chen, J. S., Reddy, V., Day, J. L., Shlykov, M. A., Wakabayashi, S. T., and Saier, J. M. H. (2012). The amino acid-polyamine-organocation superfamily. *J Mol Microb Biotech*, 22(2):105–113.
- [Wright et al., 2007] Wright, E. M., Hirayama, B. A., and Loo, D. F. (2007). Active sugar transport in health and disease. *J Intern Med*, 261(1):32–43.
- [Wright and Kadner, 2001] Wright, J. S. and Kadner, R. J. (2001). The phosphoryl transfer domain of UhpB interacts with the response regulator UhpA. *J Bacteriol*, 183:3149 – 3159.
- [Yamashita et al., 2005] Yamashita, A., Singh, S. K., Kawate, T., Jin, Y., and Gouaux, E. (2005). Crystal structure of a bacterial homologue of Na<sup>+</sup>/Cl<sup>-</sup>-dependent neurotransmitter transporters. *Nature*, 437(7056):215–223.
- [Zhang et al., 2012] Zhang, X., Chang, H., Tran, S. L., Gauntlett, J. C., Cook, G. M., and Rainey, P. B. (2012). Variation in transport explains polymorphism of histidine and urocanate utilization in a natural *Pseudomonas* population. *Environ Microbiol*, 14(8):1941–1951.
- [Zhang et al., 2015] Zhang, X.-X., Gauntlett, J. C., Oldenburg, D. G., Cook, G. M., and Rainey, P. B. (2015). Role of the transporter-like sensor kinase CbrA in histidine uptake and signal transduction. *J Bacteriol*, 197(17):2867–2878.
- [Zhang et al., 2006] Zhang, X.-X., George, A., Bailey, M. J., and Rainey, P. B. (2006). The histidine utilization (*hut*) genes of *Pseudomonas fluorescens* SBW25 are active on plant surfaces, but are not required for competitive colonization of sugar beet seedlings. *Microbiology*, 152(6):1867–1875.

- [Zhang et al., 2010] Zhang, X.-X., Liu, Y.-H., and Rainey, P. B. (2010). CbrAB-dependent regulation of *pcnB*, a poly(A) polymerase gene involved in polyadenylation of RNA in *Pseudomonas fluorescens*. *Environ Microbiol*, 12(6):1674–1683.
- [Zhang and Rainey, 2007] Zhang, X.-X. and Rainey, P. B. (2007). Genetic analysis of the histidine utilization (*hut*) genes in *Pseudomonas fluorescens* sbw25. *Genetics*, 176(4):2165–2176.
- [Zhang and Rainey, 2008] Zhang, X.-X. and Rainey, P. B. (2008). Dual involvement of CbrAB and NtrBC in the regulation of histidine utilization in *Pseudomonas fluorescens* SBW25. *Genetics*, 178(1):185–195.
- [Zhang et al., 2014] Zhang, X.-X., Ritchie, S. R., and Rainey, P. B. (2014). Urocanate as a potential signaling molecule for bacterial recognition of eukaryotic hosts. *Cell Mol Life Sci*, 71(4):541–547.

## Acknowledgements

My first and greatest thanks goes to Prof. Jung, thank you Heinrich, for my fascinating project, for your constant support, your shared experience and creative ideas. I had the best time in your lab with you as my supervisor!

Next, I would like to thank all the members of my examination and thesis advisory committee for their support.

Michelle, I could not have done it without you. For three and a half years you were the person I spent most time with. Thank you for everything, your constant help and advice, for listening and talking everyday!

Nicola, Dan and Tania, I loved having you as colleagues, thanks for many shared lunch and coffee breaks, for scientific and personal talks.

A big thanks goes to the research course and bachelor students I supervised, you were so helpful and fun to work with, Korbinian, Annabel, Simon, Franzi, Iris and especially my last student and co-author Anna!

I wish to thank my colleagues from the microbiology, all the great people working in the K Jung, Lassak, Cordes and formerly Heermann and Bramkamp groups made this a time well spent.

Thank to my office mates Lei and Marija for being so helpful with everything baby-related. Thank you, Julia, my neighbour, colleague and friend, our shared car or bike rides always brightened the day!

Two friends spent almost 10 years with me at the faculty of biology from the first semester until now, Lisa and Krisi, we shared our path and oh so many coffee breaks. You made this a great time!

My family, Mama, Papa, and Josie, you always supported me, you always listened and you always had good advice. Sigrid, Christian, Kathi and Andi I am so glad to have you and your support as well! Thank you all and my whole family for everything!

The biggest thanks goes to my husband, Maxi, you are my rock and everyday I am thankful to you. Korbinian, I am so happy to be your mother, you are the light of my life.